BELGIAN RESEARCH PROGRAMME ON THE ANTARCTIC

SCIENTIFIC RESULTS OF PHASE III (1992-1996)

VOLUME I

MARINE BIOGEOCHEMISTRY AND ECODYNAMICS

EDITED BY S. CASCHETTO

FEDERAL OFFICE FOR SCIENTIFIC, TECHNICAL AND CULTURAL AFFAIRS

BELGIAN RESEARCH PROGRAMME ON THE ANTARCTIC

SCIENTIFIC RESULTS OF PHASE III (1992-1996)

VOLUME I

MARINE BIOGEOCHEMISTRY AND ECODYNAMICS

EDITED BY S. CASCHETTO

FEDERAL OFFICE FOR SCIENTIFIC, TECHNICAL AND CULTURAL AFFAIRS

1997

LEGAL NOTICE

Additional information on the Belgian Research Programme on the Antarctic is available on Internet (http://www.belspo.be/antar)

D/1997/1191/21

Published by the Federal Office for Scientific, Technical and Cultural Affairs (OSTC)
Brussels, Belgium

Cover photograph : Dr J.-L. Tison

Serial number ANTAR/97/3

FOREWORD

This volume presents the scientific results of research projects in the area of Marine Biogeochemistry and Ecodynamics funded under the Third Phase of the Belgian Research Programme on the Antarctic (1992-1996). Achievements of research projects in the other areas of the Programme form the subject of two separate volumes (Volume II : Part A – Hydrodynamics, Part B – Marine Geophysics ; Volume III : Glaciology and Climatology)

The Programme, which was initiated by the Belgian Government in 1985, is funded, managed and co-ordinated by the Federal Office for Scientific, Technical and Cultural Affairs (OSTC). The money allocated to the Third Phase was 160 MBEF. Research-work was implemented by means of 3-years projects undertaken by university- or federal scientific institute-based scientists.

All research costs (personnel, equipment, travel, working and overheads) were financed by the OSTC.

Such research effort aimed at contributing to the development of the knowledge required for a science-based conservation and management of the Antarctic environment and to the assessment of the mechanisms through which the Antarctic and the global climate interact. Emphasis was given on a multi-disciplinary approach of the dynamics of the global functioning of Antarctic main natural systems and of their evolution and interactions. Seven research lines were selected under three priority areas :

- ECODYNAMICS OF THE SOUTHERN OCEAN AND INTERACTIONS WITH THE CLIMATE :
  - Biogeochemical fluxes and cycles in the main trophic compartments
  - Modelling the global dynamics of ecosystems
  - Assessment of the role of " new production " in the burial of atmospheric CO_2 by the Southern Ocean

- EVOLUTION AND PROTECTION OF MARINE ECOSYSTEMS :
  - Application of predictive ecological models to simulate ecosystem responses to man-made climatic disturbances
  - Study of hydrocarbons spills dispersion

- ROLE OF THE ANTARCTIC IN GLOBAL CHANGES :
  - Ocean-Cryosphere-Atmosphere interactions.
  - Sedimentary palaeoenvironment.

Belgium's commitment in scientific research on the Antarctic is currently covered by the Fourth Phase of the Programme (1997-2000). The overall budget of this new phase amounts to 236 MBEF. In addition the OSTC contributes a sum of 20 MBEF to the operational costs of the European Project for Ice Coring in Antarctica (EPICA).

CONTENTS

1 SPATIAL AND SEASONAL VARIABILITY OF NEW PRODUCTION AND EXPORT PRODUCTION IN THE SOUTHERN OCEAN

F. DEHAIRS, M. SEMENEH, M. ELSKENS and L. GOEYENS

- ABSTRACT 1
- INTRODUCTION 3
- MATERIAL AND METHODS 4
  - Cruises 4
  - Sampling and analysis of dissolved nitrogen concentrations and uptake rates 4
  - Phytoplankton species: identification and enumeration 6
  - Determination of elemental and isotopic composition of total suspended matter 7
- RESULTS AND DISCUSSION 8
  - Spatial and seasonal variability of nutrient distribution and nitrogen uptake 8
  - Phytoplankton assemblage composition and nitrogen uptake 30
  - Spatial and seasonal variability of the export process from the mixed surface layer 46
- CONCLUSIONS 70
- ACKNOWLEDGEMENT 72
- REFERENCES 73

2 ECOLOGICAL MODELLING OF THE PLANKTONIC MICROBIAL FOOD-WEB

Ch. LANCELOT, S. BECQUEVORT, P. MENON, S. MATHOT and J.-M. DANDOIS

- ABSTRACT 3
- INTRODUCTION 5
  - The Paradoxical nature of the Southern Ocean 5
  - Towards a generic model of phytoplankton development in the Southern Ocean 7
- MATERIAL AND METHODS 9
  - Polar expeditions 9
  - Methods 10
- STRUCTURE AND FUNCTIONING OF THE ANTARCTIC PELAGIC FOOD WEB 14
  - Phenomenological description at visited sites 16
  - Antarctic pelagic ecosystem functioning 23
- MODELLING C, N, Fe THROUGH THE PLANKTONIC MICROBIAL FOOD-WEB OF THE SOUTHERN OCEAN: THE SWAMCO MODEL . 27
  - Structure of the SWAMCO model .. 27
  - Equations and parameters 31
  - Model results 47
- CONCLUSION AND PERSPECTIVES 64
- REFERENCES 69

ROLE OF THE MEIOBENTHOS IN ANTARCTIC ECOSYSTEMS

S. VANHOVE, J. WITTOECK,
M. BEGHYN, D. VAN GANSBEKE,
A. VAN KENHOVE, A. COOMANS
and M. VINCX

- ABSTRACT 1
- INTRODUCTION 3
- MATERIAL AND METHODS 4

  Deep-sea study 4

  Shallow-water study 5

  Treatment of the meiofauna and nematodes 6

  Environmental data of Signy Island 6

  Statistical tests 7

  In situ grazing experiments 7

  Sediment-water nutrient concentration changes 8

  Respiration 9
- RESULTS 10

  Meiobenthos in the deep-sea floor of the Weddell Sea 10

  Meiobenthos in the low subtidal sediments of Signy Island 13

  Relations between the meiobenthos and its environment in the deep-sea 14

  Relations between the meiobenthos and its environment in the low subtidal 15

  Flux of organic matter and nutrients through the benthic system and sediment-water interface at Signy Island 17
- DISCUSSION 18

  Comparison of Antarctic meiobenthic standing stock with similar systems all over the world 18

  Meiobenthic relations with the trophic environment 19

  Bentho-pelagic coupling: direction water column to sediments 22

  Bentho-pelagic coupling: reverse direction and contribution of the meiobenthos to the mineralization processes: the case of Signy Island 23

  Meiofaunal secondary production at Signy Island 28

  Carbon balance at Signy Island .. 31
- CONCLUSIONS 33
- ACKNOWLEDGEMENTS 35
- REFERENCES 36

Contents of VOLUME II

Part A : **HYDRODYNAMICS**

OIL SPILL MODELLING IN THE WEDDELL SEA

B. PETIT

Part B : **MARINE GEOPHYSICS**

BELANTOSTRAT BELGIAN CONTRIBUTION TO THE "ANTARCTIC OFFSHORE ACOUSTIC STRATIGRAPHY PROJECT (ANTOSTRAT)"

M. DE BATIST, P.-J. BART and K. VANNESTE

Contents of VOLUME III

GLACIOLOGY AND CLIMATOLOGY

FORMATION OF THE TERRA NOVA BAY POLYNYA AND CLIMATIC IMPLICATIONS

H. GALLÉE

DYNAMICS OF THE ANTARCTIC ICE SHEET AND ENVIRONMENTAL CHANGE

F. PATTYN, H. DECLEIR and D. WILLAERT

CHEMICAL AND ISOTOPIC COMPOSITION OF ICE FROM ANTARCTIC ICE SHELVES : IMPLICATIONS FOR GLOBAL CHANGE

R. SOUCHEZ, J.-L. TISON and R. LORRAIN

RESEARCH CONTRACT A3/03/001

1

SPATIAL AND SEASONAL VARIABILITY OF NEW PRODUCTION AND EXPORT PRODUCTION IN THE SOUTHERN OCEAN

F. DEHAIRS[1],
M. SEMENEH,
M. ELSKENS and
L. GOEYENS

VRIJE UNIVERSITEIT BRUSSEL
LABORATORY OF ANALYTICAL CHEMISTRY
Pleinlaan 2
B-1050 Brussels
Belgium

[1] Corresponding author E-mail : fdehairs@vub.ac.be

CONTENTS

ABSTRACT 1

1. INTRODUCTION 3

2. MATERIAL AND METHODS 4

2.1. Cruises 4

2.2. Sampling and analysis of dissolved nitrogen concentrations and uptake rates 4

2.3. Phytoplankton species: identification and enumeration 6

2.4. Determination of elemental and isotopic composition of total suspended matter 7

3. RESULTS AND DISCUSSION 8

3.1. Spatial and seasonal variability of nutrient distribution and nitrogen uptake 8

3.1.1. Nutrient distribution patterns 8

3.1.2. The corresponding nitrate and ammonium uptake rates 11

3.1.3. Seasonal variability of the nitrate uptake rates 14

3.1.4. The nitrogen uptake regime 20

3.1.5. Effect of ammonium on the nitrate uptake rate and *f*-ratio 26

3.2. Phytoplankton assemblage composition and nitrogen uptake 30

3.2.1. Phytoplankton biomass, community structure and nitrogen uptake rates 30

3.2.2. Seasonal evolution in phytoplankton community structure and nitrogen uptake regime 39

3.3. Spatial and seasonal variability of the export process from the mixed surface layer 46

3.3.1. Estimation of the O_2 consumption rates 47

3.3.2. Particulate Ba stocks and O_2 consumption rates: the transfer function 50

3.3.3. Comparing calculated JO_2 with primary production and Ba-barite stocks 55

3.3.4. Particulate Ba and productivity in different environments of the Southern Ocean 59

3.3.5. Exported carbon respired in the mesopelagic water column 61

3.3.6. Temporal evolution of export production 65

3.3.7. Comparison of export production calculated from mesopelagic Ba and from sediment trap Ba fluxes 66

4. CONCLUSIONS 70

ACKNOWLEDGEMENT 72

REFERENCES 73

ABSTRACT

This study focuses on the investigation of two intensely related fluxes in the Southern Ocean: (a) the nutrient uptake regime, with main emphasis on the uptake of nitrogen sources and (b) the type and intensity of export production towards the deeper layers and the sediments.

The separation in Southern Ocean provinces of silicate excess at nitrate exhaustion and of nitrate excess at silicate exhaustion, as suggested by Kamykowski and Zentara (1985, 1989), was supported by our investigations of the silicate to nitrate uptake ratios. Oligotrophic Antarctic waters mainly exhibit proportionally higher silicate removal what induces a potential for nitrate excess. The nitrogen uptake regime of such areas is characterised by low absolute as well as specific nitrate uptake rates throughout. Maximal values did not exceed 0.15 μM d^{-1} and 0.005 h^{-1}, respectively. Corresponding *f*-ratios ranged from 0.39 to 0.86. This scenario contrasts strikingly to the more fertile ice edge areas. They showed a drastic but short vernal increase in nitrate uptake. Absolute uptake rates reached a maximum value of 2.18 μM d^{-1} whereas the maximal specific uptake rate was 0.063 h^{-1}. This peak nitrate utilisation during early spring led to the observed potential for silicate excess. With increasing seasonal maturity the nitrate uptake became inhibited by the presence of enhanced ammonium availability (up to 8 % of the inorganic nitrogen pool), however, and after a short period of intensive nitrate consumption the uptake rates drop to very low levels, which are comparable to the ones observed in the area of nitrate excess at silicate exhaustion.

The nitrogen uptake by phytoplankton was also studied in relation to the biomass and structure of the community in the Atlantic and Indian sectors of the Southern Ocean. Two scenarios for the seasonal evolution of the uptake regime and the phytoplankton community structure are discussed. In the Marginal Ice Zone of the Scotia-Weddell Confluence area, the transition from a predominantly nitrate based system to a predominantly ammonium based one was paralleled by the disappearance of diatom dominance and the concomitant development of a dense flagellate dominated phytoplankton community. On the other hand, in the Coastal and Continental Shelf Zone and Open Oceanic Zone of the Indian sector, the shift in the nitrogen uptake regime occurred without significant change in the

phytoplankton community structure. Diatoms dominated the assemblage throughout and about 80% of the phytoplankton biomass was in the > 10 µm size fraction. Unlike the first scenario, diatom growth was largely depending on ammonium. Thus, in areas of persistent water column stability and less selective grazing pressure, a shift in the uptake regime can occur without changes in the community structure. The dominance of diatoms under regenerated production provides, furthermore, physiological supports for the observed potential for nitrate excess in oligotrophic Antarctic waters.

Export fluxes, as traced by mesopelagic stocks of particulate Ba-barite, were found to be strongly dependent on the type of production. In environments with predominant regenerated production, export production did not sustain significant Ba-barite accumulation. This appeared to be the characteristic situation for environments having shallow mixed layers as a result of melt water input, such as the NW Weddell Sea and the Prydz Bay region. Although in these environments algae growth was high (large nitrate depletions and uptake rates at the beginning of the growth season) grazing pressure was also high, as witnessed by high subsurface ammonium. Open ocean areas, on the contrary, had larger export fluxes despite their lower surface productivities (lower integrated nitrate depletions) and algae biomass. The latter properties resulted from deeper mixed surface layers and relatively reduced grazing pressures (poor ammonium build-up). The Polar Front region appeared to be an intermediate system.

Additionally, a transfer function was used to calculated the fraction of exported carbon respired in the subsurface and intermediate waters (i.e. the mesopelagic water column). This function was first validated to the ANTARKTIS X/6 Ba data set and thereafter applied to the whole of our Southern Ocean data set. Export production obtained from mesopelagic Ba accumulation was subsequently compared to sediment trap Ba fluxes.

1. INTRODUCTION

Hart (1934) already recognised the striking disequilibrium between nutrient abundances and the paucity of phytoplankton development in Antarctic waters. There are differences, however. The productivity levels can vary by approximately two orders of magnitude, approaching that of oligotrophic systems in the open ocean and "bloom" conditions in the vicinity of the coasts and in stabilised waters nearby the ice edge. Additionally, earlier studies suggested the importance of pico-, nano- and microplankton producers and predators for the Antarctic food web (El-Sayed 1987).

The understanding of the Southern Ocean's role in the global cycling of biogenic elements relies largely on the relative seasonal variability in the different subunits of Antarctic waters. Open ocean environments generally display poor phytoplankton development and concomitantly low nutrient removal, whereas dense phytoplankton assemblages and elevated nutrient depletions usually occur in well sheltered areas bordering the retreating ice only (Goeyens *et al.* 1991, Tréguer and Jacques 1992). Our contribution focuses on the investigation of 2 intensely related fluxes: (a) the nutrient uptake regime, with main emphasis on the uptake of nitrogen, and (b) the type and intensity of export production towards the deeper layers and the sediments.

The phytoplankton development was characterised in terms of the nutrient signature in the surface layer, nitrogenous nutrient preferences and uptake rates, phytoplanktonic species distributions and stocks. Additionally, the study of the fate of primary production combined estimates of in-situ and mesopelagic remineralisation. Ammonium accumulations in the upper layer and corresponding ammonium remineralisation rates were determined to describe the former aspect; barite accumulation and oxygen consumption were determined to describe the mesopelagic remineralisation process.

2. MATERIAL AND METHODS

2.1. Cruises

Results were obtained during 7 different cruises: EPOS LEG 2 (20 November 1988 to 7 January 1989), ANTARKTIS IX/2 (14 November to 30 December 1990), ANTARKTIS X/6 (23 September to 30 November 1992) and ANTARKTIS X/7 (3 December 1992 to 22 January 1993) aboard RV Polarstern, MARINE SCIENCE VOYAGE 6 (3 January to 20 March 1991) aboard RV Aurora Australis and INDIGO 3 (03 January to 28 February 1987) and ANTARES 2 (26 January to 23 March 1994) aboard RV Marion-Dufresne. Data from the earliest cruises are used for the sake of comparison only; they were collected during the first and second phase of the research programme on the Antarctic. For the current report main emphasis is on the research carried out during ANTARKTIS X/6, ANTARKTIS X/7 and ANTARES 2.

2.2. Sampling and analysis of dissolved nitrogen concentrations and uptake rates

Samples for nutrient analyses were collected either with 12 l Niskin and Go-Flo bottles, mounted on the CTD rosette, or with 30 l Niskin bottles used for production-dissolution experiments. Nitrate was analysed by an autoanalyser system (Tréguer and Le Corre, 1975); ammonium concentrations were determined manually as described by Koroleff (1969).

We describe the nutrient signature of the upper layer in terms of nutrient stocks and availability. Nutrient stocks are defined as depth integrated amounts in the upper layer, the section of the water column confined between the surface and temperature minimum layer. The availability of nitrogenous nutrients are defined as their percentage in the total dissolved inorganic nitrogen pool. Similarly, particulate matter stocks are defined as depth integrated amounts of particulate organic carbon (POC), particulate nitrogen (PN) and chlorophyll.

The nutrient uptake regime in the surface layer is determined by nutrient depletions, which represent an estimate of seasonally integrated nutrient removal in the upper layer down to the remnant winter layer or temperature minimum layer (Le Corre and Minas, 1983; Jennings *et al.*, 1984), as well as by absolute and specific

nitrogen uptake rates obtained from ^{15}N incubation experiments. Three assumptions are implicit in the use of nutrient depletions: (1) vertical homogeneity characterises the ice covered winter water, (2) lateral and vertical mixing remain negligible and (3) melting of nutrient-poor pack ice does not obscure the signal of nutrient utilisation. A detailed discussion of the hypotheses is given by Goeyens *et al.* (1995).

In accordance with Dugdale and Wilkerson (1986) and Collos (1987), specific nitrogen uptake rates (v, in h^{-1}) are defined as nutrient taken up per unit of PN and per unit of time, whereas absolute uptake rates (ρ, in $\mu M\ h^{-1}$) are the product of specific uptake rates and PN concentration:

$$\rho_N\ (\mu M\, h^{-1}) = v_N\ (h^{-1}) \times PN\ (\mu M) \qquad (1)$$

Additionally, nitrate uptake rates were evaluated by an inverse technique (Shopova *et al.*, 1995). For this purpose we applied a vertical advection-diffusion model; the equation of conservation of nitrate is:

$$\partial_t [NO_3] = \partial_z (K\, \partial_z [NO_3] - w\, \partial_z [NO_3] + J = 0 \qquad (2)$$

with $[NO_3] = [NO_3]_{(z,t)}$ the ambient nitrate concentration, $K_{(z,t)}$ the vertical mixing coefficient, $w_{(z,t)}$ the vertical velocity and $J_{(z,t)}$ the apparent production/consumption rate.

In this model, uptake equals consumption and we assume non-constant eddy diffusivity and vertical velocity over the water column (Shopova *et al.*, 1995). In order to avoid biasing effects of horizontal advection, we contrived 2 "average" stations, the first one representing the MIZ (EPOS LEG 2 stations 157, 158, 164 and 172) and the second one representing the CCSZ (MARINE SCIENCE VOYAGE 6 stations 16, 29, 32 and 48), respectively (Goeyens and Dehairs, 1993). The average calculated nitrate uptake rates amount to 0.04 $\mu M\ d^{-1}$ and to 0.03 $\mu M\ d^{-1}$, what is in good agreement with the experimental values of 0.06 and 0.04 $\mu M\ d^{-1}$, obtained from the incubation experiments. Averaging the stations inherently signifies that they are homogeneous (no horizontal advection taking place). The similarity of theoretical and empirical results gives evidence for insignificant

advection and strengthens the use of nutrient depletions as estimates of time integrated uptake.

Furthermore, reference is made to *f-ratios* in order to characterise the relative contribution of new nitrogen (mostly nitrate) to primary production (Eppley and Peterson, 1979), and to relative preference indices (RPI), which describe the nitrogen utilisation relative to the nitrogen availability, as defined by McCarthy *et al.* (1977). Both parameters are common for assessing the interaction between nitrate and ammonium uptake (Dortch, 1990). *f*-ratios combine preference and inhibition, whereas RPI values must be treated as indicators of preference only. The precision of the RPI is low, however, because of considerable error resulting from the combination of different variables.

2.3. Phytoplankton species: identification and enumeration

Water samples for species identification and enumeration were taken from the surface layer (< 30 m) in different parts of the Southern Ocean and preserved with a hexamine-buffered formalin solution (final concentration ~0.4%). We examined a total of 147 samples of about 81 stations. Depending on the biomass, 10 or 50 ml subsample was settled for about 24 h and counted under inverted microscope according to the Utermöhl method (Utermöhl, 1958). Cell volume was calculated from cell dimensions using appropriate cell geometry. Carbon biomass was estimated from cell volume and abundance (cells l^{-1}) using the conversion factors of Eppley *et al.* (1970):

$$\text{Log}(C) = 0.76 \times \log(V) - 0.352 \text{ for diatoms,} \quad (3)$$

$$\text{Log}(C) = 0.94 \times \log(V) - 0.6 \text{ for non-diatoms} \quad (4)$$

where V is the cell's volume (μm^3) and C is cell's carbon (pg).

With this method only cells > 2 μm can be quantified and thus the biomass of pico-sized phytoplankton is excluded. Biomass data for EPOS LEG 2 and MARINE SCIENCE VOYAGE 6 cruises were kindly provided by S. Becquevort and E. Kopczynska, respectively.

2.4. Determination of elemental and isotopic composition of total suspended matter

Total suspended matter (TSM) for C, N an stable C isotope ratio analysis was collected on precombusted (at 450 °C) glass fibre filters (Whatmann GF/F), dried at 60 °C for approximately half an hour and stored dry in Petri dishes till analysis in the home lab. POC and PN concentrations were determined after processing the filters with HCl for carbonate removal. Analyses were carried out with a Carlo Erba NA-1500 CN analyser.

Stable isotope ($\partial^{13}C$) analyses were performed on a Finnigan Mat Delta E mass spectrometer connected to the Carlo Erba NA-1500 CN analyser through a Trapping Box system for automatic cryopurification of the trapped carbon dioxide generated during the combustion step and for injection into the mass spectrometer. Results are referred to PDB limestone standards and to atmospheric nitrogen, respectively.

TSM for the determination of metal concentrations was sampled on polycarbonate filters (Nuclepore, porosity 0.40 µm), dried at 60 °C for approximately half an hour and stored dry in Petri slides till analysis in the home lab. Sample filters were destructed and dissolved either by a fusion technique or by strong acid attack. Ba, Ca, Sr, Si and Al concentrations were determined by ICP-OES (Jobin-Yvon JY 48 & 38).

3. RESULTS AND DISCUSSION

3.1. Spatial and seasonal variability of nutrient distribution and nitrogen uptake

3.1.1. Nutrient distribution patterns — The surface layer of the Southern Ocean is characterised by a ubiquitous abundance of macronutrients, complete exhaustion of nutrient availability being seldom observed. We found variations from 6.6 to 31.8 μM, 0.66 to 2.17 μM and 3.5 to 82.3 μM for surface nitrate, phosphate and silicate, respectively. Corresponding depth-weighted average concentrations for the upper mixed layer are slightly less variable; they range from 22.6 to 31.7 μM, 1.49 to 2.21 μM and 24.8 to 83.2 μM. Summarised descriptive statistics of the nutrient concentrations are given in Table 1. Lowest values correspond to well-sheltered ecosystems in the vicinity of the Antarctic continent (MARINE SCIENCE VOYAGE 6, Prydz Bay area), whereas highest values were observed during an early spring transect through the Weddell Sea (ANTARKTIS IX/2). The minimal silicate concentration was measured in waters north of the Polar Front during the ANTARES 2 cruise. Lowest ambient nutrient values, reflecting intensive nutrient uptake, mainly characterise MIZ and CCSZ ecosystems, where dense blooms occur. On the contrary, phytoplankton blooms do not usually develop in the OOZ and scarce plant life corresponds with low to negligible nutrient removal. Moreover, considerable interannual variability exists in the different Southern Ocean realms (Baumann *et al.*, 1995). Therefore, nutrient depletions are very variable; the minimal and maximal values can vary by as much 3 orders of magnitude (Table 1). They range from 0 to 1574 mmol m^{-2}, from 0 to 86 mmol m^{-2} and from 0 to 1737 mmol m^{-2} for nitrate, phosphate and silicate, respectively. Strikingly high nitrate depletion (NO_3De), which occurs mainly in relatively shallow and well-stabilised upper layers of the MIZ and CCSZ, stresses the importance of nitrate in shaping the bloom development of the latter environments. Its contribution to primary production as well as its seasonal variability in Southern Ocean MIZ ecosystems was thoroughly investigated in several earlier papers (Smith and Nelson, 1990; Cota *et al.*, 1992; Goeyens *et al.*, 1995). Ammonium availability (NH_4Av) shows considerable variability too. On average it represents 1.3% and 1.7% of the dissolved inorganic

nitrogen pool in the surface and upper layer, respectively. The values vary between 0.2 and 7.6% in surface water and between 0.2 and 7.3% in the upper mixed layer (Table 1).

Table 1: Variability in nutrient signature of Southern Ocean waters; surface concentrations (su) represent values for the shallowest sampling depth (< 10m); upper layer values (ul) are depth weighted averages for the upper water column down to the temperature minimum depth.

	Mean	Median	Minimum	Maximum
NO_3,su (µM)	25.3	26.7	6.6	31.8
NO_3,ul (µM)	28.0	28.1	22.6	31.7
NO_3De (mmol m^{-2})	233	145	0	1574
PO_4,su (µM)	1.68	1.81	0.66	2.17
PO_4,ul (µM)	1.89	1.90	1.49	2.21
PO_4De (mmol m^{-2})	16	11	0	86
Si,su (µM)	55.3	61.1	3.5	82.3
Si,ul (µM)	64.4	67.8	24.8	83.2
SiDe (mmol m^{-2})	406	242	0	1737
NH_4Av,su (%)	1.32	0.84	0.15	7.55
NH_4Av,ul (%)	1.71	0.97	0.15	7.32

Production and/or consumption of nutrients by marine organisms may occur in ratios which differ from the ratios of the ambient concentrations of those nutrients (Fanning, 1992). Fanning raised already the interesting idea to compare ratios of reaction rates to ratios of upward fluxes of nutrients into the photic layer. In order to unveil the complexity of the Southern Ocean's nutrient uptake regime we compared nitrate and silicate depletions with their availability in the temperature minimum

layer. The former parameters depict new production *sensu* Dugdale and Goering (1967) and diatom production, respectively. The nitrate to silicate ratios, available for phytoplankton nutrition at the onset of the growth season, are reflected by their values in the remnant winter water (temperature minimum layer). They show a relatively constant pattern, whereas the depletion ratios are considerably more variable (Table 2).

The mean winter nitrate over winter silicate ratio amounts to 0.46, ranging from 0.36 to 1.03. The mean depletion ratio, on the contrary, is 0.78, with a minimum of 0.11 and a maximum of 4.05.

On a plot of specific silicate depletion versus specific nitrate depletion (i.e. the depletions normalised to their corresponding winter concentrations) all data fall apart in two groups (Figure 1). The first one gathers all stations with normalised silicate depletions exceeding normalised nitrate depletions. Rearrangement of the equation shows that silicate to nitrate depletion ratios which exceed ratios of the winter concentrations correspond with ratios of ambient concentrations which are inferior to the ratios of the winter concentrations:

$$\frac{SiDe}{NO_3De} > \frac{Si,tm}{NO_3,tm} \Rightarrow \frac{Si,su}{NO_3,su} < \frac{Si,tm}{NO_3,tm} \qquad (5)$$

The significance of this dissimilarity is that silicate is removed from the water at a proportionally higher rate than nitrate. Such a process generates nitrate excess at silicate exhaustion when persisting over a sufficiently long period. In the second group, on the other hand, we find all stations with proportionally higher specific nitrate depletion, meaning that those waters carry a potential for silicate excess at nitrate exhaustion:

$$\frac{SiDe}{NO_3De} < \frac{Si,tm}{NO_3,tm} \Rightarrow \frac{Si,su}{NO_3,su} > \frac{Si,tm}{NO_3,tm} \qquad (6)$$

The distinction between these two groups agrees well with the earlier separation introduced by Kamykowski and Zentara (1985, 1989). It inspired us to develop the conceptual separation between two groups, which we denominated as nitrate excess area (NEA) and silicate excess area (SEA), respectively.

Table 2: Variability in nutrient concentration ratio for the temperature minimum (tm) and upper layers (ul) and in depletion ratio.

		Mean	Median	Minimum	Maximum
$\frac{NO_3,tm}{Si,tm}$	(mol mol^{-1})	0.46	0.42	0.36	1.03
$\frac{NO_3,ul}{Si,ul}$	(mol mol^{-1})	0.46	0.41	0.33	1.14
$\frac{NO_3De}{SiDe}$	(mol mol^{-1})	0.78	0.61	0.11	4.05

3.1.2. The corresponding nitrate and ammonium uptake rates — ρ-NO_3 values for SEA stations vary largely in contrast to the situation for NEA stations where values remain relatively constant (Table 3). The maximal value observed in the SEA amounts to 2.18 µM of NO_3 d^{-1}, which is approximately 3 orders of magnitude higher than the observed minimal value and also >1 order of magnitude higher than the maximal NEA value of 0.15 µM d^{-1}. Minimal values of both groups are very similar (~0.007 µM d^{-1}). Elevated absolute nitrate uptake rates indicate either high specific uptake rates or high biomass or both (Dugdale and Goering, 1967). Inspection of ν-NO_3 reveals highest values to occur in the SEA also (Table 3), with a maximum of 0.0625 h^{-1}, exceeding by 1 order of magnitude the observed maximum of the NEA (0.0046 h^{-1}). The ammonium uptake rates fluctuate less. The mean SEA value amounts to 0.07 µM d^{-1}, ranging from 0.003 to 0.18 µM d^{-1}. Those values are but slightly higher than the ones observed in the NEA: the mean ammonium uptake rate is 0.02 µM d^{-1}, the minimal and maximal uptake rates amount to 0.004 and 0.07 µM d^{-1}, respectively. Additionally, it is clear that biomass parameters such as PN and chlorophyll a concentrations reach highest values in the SEA (Table 3). Maximal PN and chlorophyll stocks of the SEA are 3.52 µM and 2.6 µg l^{-1}, whereas the maximal values observed in the NEA amount to 1.31 µM and 0.9 µg l^{-1}, respectively.

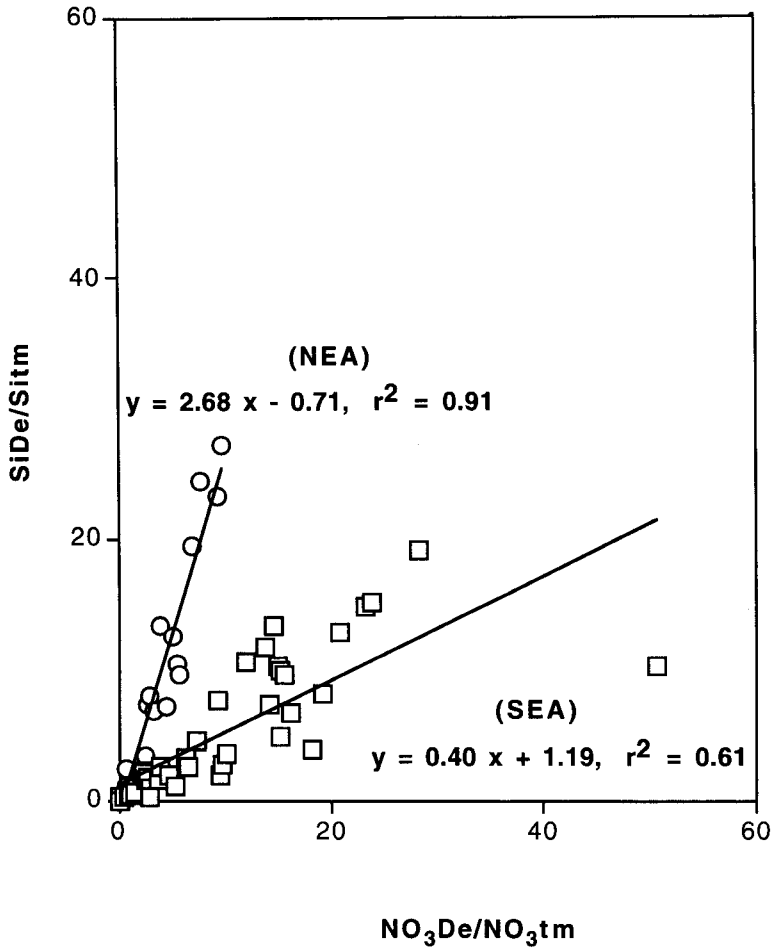

Figure 1: Specific silicate depletion *versus* specific nitrate depletion: the nitrate excess area (NEA) groups stations with a specific silicate depletion to specific nitrate depletion ratio > 1, while the silicate excess area (SEA) groups all stations with a specific silicate depletion to specific nitrate depletion ratio < 1.

Obviously, we face a twofold track in the course of Southern Ocean waters. On the one hand, a total lack of increased ecosystem's capacity to ingest nitrate into its structure depicts the NEA. All NEA stations being situated in the vicinity of the northernmost boundary of the winter ice extension, they fit well with the definition and functional characteristics of the OOZ (Tréguer and Jacques, 1992). Biomass build-up and primary production of typical OOZ ecosystems were found to be close

to those of oligotrophic waters. Especially the Indian Ocean sector, which was extensively sampled during the last decades, showed poor chlorophyll contents and low carbon assimilation rates (Jacques and Minas, 1983; Jacques, 1989). Observed biomass accumulations and primary production levels in the Scotia Sea were somewhat higher, as illustrated by the comprehensive comparison of literature data by Mathot *et al.* (1992).

Table 3: Variability in absolute uptake rate, specific uptake rate, PN concentration and chlorophyll *a* concentration in both the nitrate excess and silicate excess areas.

		Mean	Median	Minimum	Maximum
NEA	ρ-NO_3 ($\mu M\,d^{-1}$)	0.034	0.029	0.008	0.146
SEA	ρ-NO_3 ($\mu M\,d^{-1}$)	0.282	0.108	0.007	2.179
NEA	ρ-NH_4 ($\mu M\,d^{-1}$)	0.024	0.019	0.004	0.066
SEA	ρ-NH_4 ($\mu M\,d^{-1}$)	0.073	0.075	0.003	0.184
NEA	v-NO_3 (h^{-1})	0.0017	0.0016	0.0003	0.0046
SEA	v-NO_3 (h^{-1})	0.0057	0.0029	0.0002	0.0625
NEA	PN (μM)	0.75	0.78	0.14	1.31
SEA	PN (μM)	1.37	1.11	0.06	3.52
NEA	chlor a ($\mu g\,l^{-1}$)	0.21	0.19	<0.01	0.95
SEA	chlor a ($\mu g\,l^{-1}$)	0.60	0.29	0.02	2.58

On the other hand, the SEA clearly shows enhanced but short-lived capacity to remove nitrate. The latter environment, profiting by a physical trigger like upper layer stabilisation in combination with thermo-layer formation (Bauman *et al.*, 1995) and nutrient abundance (Table 1), exhibits a potential of dense phytoplankton development, generating considerable nitrate depletion but never or seldom complete exhaustion of the nitrate pool. The SEA groups typical MIZ and CCSZ stations. It is well-known that oceanographic processes within the ice edge regions

stimulate primary production: satellite observations (Sullivan *et al.*, 1988) provided clear evidence for a girdle of enhanced phytoplankton standing crops along the ice edges. Differences in primary production between the MIZ and OOZ can easily exceed two orders of magnitude (Smith and Nelson, 1986), although MIZ zones are not always productive (e.g. MIZ in Atlantic sector during ANTARKTIS X/6).

3.1.3. Seasonal variability of the nitrate uptake rates — Seasonal patterns of the nutrient status and productivity regime in the MIZ were given by Cota *et al.* (1992) and Goeyens *et al.* (1995). In an attempt to estimate the degree of seasonal progress, we introduce the seasonal maturity as a "subjective" parameter based on the observed NO_3De in the water and on the corresponding nitrate uptake rate. Assuming that the nitrate uptake rate remains constant with time, the ratio of NO_3De to ρ-NO_3 can provide an estimate of how long nitrate uptake lasted in that particular water mass. There is abundant evidence for decreasing nitrate uptake rates with seasonal progress, however, and estimates of the ongoing season's duration by NO_3De to ρ-NO_3 ratios are only realistic when the uptake rate remains constant or nearly constant. Referring to the observed seasonal evolution in typical MIZ ecosystems (Goeyens *et al.* 1995), we assume drastic increase of the nitrate uptake rate during early spring followed by progressive decline till the end of spring to correspond with maximal NO_3De occurring during late spring and minimal values during winter time (Figure 2).

With this statement in mind and the additional hypothesis that a similar scenario holds for the whole seasonally ice covered Southern Ocean we found that a stretched out S-shape curve fits best with the variation of NO_3De to ρ-NO_3 ratios. During the first 50 days, we observed a general agreement between NO_3De to ρ-NO_3 ratios and the actual season's duration. After ρ-NO_3 has reached its peak value, the discrepancy increases dramatically to become asymptotic from the moment on ρ-NO_3 has become minimal and NO_3De maximal. The asymptotic maximum occurs after approximately 117 days. In order to equate the relation between "erroneous" NO_3De to ρ-NO_3 ratios and "factual" durations of the growth season we utilised a sigmoid regression of the available data (Figure 2).

Here must be added a word of caution, however. Several factors, other than the nitrate uptake regime, determine the state of seasonal progress in the Southern Ocean (as well as in the World Ocean) and considering nitrate uptake as the only determining parameter, irrespective of other important physical biological and chemical effects, signifies anyhow a serious simplification. Therefore, we prefer to use the NO_3De to ρ-NO_3 ratios merely as an indicator of the seasonal state, which we have denoted as maturity on a scale of 0 to 100% ($\pm$ 117 days), rather than to relate the ratio to a duration expressed in days. Not its real value is important for the following discussion; the percentage of maturity was introduced as a useful tool describing seasonal progress in a qualitative way only.

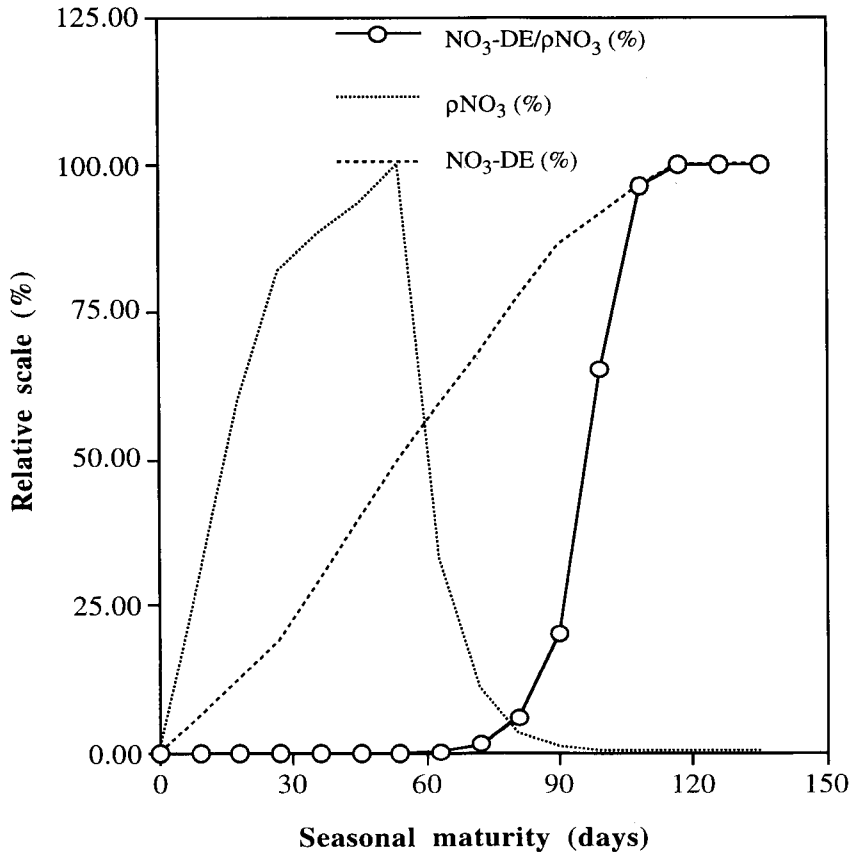

Figure 2: Seasonal maturity estimated from the ratios of nitrate depletion (NO_3De) to absolute nitrate uptake rate (ρ-NO_3).

Seasonal variability of ρ-NO_3, ν-NO_3 and PN concentration are shown in Figure 3. Both the absolute and specific uptake rates exhibit similar patterns with little seasonal variation in the NEA in contrast to enhanced variation in the SEA. The distinct pattern in the SEA is mainly evidenced by significantly increased values at the beginning of the productivity season, as observed also by others (Smith and Nelson, 1991; Cota *et al.*, 1992; Goeyens *et al.*, 1995). The PN values are somewhat scattered, on the contrary, with high values occurring during the earliest phase as well as at greater seasonal maturity.

A key parameter shaping the difference between NEA and SEA is the contrasting nitrate uptake regime of both ecosystems (Figure 3a). Observed low and seasonally constant absolute nitrate uptake rates in the NEA (mean value = 0.03 $\mu M\ d^{-1}$, Table 3) could never induce complete exhaustion of the available nitrate pool. At a constant uptake rate of 0.03 $\mu M\ d^{-1}$ and with complete absence of any refilling by physical processes as diffusion and advection or by biochemical processes as nitrification, complete removal of available nitrate would not happen before approximately 3 years. This 'unrealistic' view stresses how limited nitrate uptake in NEA waters is. On the other hand, the observed nitrate uptake rates in the SEA were remarkably higher at least during the start of the productive season but did not lead to exhaustion of the nitrate pool either. The maximal absolute uptake rate (2.2 $\mu M\ d^{-1}$, Table 3) could easily reduce the ambient nitrate stock to undetectable levels within a period of less than 1 month, but this scenario did not occur. Long before complete exhaustion of available nitrate uptake rates had decreased to low values, comparable to the ones of the NEA. The similarity of the minimal nitrate uptake rates in both systems strengthens the importance of highly increased nitrate uptake rates, observed during the early growth phase, for the configuration of silicate excess at nitrate depletion. The absence of such a vernal increase in the nitrate uptake capacity of NEA ecosystems, on the contrary, induces a potential for nitrate excess at silicate depletion. The separation between both groups is paralleled by the variability in specific nitrate uptake rate (Table 3, Figure 3b). Dugdale and Wilkerson (1991) recognised low specific nitrate uptake rates as a common feature of HNLC provinces such as the equatorial Pacific, the sub-arctic Pacific and most notably the Southern Ocean. The "traditional" values of specific nitrogen uptake

rates (Dugdale and Goering, 1967) are essentially normalised to the PN trapped on glass fibre filters, which can include non-phytoplanktonic and detrital PN.

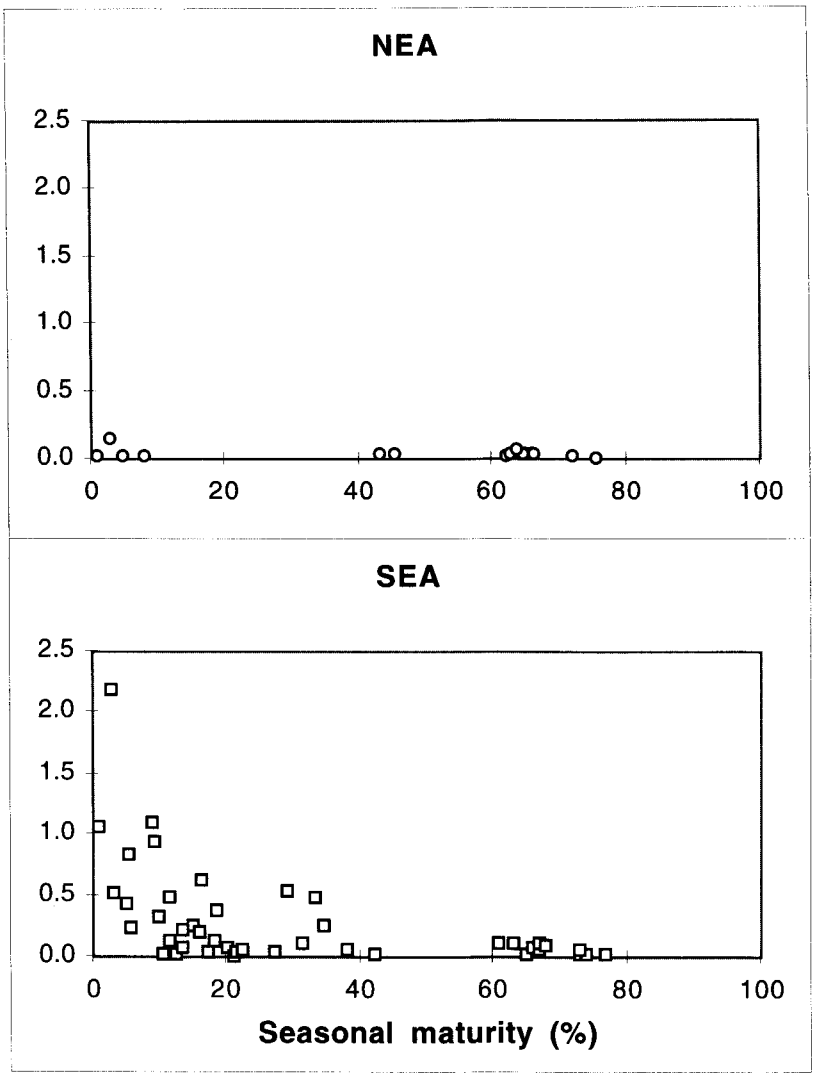

Figure 3a: Absolute nitrate uptake rate (ρ-NO_3, $\mu M\ d^{-1}$) *vs* seasonal maturity (%) plot.

On many occasions, phytoplankton made up a minor fraction of the planktonic biomass only and when this occurred PN-specific uptake rates underestimated true phytoplankton-specific nutrient uptake. A main question for this investigation

remains therefore: is there a significant difference between the highest and lowest observed values? In an attempt to remove influences of non-phytoplanktonic nitrogen we compared PN-specific uptake rates with chlorophyll-specific uptake rates and with uptake rates normalised to phytoplankton particulate nitrogen (PPN). Chlorophyll-specific uptake rates are the quotients of absolute uptake rates and the corresponding chlorophyll concentration, units are μmol (μg d)$^{-1}$. PPN-specific uptake rates are the product of chlorophyll-specific uptake rates and chlorophyll to PPN ratios; units are d^{-1}.

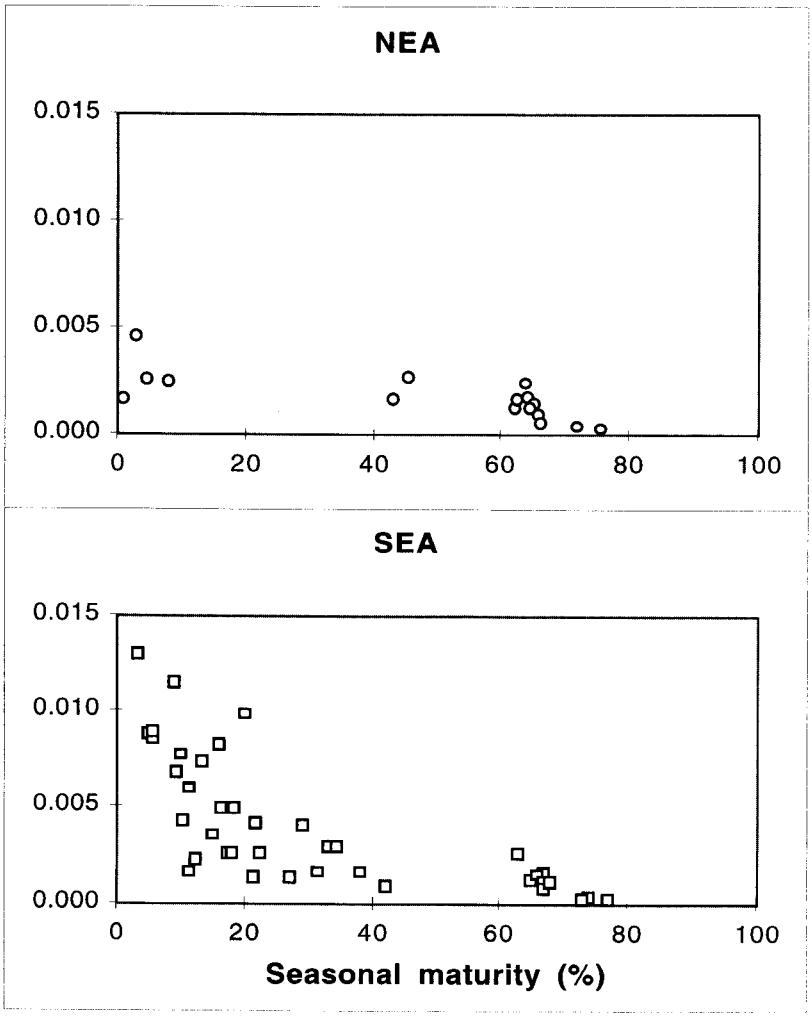

Figure 3b: Specific nitrate uptake rate (v-NO_3, d^{-1}) *vs* seasonal maturity (%) plot.

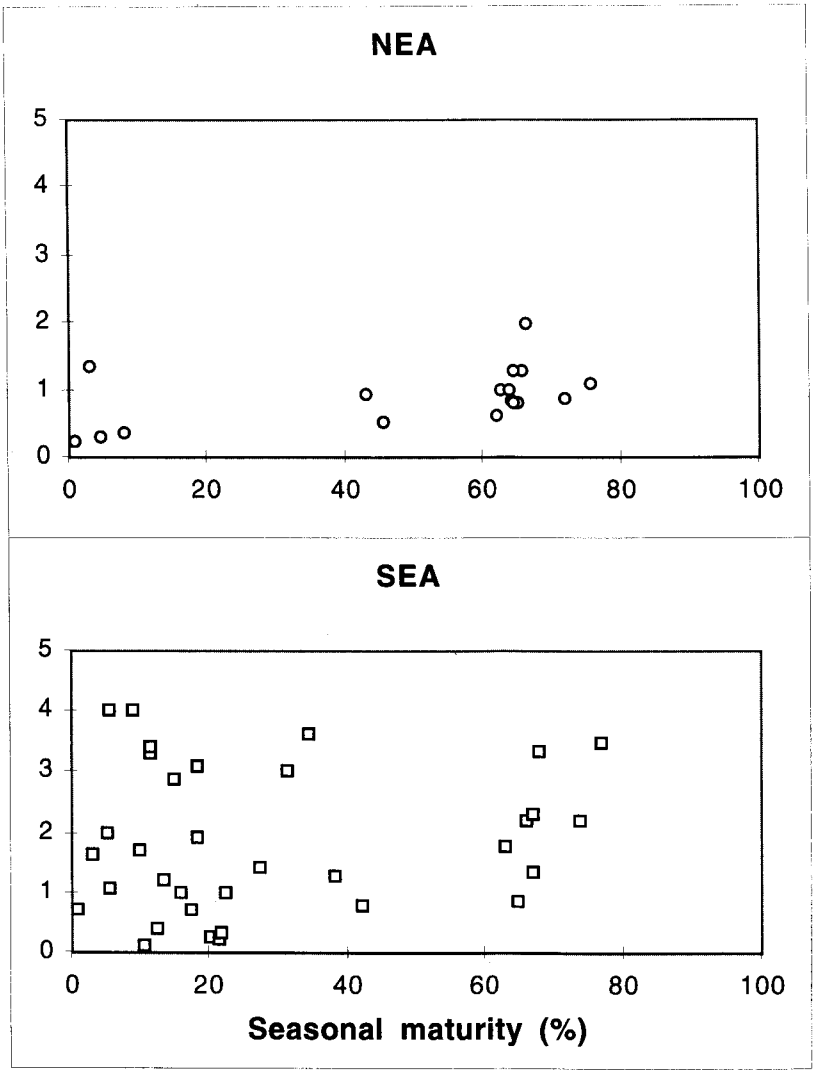

Figure 3c: Particulate nitrogen concentration (PN, µM) *vs* seasonal maturity (%) plot.

PPN values are estimates of the phytoplanktonic nitrogen biomass, obtained from cell counts and cell volume determinations, using a conversion factor of 6 for the POC to PN ratio (Semeneh, unpublished results). Both conversion techniques are somehow controversial. The POC to chlorophyll and inherently the PN to chlorophyll ratios are largely variable (Geider, 1987) and the chlorophyll

concentration per cell can be affected by variable irradiation as well as variable nutrition (Cullen and Lewis, 1988).

The different expressions of the specific nitrate uptake rate show a consistent pattern, however, with slightly less pronounced extremes for chlorophyll-specific uptake rates in the SEA though (Figure 4). Hence, we feel confident that the separation between highest and lowest uptake rates as observed in the SEA reflects significantly different situations. Moreover, a regression analysis of ρ-NO_3 *versus* ν-NO_3 and PN reveals that the variability in absolute uptake rate must be seen as a result of variable specific uptake rates rather than variable biomass. Notwithstanding predominant influence of the specific uptake rate, the results clearly show that biomass and possibly other parameters can not completely be disregarded for the variability in ρ (Table 4). This holds especially for the SEA data.

Table 4: Regression analyses of ρ-NO_3 *versus* ν-NO_3 and PN values; units are in $\mu M\ d^{-1}$, h^{-1} and μM, respectively.

		slope	intercept	R^2	p	F
NEA	ρ-NO_3 vs. ν-NO_3	24.95	-0.01	0.66	0.0001	25.52
NEA	ρ-NO_3 vs. PN	0.03	0.01	0.16	0.1129	2.84
SEA	ρ-NO_3 vs. ν-NO_3	79.02	-0.06	0.56	0.0001	47.49
SEA	ρ-NO_3 vs. PN	0.09	0.04	0.21	0.0028	10.21

3.1.4. The nitrogen uptake regime — Variable nitrate uptake rates (Figure 3) in combination with relatively constant ammonium uptake rates (Table 3) lead to important differences in the nitrogen uptake regime of the investigated environments. A summary of the leading parameters is given in Table 5. The average *f-ratio* for the NEA amounts to 0.58 ± 0.13, the corresponding average RPI value is 43 ± 15 and the minimal value is 10. Similar average values are observed for the SEA ; they amount to 0.65 ± 0.21 and to 36 ± 32 for *f*-ratio and RPI, respectively. Both parameters indicate predominance of the nitrate contribution to

primary production with rather limited occurrence of *f*-ratios < 0.5 and high demand for ammonium (RPI > 1). Despite these similar average values, both areas display important nonuniformity which is mirrored by the distinct seasonal patterns.

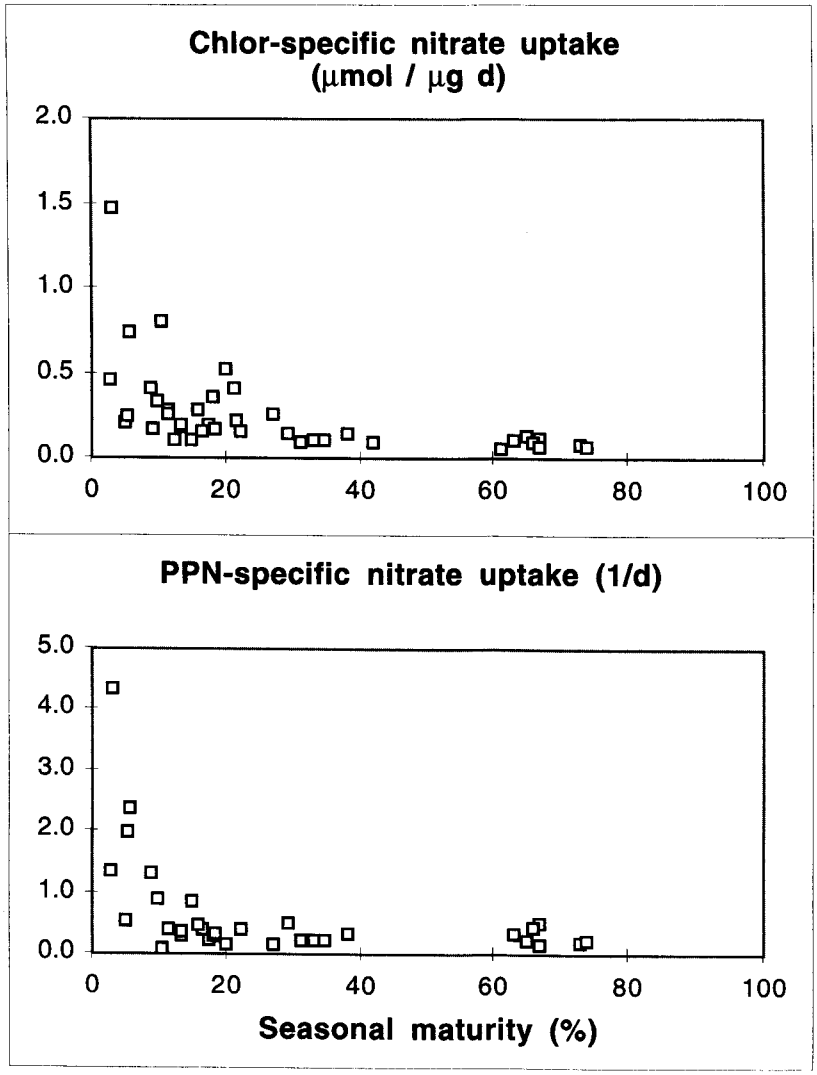

Figure 4: Chlor and PPN-specific nitrate uptake *versus* seasonal maturity (%) in the SEA area.

NEA data exhibit a constant evolution, with absence of very high and very low *f*-ratios and consistent preference for ammonium. On the other hand, the SEA data

evidence a marked decrease in *f*-ratio at greater seasonal maturity (Figure 5) and elevated RPI values in agreement with declining *f*-ratios (Figure 6).

Table 5: Variability in nitrogen uptake regime of both NEA and SEA areas.

		Mean	Median	Minimum	Maximum
NEA	*f*-ratio	0.58	0.60	0.39	0.86
SEA	*f*-ratio	0.65	0.64	0.25	0.98
NEA	RPI	43	43	10	75
SEA	RPI	36	22	2	139

The transience of the latter system confirms the earlier described variability in nitrate uptake. Both the *f*-ratio and RPI are unbiased by possible contamination with non-phytoplanktonic PN, since the latter factor is cancelled out in the formulas. Decreasing *f*-ratios primarily reflect the decrease in nitrate uptake at relatively constant ammonium uptake (Figure 7). Winter plankton in the Antarctic Ocean consist of dilute regenerating communities (Garrison *et al.*, 1993), with phytoplankton meeting their nitrogen requirements mainly by uptake of ammonium (mean *f*-ratio = 0.4, Cota *et al.*, 1992). Diatoms represent a significant, though not predominant, fraction of the autotrophs. Such communities are likely the rule in the Antarctic pelagic and superimposed blooms, utilising elevated amounts of nitrate, occur at the event scale (Smetacek *et al.*, 1990). The NEA configuration matches fairly well with these regenerating characteristics. Maximal biomass accumulations (PN stocks) and corresponding nitrate uptake rates do not exceed 1 $\mu g\ l^{-1}$ and 0.15 $\mu M\ d^{-1}$, respectively. The nitrogen uptake regime proves remarkably constant, with *f*-ratios indicating that both nutrients are removed at similarly low uptake rates throughout (Figure 5). Moreover, ammonium is consistently the preferred nutrient, not one RPI value < 1 being observed. Considering the RPI values as an expression of the ecosystem's demand for ammonium despite the abundance of nitrate, one observes limited variation of the seasonal pattern only. Any trigger for enhanced nitrate uptake (higher *f*-ratios and/or lower RPI values) and subsequent phytoplankton build-up remains conspicuously absent in this particular

environment. Seasonal as well as interannual variation in the NEA will, therefore, be much less than in the case of emerging blooms (Baumann *et al.*, 1995).

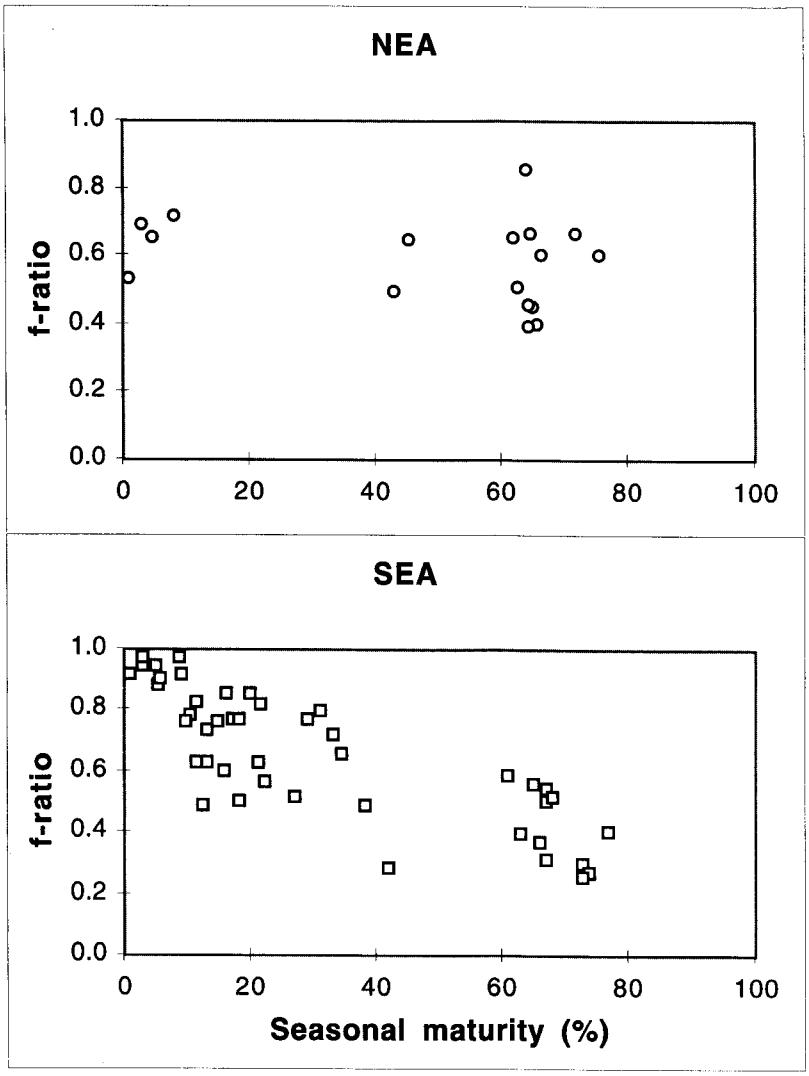

Figure 5: Comparison of the seasonal variability in *f*-ratio for both the NEA and SEA areas.

On the other hand, when spring conditions rouse phytoplankton of the SEA to an intensive awaking of life, both a biomass build-up (Figure 3c) and a parallel increase in PN-specific nitrate uptake rate are observed (Figure 3b). The rise in

nitrate uptake after winter time is consistent with the observations of Garside (1991) and Dickson and Wheeler (1995) for an upwelling area off the coast of Oregon. Enhanced PN-specific nitrate uptake rates reflect concurrent variations in phytoplanktonic biomass and more specifically in the PPN concentration relative to the total PN concentration.

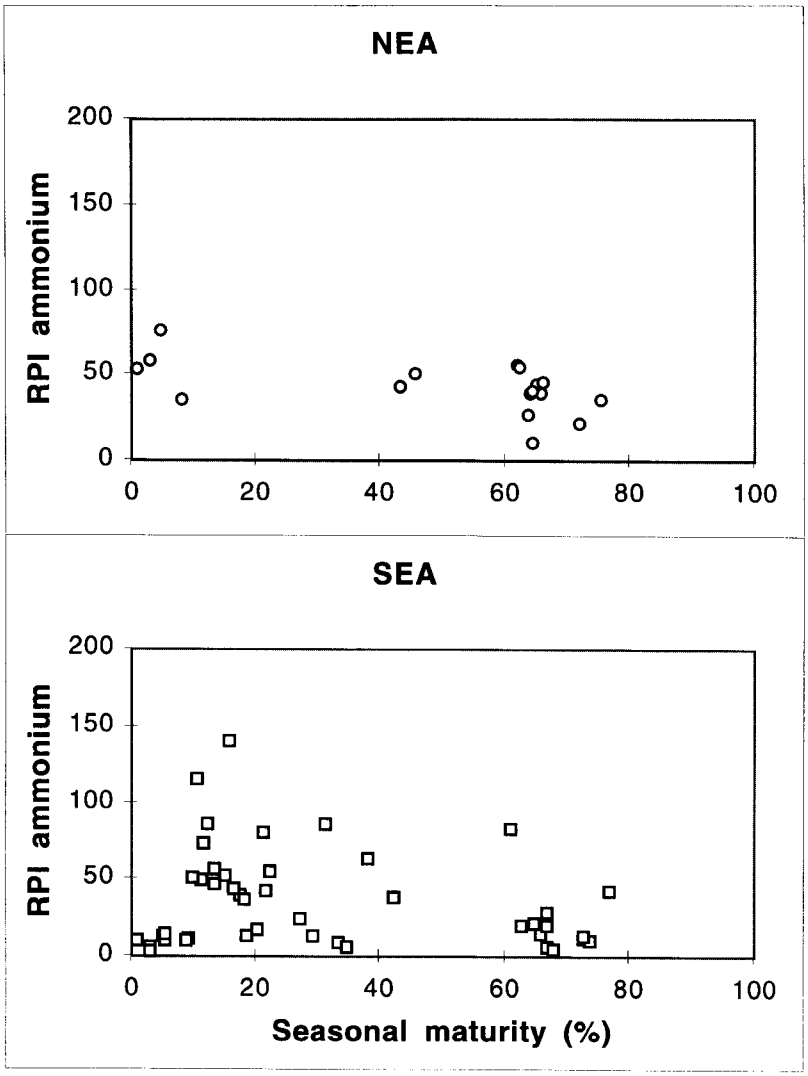

Figure 6: Comparison of the seasonal variability in relative preference index (RPI) for both the NEA and SEA areas.

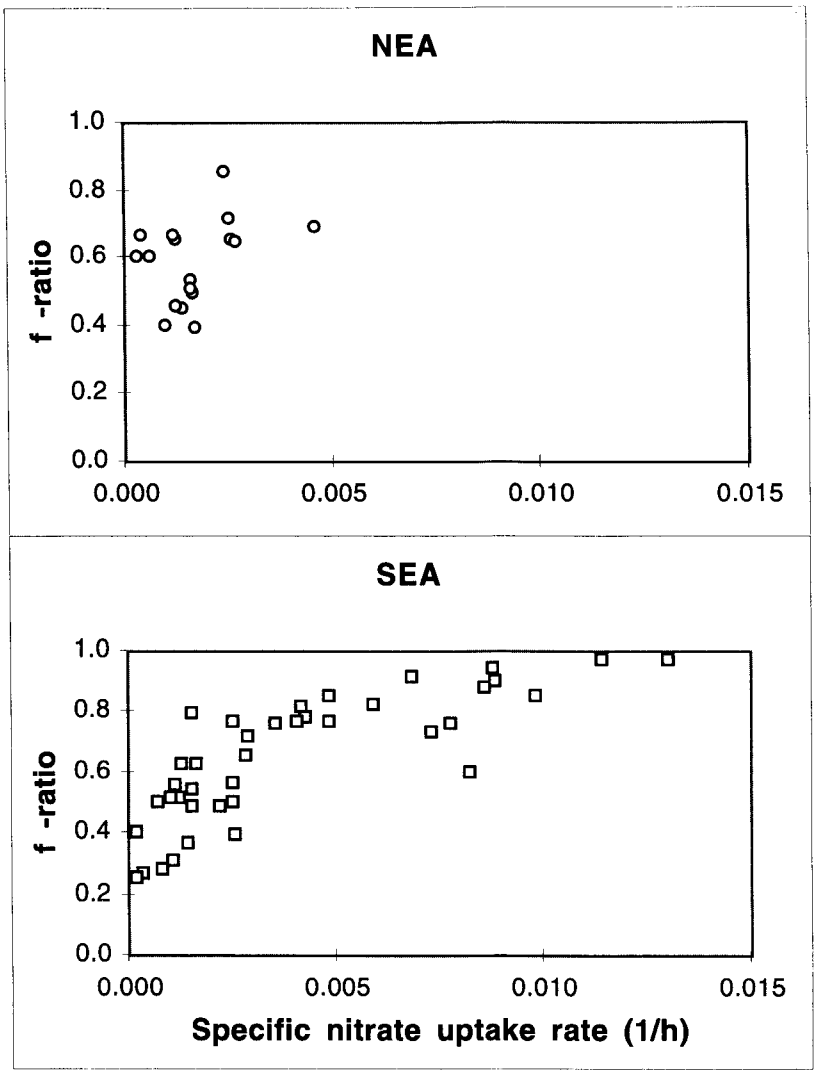

Figure 7: Relation between *f*-ratio and ν-NO_3 for both NEA and SEA areas.

PN to PPN ratios are significantly higher during the earliest phase of the growth season with maximal ratios being nearly 10. It can not be dismissed, however, that nitrogen uptake rates are also related to the distribution of nitrogenous nutrients, invoking physiological regulation of the phytoplankton (Dugdale and Wilkerson, 1991). During the EPOS LEG 2 cruise significant decreases in PN-specific nitrate uptake were not accompanied by any substantial increase of non-phytoplanktonic nitrogen (Goeyens *et al.*, 1995).

3.1.5. Effect of ammonium on the nitrate uptake rate and *f*-ratio — It is a basic tenet of nitrogen utilisation by phytoplankton that ammonium inhibits the uptake of nitrate and the severity of the inhibitory effect is usually judged from differences between values at ammonium concentrations below and superior to 1 µM (Dortch 1990). Models on external interactions between different nitrogen sources made preferentially use of the relative concentrations of each nutrient (Harrison *et al.*, 1987; Collos, 1989). Hence, we used the NH_4Av as a key parameter for the description of the regulating effect of ammonium in the ecosystem under study. Two aspects of the seasonal evolution in the SEA deserved our particular attention. The $v\text{-}NO_3$ *versus* NH_4Av plot (Figure 8) shows that increased values of NH_4Av bear upon decreased specific uptake rates, with values ≤ 0.002 h^{-1} occurring mainly at $NH_4Av > 2\%$. There is some scatter at low values of NH_4Av, however, and a closer look at the plotted values confirms that a slight increase might occur at the low end side of NH_4Av values (Figure 8).

Earlier investigations in the Scotia and Weddell Seas provided evidence for a potential of enhanced nitrate uptake at low ammonium (Glibert *et al.*, 1982), a phenomenon that was later confirmed by Dortch *et al.* (1991). Since winter water is generally devoid of high ambient ammonium (Nöthig *et al.*, 1991) and melting of pack ice contributes little to the accumulation of ammonium in the photic zone (Biggs, 1978), Antarctic waters generally display poor ammonium availability during early spring. Minor injections of ammonium through heterotrophic activity in the water column or in remote pack ice might have a stimulatory effect on the nitrate uptake rate. Unfortunately, studies of the stimulatory effect of ammonium were not planned during our field work and firm proof of such a scenario is not available. Moreover, any accumulation of ammonium in the water results from mineralisation of organic substances in excess to autotrophic ammonium removal. The organic substances such as chelates, complexes, colloids and aggregates, carry other vital elements and compounds resulting from numerous metabolic and physicochemical reactions. Their production and possible accumulation during the mineralisation process in the surface layer might as well stimulate the nitrate uptake process. Earlier experiments provided evidence for increased algal development by release of triggering substances from melting winter ice in the Weddell Sea (Baumann *et al.*, 1995). On the other hand, the hyperbolic decreasing trend of $v\text{-}NO_3$ *versus*

NH_4Av strongly suggests inhibition of nitrate uptake by increased ammonium availability, as modelled already by Zevenboom (1981) and Collos (1987). However, in this plot differences in phytoplankton species and interannual variations obscure somehow the effect of ammonium on the nitrate uptake.

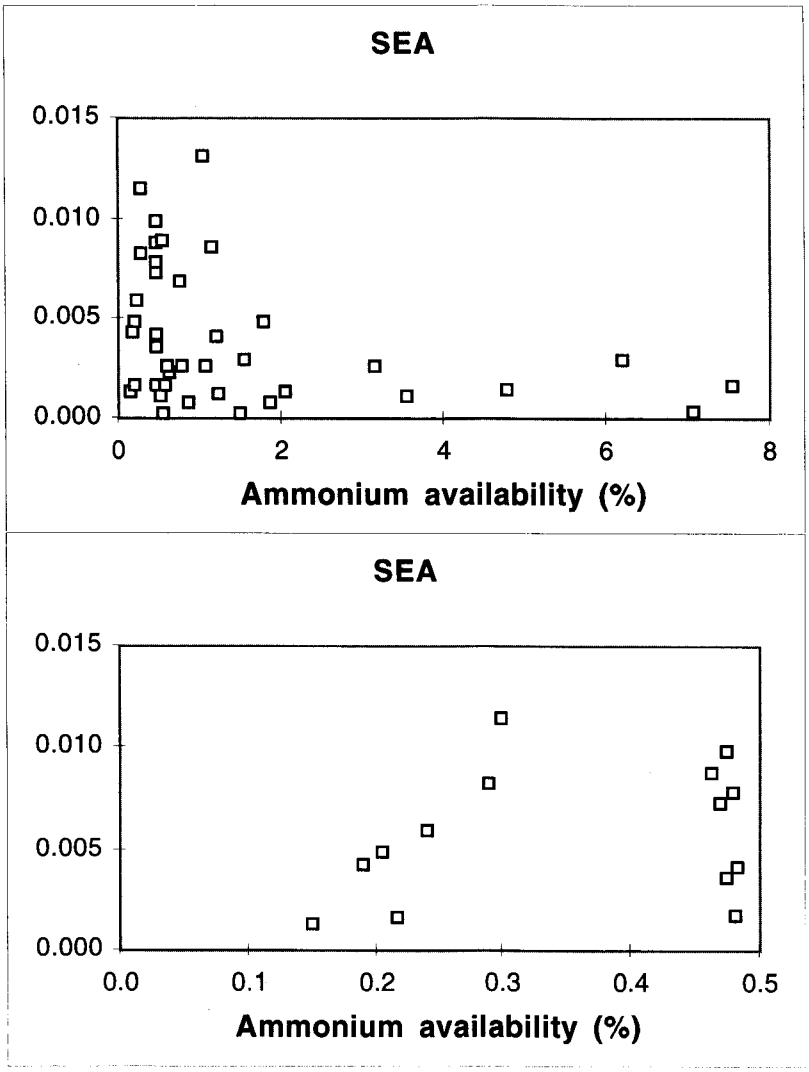

Figure 8: Relation between $\nu\text{-}NO_3$ (h^{-1}) and NH_4Av (%) for the SEA area.

Figure 9 shows an example of the susceptibility of nitrate uptake on ammonium as observed during the ANTARES 3 cruise (27 September to 8 November 1995,

preliminary results). Increased NH_4Av leads to decreased values of the nitrate uptake rates and these observations confirm a recent study that low levels of ammonium < 1 μM are capable of significant inhibition of the nitrate uptake rate (Harrison *et al.*, 1996). For Antarctic waters characterised by superfluous stocks of nitrate (and other macro-nutrients), we suspect that the elevated availability of nitrate does not suppress the inhibition by ammonium and that therefore non-competitive inhibition is more likely.

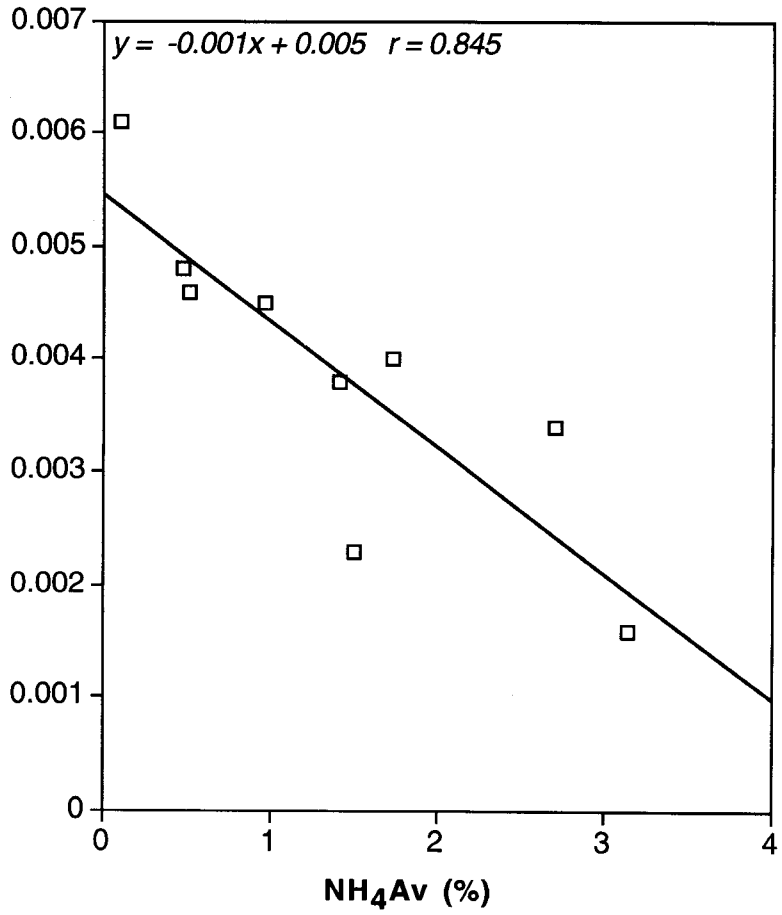

Figure 9: Effect of increasing NH_4Av (%) on $v\text{-}NO_3$ (h^{-1}) for ANTARES 3. Ammonium concentrations ranged from 0.3 to 1 μM.

Interactions between ammonium and nitrate uptake can also be illustrated by the *f*-ratio (the nitrate uptake to total nitrogen uptake ratio). The average *f*-ratios amount to 0.73, 0.59 and 0.42 for $NH_4Av < 1.54$, for $1.54 \leq NH_4Av \leq 1.97$ and for $NH_4Av > 1.94$, respectively. The latter values of NH_4Av were found to enclose the range of transition from predominant nitrate uptake (*f-ratio* > 0.5) to predominant ammonium uptake (*f*-ratio < 0.5) in typical MIZ systems of the Weddell Sea (Goeyens *et al.*, 1995). The average *f*-ratios measured in SEA surface waters confirm that these systems pivoted at about the same NH_4Av.

Both the good agreement with earlier data and the significant seasonal decrease in *f*-ratio (Figure 5) underpin that ammonium acts as a regulator of the nitrogen uptake regime in SEA waters. However, decreases in *f*-ratio were not inherently linked to a shift from diatom to non-diatom predominance. In a typical SEA of the Weddell Sea we observed the substitution of a large diatom bloom by a nearly pure cryptophycean bloom which was accompanied by a drastic decrease in *f*-ratio. On the contrary, the on shelf zone of Prydz Bay displayed a largely regeneration based community (mean *f*-ratio = 0.3), consisting mainly of diatoms (Kopczynska *et al.*, 1995).

3.2. Phytoplankton assemblage composition and nitrogen uptake

3.2.1. Phytoplankton biomass, community structure and nitrogen uptake rates — During the ANTARKTIS IX/2 cruise, the Weddell Sea was characterised by near freezing surface temperatures (~ -1.73 °C), high salinity (~ 34.36 psu) and high nutrient concentrations, indicating the early stage of the growth season (Table 6). Phytoplankton biomass was very low (Chl. *a* ~ 0.1 µg l^{-1}; Tables 6 and 7) and the assemblage was dominated by *non-Phaeocystis* flagellates (Table 7). The autotrophic community structure was characterised by dominance of small cells; about 66 % of the total biomass was due to the < 20 µm size fraction.

During the ANTARKTIS X/7 cruise the Weddell Sea was marked by large spatial and temporal variability in physico-chemical and biological parameters (Table 6). Analysis of the physico-chemical and biological data by principal component analysis (PCA) revealed three clusters of stations, each representing different stages of the growth season. These include: the central Weddell Sea, eastern Weddell Sea and Larsen Shelf region (Tables 6 and 7). In the central Weddell Sea nutrient concentrations were relatively high, phytoplankton biomass was low (Chl. *a* ~ 0.4 µg l^{-1}) and the assemblage was dominated by flagellates. Size-fractionation indicated that about 61% of the phytoplankton biomass was due to the < 10 µm size fraction (Table 7). The second group, eastern Weddell Sea, was located in the extreme eastern part of the transect. These are shallow stations, characterised by relatively low surface temperature (~ -1.36 °C), high salinity (~ 34.23 psu) and decreased levels of nutrients (Table 6). Very sharp and shallow pycnocline (~ 10-30 m) indicated stable water column. Phytoplankton bloom was apparent with surface Chl. *a* concentrations in some stations reaching up to 6 µg l^{-1}. Diatoms (~ 43%) and *Phaeocystis sp* (~ 27%) dominated the phytoplankton assemblage and micro-sized phytoplankton (> 10 µm) represented ~ 59% of the total biomass (Table 7). The third group, Larsen Shelf, represents stations along a short transect in the Larsen Shelf, located on the western side of the Weddell Sea. Like the eastern Weddell Sea, the Larsen Shelf transect covers relatively shallow waters, showing pronounced ice melting and maintaining a shallow upper mixed layer (~ 20-50 m; Table 6).

Table 6: Summaries (mean and standard deviation) of physico-chemical and biological characteristics of the surface water in Atlantic and Indian sectors of the Southern Ocean. ND = no data, *SWC* = Scotia-Weddell Confluence (*SWC A* = early season and *SWC B* = late season), *CCSZ* = Coastal and Continental Shelf Zone, *OOZ* = Open Oceanic Zone. The sampling periods were: ANTARKTIS IX/2 (14 November to 30 December 1990), ANTARKTIS X/7 (3 December 1992 to 22 January 1993), EPOS LEG 2 (20 November 1988 to 7 January 1989) and MARINE SCIENCE VOYAGE 6 (3 January to 20 march 1991).

	Temp. °C	Salinity psu	NH_4 Avail. %	NO_3 µM	PO_4 µM	$Si(OH)_4$ µM	POC µg l^{-1}	Chl a µg l^{-1}
Weddell Sea (ANT IX/2)	-1.73 ± 0.12	34.36 ± 0.03	0.5 ± 0.3	29.4 ± 1.1	2.0 ± 0.1	72.4 ± 7.3	36.8 ± 17.8	0.1 ± 0.1
Central Weddell Sea (ANT X/7)	-1.26 ± 0.42	33.95 ± 0.22	1.0 ± 0.6	27.6 ± 1.4	1.9 ± 0.1	71.7 ± 2.6	117.6 ± 68.9	0.4 ± 0.5
Eastern Weddell Sea (ANT X/7)	-1.36 ± 0.44	34.23 ± 0.02	0.8 ± 0.3	24.5 ± 3.2	1.7 ± 0.2	58.3 ± 1.0	349.9 ± 148.5	3.7 ± 1.5
Larsen Shelf (ANT X/7)	-0.67 ± 0.61	33.75 ± 0.16	0.8 ± 0.7	15.9 ± 3.6	1.1 ± 0.2	60.6 ± 12.9	473.9 ± 105.2	3.8 ± 0.8
Scotia-Weddell, SWC A (EPOS)	-1.41 ± 0.27	33.84 ± 0.27	0.7 ± 0.5	27.9 ± 2.9	1.7 ± 0.2	72.5 ± 6.0	121.0 ± 68.5	1.2 ± 0.8
Scotia-Weddell, SWC B (EPOS)	-0.29 ± 0.68	33.59 ± 0.17	4.7 ± 2.4	22.3 ± 3.4	1.4 ± 0.3	62.5 ± 10.2	157.4 ± 53.0	1.0 ± 0.8
Prydz Bay CCSZ (MSV 6)	-0.15 ± 0.47	33.49 ± 0.51	0.9 ± 0.5	12.9 ± 4.5	0.9 ± 0.3	31.7 ± 11.6	412.1 ± 182.1	ND
Prydz Bay OOZ (MSV 6)	0.98 ± 1.12	33.81 ± 0.09	1.0 ± 0.8	26.8 ± 0.9	1.8 ± 0.1	42.2 ± 7.4	84.3 ± 30.6	ND

Table 7: Total phytoplankton biomass (PPC), size-fractionated biomass (<10 µm and >10 µm equivalent spherical diameter) and the contribution of different taxonomic groups in different parts of the Southern Ocean. Also indicated are the relative contributions of each taxonomic group and size-fraction. ND = no data. * = data from Kopzynska *et al.* (1995) and ‡ = data from Becquevort *et al.* (1992).

	Biomass (µgC l^{-1})								% Contribution				
	PPC	PPC <10 µm	PPC >10 µm	Pennate Diatom	Centric Diatom	Diatoms	Dino-flagellate	Flage-llate	Diatoms	Dino-flagellate	Flage-llate	PPC <10 µm	PPC >10 µm
Weddell Sea (ANT IX/2)	19.3 ± 10.2	6.7 ± 2.1	12.6 ± 8.9	2.9 ± 2.7	1.9 ± 1.9	4.8 ± 4.4	6.2 ± 5.2	8.3 ± 3.0	22.5 ± 10.4	28.7 ± 16.6	48.8 ± 19.2	40.6 ± 15.3	59.4 ± 15.3
Central Weddell Sea (ANT X/7)	15.7 ± 10.5	8.9 ± 6.1	7.0 ± 5.6	3.6 ± 3.5	1.9 ± 1.7	5.5 ± 4.9	6.3 ± 5.6	4.0 ± 9.8	33.0 ± 12.2	35.9 ± 19.0	31.5 ± 19.2	59.1 ± 18.1	40.9 ± 17.8
Eastern Weddell Sea (ANT X/7)	53.0 ± 43.9	21.2 ± 16.8	31.7 ± 27.8	8.3 ± 4.3	11.0 ± 9.0	19.4 ± 12.7	13.9 ± 15.0	19.7 ± 19.1	43.2 ± 22.0	22.1 ± 12.6	34.7 ± 12.6	40.9 ± 10.6	59.1 ± 10.6
Larsen Shelf (ANT X/7)	95.0 ± 50.0	38.2 ± 23.6	56.5 ± 54.2	24.3 ± 14.3	15.1 ± 20.8	39.5 ± 28.8	29.0 ± 27.9	26.5 ± 14.5	39.6 ± 15.5	30.1 ± 12.0	30.3 ± 15.1	45.8 ± 22.9	54.2 ± 22.9
Scotia-Weddell‡ SWC A (EPOS)	31.4 ± 26.1	ND	ND	ND	ND	18.4 ± 24.0	1.8 ± 0.7	11.2 ± 7.4	48.7 ± 22.2	6.0 ± 2.3	45.3 ± 22.7	ND	ND
Scotia-Weddell‡ SWC B (EPOS)	26.9± 27.6	ND	ND	ND	ND	1.8 ± 2.25	0.5 ±0.43	24.9 ±28.74	19.7 ± 31.2	3.0 ± 5.2	77.3 ± 31.6	ND	ND
Prydz Bay * CCSZ (MSV 6)	110.4 ± 37.0	25.9 ± 17.2	84.5 ± 21.0	64.0 ± 32.1	26.9 ± 5.3	90.9 ± 28.4	6.7 ± 5.1	12.8 ± 17.2	83.6 ± 13.2	6.4 ± 4.3	10.0 ± 10.4	21.7 ± 7.3	78.3 ±7.29
Prydz Bay* OOZ (MSV 6)	87.9 ± 51.8	7.9 ± 8.0	80.0 ± 50.0	28.0 ± 43.6	48.5 ± 54.1	76.5 ± 51.0	6.9 ± 12.7	4.4 ± 6.8	85.6 ± 14.9	10.3 ± 14.3	4.1 ± 5.2	12.2 ± 10.8	87.8 ±10.84

High nutrient depletion, dense phytoplankton development (Chl. *a* ~ 3.8 μg l^{-1}), as well as subsurface ammonium build up (2 to 3 μM) characterised this area. Diatoms (~ 41%) and *Phaeocystis sp* (~ 23%) dominated the assemblage and about 54% of the biomass was due to the > 10 μm fraction (Tables 6 and 7). In terms of species composition, the central Weddell Sea was characterised by abundance of small diatoms (< 10 μm) and autotrophic flagellates. Cryptophytes and other unidentified flagellates formed the bulk of the biomass. *Phaeocystis sp* contributed only 8%. Pennate and centric diatoms contributed for ~ 19% and ~ 14% to the total biomass, respectively. Small pennates such as *Nitzschia cylindrus* and *Nitzschia prolongatoides* as well as centric diatoms of the genus *Coscinodiscus*, *Thalassiosira*, *Corethron*, *Asteromphalus* and *Actinocyclus* were abundant.

In the eastern Weddell Sea and Larsen Shelf the phytoplankton assemblage was dominated by diatoms and *Phaeocystis sp*. Unlike the central Weddell Sea, *Phaeocystis sp* in these regions was very dominant, representing ~ 26.5% and 23% of the total biomass in the eastern Weddell Sea and the Larsen Shelf, respectively (Table 7). Although diatoms dominated the assemblage both in the eastern Weddell Sea and Larsen Shelf, the composition of species was different. In the eastern Weddell Sea centric diatoms were predominant, representing about 56% of the diatom biomass and about 25% of the total biomass (Table 7). Important centric genera included: *Thalassiosira*, *Coscinodiscus*, and *Corethron* (*C. criophilum*). The genus *Thalassiosira* alone represented about 15% of the total biomass. Although centric diatoms were dominant, the relative contribution of one pennate diatom, *Nitzschia prolongatoides*, was significant (~ 9%). On the contrary, in the Larsen Shelf pennate diatoms were the predominant species with a relative contribution of 77% to the diatom biomass and 32% to the total biomass (Table 7). The main pennate diatoms in this region included species such as *Nitzschia cylindrus, Thalassiothrix sp*, *Fragilariopsis sp* and chains of *Nitzschia prolongatoides* and *Nitzschia lineola.*

Fast dividing cells exhibited high $v\text{–}NO_3$. In the Weddell Sea high $v\text{–}NO_3$ was associated with bloom conditions (eastern Weddell Sea and Larsen Shelf; Table 8). On the contrary, $v\text{–}NH_4$ values were rather similar both during bloom and non-bloom

conditions. ρ–NO_3 values in bloom stations (Eastern Weddell Sea and Larsen Shelf) were one order of magnitude higher than in non-bloom stations (ANTARKTIS IX/2 and central Weddell Sea; Table 8).

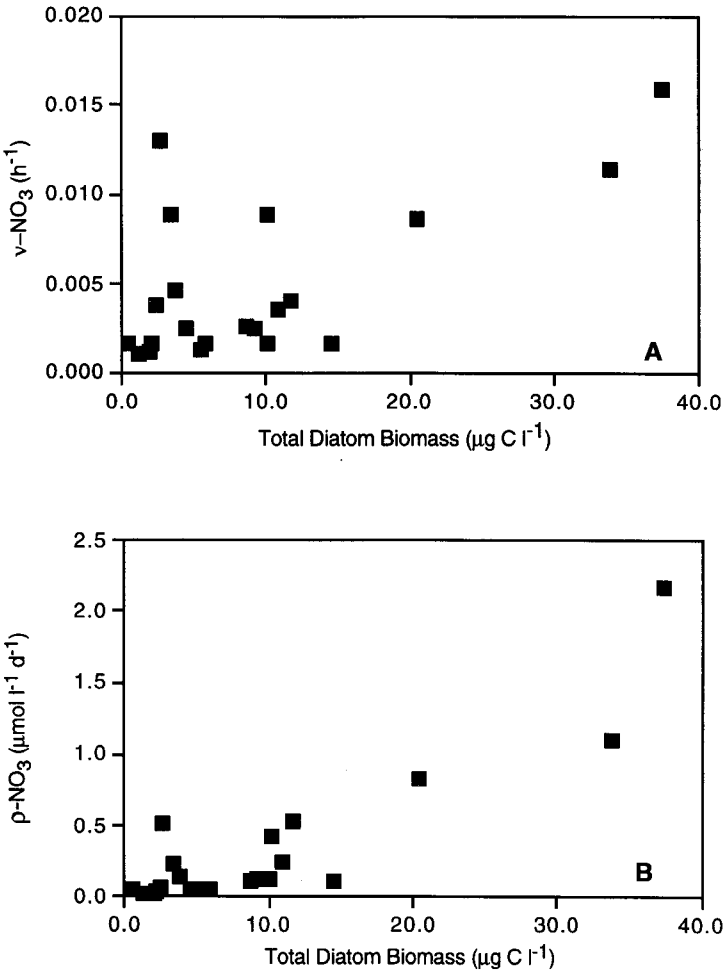

Figure 10: Scatter diagrams showing the relationship of total diatom biomass with (A) specific (v–NO_3) and (B) absolute (ρ–NO_3) nitrate uptake rate during ANTARKTIS X/7 cruise in the Weddell Sea.

Table 8: Specific (vN) and absolute (ρN) nitrogen uptake rates as well as *f*-ratios in the surface waters of the Southern Ocean.

	No. of samples (n)	Specific uptake rate ($x10^{-3}$ h^{-1}) vNO3	vNH4	ΣvN	Absolute uptake rate (nmol $l^{-1}d^{-1}$) ρNO3	ρNH4	ΣρN	*f*-ratio
Weddell Sea (ANT IX/2)	9	3.5 ± 2.6	1.3 ± 0.5	4.8 ± 2.8	22.8 ± 16.9	9.1 ± 5.6	31.9 ± 19.3	0.69 ± 0.12
Central Weddell Sea (ANT X/7)	14	3.3 ± 3.5	1.3 ± 0.6	4.6 ± 3.3	109.0 ± 131.5	40.3 ± 29.4	149.3 ± 132.5	0.62 ± 0.19
Eastern Weddell Sea (ANT X/7)	5	8.7 ± 4.5	0.9 ± 0.3	9.6 ± 4.5	919.6 ± 757.8	84.7 ± 39.0	1004.3 ±784.8	0.89 ± 0.08
Larsen Shelf (ANT X/7)	4	5.8 ± 3.8	0.9 ± 0.4	6.7 ± 3.5	678.4 ± 286.1	119.6 ± 67.2	798.0 ± 222.4	0.83 ± 0.11
Scotia-Weddell, *SWC A* (EPOS)	6	5.4 ± 2.1	2.6 ± 1.6	8.0 ± 3.4	194.3 ± 155.1	78.4 ± 34.4	272.7 ± 180.7	0.66 ± 0.10
Scotia-Weddell, *SWC B* (EPOS)	5	2.7 ± 3.0	2.0 ± 0.7	4.7 ± 3.3	122.8 ± 127.8	98.8 ± 42.9	221.7 ± 151.2	0.44 ± 0.21
Prydz Bay, *CCSZ* (MSV 6)	4	0.5 ± 0.4	0.7 ± 0.3	1.2 ± 0.7	61.4 ± 37.1	85.8 ± 47.7	147.2 ± 71.9	0.42 ± 0.12
Prydz Bay, *OOZ* (MSV 6)	5	1.0 ± 0.9	0.4 ± 0.2	1.3 ± 1.0	27.6 ± 20.5	11.3 ± 7.1	38.9 ± 24.7	0.68 ± 0.11

Early in the season (ANTARKTIS IX/2) nitrate was the predominant nitrogen source (*f*-ratio > 0.5) for the flagellate dominated assemblage (Table 7 and 8). Although flagellates dominated the assemblage (Table 7), both diatom and flagellate biomass showed similar relationship with ρ–NO_3 (diatom PPC *versus* ρ–NO_3, $r^2 = 0.70$; flagellate PPC *versus* ρ–NO_3, $r^2 = 0.7$). Among diatoms the biomass of pennate diatoms correlated strongly with nitrate uptake rate ($r^2 = 0.76$). During ANTARKTIS X/7 as a whole only diatom biomass showed strong correlation with nitrate uptake rate (Figures 10 A and B). Despite large variability in biomass and assemblage during this cruise (Tables 6 and 7), the production regime was rather similar with overwhelming importance of new production (Table 8).

During the EPOS LEG 2 cruise, the MIZ of the Scotia-Weddell Confluence zone showed large inter-station variability, leading to the distinction between the early and mature stages of the growth season (Tables 6 and 8). The early stage (*Scotia-Weddell Confluence A, SWC A*) was characterised by a relatively low temperature (~-1.41 °C), relatively high nutrient concentration and moderate ammonium availability (~ 0.7%; Tables 6 and 7). On the other hand, in stations where the season had more progressed (*SWC B*) surface water was warmer (~ 0.29 °C), nutrient levels were lower and NH_4Av was higher (4.7%). Although phytoplankton biomass was similar during the early and later stages of the MIZ, the composition of the assemblage was different. Early in the season (*SWC A*) the assemblage was dominated by diatoms (~ 49%) and late season (*SWC B*) by flagellates (~ 77.3%, *non-Phaeocystis sp*). Blooms of cryptophytes were observed in some stations. Much of the biomass during the early stage was due to micro-sized phytoplankton (> 20 µm size fraction) but as the season progressed the dominance shifted to the nanophytoplankton and this shift in community structure was caused by deep mixing and selective grazing of the microphytoplankton (mainly diatoms) by krill (Jacques and Panouse, 1991).

The uptake regime in the Scotia-Weddell Confluence zone varied depending on dominance of diatoms or flagellates. At the beginning of the season (*SWC A*) a diatom dominated microphytoplankton assemblage thriving in stabilised surface water was

characterised by high ν-NO_3 and predominance of new production (Tables 7 and 8). With the progress of the season (*SWC B*), the phytoplankton composition shifted to dominance by flagellates (mainly cryptophytes) and nanophytoplankton (Tables 7 and 8). This was accompanied by an increase in ammonium availability, a decrease in nitrate uptake rate and preponderance of regenerated production (Goeyens *et al.*, 1991).

The Prydz Bay area was investigated during the MARINE SCIENCE VOYAGE 6 cruise. Two functional zones were identified: CCSZ and OOZ (Goeyens and Dehairs, 1993). Both POC and PPC data for the CCSZ indicate dense phytoplankton bloom (Tables 6 and 7; Semeneh, 1992; Kopczynska *et al.*, 1995). We observed important differences in terms of species composition between the CCSZ and the bloom stations in the Weddell Sea (eastern Weddell Sea and Larsen Shelf). Whereas the bloom in the eastern Weddell Sea and the Larsen Shelf was due to diatoms and *Phaeocystis sp*, the bloom in the CCSZ was entirely due to diatoms. Diatoms contributed for about 84% to the total biomass. In terms of size distribution the microphytoplankton were dominant in the CCSZ, representing about 78% of the total biomass (Table 7). Pennate diatoms, in particular, were very important, representing about 70% of the diatoms biomass and ~ about 58% of the total biomass. *Nitzschia curta* was the most dominant pennate diatom which, on average, contributed 28.2 % to the PPC. At one station this species virtually formed a mono-specific bloom. This species together with *N. antarctica* and N. *subcurvata* represented over 45% of the total biomass. Important centric diatoms included: *Corethron criophilum*, *Rhizosolenia hebetata*, *Thalassiosira sp*, *Dactyliosolen sp* and *Biddulphia sp.* Unlike in the eastern Weddell Sea and Larsen Shelf, *Phaeocystis* contributed only ~ 5.4%.

As in the CCSZ, diatoms dominated the phytoplankton assemblage of the OOZ (~ 85.6%) and microphytoplankton (> 10 µm) represented about 87.8% (Table 7). Unlike the CCSZ, the dominant diatoms were centric species which constituted ~ 63.4% of diatom biomass and ~ 55% of total phytoplankton biomass. The dominant centric diatoms included: *Thalassiosira sp*, *Rhizosolenia hebetata, Corethron criophilum* and

Chaetoceros dichaeta. Moreover, pennates species such as *Nitzschia curta*, *N. lecontei* and *Fragilariopsis sp* were also important.

Notwithstanding the high biomass in the CCSZ, phytoplankton growth rates were low (Table 8). $v\text{–}NO_3$ values (~ 0.0005 h^{-1}) were one order of magnitude less than those observed in the Weddell Sea (Table 8). The production regime was characterised by predominance of regenerated production (f-ratio < 0.5, Table 8). On the contrary, the community in the OOZ was mainly based on new production (f-ratio > 0.5; Tables 7 and 8).

In Prydz Bay as a whole f-ratio correlated negatively with diatom biomass (Figure 11). However, pennate and centric diatoms showed different relationships with the f-ratio. Pennate diatom biomass correlated negatively with f-ratio and positively with $v\text{–}NH_4$ (Figures 12 A and 13). On the other hand, centric diatom biomass showed a positive correlation with f-ratio (Figure 12 B).

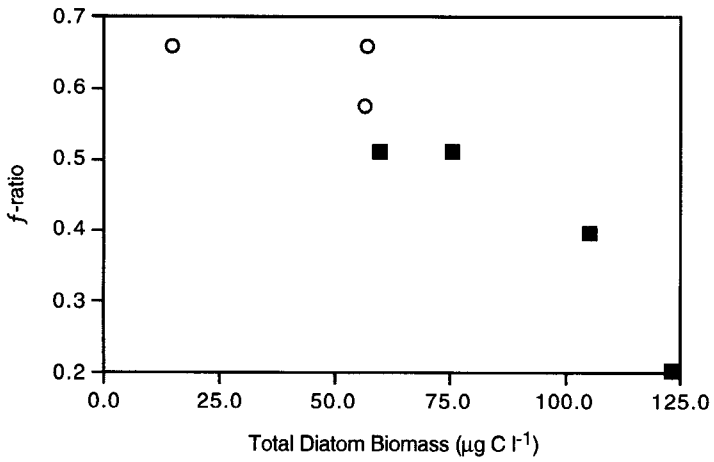

Figure 11: The relationship between total diatom biomass and f-ratio during the MARINE SCIENCE VOYAGE 6 cruise in Prydz Bay area (—○— = OOZ; —□— = CCSZ).

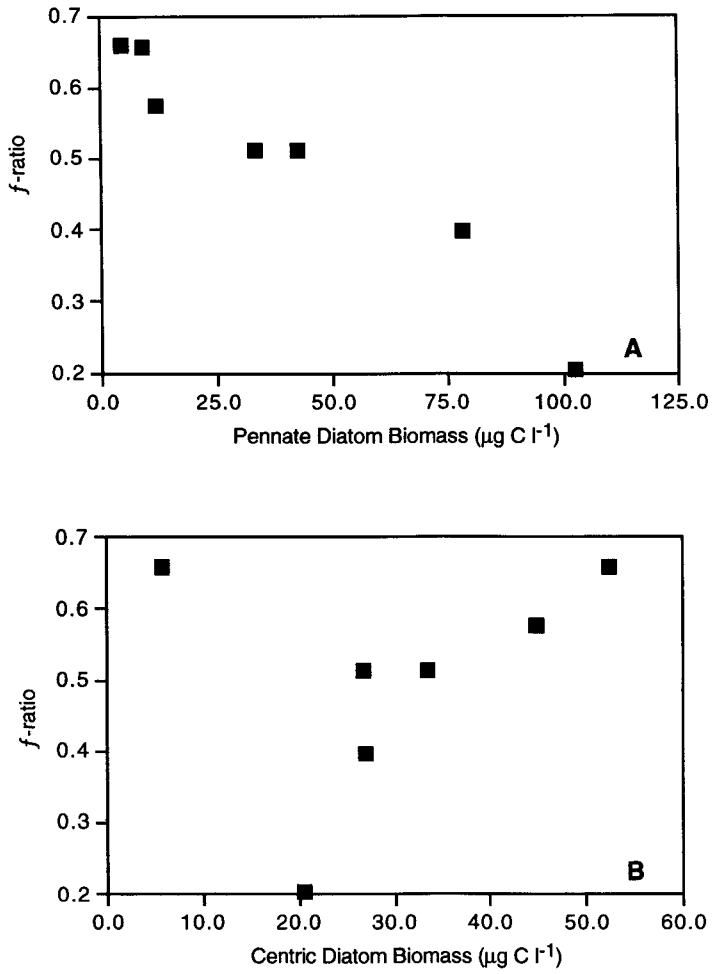

Figure 12: Relationship between the biomass of pennate (A) and centric (B) diatoms with f-ratio in the Prydz Bay area.

3.2.2. Seasonal evolution in phytoplankton community structure and nitrogen uptake regime — Two lines of seasonal evolution are apparent from the physico-chemical characteristics of the environment as well as from the relationship between nitrogen uptake regime and phytoplankton biomass, composition and structure. In the first scenario, represented by the MIZ areas of the Weddell Sea and

Scotia-Weddell Confluence, the shift from new to regenerated production was accompanied by a change in phytoplankton community structure (i.e. from a diatom dominated microphytoplankton assemblage at the beginning to a flagellate dominated nanophytoplankton assemblage at the end of the season). In the second scenario, represented by the CCSZ and OOZ of Prydz Bay, a shift in the uptake regime occurred without big changes in phytoplankton community structure. When discussing the seasonal evolution, the factors controlling the growth and maintenance of phytoplankton biomass, community structure and uptake regime are considered.

The first scenario is typical for MIZ areas of the Weddell Sea and Scotia-Weddell Confluence. Thick ice cover, high levels of nutrients and low ammonium availability characterise the early stage of MIZ (ANTARKTIS IX/2 and central Weddell Sea; Table 6). Autotrophic flagellates (non-*Phaeocystis*) dominated the phytoplankton assemblage and much of the phytoplankton biomass was dominated by the < 10 μm size fraction (Table 7). Despite low phytoplankton biomass, relatively high $v\text{–}NO_3$ indicate active phytoplankton (Table 8). During winter and early spring phytoplankton biomass is kept low by sub-optimum growth conditions (mainly due to low light availability and sub-optimal temperature) and predominance of heterotrophic activity (Garrison *et al.*, 1993). Ammonium concentrations during this stage is low and, hence, new production is predominant (Table 8).

As the season progressed (e.g. *SWC A,* eastern Weddell Sea and Larsen Shelf) the rise in temperature causes ice melting and shallow upper mixed layers (10-50 m). The shallow mixed layer optimises growth conditions and reduces loss rates induced by intense mixing, leading to dense bloom development (Chl. a > 1.5 μg l^{-1}, Table 6). Sakshaug and Holm-Hansen (1984) stressed the importance of water column stability and suggested a maximum pycnocline depth of 50 m for a bloom to develop. Within the stabilised surface water diatoms dominate the assemblage due to their fast division rates under optimum light conditions. This is corroborated by the fact that both $v\text{–}NO_3$ and $\rho\text{–}NO_3$ during bloom periods were correlated strongly to diatom biomass (Figures 10 A and B). Besides diatoms, other important species include *Phaeocystis sp* whose relative contribution increased from about 7% early in the season (central Weddell

Sea) to about 25% as the season progressed (eastern Weddell Sea and Larsen Shelf). The occurrence of a diatom bloom with *Phaeocystis* during this period implies a similar strategy to increase the biomass and reduce the loss rate. Colony formation by *Phaeocystis* is analogous to chain formation by bloom forming diatoms; a morphological strategy that possibly may reduce grazing pressure by microheterotrophs. For example, in the Bransfield Strait a rich and highly productive *Phaeocystis* dominated assemblage was associated with low copepod biomass and low feeding activity, implying the unsuitability of this species for copepods (Schnack *et al.*, 1985).

Late in the growth season (e.g. *SWC B*) the MIZ is characterised by deeper mixed layer, dominance of flagellates, high ammonium availability (~ 4.7%) and predominance of regenerated production (f-ratio ~ 0.44; Tables 6, 7 and 8). Due to decreased stability of the water column and selective grazing of diatoms by krill, the community structure shifted to dominance by smaller size fraction, mainly by cryptophytes (Jacques and Panouse, 1991; Bequevort *et al.*, 1992; Schloss and Estrada, 1994). These combined bottom-up and top-down control mechanisms selectively reduced the important and active component of the bloom (i.e. diatoms). In areas of high krill concentration and deep vertical mixing flagellates dominate over diatom (Kopczynska, 1992). High krill abundance is the main feature of the north-western Weddell Sea and Scotia-Weddell Confluence area (Priddle *et al.*, 1988). In the MIZ of Scotia-Weddell Confluence area grazing by krill not only structured the community but also enhanced ammonium availability through its direct excretion and by producing appropriate substrate for remineralisation (El-Sayed, 1988; Goeyens *et al.*, 1991b). Under this condition small cells which tend to satisfy their nitrogen requirement by assimilating ammonium dominate the assemblage (Probyn and Painting, 1985; Koike *et al.*, 1986). Exclusion of microphytoplankton from the system offers greater advantage for small phytoplankton by a reduced competition for ammonium with the larger cells.

Total specific uptake rate indicates the growth rate of phytoplankton. Much of the variability in total specific uptake rate was mainly due to nitrate uptake rate. As can be

seen in Table 8, uptake rates were low at the beginning of the season (ANTARKTIS IX/2 and central Weddell Sea), increased as the season progressed (*SWC A*), reached its maximum (eastern Weddell Sea), decreased slightly (Larsen Shelf) and became very low at the end of the season (*SWC B*). This trend in specific nitrate uptake rate was paralleled by the *f*-ratio. Thus, in the MIZ, a diatom-dominated, predominantly nitrate-based microphytoplankton assemblage thriving in a stable water at the beginning of the season was transformed into a flagellate dominated, ammonium-based nanophytoplankton assemblage towards the end of the season.

In the second scenario, applying to the CCSZ and OOZ parts of Prydz Bay, only a shift in uptake regime was observed. The main features of these areas include their stable water column (CCSZ), high phytoplankton biomass, dominance of diatoms, greater importance of the larger size fraction, low ν–NO_3, high ammonium availability (CCSZ) and predominance of regenerated production (in CCSZ; Tables 6, 7 and 8). A bloom can develop only when the rate of biomass increase exceeds the loss rate (grazing rate and sedimentation rate). Once the bloom has developed it can be sustained for a longer period under low growth rate if the loss rate is small. This appears to be the case in the CCSZ of the Prydz Bay. Stable water column due to continuous freshwater supply from the ice shelves, high biomass, low ν–NO_3 and high ammonium availability indicate prolonged phytoplankton bloom. High ammonium availability can develop without the contribution of migratory herbivores such as krill through prolonged heterotrophic activity by the microheterotrophs. This is corroborated by high heterotrophic activity of dinoflagellates, ciliates and nanoflagellates in this area (Archer *et al.*, 1995; Kopczynska *et al.* 1995). Microheterotrophs can consume as much as 48% of the daily production (Becquevort *et al.*, 1992) and this can lead to high ammonium availability. These heterotrophs preferentially graze on small cells, < 20 μm (Froneman *et al.*, 1995) and their grazing pressure increases with the progress of the season (Archer *et al.*, 1995). This keeps the biomass of small cells low thereby reducing their competition for ammonium with the large cells.

The dominance of diatoms late in the growth season implies little or no selective grazing pressure by meso- and macroheterotrophs and persistence of stable water

column. This also suggests that diatoms were dominant throughout the season. In a similar environment, the Ross Sea ice edge, diatoms (mainly pennate diatoms) dominated the phytoplankton assemblage from the beginning to the end of the season (El-Sayed *et al.*, 1983; Smith and Nelson, 1985; Nelson and Smith, 1986).

Despite bloom conditions in the CCSZ, phytoplankton production was largely based on ammonium, regenerated production (Tables 6, 7 and 8; Semeneh, 1992). In particular, large diatoms, which often are considered to live mainly on nitrate and to export organic material to deep sea, were predominantly assimilated ammonium (Figure 11). This contrast with the MIZ, where a mixed diatom-*Phaeocystis sp* bloom was based on nitrate (Tables 7 and 8; Figures 10 A and B). Although the Prydz Bay phytoplankton community was largely based on ammonium, pennate and centric diatoms exhibited differences in their nitrogen nutrition. Centric diatoms were more abundant in the OOZ and were mainly based on nitrate (Tables 7 and 8). Their biomass correlated positively with f-ratio (Figure 11 B). On the other hand, pennate diatoms were more abundant in shallow areas where the water column was stable and ammonium availability was high (e.g. Larsen Shelf and CCSZ; Tables 6 and 7). Their biomass correlated negatively with f-ratio (Figure 12 A). In these areas pennate diatoms constituted a major fraction of the total biomass (~26% in CCSZ and ~ 58% in Larsen Shelf; Table 7). Moreover, these diatoms often dominate ice assemblages (Garrison and Buck, 1985) and often get exposed to high levels of ammonium in the ice (e.g. 1.5 to 2.4 µM; Fritsen *et al.*, 1994). When exposed to elevated levels of ammonium (as in the CCSZ), these diatoms can increase their ammonium uptake capacity, v–NH_4 (Figure 13; Smith and Nelson, 1990).

This enables them to change their nitrogen source depending on the availability of ammonium. Therefore, pennate diatoms are opportunistic species with a flexible physiology that enables them to live successfully both in the ice and the water column. Such flexible nitrogen nutrition is particularly important in systems such as the Southern Ocean, where nitrate utilisation can be limited by iron availability (Martin *et al.*, 1990b). Severe nitrate depletion (as low as 2.8 µM) in the CCSZ could be attributed to the land-mass effect (high iron availability). It could also be attributed to

enhanced availability of both ammonium and iron through increased heterotrophy by microheterotrophs (Hutchins *et al.*, 1993). Greater dependence on ammonium offers more advantage for slowly dividing large diatom cells (low ν–NO_3, Table 8). This is because large cells have a high iron requirement and, in particular, this requirement is higher when they assimilate nitrate. The shift in nitrogen nutrition from nitrate to ammonium reduces the overall community demand for iron, thus, enable part of the community to subsist on nitrate. Although the relative contribution of nitrate in the CCSZ was low (*f*-ratio ~ 0.42), its absolute uptake rate was relatively high due high phytoplankton biomass (Tables 6 and 8).

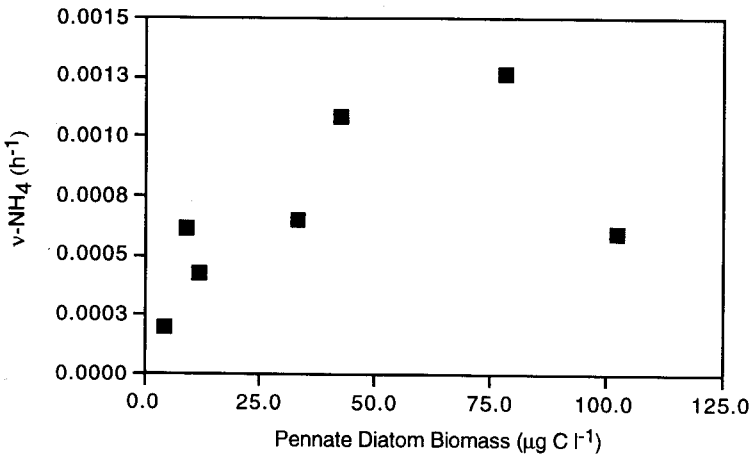

Figure 13: Specific ammonium uptake rate (ν-NH_4) *versus* pennate diatom biomass in Prydz Bay area.

This explains the observed low ambient nitrate concentrations in the CCSZ. On the contrary, in the MIZ large diatoms, which formed the bulk of the bloom, were selectively removed from the euphotic zone through grazing and water column destabilisation. The remaining phytoplankton, mainly composed of nanoplanktonic flagellates, had low biomass and was sustained by ammonium (*SWC B*, Tables 7 and 8).

The community structure in the CCSZ, unlike the MIZ, did not change during the season. The > 10 µm size fraction in Prydz Bay represented from 28.9 to 98.8 % (average ~ 80.6 %) of the total phytoplankton biomass (Table 7). The dominance of the > 10 µm size fraction was concurrent with predominance of regenerated production (Tables 7 and 8). The situation in the CCSZ is the extension of the first stages of the MIZ in the Weddell Sea and adjacent areas, i.e. diatoms persisted to late season but shifted their nitrogen nutrition from largely nitrate to ammonium. Therefore, under persistent physical stability and reduced selective grazing pressure, a diatom dominated nitrate based microphytoplankton assemblage at the beginning of the season shifts its uptake regime in response to increased ammonium availability.

From the above discussion we conclude that, depending on the underlying biological and physico-chemical factors governing the growth and maintenance of phytoplankton in euphotic zone, a shift in nitrogen uptake regime (i.e. from new to regenerated production) can proceed with or without big change in community structure.

3.3. Spatial and seasonal variability of the export process from the mixed surface layer

Earlier studies have shown that in the particulate material suspended in the oceanic water column, barium is present to a large extent as microcrystals of the sulphate mineral barite, concentrations of which appear to be correlated with productivity. The causal relationship between surface ocean productivity and content of barite in the water column is rather well documented but the exact pathway is not fully understood. From thermodynamical considerations it is clear that most of the world ocean surface waters are undersaturated with respect to $BaSO_4$ (Church, 1970; Church and Wolgemuth, 1972). Recent data (Jeandel *et al.*, 1996a; C. Monnin pers. communic., 1996) indicate that it is probably only in the dissolved Ba rich cold Southern Ocean surface and deep water column that $BaSO_4$ is saturated. However, oversaturation remains weak (saturation index is close to 1) and is unlikely to induce barite precipitation. This stresses the important role played by micro-environments within which saturation conditions are reached favourable for barite precipitation, an idea initially proposed by Chow and Goldberg (1960). There is evidence that aggregates of biogenic detritus function as such micro-environments. Indeed in surface waters Ba content is highest in the large particle size class (> 50 µm), while below 200m it becomes enriched in the smaller particles (< 50 µm) (Bishop, 1988), suggesting a formation related with the presence of larger aggregates in surface waters and a breakdown of these aggregates in deeper layers, whereby the smaller constituent particles are released. Furthermore, barite presence in biogenic aggregates has been documented from electron microscopy studies (Dehairs *et al.* 1980; Stroobants *et al.* 1991). The general process of barite formation and redistribution in the water column could therefore look like this: Dissolved barium is taken up actively or passively by living plankton. Plankton mortality, in the absence of significant grazing pressure leads to detritus formation which is prone to aggregate formation. High Ba contents and enhanced sulphate concentrations resulting from the oxidation of reduced organic sulphur compounds produce conditions of significant $BaSO_4$ oversaturation in the aggregates, leading to the precipitation of barite crystals. If such biogenic aggregates are solid and dense enough they will just settle trough the water column and will eventually reach the sediments with their barite load. However, loosely packed and less dense

specimens are more prone to fast bacterial breakdown during their descend in the water column and will disintegrate in intermediate waters, releasing their load of discrete barite crystals in the ambient water. This latter scenario fits with observations of Ba-barite maxima in the depth region between 200 and 600 m. Such maxima appear to be a world wide feature (Dehairs *et al.*, 1980; 1987; 1991; 1992; 1996). Barite crystals released from their protecting micro-environments will be subject to dissolution (except probably in the Southern Ocean surface and deep water column), but dissolution of barite is a relatively slow process (Dehairs *et al.*, 1980). Therefore, the water column stocks of these crystals are likely to reflect not only the magnitude of the biogenic matter export flux but also the extent of the heterotrophic oxidation of associated POM in subsurface and intermediate waters. Thus, the possibility existed to elaborate a transfer function allowing to assess the fraction of exported carbon respired in the subsurface and intermediate waters (i.e. the mesopelagic water column). This was attempted in the present study using the ANTARKTIS X/6 Ba data set. The obtained transfer function was thereafter applied to the whole of our Southern Ocean data set.

3.3.1. Estimation of the O_2 consumption rates — From our earlier Southern Ocean results it became apparent that mesopelagic particulate Ba maxima occurred in the vicinity of the oxygen minimum and that Ba was inversely correlated with oxygen in the oxygen minimum region (Dehairs *et al.* 1990; Dehairs *et al.*, 1992). It can be debated whether such a relationship is fortuitous, especially in view of the well documented evidence of at least a partially advective origin of the oxygen minimum in the Southern Ocean (Callahan, 1972; Reid *et al.*, 1977; Georgi, 1981; Piola and Georgi, 1982; Whitworth and Nowlin, 1987; Jamous *et al.*, 1992; Roether *et al.*, 1993). Therefore, we focused our attention on calculating profiles of oxygen consumption rates using a modelling approach. This modelling approach, outlined below, has been discussed previously in Shopova *et al.* (1995) and Dehairs *et al.* (1996). O_2 consumption rates were deduced from the dissolved oxygen profiles using a 1-D inverse model described elsewhere (Shopova *et al.*, 1995). This model approach is outlined briefly. A vertical advection - diffusion model of the steady state distribution of conservative and non-conservative tracers in the water column was used:

$$-\frac{\partial}{\partial z}K\frac{\partial C}{\partial z}+w\frac{\partial C}{\partial z}=J$$
$$C(z)\Big|_{z=z_s}=h(z_s) \qquad C(z)\Big|_{z=z_b}=h(z_b) \tag{7}$$

where z is the downward vertical co-ordinate, *K(z)* is the vertical eddy diffusivity, *C=C(z)* is the concentration of the tracer, *w(z)* is the upwelling (downwelling) velocity, *J(z)* is the total production (consumption) rate (it is zero for conservative tracers). We consider the water column between the centre of the well mixed layer and 1000m.

Qualitative information about the considered water column is obtained using the effective parameters. From Eqn. (7) we get for a conservative tracer:

$$-\frac{\partial^2 C}{\partial z^2}+w_{eff}\frac{\partial C}{\partial z}=0, \quad w_{eff}=\frac{w(z)-K'(z)}{K(z)}, \quad \frac{1}{w_{eff}}=z^* \tag{8}$$

where z* has the dimension of length. Applying the same procedure to a non-conservative tracer, we obtain:

$$-\frac{\partial^2 C^{nc}}{\partial z^2}+w_{eff}\frac{\partial C^{nc}}{\partial z}=J_{eff}, \quad J_{eff}(z)=\frac{J(z)}{K(z)} \tag{9}$$

where C^{nc} is the concentration of the non-conservative tracer and J_{eff} is the effective consumption. The effective consumption J_{eff} has the dimension of mol m^{-5} and allows comparison of stations on a qualitative basis without requiring the knowledge of the eddy diffusivity. However, in order to allow for a quantitative estimation of the upwelling and downwelling and the oxygen consumption rate we need to know the distribution of the eddy diffusivity.

The difficulties associated with the determination of eddy diffusivity are well known (e.g. Gargett, 1989). Recently, Ledwell *et al.* (1993) have shown that mixing in the upper 1000 m of the open ocean is around 10^{-5} m^2 s^{-1}. For the determination of the eddy diffusivity in the transition zone at the lower boundary of the upper mixed layer we have used Osborn's expression (Osborn, 1980) which relates the diffusivity K to the buoyancy frequency N ($K = \Gamma\varepsilon N^{-2}$; $N^{-2} = (g/\rho 0)\ (\partial\rho/\partial z)$; with Γ = proportionality constant; ε = dissipation rate of turbulent kinetic energy and ρ = density). However, for the water column extending below the thermocline a constant

mixing of 5 10^{-5} m^2 s^{-1} is used. The same value is used by Webb *et al.* (1991) for the Fine Resolution Antarctic Model.

Horizontal homogeneity of the considered water column is generally assumed in this model approach. This assumption implies that the horizontal length scale of the water column concerned is set by the distance over which the oxygen gradient is negligible. Practically this length scale is at least a few kilometres, as a result of ship- and bottle-drifting, measurement errors, variability in mixing processes and in concentration. Careful comparison of the data between nearest stations suggests that even for distances of 10 to 40 km oxygen gradients are of the order of the measurement error. Nevertheless, if the horizontal velocity and oxygen gradients are known in the region of the considered station we can use them to correct the oxygen consumption rates *J*. Actually the consumption rate calculated from the data of a single station contains 2 parts:

$$J = J_l + J_h \tag{10}$$

where J_l is the contribution of the local processes and:

$$J_h = (u/\partial_z C)(\partial_x C \partial_z C^{nc} - \partial_x C^{nc} \partial_z C) \tag{11}$$

is the contribution of the horizontal advection (Shopova *et al.*, 1995). It is clear from (11) that the contribution of the horizontal advection is negligible for small horizontal concentration gradients. Generally the horizontal advection will not influence the consumption rates if the gradients of the conservative and the non-conservative tracers are proportional for any depth.

For the latitudinal belt between 57°15'S and 58°S a series of stations were occupied both along the 6°W and the 6°30'W meridians. These stations represent the nearest ones along the main path of the ACC and we have compared the oxygen data between both meridians. The oxygen concentrations are very similar for every pair of stations located at the same latitude. The comparison of the oxygen profiles was limited to the water column below the transition zone between surface mixed layer and deep waters where surface forcing has no strong influence. We have assumed an average horizontal velocity of 0.05m s^{-1} (Whitworth and Nowlin, 1987; Webb *et al.*, 1991) and have applied Eqn. (11) to all pairs of stations between 57°15'S and 58°S. The calculated advection term J_h for the depth region between

the transition zone and 1000 m appears to induce an underestimation of J by 10% to 15%. This J_h term is larger in the vicinity of the transition zone (J_h increases to between 20% and 50%) but generally decrease to 0 at greater depths where pure vertical advection is prevailing (zero horizontal gradients). However, on some occasions J_h can be significant even at 1000m depth, reaching 10 to 20%. These results for a limited set of stations indicate that advection represents an input of oxygen (J_h is opposite in sign to J_l) and suggest that our calculations of the local O_2 consumption rates are in general underestimated and represent a conservative estimate of local oxygen consumption.

3.3.2. Particulate Ba stocks and O_2 consumption rates: the transfer function — The 1-D O_2 consumption model was applied to the ANTARKTIS X/6 data for which a high quality data set on dissolved oxygen and primary production was available next to an extensive data set for particulate Ba.

In the following discussion particulate Ba concentrations always represent total concentrations corrected for the lithogenic fraction. The lithogenic fraction is calculated using an average crustal Ba/Al molar ratio of 0.00118 and assuming all particulate Al in the sample is lithogenic in origin. This correction typically reduces total particulate Ba concentrations by only 2 to 3%, emphasising the importance of other carrier phases (mainly barite but also Ba dispersed in biogenic materials).

Depth weighted average values for Bap in the surface layer (upper 100 m) and for the mesopelagic depth area (200 to 400 m depth interval) are given in Table 9, together with data for primary production integrated over the euphotic layer (from Jochem *et al.*, 1995 and Rommets *et al.*, 1993) and depth weighted (200 m interval) average dissolved oxygen content in the O_2 minimum (from Rommets *et al.*, 1993 and Dehairs *et al.*, 1996).

In order to estimate the rate of O_2 consumption the mixing coefficient K was calculated (see previous section) for the transition zone between the well mixed surface layer and the mesopelagic water column and was taken equal to $5\ 10^{-5}\ m^2\ s^{-1}$ below this transition zone. For the PFZ, characterised by a much more intense and complex mixing, this latter value for K is probably too small and so are probably the calculated O_2 consumption rates.

Table 9: Depth weighted average particulate Ba concentrations in the surface (upper 100 m) and at mesopelagic depth (200 to 400 m depth interval); O_2 consumption rates and primary production at transects 2, 5 and 11 during ANTX/6.

Station	Lat.	Long	Surface Bap pmol/l	Mesopel. Bap pmol/l	Depth of Bap max m	Depth of O_2 min m	Av. O_2 in O_2 min µmol/l	Integrated O_2 Cons mmol/m²/d	Max O_2 Cons µmol/l/d	Depth Max O_2 cons m	O_2 Cons at 1000m µmol/l/d	Primary Production* mg C/m²/d
Transect 2; 12 to 18 October 1992												
869	56°30' S	6° W	201	293	200	300	193.4	N.D.	N.D.	N.D.	N.D.	N.D.
872	55° S	6° W				415	188.5	2.59	7.00E-03	200-300	4.18E-04	78
873	54°30' S	6° W	234	275	200	430	191.9	2.17	7.20E-03	250	3.86E-04	N.D.
876	53° S	6° W				410	182.9	2.39	9.40E-03	250	1.82E-03	N.D.
877	49° S	6° W				820	183.0	2.03	1.30E-02	200	1.25E-03	N.D.
878	48°30' S	6° W	411	494	300	790	183.5	2.69	1.20E-02	200-300	1.40E-03	244
Transect 5; 24 to 30 October 1992												
886	56° S	6° W	355	268	200	370	195.5	1.86	1.19E-02	200	7.41E-05	N.D.
891	55° S	6° W	252	325	250	360	185.5	4.50	2.05E-02	250	6.25E-04	191
895	53° S	6° W	181	297	300	385	185.8	2.57	1.80E-02	200	4.40E-04	127
899	51° S	6° W	161	356	300	380	180.0	4.54	1.70E-02	250	5.74E-04	335
903	49° S	6° W	488	368	250	680	182.3	2.07	1.73E-02	250	8.52E-04	1535
907	47° S	6° W	368	368	300	775	184.0	1.19	5.70E-03	400	1.10E-04	1202
Transect 11; 10 to 21 November 1992												
939	57°30' S	6° W	318	274	250	420	203.7	0.95	1.00E-02	250	1.24E-04	N.D.
945	55° S	6° W	256	326	300	430	187.2	5.82	5.30E-02	200	3.80E-04	347
949	53° S	6° W	397	303	200	345	181.9	3.50	2.50E-02	200	6.07E-04	258
953	51° S	6° W	139	509	300	500	179.2	4.87	4.36E-02	250	2.10E-03	388
960	49° S	6° W	7997	437	250	650	184.2	2.15	8.70E-03	250-300	1.05E-03	2892
969	47° S	6° W	910	393	200	800	185.4	1.27	2.90E-03	400	1.39E-03	1074
Transect 12 &13; 22 to 23 November 1992												
972	48°30' S	6° W	502	419	200	790	182.5	2.87	1.60E-02	250	2.80E-03	N.D.
978	49°50' S	6° W	1741	390	250	495	184.3	N.D.	N.D.	N.D.	N.D.	N.D.

N.D. = no data. * Data from Jochem *et al.* (1995) and Rommets *et al.* (1993)

Despite the uncertainty on the applicability of the selected mixing coefficient value internal comparison of O_2 consumption rates at a single station is valid in the PFZ. Table 9 reports the integrated O_2 consumption rates (mmol m^{-2} d^{-1}) in the water column between 175m and 1000m as well as the maximum O_2 consumption rate and the O_2 consumption rate at 1000m (both in µmol l^{-1} d^{-1}). O_2 consumption rates at 1000m are similar in magnitude to those observed by Kroopnick (1974) for the deep Pacific Ocean and by Broecker *et al.* (1991) for the deep (> 2000m) Atlantic Ocean. At depths shallower than 1000m consumption rates can be up to two orders of magnitude larger than rates at 1000m and water column integrated values range between 0.95 and 5.82 mmol m^{-2} d^{-1} (Table 10). Such values are 2.5 to 15 times smaller than the mean oxygen consumption rates for the northern North Atlantic inferred from a vertical two-box model approach (Peng *et al.*, 1987). Maximal O_2 consumption rates occur in the 200 to 300m depth range and vary between 0.007 and 0.053 µmol l^{-1} d^{-1} (Table 9). There is a general tendency for an increase of O_2 consumption rate with advancing season. This is especially true for the 55°S position visited during transects 2, 5 and 11.

The temporal variability of the O_2 consumption rate is highest in the region of the ACC - Weddell Gyre boundary at 55°S, with an increase from 2.59 mmol m^{-2} d^{-1} (Station 872; transect 2; October 14) over 4.50 mmol m^{-2} d^{-1} (Station 891; transect 5; October 25) to 5.82 mmol m^{-2} d^{-1} (Station 945; transect 11; November 14). Temperature *versus* salinity diagrams (not shown) indicate that the same water body was sampled over the one month time interval. Since during this one month period ice cover was reduced from 70% to 0% (observations by J. van Franeker, reported in Rommets *et al.*, 1993), we wonder whether the variability in O_2 consumption rate could be related to release events of sea-ice such as described by Riebesell *et al.* (1991). Antarctic sea-ice has been observed to contain large amounts of phytoplankton (between 10 and 80 mg Chl. *a* m^{-2}; see e.g. Table 3 in Legendre *et al.*, 1992). Likewise, Mathot (1993) observed POC carried by sea-ice phytoplankton in the northern Weddell Sea to reach values up to 2.7 mg C l^{-1} (EPOS-2 expedition; November - December 1988). During the same EPOS expedition we observed total POC contents of brown ice to be as high as 9 mg POC l^{-1} (F. Dehairs, unpublished results). If it is assumed that POC is distributed homogeneously over 2m of sea ice, the release of such amounts of POC as

induced by break-up of the pack-ice represents enough fuel over one month to account for the large increase in combustion rate in the mesopelagic region. Thus it appears that sedimentation and breakdown of POM released from sea-ice during sudden events has the potential to affect significantly the O_2 consumption rate in the water column and this on time scales of the order of days. Although these processes have led to an increase of the mesopelagic particulate Ba contents (Table 9), this increase, relative to the observed oxygen consumption, is less than observed for the ice-free southern ACC stations (see discussion below).

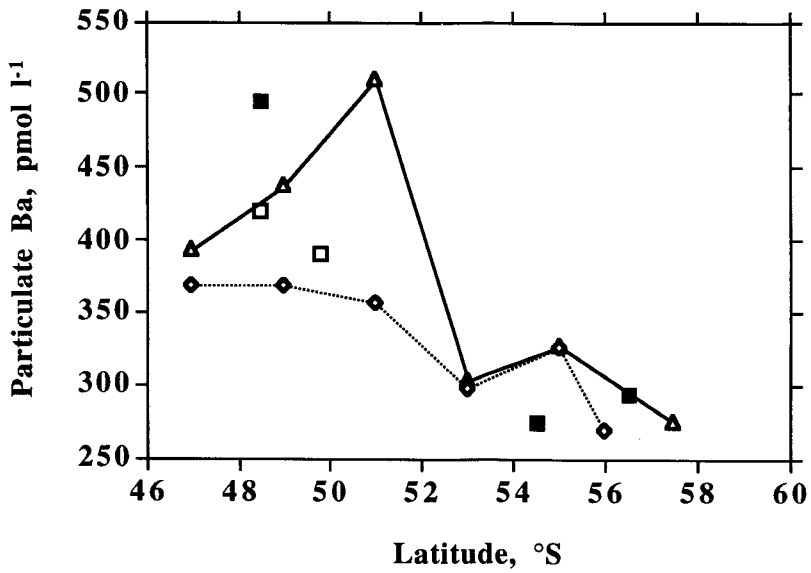

Figure 14: Latitudinal distribution of mesopelagic particulate Ba (pmol l^{-1}) during ANTARKTIS X/6 transects 2 (closed squares), 5 (open diamonds), 11 (open circles) and 12, 13 (open squares). Ba concentrations represent depth weighted average values for the 200 to 400m depth interval.

In general, mesopelagic Bap stocks increase from south to north and reach highest values in the PFZ (Figure 14), indicating increased export of material from the upper mixed layer in the PFZ relative to the southern ACC. However, the difference of mesopelagic Bap between PFZ and southern ACC is much smaller than observed for Bap in surface waters and for primary production (Figures 14 and 15). For the PFZ this may indicate that the Ba which is translocated from the

dissolved to the particulate phase in the surface waters is delivered to a significant degree below the mesopelagic depth region. The efficiency of this transfer to depths extending below the mesopelagic zone might be greater in the PFZ because of the much larger primary production and resulting larger export flux (see e.g. Boyle, 1988).

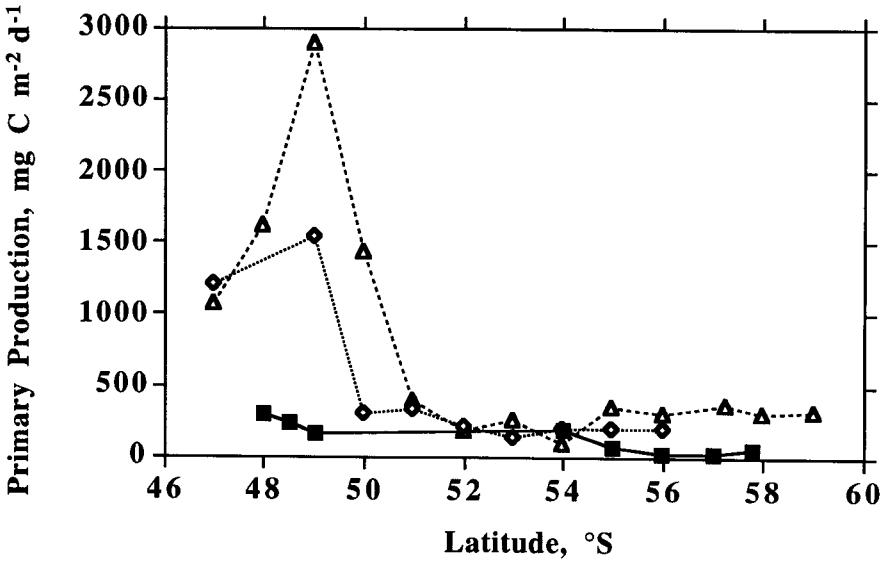

Figure 15: Latitudinal distribution of primary production (mg C m^{-2} d^{-1}; data from Jochem *et al.*, 1995 and Rommets *et al.*, 1993) during ANTARKTIS X/6 transects 2 (closed squares), 5 (open diamonds) and 11 (open circles).

Comparison of Bap profiles from fixed latitudes sampled during the three consecutive transects provides information on the degree of transience of the Bap tracer. For the southern ACC, temperature *versus* salinity plots indicate that over the investigation period of one month, water masses at 6°W varied little except for warming in the upper layer, suggesting that sampling over time occurred essentially within the same water masses. In the period between transects 2 and 11 little change in mesopelagic Bap content is observed at latitudes south of 55°S, while north of 55°S temporal changes become more and more pronounced (Table 9). This is especially marked at 51°S where average mesopelagic Bap increases from 356 pmol l^{-1} on October 27 (Station 899; transect 5) to 509 pmol l^{-1} on November 17

(Station 953; transect 11). Temperature *versus* salinity plots of station 899 and 953 (graphs not shown) overlap perfectly for the depth region extending below the upper mixed layer, indicating that over a three weeks period essentially the same mesopelagic and deep water body was sampled. Thus, even over relatively short time intervals mesopelagic Bap stocks can increase significantly, in general concordance with the increase of primary production in the upper mixed layer. North of 51°S, in the PFZ, temporal evolutions are less clear probably as a result of significant meandering of the Polar Front between 47°S and 49°S (Veth *et al.*, 1995). For instance, Station 878 sampled early in the season (transect 2; 48°30'S) shows a high average mesopelagic Bap value (494 pmol l^{-1}). The anomalously high temperatures along this profile suggest, however, that a watermass was sampled which intruded from the northern side of the PFZ and this probably as a result of meandering of the Polar Front.

3.3.3. Comparing calculated JO_2 with primary production and Ba-barite stocks (ANTARKTIS X/6) — For the southern ACC region, for which we are confident that the chosen mixing coefficient is realistic, the regression of computed oxygen consumption rates *versus* primary production (Figure 16) is highly significant ($p = 0.004$; $r^2 = 0.715$). This correlation is improved when the data for 55°S, where release of organic matter associated with production by ice algae could have increased the vertical flux (see discussion above), are not considered in the regression (Figure 16). This co-variation suggests a close coupling exists between both processes with time scales of the order of days rather than weeks. This is possible only if export of organic matter is sustained by fast settling aggregates which are sensitive to mineralisation in the mesopelagic depth region. Such a scenario is also consistent with the mechanism for barite crystal formation and release invoked to explain the Ba-barite maximum in the mesopelagic water column (Dehairs *et al.*, 1991; Stroobants *et al.*, 1991) and the coincidence of the Bap concentration and oxygen consumption rate extremes. The slope of the regression line between oxygen consumption and primary production suggests that 9.6% of the organic carbon synthesised in local surface waters is oxidised in the water column between bottom of surface mixed layer and 1000m (assuming a Redfield O_2/C mole ratio of 175/127 to apply during oxidation; Broecker *et al.*, 1985). This value is in good agreement with estimates for the open oceanic system in general (e.g. Berger, 1989) and leaves the major fraction of carbon synthesised in

surface waters for mineralisation at shallower depths and also for export to the ocean floor.

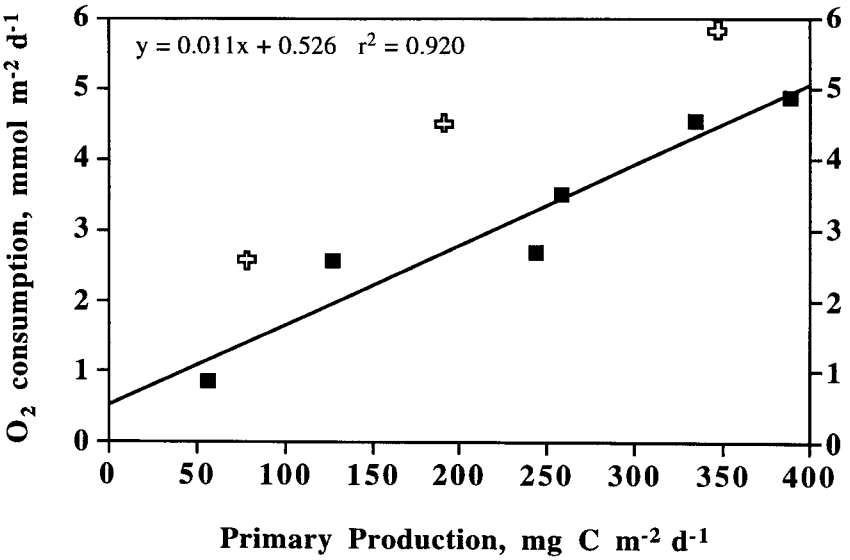

Figure 16: Regression of calculated O_2 consumption rates (mmol m^{-2} d^{-1}) *versus* primary production (mg C m^{-2} d^{-1}, data from Jochem *et al.*, 1995 and Rommets *et al.*, 1993) for stations in the southern ACC region. O_2 consumption rates represent values integrated over the depth extending between centre of the well mixed surface layer and 1000m. The regression shown does not include the stations at 55°S (crosses), which were still partially covered by ice during transects 2 and 5.

The vertical profiles of Bap and O_2 consumption rate for southern ACC and PFZ stations show a striking similarity as illustrated in Figures 17 a, b for a southern ACC and a PFZ station of transect 11. This suggests that the intrinsic process controlling Ba-barite release and oxygen consumption at mesopelagic depth is the same and that it is operating similarly in the southern ACC and the PFZ.

We now compare the calculated oxygen consumption rates with Bap contents for the southern ACC stations. Therefore, we calculated depth weighted average Bap contents and oxygen consumption rates (on volume basis) for the 200 to 400m depth interval where the extremes of both parameters are located. Taking only the

ice free stations into account (i.e. excluding the data for 55°S from the regression analysis) we observe a significant correlation (Figure 18):

$$\text{or} \quad \begin{aligned} Bap &= 218 * 10^{20.JO_2} \quad & r^2 &= 0.884 \\ Bap &= 17198 * JO_2 + 185 \quad & r^2 &= 0.869 \end{aligned} \qquad (12)$$

The data point at 55°S for transect 11 does not show a proportionally enhanced Bap stock. This is likely to reflect differences between the high-biomass pack-ice environment and the low-biomass open sea environment in mode of aggregation, water column transit time of aggregates and barite production and release.

It would be of interest to investigate whether the observed relationship between Bap and oxygen consumption is maintained during the whole growth season. Considering the observed close relationship between oxygen consumption at depth and primary production and the fact that micro-crystals of barite, once released from the aggregates, will tend to accumulate because of slow dissolution rate and slow settling rate (e.g. Dehairs *et al.*, 1980 and 1990), we expect such a relationship would not be persistent over the season.

Another point of interest is the non-zero Bap intercept (Bap intercept is 218 pmol l^{-1} for the exponential function and 185 pmol l^{-1} for the linear function). This suggests there can be a significant background content of Bap in the water column even during periods without significant plankton growth. As a result significant carry over of Bap between successive plankton growth seasons might occur. This represents a major problem when applying such a transfer function to other environments.

For oceanic environments undersaturated with respect to $BaSO_4$ it is likely that the background Ba signal is reduced because of dissolution, while for $BaSO_4$ saturated environments, such as the Southern Ocean cold surface and deep waters (Jeandel *et al.*, 1996a) it can represent a significant fraction of the total.

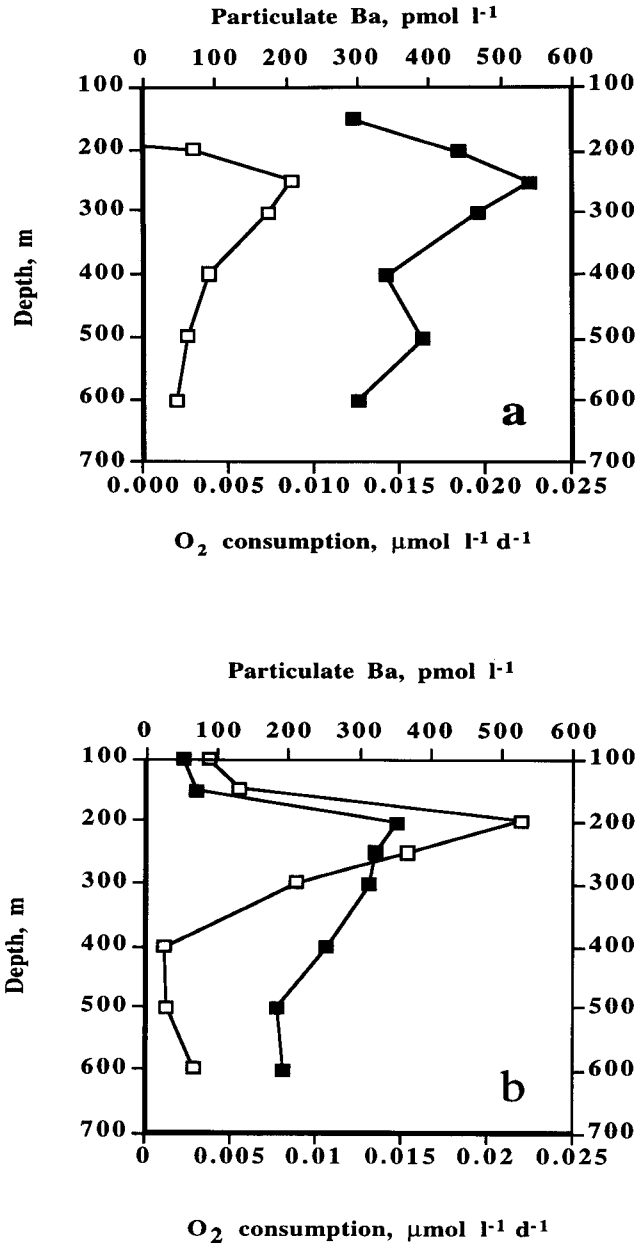

Figure 17: Comparison of the vertical profiles of O_2 consumption rate (open squares; mmol m^{-2} d^{-1}) and particulate Ba (closed squares; pmol l^{-1}) at: (a) Station 960, 49°S, transect 11; (b) Station 949, 53°S, transect 11.

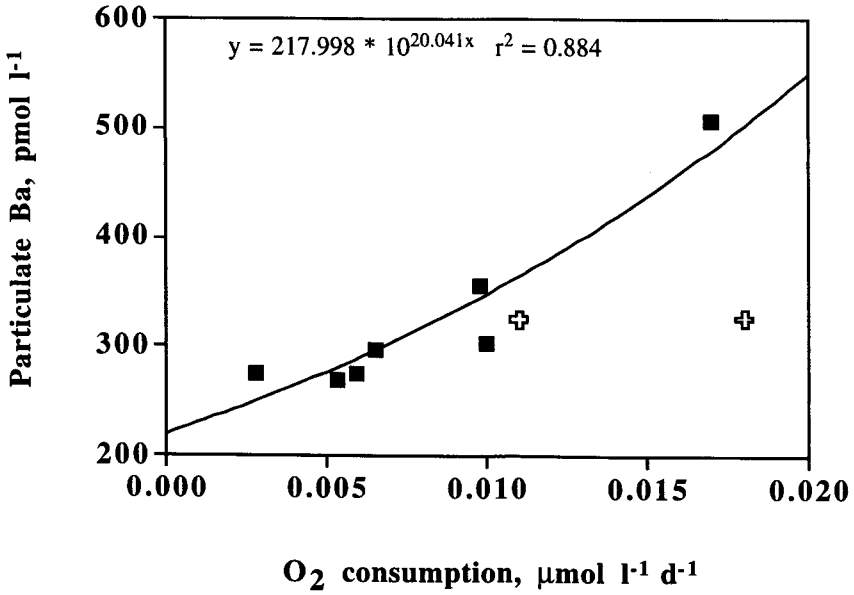

Figure 18: Regression of calculated O_2 consumption rates (mmol m^{-2} d^{-1}) *versus* primary production (mg C m^{-2} d^{-1}; Jochem *et al.*, 1995 and Rommets *et al.*, 1993) for stations in the southern ACC region. O_2 consumption rates represent values integrated over the depth extending between centre of the well mixed surface layer and 1000 m. The regression shown does not include the stations at 55°S (crosses), which were still partially covered by ice during transects 2 and 5 (see text).

3.3.4. Particulate Ba and productivity in different environments of the Southern Ocean — Table 10 gives the mesopelagic particulate Ba data available for the following different regions of the Southern Ocean: PFZ, ACC and AD zones in the Indian Ocean sector; the CCSZ in Prydz Bay; the ACC and the PFZ in the Atlantic Ocean sector; the MIZ and the CPIZ in the Weddell Sea and the MIZ and OOZ in the Scotia-Weddell Confluence area. As discussed below these different environments are characterised by different regimes of plankton community composition and productivity. Primary production rates for corresponding stations are shown as well in Table 10, with reference to data sources.

Figure 19 shows the distribution of all mesopelagic Ba data *versus* primary production rates. From Figure 19 a whole spectrum of different regimes can be

discerned, from weak to strong Ba response to primary productivity. Generalising, three regimes can be identified: Regime 1 with the highest mesopelagic Ba response to primary productivity (mainly the OOZ and POOZ of the ACC region in general and the Weddell Sea CPIZ); Regime 2 with the lowest Ba response (mainly the MIZ regions of the Scotia-Weddell Confluence area and the Prydz Bay shelf) and Regime 3, showing an intermediate situation (region of the PFZ). If the mesopelagic Ba is indeed a faithful tracer of the export production, this observation suggest significant differences in the relative importance of export production in total production between the different Southern Ocean environments investigated. This was indeed verified by careful comparison between mesopelagic Ba contents and parameters tracing the extent of phytoplankton development (nitrate depletion over the growth season) and of the recycling efficiency (build-up of ammonium stocks).

As described in Dehairs *et al.* (1992), this was done for OOZ, MIZ and CPIZ in the Scotia-Weddell Confluence area and for the OOZ and MIZ in the Prydz Bay area. MIZ areas showed the highest nitrate depletion levels, indicating phytoplankton growth to have been highest. This is the result of the well stabilised and relatively shallow mixed layer water column induced by pack-ice and ice-shelf melting in these areas. However, the proportionally enhanced ammonium stocks observed in the MIZ areas indicate that primary production was intensively recycled via micro-grazers and bacterial activity. The potential effect of the micro-grazers was documented for Prydz Bay, where inshore waters had size matching between diatoms (the prevailing autotrophs) and heterotrophic dinoflagellates, while in offshore waters this was not the case and diatoms significantly outsized the dinoflagellates (Kopczynska *et al.*, 1995). From this it can be concluded that the high productivity generally associated with stable, shallow mixed layers do not necessarily sustain a large export flux, as witnessed by the low Ba stocks in the mesopelagic waters of such environments. In these systems the primary carbon is mainly recycled through the microbial food web and little is left for export. In the OOZ but also the CPIZ areas a proportionally much larger fraction of the production is left for aggregation and sedimentation as witnessed by the higher stocks of mesopelagic Ba for given primary production. The PFZ on the Atlantic sector exhibits a behaviour which is intermediate between the MIZ and the OOZ.

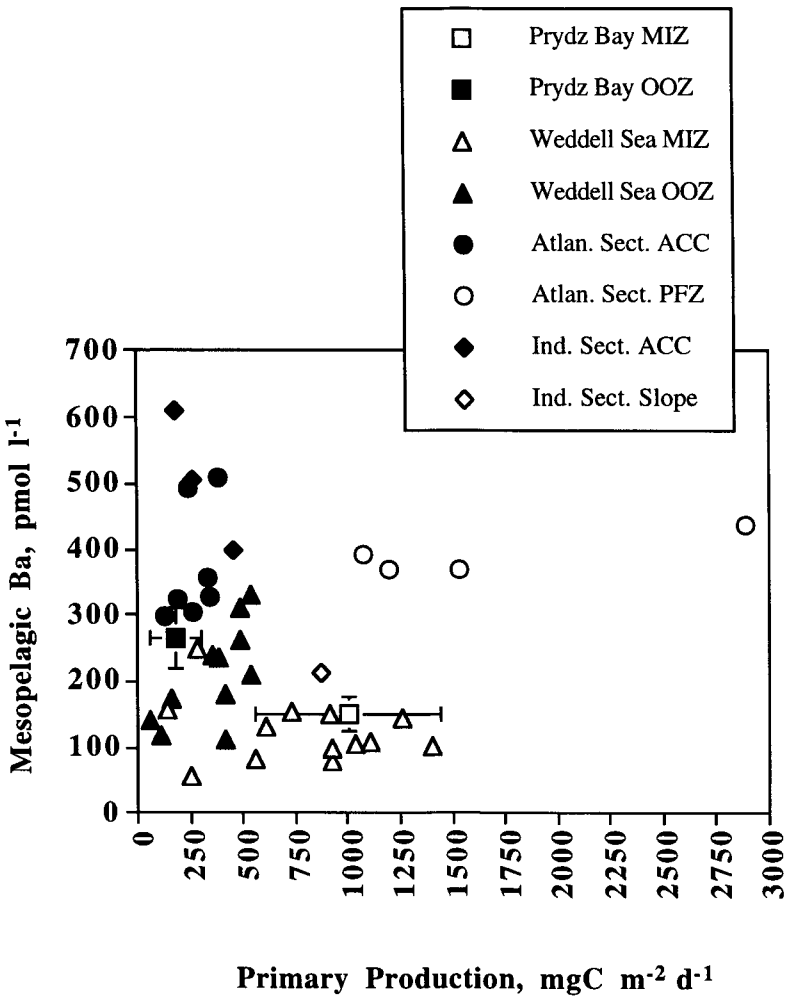

Figure 19: Mesopelagic particulate Ba content (depth weighted averages) *versus* primary production for different area of the Southern Ocean. Sources for primary production data, as indicated in Table 10.

3.3.5. Exported carbon respired in the mesopelagic water column — From the mesopelagic Ba contents the corresponding oxygen consumption rates and organic carbon respiration rates were calculated using Eqn. (8) and considering a value of 50 pmol l^{-1} for the background Ba signal (Table 10). This background Ba value is arbitrary and was chosen because it is close to the lowest particulate Ba values observed during the growth season (i.e. in the MIZ of the

Scotia Weddell Confluence). Selecting a higher value will of course reduce the calculated fraction of export production that is oxidised in the mesopelagic water column. For example, taking the background Ba equal to 185 pmol l^{-1} (i.e. the value observed for the ACC in the Atlantic sector), would reduce to zero the mesopelagic oxidation of exported POC for the MIZ's of the Prydz Bay Shelf and the Scotia-Weddell Confluence and for the sub-Tropical waters of the Indian sector. Inspecting the larger data set for the Indian Ocean (Figure 20a, b) it appears that export production (in fact respiration of exported carbon in the mesopelagic area) gradually increases away from the Antarctic shelf region to reach highest rates in the PFZ.

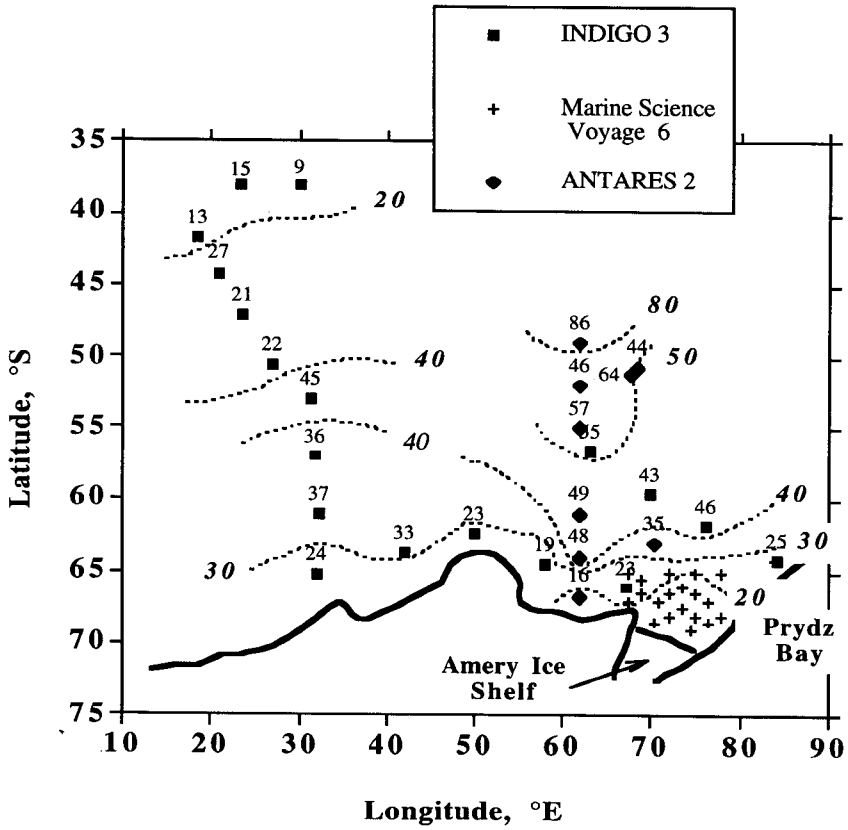

Figure 20a: Spatial variability of export production (mg C m^{-2} d^{-1}) respired in the mesopelagic water column in the Indian sector; summer situation (January to March): General view.

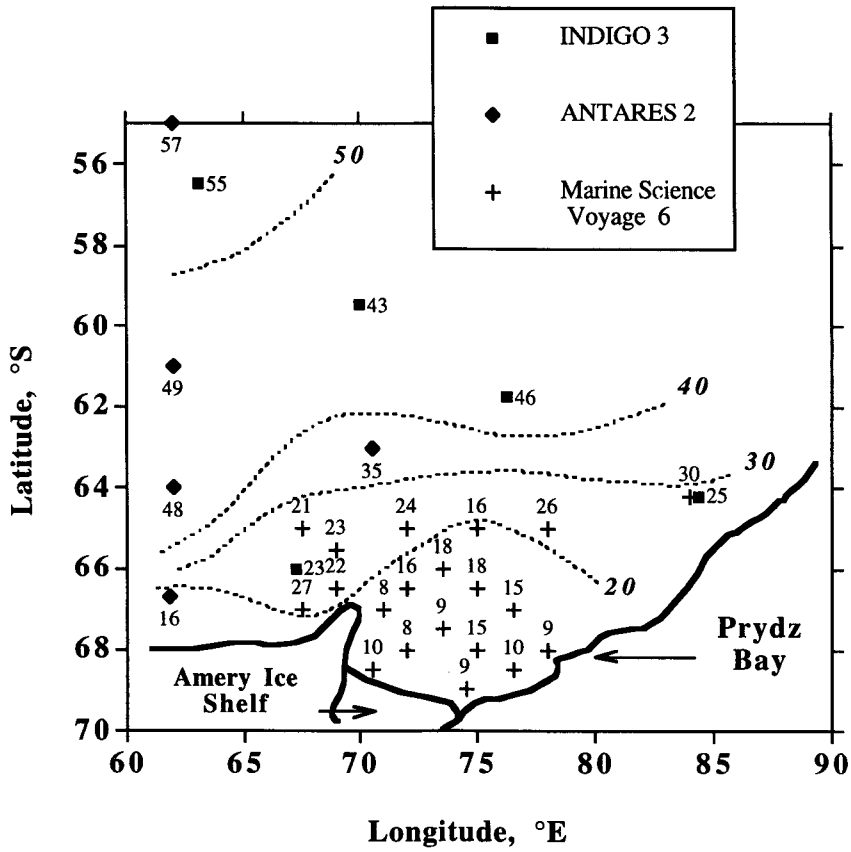

Figure 20b: Spatial variability of export production (mg C m^{-2} d^{-1}) respired in the mesopelagic water column in the Indian sector; summer situation (January to March): Zoom on Prydz Bay area.

The PFZ between 60° and 70°E has higher export production than at 30°E. Sub-Antarctic and sub-tropical waters have again lower export production. For the Atlantic sector and the Weddell Sea highest export production occur in open ocean systems (ACC and PFZ and open central Weddell Sea), while lowest values are associated with shelf areas and the MIZ of the Scotia-Weddell Confluence area. The latter area behaves differently from the central Weddell Sea in that it is characterised by larger melt water input as a result of ice being continuously advected into this area by the Weddell gyre.

Table 10: Mesopelagic particulate Ba, Primary Production and Export Production for different environments of the Southern Ocean; n = number of samples. Calculations for background particulate Ba concentration = 50 pmol/l.

Station	Lat	Long	Prim. Prod. mgC/m²/d	n	MesoBa pmol/l	n	JO_2 µmol/l/d	ExP mgC/m²/d	ExP/Prim. Prod. %
Indian Sector									
INDIGO 3 (January - February 1987)									
ACC	57°-66°S	31°-85°E	n.d.		377 ± 111	11	0.010 ± 0.006	33 + 11	
PFZ	53°-57°S	31-64°E	n.d.		494	1	0.026	45	
Sub-Antarctic	44°-51°S	20-27°E	n.d.		280 ± 34	3	0.013 ± 0.002	22 ± 3	
Sub-Tropical	38°-42°S	18°-30°E	n.d.		173 ± 31	3	0.007 ± 0.002	12 ± 3	
ANTARES-2 (February - March 1994)									
Contin. Slope	66°41' S	61°51'E	262 (a)	1	212	1	0.009	16	6.3
ACC	55°-64° S	62°-70°30'E	336 ± 221 (a)	4	517 ± 88	4	0.027 ± 0.005	47 ± 9	18.9 ± 10.6
PFZ	49°-52° S	62°-68°25' E	164 ± 8 (a)	2	642 ± 193	4	0.034 ± 0.011	60 ± 20	40.7 ± 19.3
PRYDZ BAY; Marine Science Voyage 6 (January - March 1991)									
OOZ	64°10'-66°30'S	67°30'-84° E	182 ± 125 (b)	17	261 ± 45	11	0.012 ± 0.003	21 ± 5	12 ± 3
Contin. Shelf	67°-69°S	67°30'-70°30'E	1002 ±443 (b)	24	168 ± 59	10	0.007 ± 0.003	12 ± 6	1.2 ± 0.6
Atlantic Sector & Weddell Sea									
Scotia-Weddell Confluence: EPOS-2 (December 1988 - January 1989)									
Scotia Front	57°-59°S	47°-49°W	656 ± 140 (c)	8	253 ± 48	8	0.012 ± 0.003	21 ± 5	3.3 ± 0.7
MIZ	58°-62°S	47°-49°W	1113 ± 687 (c)	17	125 ± 38	17	0.004 ± 0.002	8 ± 4	2.9 ± 2.9
ANTX/6 (October - November 1992)									
ACC	53°-57°30'S	6°W	231 ± 94 (d)	4	295 ± 22	8	0.014 ± 0.001	25 ± 2	13.1 ± 5.2
PFZ	47°-51°S	6°W	1096 ± 934 (d)	7	415 ± 55	9	0.021 ± 0.003	37 ± 6	7.0 ± 6.4
Weddell Sea									
ANTX/7 (December 1992 - January 1993)									
Larsen Shelf	70°42' S	12°34'W			133	1	0.005	8	
Weddell Sea	63°19'-69° S	15°43'-53°04'W			388 ± 83	7	0.020 ± 0.005	34 ± 8	

n.d. = no data. (a) Piraux (1995). (b) Data for Jan. - March 1987, from Mathot (1993). (c) Mathot (1993). (d) Jochem *et al.* (1995) & Rommets *et al.* (1993)

In that aspect the Scotia Sea MIZ resembles the shelf area of Prydz Bay also continuously affected by melt water from Amery glacier. Furthermore, for the Scotia-weddell Confluence area, the Scotia Front to the north of the MIZ, might act as a physical barrier confining the effect of melt water input to a restricted area and hence increasing surface layer stabilisation.

For OOZ and areas of the Atlantic and Indian ACC respiration of exported carbon in the mesopelagic depth zone represents between 13 and 19 % of local primary production. For the PFZ these values vary more widely, between 7 and 41 % for the Atlantic and Indian sector, respectively. The higher values for the PFZ in the Indian sector probably also reflect a seasonal effect. Indeed, In the Indian sector sampling was always during late summer, early autumn while for the PFZ in the Atlantic sector it was early spring. Thus, accumulation of mesopelagic barite since the onset of the growth season proceeded over a longer time span in the Indian sector than in the Atlantic sector. For the MIZ areas of the Weddell - Scotia Confluence and the Prydz Bay continental shelf, mesopelagic POC respiration is much lower with values ranging between 1 and 3 % respectively.

3.3.6. Temporal evolution of export production — The data presented in Table 10 cover the southern hemisphere spring to autumn period (October - March). A more complete picture of the year round temporal evolution was obtained for the Indian Ocean sector where a fixed site (Kerfix station; 50°40'S -68°25'E) was sampled on a monthly basis from 1992 to 1994 (Jeandel *et al.*, 1996b).

The particulate Ba data in Figure 21 were obtained from SEM-EMP barite micro-crystal counting and sizing in suspended matter from 150m, 350m and 500m depth. Deduced heterotrophic respiration rates of carbon indicate highest values for January and February and November 94. For end of 93, beginning of 94 there is about a one month delay between the mesopelagic Ba maximum and the upper water column Chl. *a* maximum which is centred on December 93 (Fiala *et al.*, 1995 and Jeandel *et al.*, 1996b).

The observed temporal evolution indicates a relatively close coupling (in the order of a few weeks) between increase of primary production and phytoplankton biomass and the mesopelagic Ba signal. This conclusion is also corroborated by

the observed temporal evolution of particulate Ba profiles in the ACC and PFZ of the Atlantic sector (expedition ANTARKTIS X/6). Indeed, stations which were re-occupied at two to three weeks interval and for which we had evidence (from T-S diagrams) that the same water body was sampled, showed very similar particulate profiles. However, for the areas where primary production increase indicated onset of the spring bloom, slight increases of the mesopelagic Ba signal were apparent (Dehairs *et al.*, 1996), again suggesting a rather close coupling between production and export + respiration of organic carbon at depth.

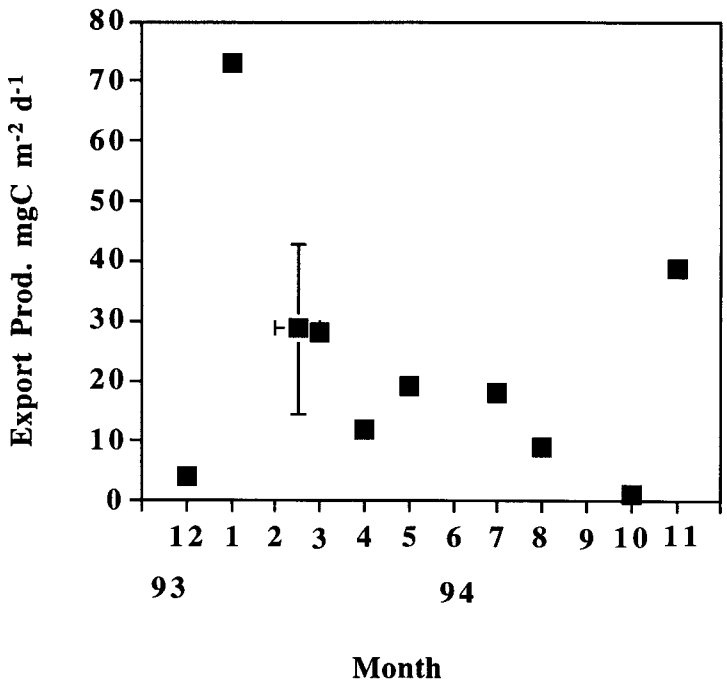

Figure 21: Seasonal evolution of exported POC oxidised in the mesopelagic water column at Kerfix station (50°40'S - 68°25'E).

3.3.7. Comparison of export production calculated from mesopelagic Ba and from sediment trap Ba fluxes — We have compared the calculated organic carbon respiration rates (which represent part of the carbon export flux) with new production derived from sediment trap Ba fluxes and which reflect the output rate of POC from the euphotic zone (Dymond *et al.*, 1992; Gingele and Dahmke,

1994; Nürnberg, 1995). Francois *et al.* (1995) have shown that organic carbon fluxes collected by sediment traps can be significantly contaminated with refractory carbon, advected from slope regions. Considering only stations well outside any influence of advected slope material. They observed the following empirical relationship between C_{org} and Ba fluxes:

$$\frac{FC_{org}}{FBa} = 4787.z^{-0.616} \qquad (13)$$

with FC_{org} and FBa the measured fluxes of organic carbon and Ba in µg cm^{-2} y^{-1} ; z = the depth of sampling in m.

This relationship was then substituted in another empirical relationship described by Sarnthein *et al.* (1988) and relating new, export production with the water column organic carbon flux and with depth:

$$ExP = exp[^{(LnFC_{org} + (0.5537.Lnz) - 3.023)}/_{0.6648}] \qquad (14)$$

with ExP = export production in g C m^{-2} y^{-1}, FC_{org} = organic carbon flux in mg C m^{-2} y^{-1} z = depth of sampling in m. Substitution of (3) in (4) gives (Nürnberg, 1995):

$$ExP = 3.56.(FBa)^{1.54}.z^{-0.0937} \qquad (15)$$

This equation is equivalent to the one given by Francois *et al.* (1995):

$$ExP = 1.95.(FBa)^{1.41} \qquad (16)$$

Eqn. (16) stresses the fact that FBa is rather independent of depth and is essentially controlled by surface water processes.

We have applied Eqn. (15) to two FBa sediment trap data sets from Nürnberg (1995): (1) PF3a; 614m; Polar Front Zone and (2) KG1a; 494m;.Bransfield Strait). We compare the data for sediment trap PF3a with our export production (i.e. rather rates of POC respired in the mesopelagic water column) estimates based on data for the same general region sampled during expedition ANTARKTIS X/6; Table 9 and 10). The KG1a Bransfield Strait data set will be compared with our export production estimates from the Scotia-Weddell Confluence area (EPOS-2 expedition; Table 10). From Figure 22a, b it appears that export production, as calculated from sediment trap data, is similar in magnitude to the value of mesopelagic POC oxidation, obtained from the mesopelagic Ba-barite stocks.

Implicitly this means that a major fraction of the exported carbon is heterotrophically respired in the mesopelagic depth region as also indicated by the vertical profiles of POC, showing largest concentration gradients in the epi- and mesopelagic waters (e.g. Francois *et al.*, 1995).

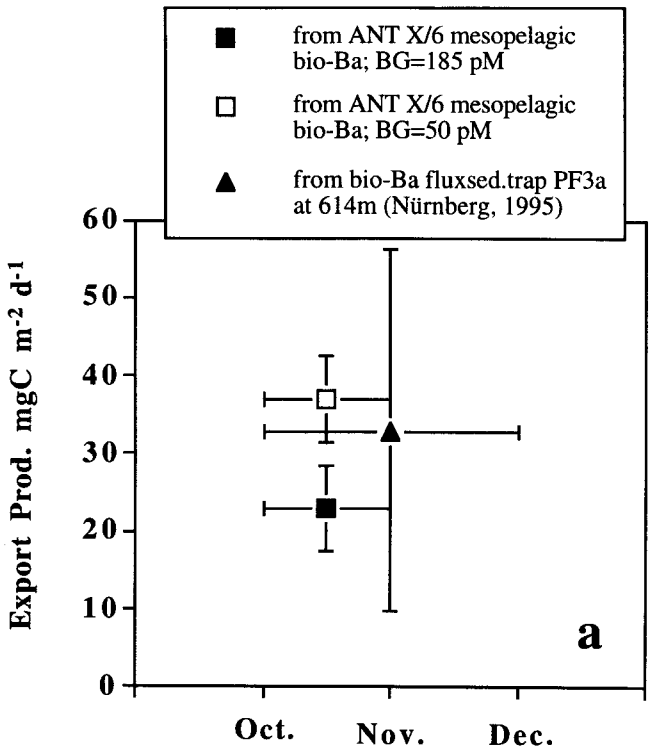

Figure 22a: Comparison of export production calculated from mesopelagic Ba data (i.e. export production respired in the mesopelagic area) with export production calculated from sediment trap bio-Ba fluxes in the Polar Front Zone and Atlantic sector: from mesopelagic Ba data for expedition ANTARKTIS X/6 (Table 10; Dehairs *et al.*, 1996) and sediment trap data (Δ) from Nürnberg (1995).

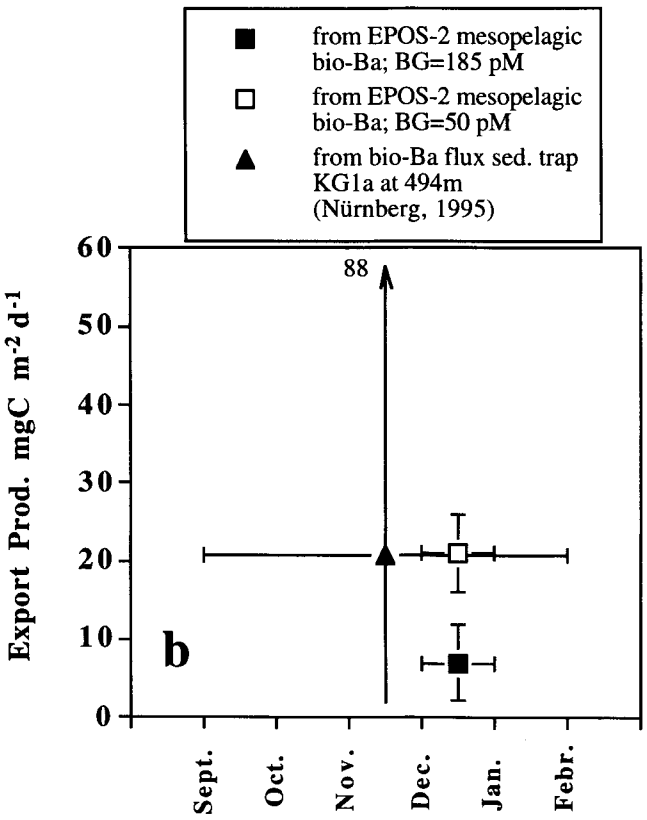

Figure 22b: Comparison of export production calculated from mesopelagic Ba data (i.e. export production respired in the mesopelagic area) with export production calculated from sediment trap bio-Ba fluxes in the Scotia Weddell area: from mesopelagic Ba data for EPOS-2 expedition (Table 10; Dehairs *et al.*, 1992) and sediment trap data (Δ) from Nürnberg (1995).

4. CONCLUSIONS

The Southern Ocean is the world's largest water body with an enormous stock of likely superfluous nutrients in its euphotic layer. Except for a few very sheltered sites the available nutrients are not completely removed from the water by primary producers. The general scenario is one of limited nutrient uptake and corresponding oligotrophy. In contrast to a seemingly monotonous nutrient signature, very important differences in nutrient uptake were observed. They underbuild the separation between two major groups, the NEA and SEA respectively.

The former group, largely representative of the OOZ environment, exhibited a relatively constant seasonal evolution. Despite nitrate abundance, absolute as well as specific nitrate uptake rates remained low throughout the season and dense bloom development did not occur. The dilute phytoplankton communities generally evidenced a significant presence of diatoms, although they were not always the predominant component. This constant lack of fertility contrasted strikingly with the temporal bloom events in the SEA.

The key process governing the SEA configuration was the enhanced nitrate uptake at the start of the productive season. The combination of several triggering effects resulting in an "ideal" physical and chemical environment as observed in the Antarctic MIZ and CCSZ, stimulated proportionally higher uptake of nitrate and induced the observed potential for silicate excess at nitrate depletion. In addition to those well described bloom enhancing effects, small injections of ammonium or other essential compounds in a sea of nitrate constituted a possible stimulation of nitrate uptake rates. The elevated nitrate consumption was quickly terminated, however, and severe exhaustion of the nitrate pool did generally not occur in Antarctic waters. Kamykowski and Zentara (1985) argued already that variations in the slopes of nitrate to silicate regressions were sensitive to the dominant nitrogen source. We conclude that the second nitrogenous nutrient has a major role in the decrease of specific nitrate uptake rates and consequently in the decrease of *f*-ratios. Build-up of exceptionally high ammonium stocks through heterotrophic activity inhibits phytoplanktonic nitrate uptake. The fertility of the SEA dwindles

rapidly due to a combination of top-down control (grazing pressure reducing the phytoplankton biomass) and bottom-up control (reduced nitrate uptake as a result of higher ammonium availability).

The latter controls seemed completely absent in the desert-like NEA. Both nutrients, nitrate and ammonium, contributed in a similarly low way to primary production. Nitrate concentrations remained high since the system was characterised by a reduced capacity to remove the ambient stock and ammonium accumulation as a result of heterotrophic remineralisation was absent. The system ran in a "steady state" mode, with low ammonium concentrations resulting from balanced uptake and remineralisation.

The variable nitrogen uptake regime and its possible implications for the phytoplankton community structure might open new research interests in view of describing and modelling the development of lower trophic levels in Antarctic waters. Could differences in fate gear the uptake of "functional" nutrients as nitrate and "structural" nutrients as silicate in the SEA?

Depending on the underlying biological and physico-chemical factors governing the growth and maintenance of phytoplankton in the euphotic zone, we demonstrated that the shift from new production to regenerated production can proceed with and without significant changes in the phytoplankton community structure. In the Antarctic MIZ zones, this shift was paralleled by a change in the community structure from a diatom dominated microplankton assemblage early in the season to a flagellate dominated nanoplankton assemblage during late season. While the change in the nitrogen uptake regime was apparently caused by an increased ammonium availability, as mentioned above, the change in the community structure was brought about by selective grazing by large grazers and reduced water column stability. In areas such as the CCSZ, where the water column stability persisted and selective grazing pressure was less pronounced, diatoms dominated the assemblage throughout the season and modified their uptake regime in response to enhanced ammonium availability.

Export fluxes as traced by water column stocks of particulate Ba-barite, were found to be strongly dependent on the type of production. In regimes with predominant regenerated production, export production did not sustain significant mesopelagic stocks of Ba-barite. This appeared to be the characteristic situation for environments having shallow mixed layers as a result of melt water input, such as the N.W. Weddell Sea MIZ and the CCSZ in Prydz Bay. Although in these environments algae growth was high (large nitrate depletions and uptake rates at the beginning of the growth season) there was heavy grazing pressure also at least in the MIZ zones, as witnessed by high subsurface ammonium. Open ocean areas (OOZ and POOZ) of the ACC, on the contrary, had larger export fluxes despite their lower surface productivities (lower integrated nitrate depletions) and algae biomass. The latter properties were the result of deeper mixed surface layers and relatively reduced grazing pressures (lower subsurface ammonium build-up). The Polar Front region appear to be an intermediate system between MIZ-CCSZ and OOZ environments described above.

ACKNOWLEDGEMENTS

The authors take the opportunity to thank AWI, IFRTP and AAD, the captains and crew members of the research vessels (R.V. Polarstern, R.V. Marion Dufresne and R.V. Aurora Australis), the chief scientists and all colleagues for their magnificent treatment and assistance during work. They are very grateful to Jean-Pierre Clement for tireless technical assistance and to Olivier Collette, Sandra Marguiller and Jacques Navez for analysing numerous samples in the home lab.

Frank Dehairs is Research Associate at the Fund for Scientific Research-Flanders; Mengesha Semeneh was awarded a VUBAROS fellowship by the Vrije Universiteit Brussel.

The present study was funded by the Belgian Scientific Research Programme on the Antarctic (research project A3/03/001).

REFERENCES

Archer, S., Leakey, R., Sleigh, M., Burkill, P., and Appleby, C. 1995. Microbial dynamics in sea ice at a coastal Antarctic site: taxonomy, biomass and production, Southern Ocean JGOFS international symposium on "Carbon Fluxes and Dynamic Processes in the Southern Ocean: Present and Past", Brest 28–31 August 1995, abstract.

Becquevort, S., Mathot, S. and Lancelot, C. 1992. Interaction of the microbial community of the marginal ice zone of the north-western Weddell Sea through size distribution analysis. Polar Biol., 12: 211-218.

Bishop, J. K. B. 1988. The barite-opal-organic carbon association in oceanic particulate matter. Nature, 332: 341-343.

Boyle, E.A. 1988. The role of vertical chemical fractionation in controlling late quaternary atmospheric carbon dioxide. Journal of Geophysical Research, 93: 15701-15714.

Broecker, W.S., Blanton, S. , Smethie, W.M. and Ostlund, G. 1991. Radiocarbon decay and oxygen utilization in the deep Atlantic Ocean. Global Biogeochemical Cycles, 5: 87-111.

Broecker, W.S., Takahashi, T. and Takahashi, T. 1985. Sources and flow patterns of deep-ocean waters as deduced from potential temperature, salinity and initial phosphate concentration. Journal of Geophysical Research, 90: 6925-6939.

Callahan, J.E. 1972. The structure and circulation of deep water in the Antarctic. Deep-Sea Research, 19: 563-575.

Chow, T. J. and Goldberg, E. D. 1960. On the marine geochemistry of barium. Geochimica et Cosmochimica Acta, 20: 192-198.

Church, T. M. 1970. Marine barite, Ph.D. thesis, University of California, San Diego, 100 pp.

Church, T.M. and Wolgemuth, K. 1972. Marine barite saturation, Earth and Planetary Science Letters, 15: 35-44.

Collos, Y. 1987. Calculations of ^{15}N uptake rates by phytoplankton assimilating one or several nitrogen sources. Appl. Radiat. Isot., 38: 275 - 282.

Cota, G. F., Smith, W. O. Jr., Nelson, D. M., Muench, R. D., and Gordon, L. I. 1992. Nutrient and biogenic particle distributions, primary productivity and nitrogen uptake in the Weddell-Scotia Sea marginal ice zone during winter. J. Mar. Res., 50: 155 - 181.

Cullen, J. J. 1991. Hypotheses to explain high-nutrient conditions in the open sea. Limnol. Oceanogr., 36: 1578 - 1599.

de Baar, H. J. W. 1994. Von Liebig's law of the minimum and plankton ecology (1899 - 1991). Prog. Oceanog., 33: 347 - 386.

Dehairs, F. , Baeyens, W. and Goeyens, L. 1992. Accumulation of suspended barite at mesopelagic depths and export production in the Southern Ocean. Science, 258: 1332-1335.

Dehairs, F., Chesselet, R. and Jedwab, J. 1980. Discrete suspended particles of barite and the barium cycle in the open ocean. Earth and Planetary Science Letters, 49: 528-550.

Dehairs, F., Goeyens, L., Stroobants, N., Bernard, P., Goyet, C., Poisson, A. and Chesselet, R. 1990. On suspended barite and the oxygen minimum in the Southern Ocean. Global Biogeochemical Cycles, 4: 85-102.

Dehairs, F., Lambert, C.E., Chesselet, R. and Risler, N. 1987. The biological production of marine suspended barite and the barium cycle in the Western Mediterranean Sea, Biogeochemistry, 4: 119-139.

Dehairs, F., Shopova, D., Ober, S., Veth, C. and Goeyens, L. 1996. Particulate barium stocks and oxygen consumption in the Southern Ocean mesoplegaic

water column during spring and early summer: Relationship with export production. Deep-Sea Research, in press.

Dehairs, F., Stroobants, N. and Goeyens, L. 1991. Suspended barite as a tracer of biological activity in the Southern Ocean. Marine Chemistry, 35: 399-410.

Dortch, Q.,1990. The interaction between ammonium and nitrate uptake in phytoplankton. Mar. Ecol. Progr. Ser. 61: 183 - 201.

Dugdale, R. C., and Goering, J. J., 1967. Uptake of new and regenerated forms of nitrogen in primary productivity. Limnol. Oceanogr., 23: 196 - 206.

Dugdale, R. C., and Wilkerson, F. P., 1986. The use of 15N to measure nitrogen uptake in eutrophic oceans; experimental considerations. Limnol. Oceanogr., 31: 673 - 680.

Dugdale, R. C., and Wilkerson, F. P., 1991. Low specific nitrate uptake rate : A common feature of high-nutrient, low-chlorophyll marine ecosystems. Limnol. and Oceanogr., 36: 1678 - 1688.

Dymond J., Suess, E. and Lyle, M. 1992. Barium in deep-sea sediment: A geochemical proxy for paleoproductivity. Paleoceanography, 7: 163-181.

El-Sayed, S. 1988. Seasonal and interannual variabilities in Antarctic phytoplankton with reference to krill distribution. In: D. Sarhage (ed.), Antarctic Ocean and Resources Variability. Springer-Verlag, Berlin Heidelberg, New York, p 101-119.

El-Sayed, S. Z., 1987. Biological productivity of antarctic waters: present paradoxes and emerging paradigms. In: El-Sayed S. Z. and Tomo A. P. (Editors.), Antarctic Aquatic Biology. SCAR, Cambridge, pp. 1 - 21.

El-Sayed, S., Biggs, D. C. and Holm-Hansen, O. 1983. Phytoplankton standingcrop, primary productivity, and near-surface nitrogenous nutrient fields in the Ross Sea. Antarctica. Deep-Sea Res., 30(8): 871-886.

Eppley, R. W., and Peterson, B. J., 1979. Particulate organic matter flux and planktonic new production in the deep ocean. Nature, 282: 677 - 680.

Fanning, K. A., 1992. Nutrient provinces in the sea: concentration ratios, reaction rate ratios, and ideal covariation. J. Geophys. Res., 97: 5693 - 5712.

Fiala, M., Oriol, L., Vetion, G., Guillot, P., Mason, J. and Dureau, G. 1995. Seasonal changes in the size fractionated phytoplankton phytoplankton biomass off Kerguelen islands, Southern Ocean JGOFS International Symposium, "Carbon fluxes and Dynamic Processes in the Southern Ocean: Present and Past", Brest 28-31 August 1995, abstract.

Francois, R., Honjo, S., Manganini, S.J. and Ravizza, G.E. 1995. Biogenic barium fluxes to the deep sea: Implications for paleoproductivity reconstruction. Global Biogeochemical Cycles, 9: 289-303.

Fritsen, C. H., Lytle, V. I., Ackley, S. F. and Sullivan, C. W. 1994. Autumn bloom of Antarctic pack-ice algae. Science, 266: 782-784.

Froneman, P. W., Perissinotto, R. and McQuaid, C. D. 1995. Microzooplankton grazing andcommunity structure in the Southern Ocean: Seasonal variations and implications for carbon cycling, Southern Ocean JGOFS international symposium on "Carbon Fluxes and Dynamic Processes in the Southern Ocean: Present and Past", Brest 28–31 August 1995, abstract.

Gargett, A. E. 1989. Ocean turbulence. Annual Review of Fluid Mechanics, 21: 419-451.

Garrison, D. L. and Buck, K. R. 1985. Sea-ice algal communities in the Weddell Sea: species composition in the ice and plankton assemblages. In: J. S. Gray and M. E. Chritiansen (Eds.), Marine Biology of Polar Regions and Effects of Stress on Marine Organisms. John Wiley and Sons, p 103-122.

Garrison, D. L., Buck, K. R. and Gowing, M. M. 1993. Winter plankton assemblage in the ice edge zone of the Weddell and Scotia Seas: composition, biomass and spatial distributions. Deep-Sea Res., 40(2): 311-338.

Georgi, D.T. 1981. On the relationship between large-scale property variations and fine structure in the Circumpolar Deep Water. Journal of Geophysical Rsearch, 86: 6556-6566.

Gingele, F. and Dahmke, A. 1994. Discrete barite particles and barium as tracers of paleoproductivity in South Atlantic sediments. Paleoceanography, 9: 151-168.

Goeyens L., Sörensson F., Tréguer P., Morvan J., Panouse M. and Dehairs, F. (1991). Spatiotemporal variability of inorganic nitrogen stocks and assimilatory fluxes in the Scotia-Weddell Confluence area, Marine Ecology Progress Series 77: 7

Goeyens, L. and Dehairs, F. 1993. Seasonal fluctuation of export and recycled production in different subareas of the Southern Ocean. Belgian Scientific Research Programme on Antarctica, Prime Mister's Services, Science Policy Office, Contract ANTAR II/08, Brussels, Belgium.

Goeyens, L., Tréguer, P., Baumann, M. E. M., Baeyens, W., and Dehairs, F., 1995. The leading role of ammonium in the nitrogen uptake regime of Southern Ocean marginal ice zones. J. Mar. Syst., 6: 345 - 361.

Goeyens, L., Tréguer, P., Lancelot, C., Mathot,S., Becquevort, S., Morvan, J., Dehairs, F. and Baeyens, W. 1991b. Ammonium regeneration in the Scotia-Weddell Confluence area during spring 1988. Mar. Ecol. Prog. Ser., 78: 241-252.

Harrison, W.G., Harris, L.R. and Irwin, B.D. 1996. The kinetics of nitrogen utilization in the oceanic mixed layer: Nitrate and ammonium interactions at nonomolar concentrations. Limnol. Oceanogr., 41: 16 - 32.

Hart, T. J., 1934. On the phytoplankton of the southwest Atlantic and Bellingshausen Sea, 1929 - 31. Discovery Rep., 8: 1 - 268.

Hutchins, D. A., DiTullio, G. R. and Bruland, K. W. 1993. Iron and regenerated production: Evidence for biological recycling in two marine environments. Limol. Oceanogr. 38(6):1242-1255.

Jacques, G. and Panouse, M. 1991. Biomass and composition of size fractionated phytoplankton in the Weddell-Scotia Confluence area. Polar Biol., 11: 315-328.

Jacques, G., 1983. Some ecological aspects of Antarctic phytoplankton. Polar Biol., 2: 27 - 33.

Jamous D., Mémery, L., Andrié, C., Jean-Baptiste, P. and Merlivat, L. 1992. The distribution of Helium 3 in the deep western and southern Indian Ocean. Journal of Geophysical Research, 97: 2243-2250.

Jeandel, C., Dupré, B., Lebaron, G., Monnin, C. and Minster, J.-F. 1996a. Longitudinal distributions of dissolved barium, silica and alkalinity in the western and southern Indian Ocean, Deep-Sea Research, 43: 1-31.

Jeandel, C., Ruiz-Pino, D., Gjata, E., Poisson, A., Brunet, C., Charriaud, E., Dehairs, F., Delille, D., Fiala, M., Fravalo, C., Miquel, J.-C., Park, Y.-H., Quéguiner, B., Razouls, S., Shauer, B. and Tréguer, P. 1996b. KERFIX, A time series station in the Southern Ocean: A presentation, Journal of Marine Systems, in press.

Jennings, J. C. Jr., Gordon, L. I., and Nelson, D. M., 1984. Nutrient depletion indicates high primary productivity in the Weddell Sea. Nature, 309: 51 - 54.

Jochem, F.J., Mathot, S. and Quéguiner, B. 1995. Size-fractionated primary production in the open Southern Ocean in austral spring. Polar Biology, 15: 381-392.

Kamykowski, D., and Zentara, S. J., 1985. Nitrate and silicic acid in the world ocean: patterns and processes. Mar. Ecol. Prog. Ser., 26: 47 - 59.

Kamykowski, D., and Zentara, S. J., 1989. Circumpolar plant nutrient covariation in the Southern Ocean: patterns and processes. Mar. Ecol. Prog. Ser., 58: 101 - 111.

Koike, I., Holm-Hansen, O. and Biggs, C. 1986. Inorganic nitrogen metabolism by Antarctic phytoplankton with special reference to ammonium recycling. Mar. Ecol. Prog. Ser., 30: 105-116.

Kopczynska, E. 1992. Dominance of microflagellates over diatoms in the Antarctic areas of deep vertical mixing and krill concentrations. J. Plankton Res., 14(8): 1031-1054.

Kopczynska, E., Goeyens, L., Semeneh, M. and Dehairs, F. 1995. Phytoplankton composition and cell carbon distribution in Prydz Bay, Antarctica: Relation to organic particulate matter and its $\partial^{13}C$ values, Journal of Plankton Research, 17: 685-707.

Koroleff, F. 1969. Direct determination of ammonia in natural waters as indophenol blue. International Council for the Exploration of the Sea 9: 19-22.

Kroopnick, P. 1974. The dissolved system in the eastern equatorial Pacific. Deep-Sea Research, 21, 211-227.

Le Corre, P., and Minas, H. J. 1983. Distributions et évolution des elements nutritifs dans le secteur indien de l' Ocean Antarctique en fin de periode estivale. Oceanol. Acta, 6 : 365 - 381.

Ledwell J.R., Watson, A.J. and Law, C. S. 1993. Evidence for slow mixing across the pycnocline from an open-ocean tracer-release experiment. Nature, 364: 701-703.

Legendre, L., Ackley, S.F., Dieckmann, G.S., Gulliksen, B., Horner, R., Hoshiasi, T., Melnikov, I.A., Reeburgh, W.S., Spindler, M. and Sullivan, C.W. 1992. Ecology of sea ice biota: Global significance. Polar Biology, 12: 429-444.

Martin, J. H. 1990. Glacial-interglacial CO2 change: the iron hypothesis. Paleoceanography, 5: 1 - 13.

Martin, J. H., and Fitzwater, S. E. 1988. Iron deficiency limits phytoplankton growth in the north-east Pacific subarctic. Nature, 331: 341 - 343.

Martin, J. H., Fitzwater, S. E. and Gordon, R. M. 1990b. Iron deficiency limits phytoplankton growth in Antarctic waters. Global Biogeochem. Cycles 4: 5-12.

Mathot, S. 1993. Phytoplankton in the Marginal Ice Zone and its contribution to the annual primary production of the Southern Ocean, Doctoral Thesis, Université Libre de Bruxelles, 201 pp.

McCarthy, J. J., Taylor, W. R., and Taft, J. L. 1977. Nitrogenous nutrition of the plankton in the Chesapeake Bay. 1. Nutrient availability and phytoplankton preferences. Limnol. Oceanogr., 22: 996 - 1011.

Minas, H. J., Minas, M., and Packard, T. T. 1986. Productivity in upwelling areas deduced from hydrographic and chemical fields. Limnol. Oceanogr., 31: 1182 - 1206.

Neori, A., and Holm-Hansen, O. 1982. Effect of temperature on rates of photosynthesis in Antarctic phytoplankton. Polar Biol., 1: 33 - 38.

Nürnberg, C.C. 1995. Bariumfluss und Sedimentation im südlichen Südatlantik - Hinweise auf Produktivitätsänderungen im Quartär, Geomar Report 38, 105 pp.

Osborn, T.R. 1980. Estimates of the local rate of vertical diffusion from dissipation measurements. Journal of Physical Oceanography, 10: 83-89.

Peng, T.-H., Takahashi, T. and Broecker, W.S. 1987. Seasonal variability of carbon dioxide, nutrients and oxygen in the northern North Atlantic surface water: Observations and a model. Tellus, 39B: 439-458.

Piola, A.R. and Georgi, D.T. 1982. Circumpolar properties of Antarctic Intermediate Water and Subantarctic Mode Water. Deep-Sea Research, 29: 687-711.

Piraux, J. 1995. De l'utilisation du profileur PNF-300, pour la mesure *in-situ* de la biomasse phytoplanctonique et de la photosynthèse chlorophyllienne en milieu marin, Travail de fin d'étude, Université Libre de Bruxelles, 95 pp.

Priddle, J., Croxall, J. P., Everson, I., Heywood, R. B., Murphy, E. J., Prince, P. A. and Sear, C. B. 1988. Large scale fluctuations in distribution and abundance of krill—a discussion of possible causes. In: D. Sarhage (ed.), Antarctic Ocean and Resources Variability. Springer, Berlin Heidelberg, New York, p 1-18.

Probyn, T. A. and Painting, S. J. 1985. Nitrogen uptake by size-fractionated phytoplankton in Antarctic surface waters. Limnol. Oceanogr., 30: 1237-1332.

Reid, J.L., Nowlin, W.D. and Patzert, W.C. 1977. On the characteristics and circulation of the southwestern Alantic Ocean. Journal of Physical Oceanography, 7: 62-91.

Riebesell, U., Schloss, I. and Smetacek, V. 1991. Aggregation of algae released from melting sea ice: Implications for seeding and sedimentation. Polar Biology, 11: 239-248.

Roether, W., Schlitzer, R., Putzka, A., Beining, P., Bulsiewicz, K, Rohardt, G. and Delahoyde, F. 1993. A chlorofluoromethane and hydrographic section across Drake Passage: Deep water ventilation and meridional property transport. Journal of Physical Oceanography, 98: 14423-14435.

Rommets, J.W., Stoll, M.H.C., Dapper, R., de Baar, H.J.W. and Veth, C. 1993. Bottle Casts databases, Frühling Im Eis, R.V. Polarstern Cruise ANTARKTIS X/6, Punta Arenas to Capetown, 29 September - 29 November 1992, V. Smetacek Chief Scientist.

Sakshaug, E. and Holm-Hansen, O. 1984. Factors governing pelagic production. In O. Holm-Hansen, L. Bolis and R. Gilles (Ed.), Marine Phytoplankton and Productivity. Springer, Berlin, p 1-18.

Sarnthein, M.K., Winn, K., Duplessy, J.C. and Fontugne, M.R. 1988. Global variations of surface ocean productivity in low and midlatitudes: Influence on CO2 reservoirs of the deep ocean and atmosphere during the last 21,000 years, Paleoceanography, 3: 361-399.

Schloss, I. and Estrada, M. 1994. Phytoplankton composition in the Weddell-Scotia Confluence area during austral spring in relation to hydrography. Polar Biol., 14: 77-90.

Schnack, S. B., Smetacek, V., Bodungen, B. V. and Stegmann, P. 1985. Utilisation of phytoplankton by copepods in Antarctic waters during spring. In J. S. Gray and

M. E. Chritiansen (Eds.), Marine Biology of Polar Regions and Effects of Stress on Marine Organisms. John Wiley and Sons, p 65-81.

Semeneh, M. 1992. Variation in new and regenerated production in the Southern Ocean. M. Sc Thesis, Vrije Universiteit Brussel, Brussels, PP 1-63.

Semeneh, M., Dehairs, F., Baumann, M. E. M., Lancelot, C., Elskens, M., Kopczy´nska, E. E. and Goeyens, L. 1995. Nitrogen uptake regime and phytoplankton community structure in the Atlantic and Indian sectors of the Southern Ocean, J. Mar. Sys. (submitted).

Shopova D., Dehairs, F. and Baeyens, W. 1995. A simple model of biogeochemical element distribution on the water column of the Southern Ocean. Journal of Marine Systems, 6: 331-344.

Smith, W. O. and Nelson, D. M. 1985. Phytoplankton bloom produced by a receding ice edge in the Ross Sea: Spatial coherence with the density field. Science, 227: 163-166.

Smith, W. O. Jr., and Nelson, D. M., 1990. Phytoplankton growth and new production in the Weddell Sea marginal ice zone in the austral spring and autumn. Limnol. Oceanogr., 35 : 809 - 821.

Stroobants, N., Dehairs, F., Goeyens, L., Vandereijden, L. and Van Grieken, R. 1991. Barite formation in the Southern Ocean water column. Marine Chemistry, 35: 411-421.

Tréguer, P. and Jacques, G. 1992. Dynamics of nutrients and phytoplankton, and fluxes of carbon, nitrogen and silicon in the Antarctic Ocean. Polar Biol., 12: 149 - 162.

Tréguer, P.and Le Corre, P. 1975. Manuel d'analyse des sels nutritifs: utilisation de l' Autoanalyser II Technicon. Laboratoire de Chimie des Ecosystèmes Marins. Université de Bretagne Occidentale, pp. 50.

Veth, C., Peeken, I. and Scharek, R. 1996. Physical anatomy of fronts and surface waters in the ACC near the 6°W meridian during austral spring 1992. Deep-Sea Research, in press.

Webb, D.J., Killworth, P.D., Coward, A.C. and Thomson, S.R. 1991. The FRAM Atlas of the Southern Ocean, Natural Environment Research Council, Swindon, Archway Press, 67 pp.

Whitworth, T. and Nowlin Jr., S.R. 1987. Water masses and currents of the Southern Ocean at the Greenwich Meridian. Journal of Geophysical Research, 92: 6462-6476.

RESEARCH CONTRACT A3/11/001

2

ECOLOGICAL MODELLING OF THE PLANKTONIC MICROBIAL FOOD-WEB

Ch. LANCELOT[1],
S. BECQUEVORT,
P. MENON,
S. MATHOT and
J.-M. DANDOIS

UNIVERSITÉ LIBRE DE BRUXELLES
GROUPE DE MICROBIOLOGIE DES MILIEUX AQUATIQUES
CP 221
Campus de la Plaine
Bd du Triomphe
B-1050 Brussels
Belgium

[1] Corresponding author E-mail : lancelot@ulb.ac.be

TABLE OF CONTENTS

1. INTRODUCTION 5

1.1 The Paradoxical nature of the Southern Ocean 5

1.2 Towards a generic model of phytoplankton development in the Southern Ocean 7

2. MATERIEL AND METHODS 9

2.1 Polar expeditions 9

2.2 Methods 10
2.2.1 Enumeration and biomass estimate of auto and heterotrophic micro-organisms 10
2.2.2 Microbial activities 11

3. STRUCTURE AND FUNCTIONING OF THE ANTARCTIC PELAGIC FOOD WEB14

3.1 Phenomenological description at visited sites 16
3.1.1 Spring bloom at ANTX/6 site : low and high iron availability; severe meteorological conditions 16
3.1.2 Spring bloom at EPOS site : suffisant iron availability; favourable meteorological conditions; krill swarm passage 19
3.1.3 Late summer at ANTARES 2 site : suffisant iron availability; favourable meteorological conditions 22

3.2 Antarctic pelagic ecosystem functioning 23
3.2.1 Linear food chain, microbial food web : where and when in the Southern Ocean? 23
3.2.2 Microbial Food Web: the key role of by protozooplankton. 23

4. MODELLING C, N, FE THROUGH THE PLANKTONIC MICROBIAL FOOD-WEB OF THE SOUTHERN OCEAN : THE SWAMCO MODEL 27

4.1 Structure of the SWAMCO model 27

4.2 Equations and parameters 31
4.2.1 AQUAPHY : the phytoplankton model 31
4.2.2 HSB : the microbial loop model 43
4.2.3 The inorganic loop 45

4.3 Model results 47
4.3.1 Validation : application of the swamco model to the ANTX/6 site 47
4.3.2 SWAMCO scenarios : phytoplankton blooms and food web structure in the Southern Ocean : iron, krill, sea ice and wind 53

5. CONCLUSION AND PERSPECTIVES 64

6. REFERENCES 69

ABSTRACT

Physical, chemical and biological conditions governing phytoplankton bloom development and food chain structure in the Southern Ocean were investigated, based on field observations and mathematical modelling. Particular attention was given to sea-ice dynamics and wind stress in triggering phytoplankton bloom induction; and iron and krill as vector of food chain structure and related surface carbon retention versus exportation. Within this framework, research was focusing on conditions determining the development of diatoms- versus nanoflagellates-dominated phytoplankton communities as well as on the dynamics of the microbial food web. Sampled sites were crossing areas with contrasting meteorological conditions and sea-ice dynamics, dissolved iron availability and krill inhabitence : the EPOS site in the iron-rich marginal ice zone of the northwestern Weddell Sea, crossed by krill swarms and experiencing in spring-summer 1988 extremely favourable meteorological conditions (average wind : $7 m.s^{-1}$); the ANTX/6 site crossing at 6°W the iron-rich Polar Frontal Jet and the sea-ice-associated iron-deficient Antarctic Circumpolar Current while submitted in early spring 1992 to severe meteorological conditions (average wind : $11 m.s^{-1}$); the iron-suffisant ANTARES 2 site in the Indian sector of the Soutern Ocean and experiencing in late summer 1994 auspicious meteorological conditions.

Biomass of auto- (diatoms and nanoflagellates) and hetero- (bacteria, bactivorous and herbivorous protozoa) trophic microorganisms were spatio-temporaly measured and their mutual interactions were assessed. Process-oriented studies were conducted for determining the physiological characteristics of diatoms and nanoflagellates growth and the feeding functional properties of the protozoan community. It is shown that diatoms and nanoflagellates growth differs by the only iron biochemistry and affinity for iron concentration, photosynthetic properties being identical for both phytoplankton groups. The protozoan community can be regarded as composed of two groups characterized by their own diet and feeding characteristics : the strictly bactivorous heterotrophic nanoflagellates and the protistovorous protozoa feeding on almost exclusively the auto- and heterotrophic flagellates. Furthermore ingestion rates of these two communities can be described by a specific food saturation function above a threshold food concentration below which feeding does not occurr. Based on these results, the numerical code of the 1D mechanistic SWAMCO model, describing carbon, nitrogen and iron cycling through the microbial food chain closed by copepod grazing pressure was established. The SWAMCO model was calibrated and validated on the ANTX/6 site.

Observational ecosystem analysis and mathematical simulations with the 1D-coupled physical-biological SWAMCO model forced by the chemical and meteorological conditions during the EPOS and ANTX/6 expeditions show the tight coupling between atmospheric forcing - most notable in frequency, duration and strenght of storm events - and phytoplankton blooms occurrence. In particular it is demonstrated that the sustained windy meteorological conditions prevailing during

the ANTX/6 expedition was the main factor preventing blooms from developping at the receeding ice-edge. Furthermore it is demonstrated that under events of favourable meteorological conditions for phytoplankton bloom initiation, the structure of the developing phytoplankton community is determined by iron availability with nanoflagellates outcompeting diatoms at iron subnanomolar concentration . Hence it can be savely concluded that the general HNLC (High Nutrient Low Chlorophyll) conditions of the Southern Ocean are resulting from the sucessfull development of grazer-controlled nanophytoplanktonic communities in a low-iron environment. Superimposing this active microbial food web, episodic blooms of diatoms are well developping in iron-enriched areas experiencing favourable meteorological conditions like near-shore neretic areas supplied with iron from shelf sediments, the rapidly eastward flowing Polar Frontal Jet retaining a significant signal of iron from shelf source and to a less extent some sea-ice covered areas having cumulated minor annual aerosol inputs. When optimal light conditions are maintained diatom growth is however limited by iron avalaibility and/or krill grazing pressure and the phytoplankton community structure shifts towards a nanoflagellates dominance.

Further research development would sake for coupling the generic SWAMCO mechanistic model with a 3D coupled sea-ice-ocean model of the global Southern Ocean to properly address the role of this remote ocean in global carbon cycle.

1. INTRODUCTION

1.1 THE PARADOXICAL NATURE OF THE SOUTHERN OCEAN

Besides the international interest in exploitation of Antarctic marine biological resources commenced in the eighteen century with the well-known disastrous consequences for biodiversity, the last few years have seen the development of numerous national and international programmes addressing the role played by the Southern Ocean in global carbon cycling and hence its influence on global climate regulation. From this respect, primary production constitutes a key process relating atmospheric and oceanic biogeochemical cycles. A significant amount of atmospheric carbon dioxide is indeed susceptible to be fixed by surface waters and exported to the deep ocean after incorporation into the food-web, giving support to the concept of the biological pump.

In most marine areas, inorganic nutrients are exhausted by phytoplankton uptake during the growing season; the transport of carbon to deep layers is then controlled by the flux of inorganic nutrients to surface waters. In this case, the biological pump works at its maximum capacity.

Some regions of the open ocean, however, are large surface ocean repositories of unused nitrate, phosphate and silicate throughout the year; phytoplankton biomass and primary production are lower than expected from nutrient availability. Among these, the Southern Ocean, that body of water South of the Antarctic Polar Front, covering 10% of the global ocean surface area. Within this region, the combined effects of wind stress and thermohaline circulation result in circumpolar surface divergence and upwelling which maintain high concentrations of all major nutrients (nitrate : 32.5 $mM.m^{-3}$; phosphate : 2.5 $mM.m^{-3}$; silicate : 100 $mM.m^{-3}$) in the surface layer (Bainbridge, 1980). The light regime, while highly seasonal, reaches during summer daily integrated values as high as in the tropics (Campbell and Aarup, 1989). Despite the permanently high nutrient concentrations and seasonally high incident surface light, primary production is generally low (e.g. the review by Mathot et al.,1992, Mathot et al., submitted). Mesoscale events of high productivity do however occur in (i) the polar front zone between 45° and 50°S (e.g. Bathmann et al., 1994); (ii) shallow, coastal embaymennts (e.g. Holm-Hansen and Mitchell, 1991) and (iii) the vicinity of the retreating ice-edge (e.g; Smith and Nelson, 1985; Lancelot et al.,1993b). Yet recorded maximum phytoplankton biomasses seldom reach the 25 mg Chl. a m^{-3} expected from the nutrients stocks (Mitchell and Holm-Hansen, 1991).

Several hypotheses have tempted to explain the paradox of high nutrients and low chlorophyll a concentrations (HNLC) in the Southern Ocean [e.g. special issue of Limnology and Oceanography (36(8), 1991) on "What controls phytoplankton production in nutrient-rich areas of the open sea?"; Lancelot et al., 1993a]. To date a

large consensus reunites the scientific community (e.g; Price et al., 1994; de Baar et al.1996, Lancelot et al., 1996) : phytoplankton growth in the Southern Ocean is under the triple control of (i) light availability driven by incident light and wind stress (e.g. Veth et al., 1993); (ii) iron availability and (iii) grazing pressure. However, the degrees to which physical, chemical and biological factors are co-limiting phytoplankton development is not fully understood and their relative importance may vary with location, time and local meteorological conditions (Lancelot et al., 1993a,b).

The major role played by ice cover and the turbulence of the water column in controlling available light to phytoplankton and hence blooming development has been evidenced by numerous field data. It is now admitted that deep-mixed ice-free areas are not highly productive and are dominated by nanoplanktonic communities (El-Sayed, 1984; Smetacek et al., 1990). On the other hand many observational evidences (e.g. Smith and Nelson 1985, 1986; Sakhaug and Holm-Hansen 1984; Nelson et al. 1987; Sullivan et al. 1988; Lancelot et al. 1991a,b) indicate that the circumpolar marginal ice zone is a region of enhanced primary production owing to the formation, at the time of ice melting, of a shallow vertically stable upper layer as a result of the production of meltwater and the subsequent seeding by actively growing sea ice microbes (Garrison et al., 1987). Provided the ice-edge is well-defined, these ice-edge related phytoplankton blooms trail the ice-edge as a narrow band 50 - 200 km wide (Smith and Nelson, 1985; Lancelot et al., 1993a). Yet phytoplankton biomass reached in these hydrodynamically stable areas, either dominated by nanophytoplankton (Hewes et al., 1990; Lancelot et al., 1993) or diatoms (Bianchi et al., 1993), remains modest, less than 10 mg Chl *a* m^{-3}, significantly lower than expected from nutrients concentrations (Hayes et al., 1984).

Trace metal limitation of phytoplankton growth development, in particular iron (Martin and Fitswater, 1988), has been investigated since 1988 in several regions of the Southern Ocean : the Weddell and Scotia Sea (de Baar et al., 1990), the Drake Passage (Helbling et al., 1991, Martin et al., 1990), the Ross Sea (Martin et al., 1990) and the Atlantic and Pacific sectors of the Antarctic Circumpolar Current (de Baar et al., 1995). Results indicate that the low availability of dissolved Fe would limit phytoplankton growth rate 'per se'. Rather Fe availability would structure the phytoplankton community that drives in turn the structure of the dominant food web (microbial food-web versus linear diatom-mesozooplankton food chain) and exportation. Low Fe supply is indeed limiting the growth rate of large diatoms while non affecting the development of pico- and nano-sized cells, better competitors at low nutrient concentration due to their large surface:volume ratio (Morel, 1990). The biomass of these minute organisms is kept at very low level, grazed by the ubiquitous fast-growing protozoa. Supporting this, Fe-rich (>2nM) areas like neritic nearshore Antarctic waters, Smith and Nelson, (1985) and the Polar front (de Baar et al., 1995, 1996) are developing diatom-dominated blooms. Furthermore, Fe-enrichment experiments in shipboard mesocosms (Martin et al., 1990; van Leeuwe et al., 1996; Scharek et al., 1996) show a positive response of the diatom component of the phytoplankton community at Fe >0.4 nM. However diatom dominance in Fe-sufficient regions of the Southern Ocean is not always observed. For instances the summer phytoplankton bloom recorded in the north-western Weddell Sea area in

1988 was dominated by nanoflagellates, mainly cryptomonas (Becquevort et al., 1993). Observational evidence suggests that the dominance of nano-sized microbes in that particular Fe-non-limiting area (Nolting et al., 199), was the consequence of a krill swarm passage (Jacques and Panouse, 1992; Lancelot et al., 1993b). Krill by selectively eliminating micro-sized microbes and mesozooplankton from the water column could have fasten the development of nano-sized phytoplankton and of herbivorous protozoa (Lancelot et al., 1993b). In this area, the dominant food-web structure is mainly driven by random top predator control.

Considering the circumpolar patchiness of krill (Cole, 1994) and dissolved iron (de Baar et al., 1996) distribution and the large variation of meteorological conditions, -in particular wind stress and sea ice prevailing at these high latitudes- the contribution of physical, chemical and biological factors to the control of phytoplankton bloom development will greatly vary within the Southern Ocean, both geographically and temporally. Phytoplankton of marginal ice zones in particular would experience forcing between two extrema - low trace metal concentration and windy meteorological conditions or sufficient trace metal concentration and serene meteorological conditions - giving rise to quite different phytoplankton species dominance and biomass and food-web structure. In regions where the former environmental conditions prevail, as for instances the Antarctic Circumpolar Current, modest nano-sized phytoplankton blooms, actively controlled by protozoa would be expected. The latter extreme conditions -high iron, low wind- on the other hand, are to be foreseen close to the continent e.g. the Ross Sea or the Prydz Bay and would stimulate the development of intensive blooms dominated by large diatoms.

1.2 Towards a generic model of phytoplankton development in the Southern Ocean

Addressing the role of the Southern Ocean in global carbon cycling and its response to or influence on climate change, stress then the need to write mechanistic models of marine ecology that describe and predict carbon, nitrogen and iron circulation through the polar ocean over seasons and years, in response to the physical forcing. These biogeochemical models have to be based on the best available understanding of biological processes of importance in carbon biomass formation and mineralisation in the surface waters of the ocean; carbon exportation to deeper layers of the ocean and have to take into consideration the dynamics of sea-ice retreat and formation. As a first step in this direction, a coupled-physical-biological model - the SWAMCO model (Lancelot et al., 1991,a,b; Lancelot et al., 1993a,b) - has been developed during the phase II of the Belgian Antarctic Programme for the simulation of nanophytoplankton development in the marginal ice zone of the north-western Weddell Sea associated to the dynamic process of ice retreat. The published SWAMCO model describes C and N circulation through aggregated biological components of the planktonic microbial food-web - nanophytoplankton, bacteria -, using temperature-dependent first-order kinetics for describing protozoan grazing pressure. Although outstanding for describing C cycling in regions of low Fe availability - the most important part of the Southern

Ocean -, the SWAMCO model does not apply in regions of Fe supply as the neritic continental waters and the Polar Front (de Baar et al., 1996). The current SWAMCO model is thus of little value for estimating the carbon sequestration capability of the Southern Ocean, as well as the ecosystem efficiency.

Complementing the structure of the SWAMCO model for its application at the scale of the whole Southern Ocean was our main objective in the scope of the Phase III of the Belgian Antarctic Programme. In order to take into consideration the key role of iron in driving the structure and functioning of the Southern Ocean ecosystem and then carbon exportation to the deep ocean versus its retention in the surface waters, the SWAMCO model structure was extended by (i) adding dissolved Fe as explicite state variable; (ii) considering two phytoplankton groups : nano-sized flagellates under control of protozoa grazing and large diatoms feeding mesozooplankton and krill and (iii) elaborating an explicite mathematical module of protozoan feeding activities and related ammonium and dissolved Fe regeneration.

Appropriate definition of the state variables and their controlling factors was derived from a comprehensive analysis of the structure and functioning of the microbial food-web as based on data gained during EPOS 88/89 (north-western Weddell Sea), ANTX/6 92 (Polar Front, ACC) and ANTARES 2 94 (Polar Front, Prydz Bay) and of current literature data. This ecosystem analysis was conducted on a regional basis considering the main areas (Polar Front, Marginal Ice Zone) of the Southern Ocean, in a dynamical view of the process of sea-ice melting and formation. This synthesis work is given in section 3 of the present report. Parametrization of the extended numerical code was derived from data on phytoplankton physiology and feeding activity of bactivorous and herbivorous protozoa gained during the SO-JGOFS expeditions ANT X/6 on board of RV Polarstern in the Atlantic sector of the Southern Ocean, in early spring 1992 (29th September - 29th November) and ANTARES 2 on board of RV Marion Dufresne in the Indian sector of the Southern Ocean in late summer 1994.

The model was validated through its application in the Atlantic sector of the Southern Ocean : the EPOS area (north-western Weddell Sea), an iron-rich, krill-abundant area and the ANTX/6 area covering both the iron rich-low krill Polar Front and the low iron-low krill ACC marginal zone. Model calibration and validation are presented in section 4 of the present rapport. Finally conditions that stimulate diatom-dominated blooms development in the Southern Ocean are investigated, based upon mathematical simulations with the one-dimensional coupled physical-biological SWAMCO, forced by either the moderate or the extremely windy weather conditions experienced during the *Polarstern* marginal ice zone expeditions EPOS and ANT X/6 and different conditions of dissolved Fe availability . Furthermore, the impact of krill on the ecosystem structure and functioning is considered.

2. MATERIEL AND METHODS

2.1 Polar expeditions

Field data were collected during 3 oceanographic cruises crossing different areas of the Southern Ocean at different time of the vernal season. Sampling includes transects in the Atlantic sector along the 6°W meridian, from September 29th to November 29th 1992 during the Southern Ocean - Joint Global Ocean Flux Study (Polarstern ANT X/6); in the Scotia-Weddell Sea area from November 22nd 1988 to January 9th 1989 during the European Polarstern Study (Epos leg 2); in the Indian sector along 62°E meridian, from January 29th to March 23th 1994 (ANTARES 2) in the scope of the ANTARES program (JGOFS-France). The different sampling areas are reported on Figure 2.1.

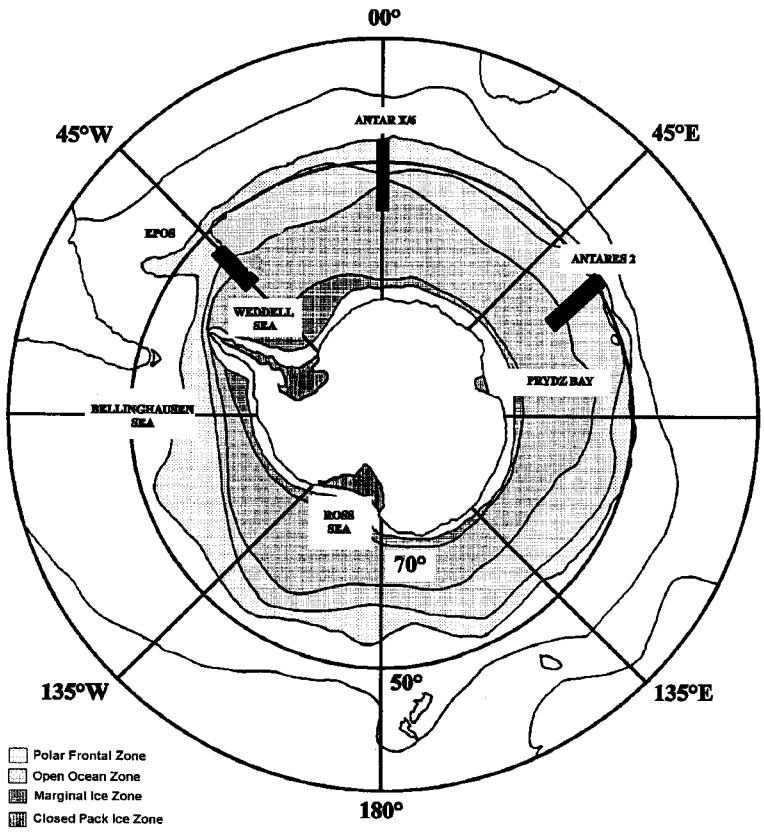

Figure 2.1: Location of ANT X/6, EPOS and ANTARES 2 cruises.

2.2 METHODS

2.2.1 Enumeration and biomass estimate of auto and heterotrophic micro-organisms

Due to the high diversity and broad range of sizes covered by microbial assemblages (0.2 to 200 µm), different preservation solutions, staining dyes (when required) and microscopy techniques have been applied for specific taxonomic groups (Table 2.I.).

Carbon biomass of each taxonomic group was calculated from biovolume measurement using the conversion factors listed in Table 2.II

Table 2.I.: Taxon definition and related sampling and preservation conditionning for microscopical analysis.

Taxon	Size, µm	Sampling volume, ml	Preservation solution	Microscopic analysis	Reference
Diatoms	> 20 < 20	50 - 100 10 - 20	Acid lugol (1 % final conc.)	Inverted light microscopy	Utermöhl, 1958
Autotrophic and heterotrophic flagellates	> 20	10 - 20	Glutardialdehyde (0.5 % final conc.)	Epifluorescence microscopy after DAPI staining	Porter and Feig, 1980
Ciliates	< 20	80			
Ciliates	> 20	50 - 100	Acid lugol (1 % final conc.)	Inverted light microscopy	Utermöhl, 1958
Bacteria	0.2 - 2	2 - 5	Formaldehyde (2 % final conc.)	Epifluorescence microscopy after DAPI staining	Porter and Feig, 1980

Table 2.II.: Conversion factors for carbon biomass estimate from biovolume measurement.

Taxon	Carbon Biovolume^{-1}, pgC µm^{-3}	Reference
Diatoms	0.11	Edler, 1979
Flagellates	0.22	Borsheim and Bratbak, 1987
Dinoflagellates	0.14	Lessard, 1991
Ciliates	0.19	Putt and Stoecker, 1989
Bacteria	Biovolume dependent Carbon/biovolume ratio	Simon and Azam, 1989

2.2.2 Microbial activities

Phytoplankton photosynthesis, growth and respiration

Physiological parameters characteristic of phytoplankton metabolism - photosynthesis, growth, respiration- were determined by mathematical fitting of two kinds of tracer experiments conducted in parallel under simulated *in situ* conditions, using equations of the AQUAPHY model of phytoplankton growth (Lancelot et al., 1991a). The method is described in extenso in Mathot et al. (1992). Shortly, photosynthetic parameters, on the one hand, were calculated from short-term (4-5h) ^{14}C incubations carried out at in situ temperature and various light intensities. Growth and respiration parameters, on the other hand, were deduced from long-term (24h) kinetics of ^{14}C assimilation into key cellular metabolites - proteins, polysaccharides, lipids and monomers - simulating, at in situ temperature and under either natural or constant saturating light intensity simulating the observed daily cycle.

Incident Photosynthetically Available Radiation (PAR) was continuously measured by means of a cosine Li-Cor sensor set up on the upper deck of the ship.

Protozooplankton feeding activity

The ingestion rates of bacteria and nanoplanktonic algae by protozooplankton were measured using the method based on the uptake of fluorescently labelled prey (Sherr et al., 1987; Rubblee and Gallegos, 1989). Bacteria or nanophytoplanktonic organisms were previously stained with 5-(4,6-dichlorotriazin-2yl)amino fluoresceine (DTAF). The method consists in inoculating natural microbial assemblages with either fluorescently labelled bacteria (FLB) or autotrophic flagellates and observe as a function of time the number of fluorescent prey ingested by protozoa. The initial slope of increase of fluorescent labelled prey ingested per protozoa is taken as a measure of ingestion rates.

Fluorescent labelled bacteria (FLB) were prepared from natural assemblages of bacterioplankton (mean biovolume of 0.06 μm^3) according to the procedure of Sherr et al. (1987). Fluorescent labelled algae (FLA) were supplied from culture of Antarctic Phaeocystis cells (Equivalent spherical diameters of 4 µm and mean biovolume of 33.5 μm^3) and stained according to Rubblee and Gallegos (1989).

Two types of experiments were conducted to study the functional behavior of protozooplankton.

- On the one hand the dependance of protozoan ingestion rate on prey abundance was determined by incubating at in situ temperature, natural assemblages of heterotrophic protozooplankton (250 to 1000 ml) at various concentrations of fluorescent preys between 10^6 and 2.5 10^7 FLA l^{-1} ,and 10^7 and 10^{10} FLB l^{-1}.

- On the other hand the influence of the presence of one type of prey (auto and heterotrophic flagellates) on the ingestion of the other type of prey (bacteria) was experimentally studied using the set-up of competitive experiments of Figure 2.2 (Menon et al., 1995). The methodology was the following: protozoan assemblages of several densities, obtained by dilution or concentration of natural communities in order to cover a large range of flagellate prey ($Np_{1,4}$) were incubated in the presence of four concentrations of fluorescently labelled bacteria ($Nb_{1,4}$).

For each experiment, the protozoan ingestion rate was measured kinetically as follows:

Sub-samples (50 to100 ml) were removed every 15 to 60 min. along the incubation period (2 to 8 h). Biological activity was immediately stopped through the sequential addition of the following preservatives: alkaline lugol solution (0.5% final concentration), borate buffered formalin (3% final concentration), and a drop of 3% sodium thiosulfate (Sherr et al., 1989). Samples were stored in glass vials at 4°C in the dark until preparation for microscopic analyses.

Preserved samples (10 to 80 ml) were stained with DAPI (Porter and Feig 1980). Protozoa were collected by filtration on 0.8 and 10 µm pore size polycarbonate membranes. Protozoan abundance and biomass and average number of FLB/FLA ingested per protozoa were determined by epifluorescence microscopy. Ingestion rates of bacteria and autotrophic flagellates were then calculated for different groups of protozoa from the linear slope of the time dependence curve of average FLB and FLA number ingested per protozoa (Sherr et al., 1987).

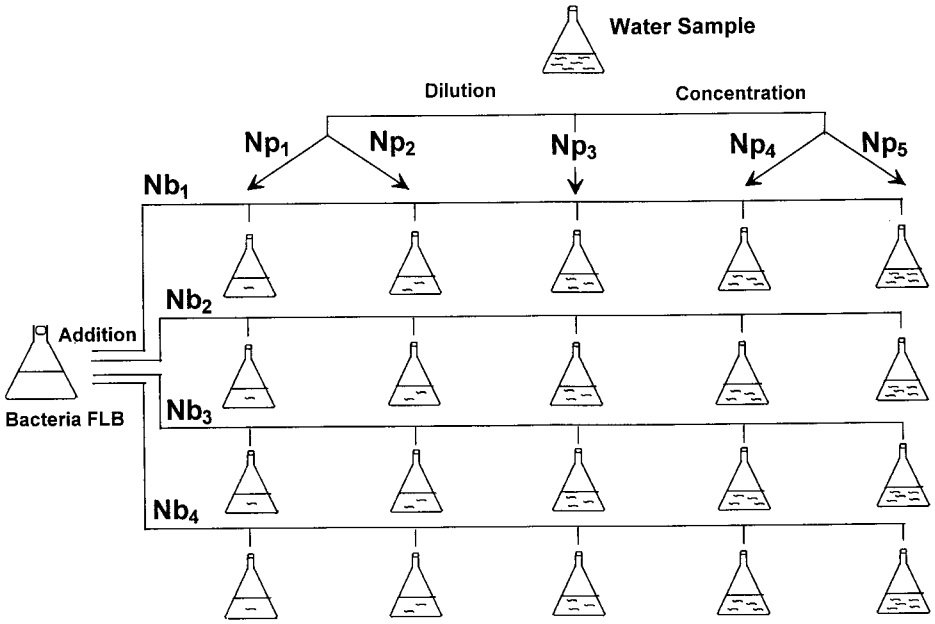

Figure 2.2: Competitive experiments of protozoan ingestion on bacteria and flagellates: experimental procedure. Nb_{1-4}: FLB at 4 concentrations, Np_{1-4}: Protozoan and autotrophic communities at 4 concentrations.

3. STRUCTURE AND FUNCTIONING OF THE ANTARCTIC PELAGIC FOOD WEB

The Antarctic pelagic food web can be regarded as a trophic continuum composed of two trophic branches (Figure 3.1.) : the linear food chain composed of microsized phytoplankters, herbivorous meso- and meta-zooplankters, krill and mammals and the microbial food web composed of pico- and nano-sized auto- and hetero-trophic microbes. Within this trophic network, two secondary producers occupy a key trophic position : protozooplankton as a link between the microbial food web and the linear food chain; krill as a link between the microbial food web and mammals. The dominance of one trophic branch over the other is not equivallent in terms of either trophic efficiency and biological ressources or geochemical balance. Indeed the linear food chain is often associated to high biological production and efficiency of the biological pump (high carbon exportation to the deep ocean and the sediments). Contrasting the dominance of an active network is often associated to regeneration processes i.e. nutrients and carbon retention in surface waters. Light environment and iron availability directly and krill indirectly (Lancelot et al., 1992; 1993b) have been reported as main factors controlling phytoplankton developments and biological production in the Southern Ocean. However their role as structuring vehicle of the Antarctic food web has not yet been assessed properly.

The relative importance of these physico-chemical and biological factors in structuring the Antarctic food chain is discussed in the following paragraphs, based on a comprehensive analysis of data collected. Three polar expeditions where contrasting environmental conditions were met: the windy 1992 early-spring ANTX/6 expedition crossing the iron-rich Polar Frontal jet and the iron-low Antarctic circumpolar current (47-58°S) around 6°W; the calm spring-summer EPOS cruise in the iron-rich, krill-inhabited northwestern Weddell Sea , the late-summer iron-rich ANTARES 2 expedition in the Indian sector of the Southern Ocean (50-66°S) both experiencing very favourable meteorological conditions.

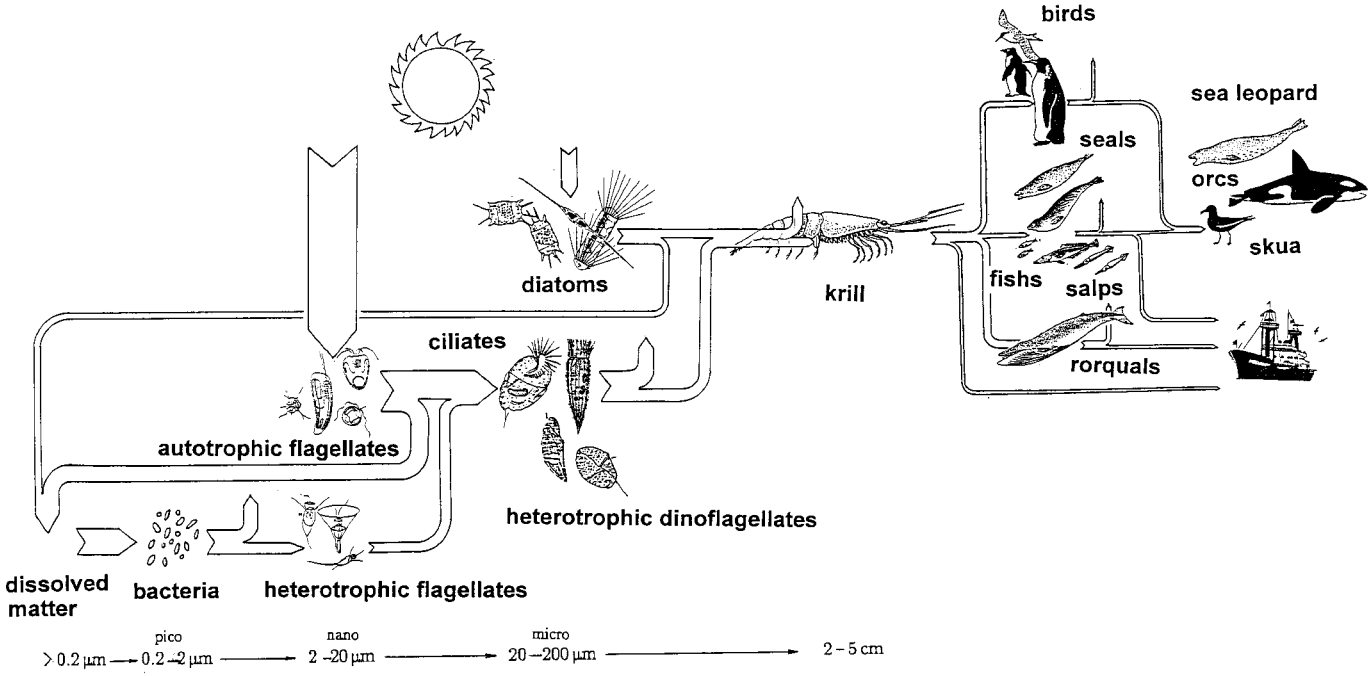

Figure 3.1: Schematic representation of the Antarctic pelagic food web.

3.1 PHENOMENOLOGICAL DESCRIPTION AT VISITED SITES

3.1.1 Spring bloom at ANTX/6 site : low and high iron availability; severe meteorological conditions

The ANTX/6 sampling site, at 6°W in the Atlantic sector of the Southern Ocean (Figure 2.1) is crossed by two contrasting water masses : the iron-depleted (~0.4nM) but partly sea-ice-associated southern branch of the ACC (~ 51-56°S) and the iron-enriched (1.8nM) Polar Frontal Jet (~ 47-50°S, Veth et al., 1996). Results of this cruise are publishing in a special issue of Deep-Sea Research. Transects were repeatedly sampled over a one-month period, at the early beginning of the growth season. During the early-spring period of 1992, meteorological conditions were severe, in particular wind speed and storm frequency (Figure 3.2.).

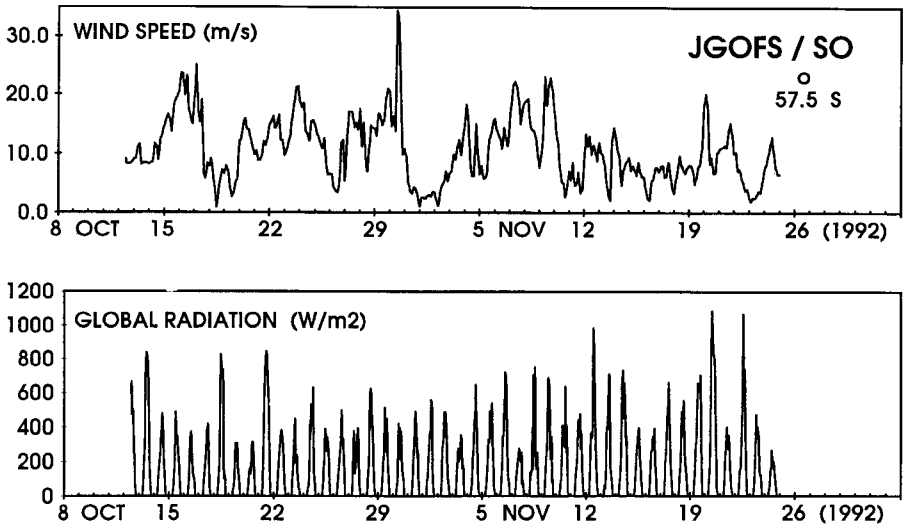

Figure 3.2: Wind speed (m s^{-1}) and global radiation (W m^{-2}) at 57.5 °S along 6°W meridian during ANTX/6 cruise.

Sea ice retreated abruptly from 54°S to 58°S and no phytoplankton bloom could be observed at the receding ice-edge (Figure 3.3.; Bathmann et al., 1996). Chlorophyll a concentrations were significantly less than 1 mg.m^{-3} (Bathmann et al., 1996) and the spring microbial community was organized in a complex microbial food network composed of autrophic nanoflagellates, bacteria, bactivorous (heterotrophic flagellates) and protistovorous protozoa (microprotozoa) of low and relatively stable biomass (Figure 3.4).

Contrasting, chlorophyll a concentrations as high as 3 $mg.m^{-3}$ were recorded in the Polar Frontal Jet, at the end of the sampling period (Figure 3.3; Bathmann et al., 1996). In about three weeks, chlorophyll a increased from 0.6-1.6 to 1.2-2.4 $mg.m^{-3}$ while dissolved iron exhibited a concomitant seasonal decrease of 1nM (de Baar et al., 1995). Elevated primary production between 1000 and 3000 mgC m^{-2} d^{-1} were recorded in the Polar Frontal Jet as well (Jochem et al., 1995) and the phytoplankton community was dominated by neretic diatoms such as Corethron criophilum and Fragilariopsis kerguelensis (Veth et al., 1996).

A complex microbial food-web developed in parallel with the linear food-chain initiated by significant biomass of diatoms (Figure 3.4). Biomass reached by bacteria, auto-and heterotrophic flagellates and microprotozoa were significantly higher (around a factor 2) compared to those reached in the ACC area (Figure 3.4). However, its importance compared to the linear food chain could be neglected as deduced from the comparison between diatoms and nanophytoplankton biomasses. The flagellated community indeed represented at a maximum 39 % of the diatom biomass. Furthermore, a strong control of microprotozoa on nanoflagellates was suggested by the observed concomittant variations of consumers and prey (Figure 3.4).

All together, it appears that iron availability was the critical factor determining the occurrence or the lack of phytoplankton blooms in these two systems, while the microbial food-web was operating over the whole area.

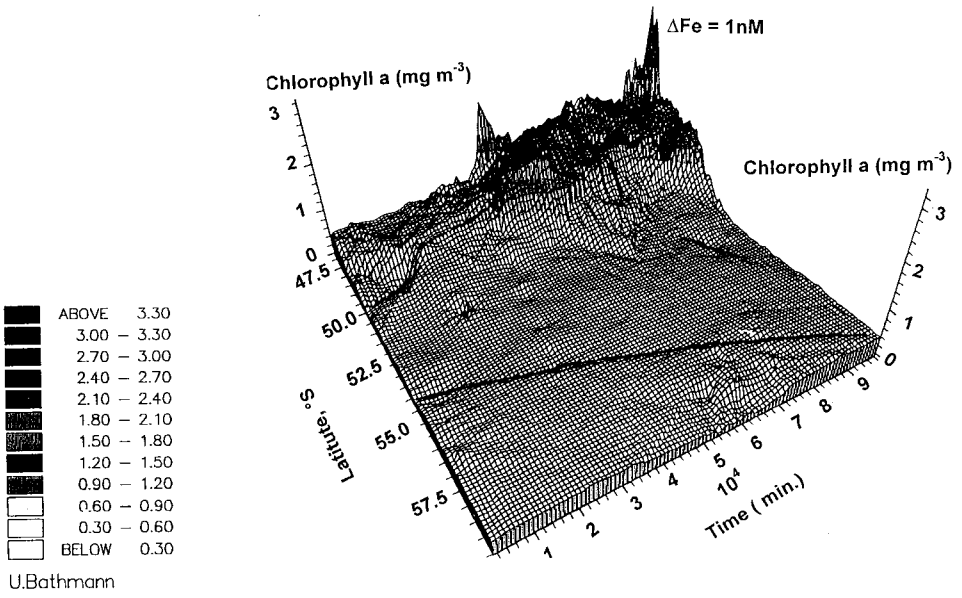

Figure 3.3: The ANTX/6 site in early spring 1992 : surface chlorophyll a and ice retreat (from Bathmann et al., 1996).

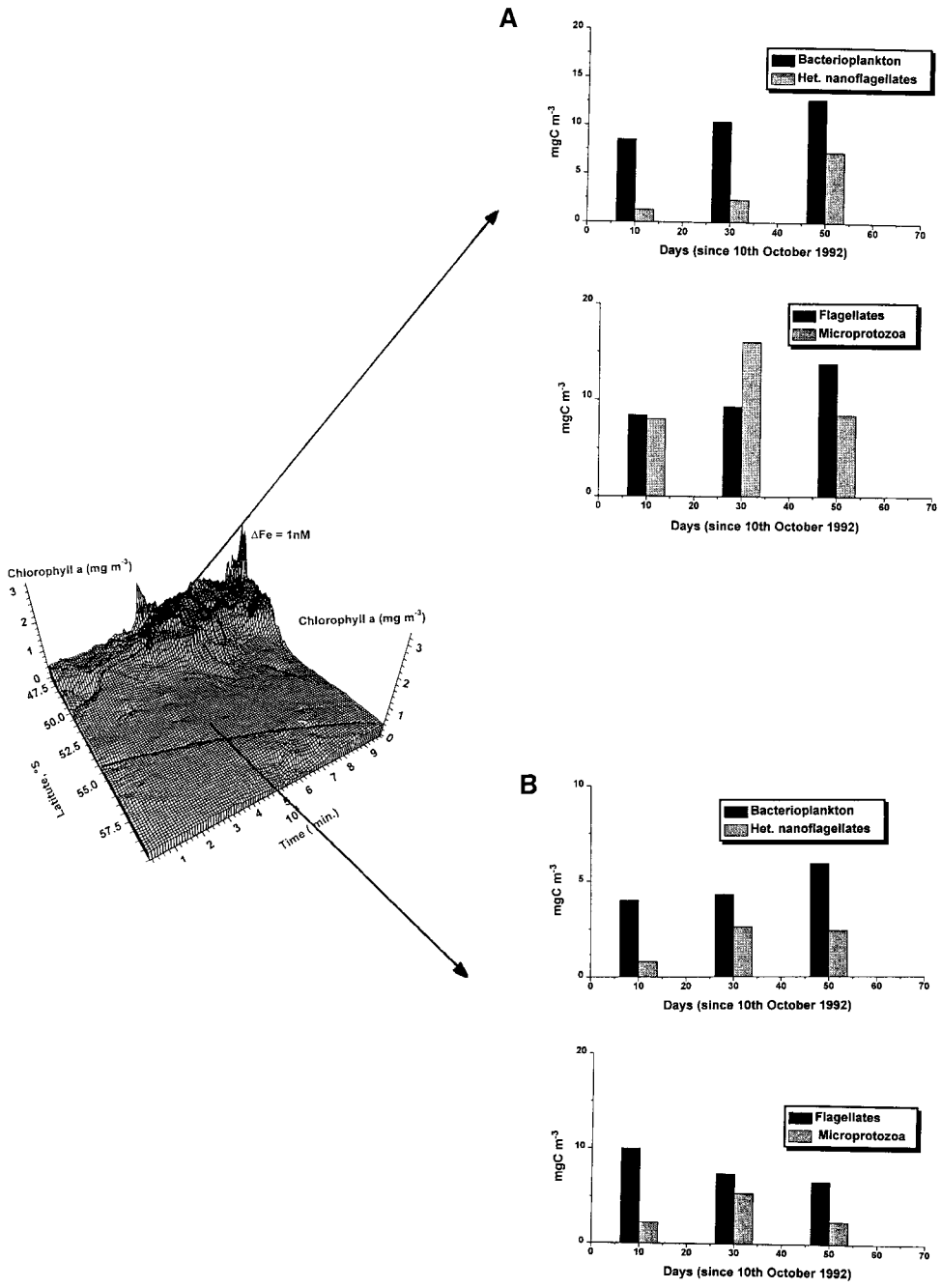

Figure 3.4: Temporal evolution of microbial assemblages (C-biomass) in the Polar Frontal (A) and ACC area (B) during the ANT X/6 cruise.

3.1.2 Spring bloom at EPOS site : suffisant iron availability; favourable meteorological conditions; krill swarm passage

The EPOS cruise took place in late spring, at meridian 49°W in the marginal ice zone of the Northwestern Weddell Sea and at the Scotia/Weddell Sea Confluence. The results of this cruise, as far as directly relevant to this discussion are described in Becquevort et al., 1993, Lancelot et al. (1991), Lancelot et al. (1993a,b), Mathot et al., 1992a,b; Nolting (1992); Veth (1991a), Veth et al. (1992) and more general in Hempel (1992). A number of transects have been worked between the Scotia Sea and the Weddell Sea crossing the Weddell-Scotia Confluence. Iron concentrations, well above 1nM, were considered as not limiting (Nolting et al., 1991). The ice-edge retreated slowly and regularly during the investigated period from 58.5° S to 60.5° S (Figure 3.5).The EPOS expedition was, for most of the time, characterized by weak (2 m s^{-1}) to moderate (16 m s^{-1}) wind speeds.

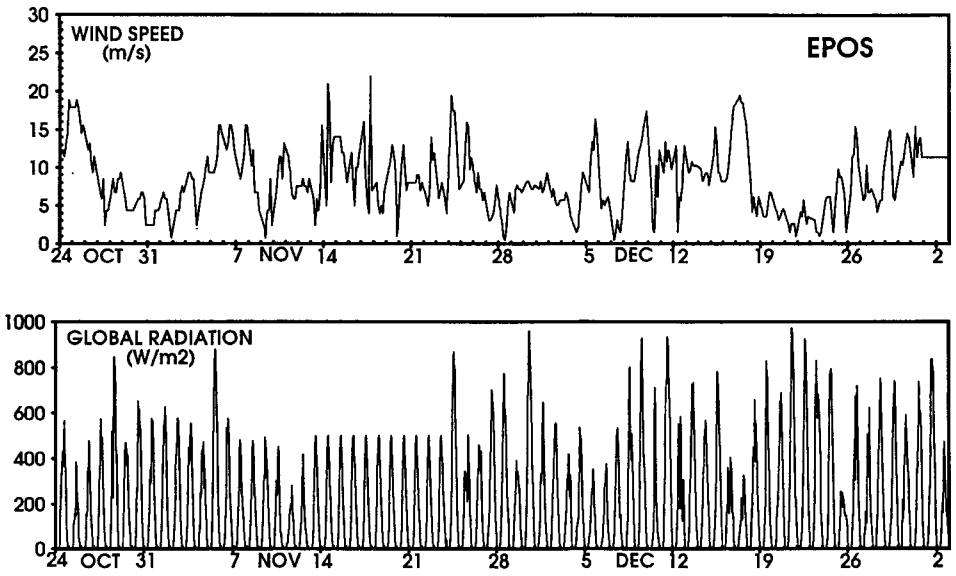

Figure 3.5: Wind speed (m/s), global radiation (W/m^2) and ice cover (%) at 60°S along 47°W meridian during Epos cruise.

Vertical salinity profiles clearly evidenced layers of lowered salinity by sea ice melting of up to 0.25 over depths between 5 to 40 m (Veth, 1991b). Despite this, the microalgal seeding of the water column upon ice melting was not critical, as revealed by the absence of significant sea-ice microalgal biomass in surface layers of the ice-covered area (Mathot et al., 1992a; Lancelot et al., 1993b).

A phytoplankton bloom reaching 3-4 mgChla m^{-3} was trailing the receeding ice-edge (Figure 3.6), due to the increased vertical stability of the surface layer induced by ice melt (Lancelot et al., 1993). Interestingly enough the phytoplankton community structure at the receeding ice-edge shifted from a diatom-dominant population in early-November (Bianchi et al., 1992) to a nanophytoplankton community in end-December (Becquevort et al., 1992). The latter community stimulated the activity of all heterotroph micro-organisms and their development was controlled by protozoan grazing pressure (Becquevort et al., 1992). The change in phytoplankton community structure was interpreted as resulting from a krill swarm passage such as that observed by chance at latitude 59°S (Figure 3.7). The sequence of ecological events are typically illustrated by Figure 3.8 that shows the time evolution of the different auto-and heterotrophic microbes that were succeeding within one month at latitude 59°S. The early spring phytoplankton bloom at the receeding ice-edge was dominated by diatoms; nanophytoplankton was contributing for less than 20 % of the total phytoplankton biomass (Figure 3.8a). The microbial food-web organisms were present but at low concentrations (Figure 3.8b,c). After the krill swarm passage, biomass of all microorganisms, excepted bacteria, was dramatically reduced (Figure 3.8). It is assumed that bacterial growth was enhanced by extra supply of labile organic matter after krill feeding. The observed shift of diatom-dominance to a near-specific nanophytoplankton community after the krill event could be interpreted as resulting from the extremely low diatom concentration after the krill passage preventing exponential growth (Figure 3.8a) or by iron depletion at the time of maximum development.

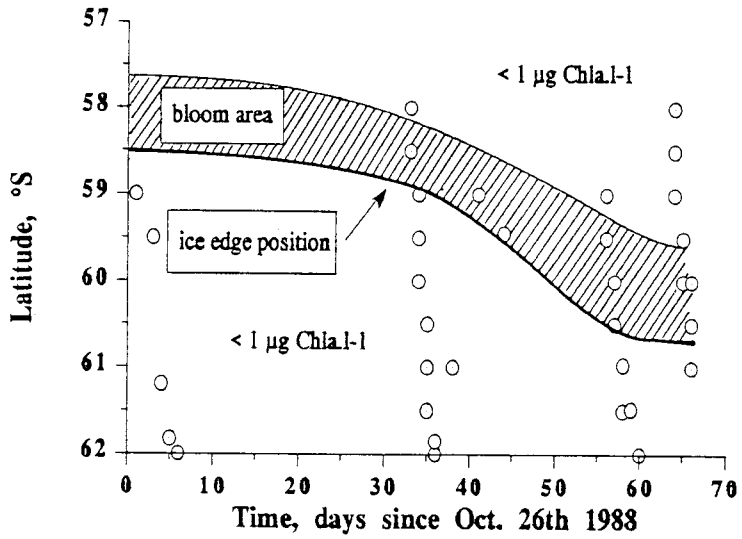

Figure 3.6: Sea ice retreat and related Chlorophyll a spatio-temporal distribution. Sampling stations (□, EPOS Leg 1; o, EPOS Leg 2) and position of the ice-edge.

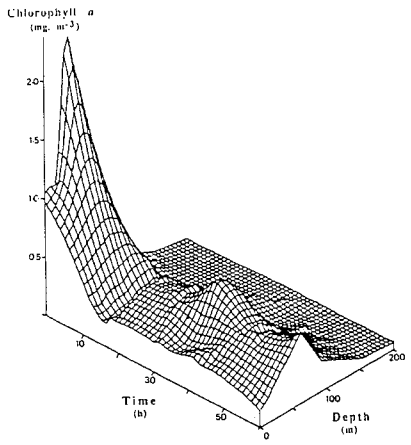

Figure 3.7: Time evolution of a diatom bloom at 59°S in the Weddell Sea (5th December 1988). The diatom bloom vanished in less than 10 h grazed down by a krill swarm (from Jacques and Panouse, 1991).

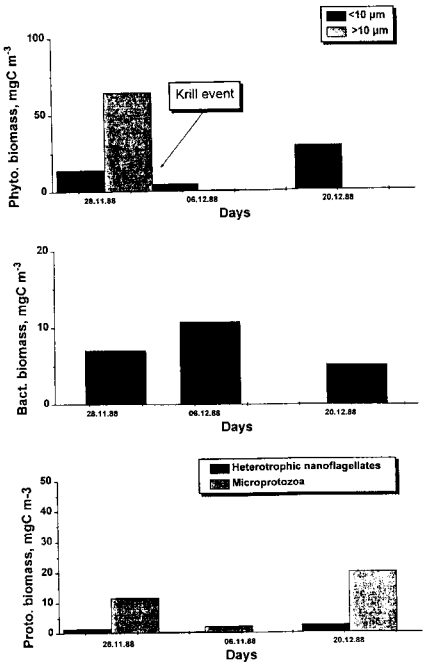

Figure 3.6: Temporal variation of phytoplankton (< and > 10 µm), bacterioplankton and protozoa (bacterivorous flagellates and protistovorous microprotozoa) at 59°S during Epos from December 5th to December 28th 1988.

3.1.3 Late summer at ANTARES 2 site : suffisant iron availability; favourable meteorological conditions

ANTARES 2 cruise took place in late summer in the Indian Sector of the Southern Ocean. Preliminary results were reported in Fiala (1995) and are publishing in a special issue of J. Mar. Syst. At this time, the whole sampling area was already ice-free since one month and open ocean conditions were met. In spite of suffisant iron concentration (0.7 - 1.8 nM, Sarthou et al., 1995), and meteorological conditions favorable to phytoplankton development, phytoplankton biomass was very low (below 0.6 mgChla m^{-3}) and did not show significant variation along the transect (Figure 3.9a). The phytoplankton community was composed of diatoms as well as nanoflagellates. Protozoa biomass (heterotrophic nanoflagellates and microprotozoa) remained low as well (Figure 3.9b). Contrasting bacterioplankton showed relatively high biomass (around 9 mgC m^{-3}, Figure 3.9c). Furthermore, the metazooplankton reached a significant biomasses (Figure 3.9.d) all over the transect but especially in the northern part below 55°S and, thus, could control the development of microorganisms such as phytoplankton and protozooplankton.

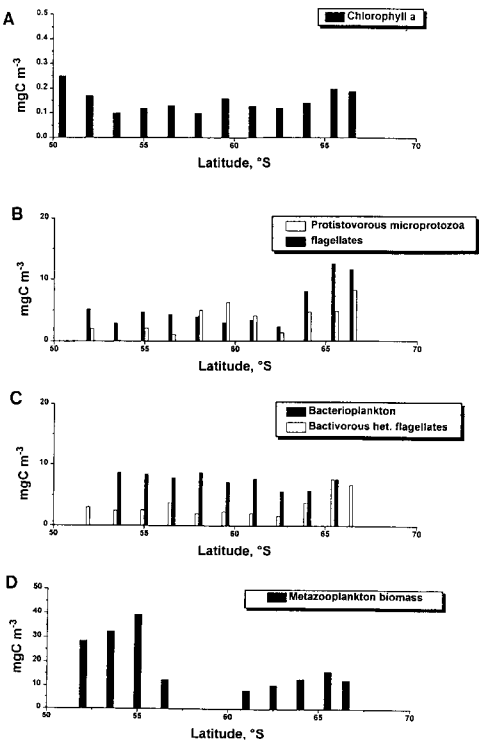

Figure 3.9:Geographical distribution of Chlorophyll a (a), microprotozoa and flagellates (b), bacteria (c) and metazooplankton (d) biomass along 62°E meridian during ANTARES 2.

Summarizing, it can be savely concluded that ANTARES 2 sampling site depicted a typical steady-state situation of end-summer where the microorganism biomasses were maintained at low concentration due to the direct control by metazooplankton.

3.2 ANTARCTIC PELAGIC ECOSYSTEM FUNCTIONING

3.2.1 Linear food chain, microbial food web : where and when in the Southern Ocean?

From the above analysis of ecosystem functioning in peculiar areas of the Southern Ocean and given the generally low dissolved iron availability in the whole Southern Ocean, it can be savely concluded that the Antarctic pelagic ecosystem is mostly dominated by an active microbial food web, the importance of which is determined by meteorological conditions. The latter, by enhancing vertical stability of the upper water provide optimal light conditions for phytoplankton exponential growth. Superimposing the microbial food web present all over the polar ocean, episodic diatom blooms stimulating the linear food chain are expected to occur in stabilized iron-rich areas : the Polar Frontal Jet and neretic waters around the continent or in the vicinity of islands. In this particular ocean inhabited by krill, diatoms blooms vanished very abruptely, victims of krill swarm passages. When occurring at depleted iron concentrations, the krill event induces a shift in the phytoplankton community structure from a diatom- to a nanophytoplankton- dominant community with related consesquences for the food-web structure and functioning.

Summarizing, it may be savely concluded that HNLC conditions in the Southern Ocean are resulting from the dominance of grazer-controlled nanophytoplanktonic communities in a Fe-limited environment. Episodic diatoms blooms are well developping in Fe-enriched areas, provided optimal light conditions are reached and maintained. These blooms are however vulnerable to krill swarm passages, as well as to sedimentation due to the large-size of the dominant phytoplankton.

3.2.2 Microbial Food Web: the key role of by protozooplankton.

Microbial communities that comprise bacteria, minute phytoplankton (< 10 µm) and protozooplankton are ubiquitous in the Antarctic pelagial system (Nöthig, 1988; Garrison and Buck, 1989a; Garrison et al., 1991; 1993; Becquevort et al., 1993; Scharek et al., 1994; Burkill et al., 1995; Becquevort, 1996; Klaas, 1996) as well as in the global ocean (Kiorboe, 1993). Their biomass is generally maintained low and shows little spatio-temporal variation.

Protozooplankton populations apparently increase in response to seasonal increase of primary and/or bacterial production (Becquevort et al., 1993; Burkill et al., 1995; Becquevort, 1996; Klaas, 1996). These results are consistent with the hypothesis that protozoan consumers display life time similar to those of their prey - phytoplankton and bacteria- and consequently control their development.

Indirect evidence of the strong control of bacterioplankton and nanophytoplankton by protozoa grazing pressure are given by the positive correlation between the biomass of prey and predators (Figures 3.10, 3.11). The positive X-intercept of the regression relating microprotozoa biomass to flagellate suggests that protozoa do not control the development of flagellates below a threshold flagellate biomass of 2 mgC m^{-3}. Accordingly, heterotrophic nanoflagellates correlate positively with bacteria, representing 42 % of bacterioplankton biomass. Also the positive X-intercept of 2.4 mgC m^{-3} suggests that heterotrophic nanoflagellate grazing pressure on bacteria is not operating at bacterial concentration lower than 2.4 mgC m^{-3}.

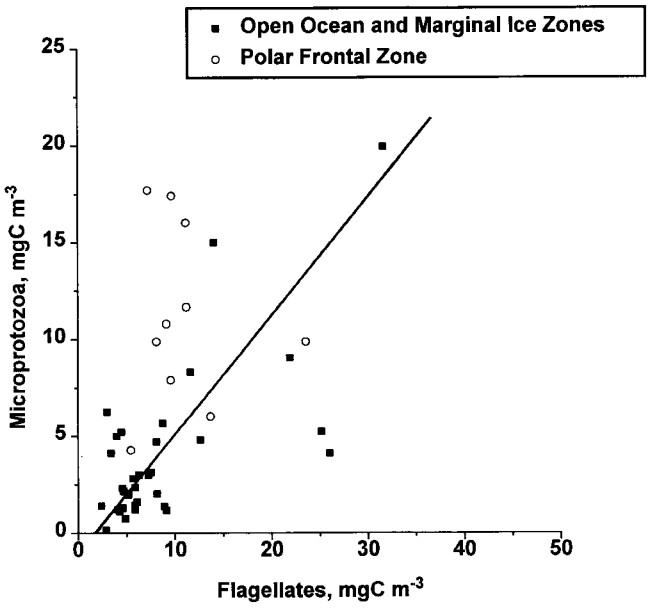

Figure 3.10: Relationship between microprotozooplankton and flagellate biomass. y = 0.39 x - 1.19.

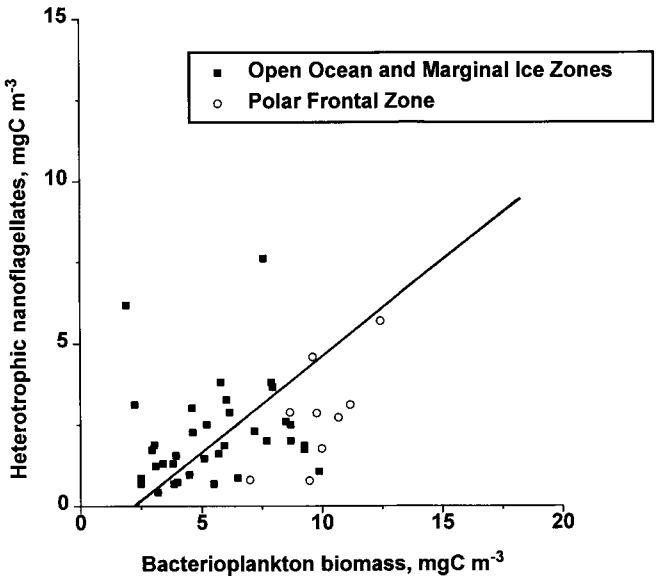

Figure 3.11: Relationship between heterotrophic nanoflagellates and bacterioplankton biomass. y = 0.42 x - 1.67

Supporting this, protozoan grazing activities recorded in different regions of the Southern Ocean at different time of the seasonal succession amount to 2-68 % of primary production and 2-90 % of bacterial production (Table 3.I).

As expected the highest percentages were generally observed at the end of the vegetative period and during the Austral winter. Furthermore, percentage less than 50 % were recorded in early spring.

Table 3.I.: Estimated protozoan ingestion in the Southern Ocean: in percentage of daily primary and bacterial production.

Area	Period	% of primary production grazed per day	% of bacterial production grazed per day	References
Atlantic sector	October-November	40	32	Becquevort, 1996
ACC	October/ November	34		Klass, in press
Polar front area	October/ November	44		Klass, in press
Weddell/ Scotia Sea	November	10	11	Garrison and Buck, 1989
Weddell/ Scotia Sea	November	68	53	Garrison and Buck, 1989
Weddell/ Scotia Sea	March	58		Garrison and Buck, 1989
Weddell/ Scotia Sea	June/July	53	68	Garrison et al. 1990c,d; 1992, 1993.
McMurdo Sound	December		9	Putt et al., 1991
McMurdo Sound	January		13	Putt et al., 1991
Indian sector	March	50	90	Menon et al., 1995
Indian sector		(47->100)		Taylor and Haberstroh, 1988
Prydz Bay	January	9		Archer et al., submitted
Prydz Bay	February	22		Archer et al., submitted

4. MODELLING C, N, FE THROUGH THE PLANKTONIC MICROBIAL FOOD-WEB OF THE SOUTHERN OCEAN : THE SWAMCO MODEL

The mechanistic SWAMCO model describing C, N and Fe circulation through aggregated chemical and biological compartments of the pelagic ecosystem has been developed to better understand and predict the complex interaction between physical, chemical and biological factors in generating and controlling diatoms and nanophytoplankton blooms in the global Southern Ocean. The generic property of this approach is demonstrated in the following chapters.

4.1 STRUCTURE OF THE SWAMCO MODEL

The coupled-physical-biogeochemical model results from the 'offline' coupling of the mechanistic biological model SWAMCO with a one-dimensional physical model. It consists of a two-layer 1D model composed of a well-mixed upper layer and a stratified deeper layer up to the euphotic depth bordered at 100m (Lancelot et al., 1993b).

The physical model is an adaptation to polar seas of the wind-mixed layer model of Denman (1973). The current numerical code has been extended with terms describing freshwater fluxes from ice-melting and the effects of wind friction changes over ice-covered regions. Basic concepts, mathematical description and parametrization are described in extenso in Veth (1991a,b). Performance and limits of the model are discussed in Veth et al., 1992.

The structure of the SWAMCO model is schematically illustrated by Figure 4.1. It results from the assemblage of 3 submodels describing the physiological growth of autotrophic flagellates and diatom (the AQUAPHY model, Lancelot et al., 1991); the dynamics of microbial organic matter degradation (the HSB model, Billen and Servais, 1989); the dynamics of bactivorous and herbivorous protozoa (the HBP model, Becquevort, in preparation).

Nitrate, ammonium and iron are assimilated by both phytoplankton groups whilst ammonium and iron can be taken up by bacteria and protozoa when the chemical composition of their food resource is N- or Fe-depleted. Both ammonium and iron are regenerated through bacterial and protozoan activity. Mesozooplankton grazing pressure on phytoplankton and protozooplankton is described as a first-order implicite forcing function and no food preference is considered. C, N and Fe exportation to the deep ocean is calculated from diatom sedimentation and faecal pellets production by mesozooplankton and krill when relevant. Nanophytoplankton and protozooplankton losses by sedimentation are neglected. All microorganisms undergo autolytic processes which release dissolved polymeric organic matter in the water column. All living particles are reduced to initial values after a krill 'event'.

The state variables of the SWAMCO model and the processes linking them are depicted in Figure 4.2. The differential equations describing changes in the state variables are summarized in Table 4.I

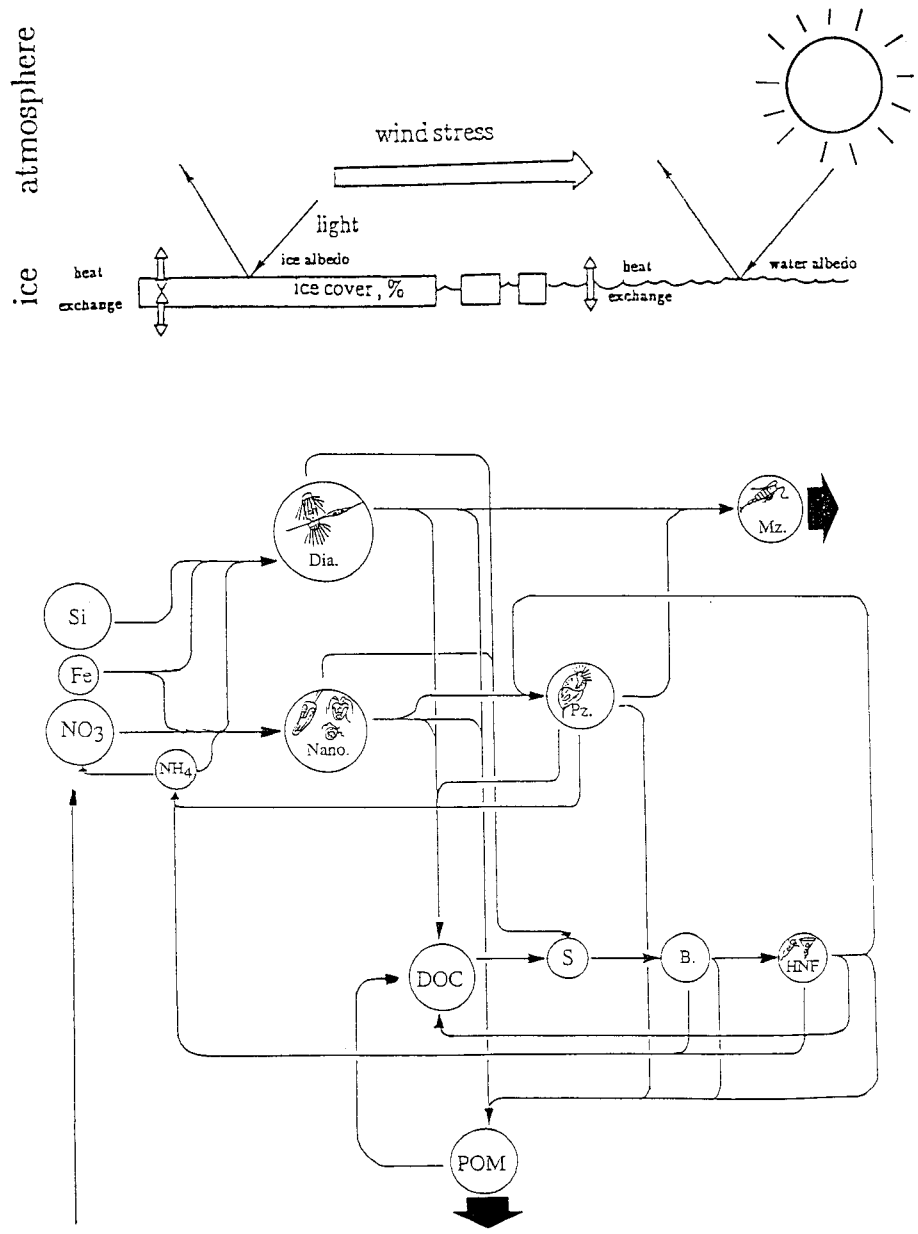

Figure 4.1: Diagrammatic representation of the mechanistic biogeochemical model SWAMCO.

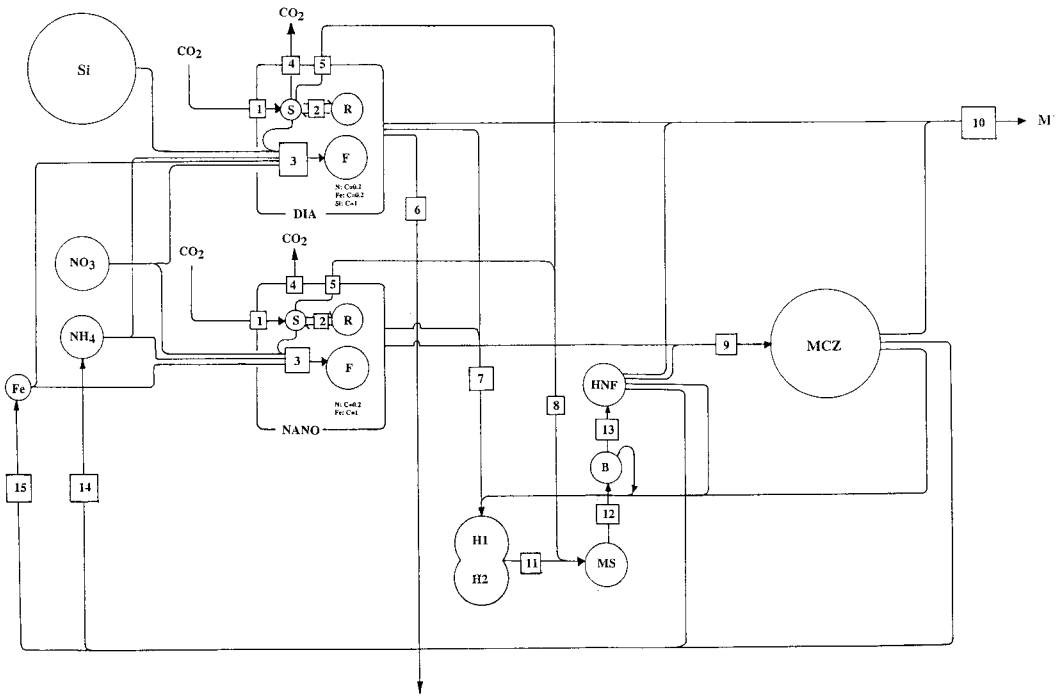

Figure 4.2: Structure of the biological model SWAMCO. DIA = diatoms; NANO = autotrophic nanoflagellates; R = reserve products; S = monomers; F = functional macromolecules; B = bacteria; HNF = bacterivorous heterotrophic nanoflagellates; MCZ = protistovorous microprotozoa and MZ= metazooplankton

Table 4.I. Differential equations of the SWAMCO model

Phytoplankton

$$\frac{dF_{DIA}}{dt} = \text{synthesis} - \text{MZ grazing} - \text{autolysis} - \text{sedimentation}$$

$$\frac{dR_{DIA}}{dt} = \text{synthesis} - \text{catabolism} - \text{MZ grazing} - \text{autolysis} - \text{sedimentation}$$

$$\frac{dS_{DIA}}{dt} = \text{synthesis} - \text{R\&F synthesis} + \text{R catabolism} - \text{exudation} - \text{respiration} - \text{autolysis} - \text{sedimentation} - \text{MZ grazing}$$

$$\frac{dF_{NANO}}{dt} = \text{synthesis} - \text{MCZ grazing} - \text{MZ grazing} - \text{autolysis}$$

$$\frac{dR_{NANO}}{dt} = \text{synthesis} - \text{catabolism} - \text{MCZ grazing} - \text{MZ grazing} - \text{autolysis}$$

$$\frac{dS_{NANO}}{dt} = \text{synthesis} - \text{R\&F synthesis} + \text{R catabolism} - \text{exudation} - \text{respiration} - \text{autolysis} - \text{MCZ grazing} - \text{MZ grazing}$$

Protozooplankton

$$\frac{dHNF}{dt} = \text{growth} - \text{autolysis} - \text{MCZ grazing} - \text{MZ grazing}$$

$$\frac{dMCZ}{dt} = \text{growth} - \text{autolysis} - \text{MZ grazing}$$

Microbial loop

$$\frac{dB}{dt} = \text{growth} - \text{HNF grazing} - \text{autolysis}$$

$$\frac{dH_i}{dt} = \text{R\&F}_{DIA}\,\text{autolysis} + \text{R\&F}_{NANO}\,\text{autolysis} + \text{MCZ autolysis} + \text{HNF autolysis} + \text{B autolysis} - H_i\,\text{ectoenzymatic hydrolysis}$$

$$\frac{dMS}{dt} = H_i\,\text{ectoenzymatic hydrolysis} + S_{DIA}\,\text{exudation} + S_{NANO}\,\text{exudation} - \text{B uptake} + S_{DIA}\,\text{autolysis} + S_{NANO}\,\text{autolysis}$$

Inorganic nutrient loop

$$\frac{dNO_3}{dt} = -\,\text{DIA uptake} - \text{NANO uptake}$$

$$\frac{dNH_4}{dt} = -\,\text{DIA uptake} - \text{NANO uptake} + \text{B regeneration} + \text{HNF regeneration} + \text{MCZ regeneration}$$

$$\frac{dFe}{dt} = -\,\text{DIA uptake} - \text{NANO uptake} - \text{B uptake} - \text{HNF uptake} - \text{MCZ uptake} + \text{MCZ regeneration} + \text{B regeneration} + \text{HNF regeneration}$$

$$\frac{dSi}{dt} = -\,\text{DIA uptake}$$

4.2 Equations and parameters

4.2.1 AQUAPHY : the phytoplankton model

Mathematical description :

The phytoplankton community is represented by two groups - the autotrophic flagellates and diatoms -, each described by 3 state variables (functional cellular constituents F, reserve products R, monomers S) as defined by the AQUAPHY model (Figure 4.2.; Lancelot et al., 1991). Rate equations are the following :

$$\frac{dF_i}{dt} = sF_i - lF_i - sed\,F_i - \alpha g_j F_i$$

$$\frac{dS_i}{dt} = p_i - sR_i + cR_i - sF_i - e_i - r_i - lS_i - sed\,S_i - \alpha g_j S_i$$

$$\frac{dR_i}{dt} = sR_i - cR_i - lR_i - sed\,R_i - \alpha g_j R_i$$

in which : F_i = DIA (diatoms) or NANO (nanophytoplankton)
αg_j = protozoan, metazoan or krill grazing pressure (h^{-1}).

In these equations :

- the rate of phytoplankton growth sF_i is governed by monomeric substrate S and nutrient availability according to a multiplicative Michaelis-Menten kinetics characterized by 3 constants: the maximum specific growth rate μF_{maxi} and the half-saturation constants for S and N assimilation respectively K_{Si} and K_{Ni} :

$$sF_i = mF_{max_i} \frac{S_i}{K_{S_i} + S_i} \frac{N}{K_{N_i} + N} F_i$$

  N corresponds to the limiting nutrient, i.e. the nutrient which displays the lowest ambient concentration compared to the half-saturation constant for phytoplankton uptake. Conceptually, it can be either inorganic nitrogen, phosphate, silicate or dissolved iron. In the remote Antarctic waters, it is considered that iron is the limiting nutrient (N = Fe; $K_{Ni} = K_{Fei}$) and phytoplankton physiological growth is governed by light and dissolved Fe availability. The better ability of nanoflagellates over diatoms to grow at low ambient dissolved Fe is expressed by the values of the half-saturation constants of Fe uptake K_{Fei} which differ from 2 orders of magnitude between the two phytoplankton groups (Table 4.II).

- The photosynthetic process p_i is governed by irradiance I according to the relationship of Platt et al. (1980); it is characterized by three parameters normalized to biomass, the maximal photosynthetic capacity $K_{max,}$ the photosynthetic efficiency α and a description of the photoinhibition β:

$$p = K_{maxi} (1 - \exp(-\alpha\, I / K_{maxi})) \exp(-\beta\, I / K_{maxi})\, F_i$$

- The synthesis of storage products sR_i is governed by the size of S_i following a Michaelis-Menten kinetic characterized by the constants ρ_{maxi} and K_{Si} :

$$sR_i = \rho_{max_i} \frac{S'_i}{K_{S_i} + S'_i} F_i$$

where $S'_i = \frac{S_i}{F_i} - Qs$

Qs being the monomers cellular quota.

- The catabolism cR_i of storage products R_i is postulated to obey a first kinetic characterized by the constant k_{Ri}.

$$cR_i = k_{Ri} R_i$$

- The metabolic costs, in terms of a demand for ATP and reductors, are primarily met by cellular respiration r. This process is expressed by the sum of two terms, associated with maintenance processes, and the synthesis of new cellular material (Shuter, 1979) :

$$r_i = k_{Fi} F_i + \xi sF_i$$

where k_{Fi} is a first order constant and ξ a dimensionless constant assumed to vary according to the inorganic nitrogen source.

- The exudation process e, the rate of cell autolysis l and the sedimentation rate of diatoms -sed- are described by first order kinetics :

$$e_i = \varepsilon_i S_i$$

$$l_i R_i = k_{Li} R_i; \quad l_i S_i = k_{Li} S_i; \quad l_{Fi} = k_{Li} F_i$$

$$sed\ F_{DIA} = k_{sed}\ F_{DIA};\ sed\ R_{DIA} = k_{sed}\ R_{DIA};\ sed\ S_{DIA} = k_{sed}\ S_{DIA}$$

in which ε_i, k_{Li} and k_{sed} are first order constant.

Parameters:

The physiological parameters of phytoplankton growth were determined experimentally by mathematical fitting of ^{14}C experimental data describing the photosynthesis-light relationship and time-course C assimilation in phytoplankton cellular constituents along a 24 hours cycle, making use of the AQUAPHY set of equations. When conducted at non-limiting iron concentration, no significant difference in either photosynthetic (Table 4.II.) or growth (Figure 4.3.) parameters of the nanophytoplankton-dominant or diatom-dominant communities could be evidenced.

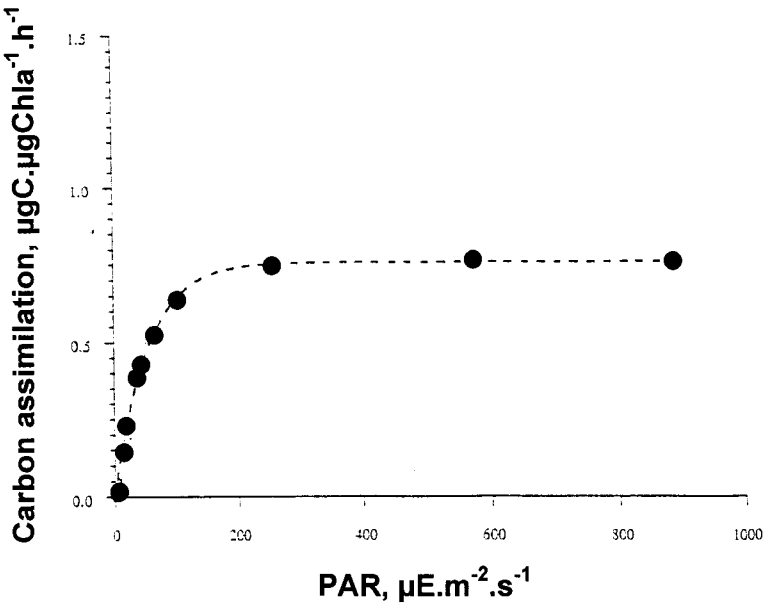

Figure 4.3.: Experimental determination of the photosynthesis-light relationship typical of phytoplankton communities of latitude 55°S (ANTX/6 st.872).

Table 4.II.: Typical photosynthetic parameters for spring-summer Antarctic phytoplankton.

Geographical site	K_{max} h^{-1}			alpha h^{-1} ($\mu E .m^{-2} s^{-1}$)$^{-1}$		
	min	max	mean	min	max	mean
ATLANTIC SECTOR						
EPOS cruise 1988						
MIZ NW Weddell Sea	0.01	0.11	0.06	0.0003	0.0012	0.0009
SO-JGOFS ANTX/6 1992						
MIZ ACC	0.015	0.091	0.051	0.0004	0.0011	0.001
Polar front	0.046	0.08	0.065	0.0006	0.0011	0.0008
INDIAN SECTOR						
ANTARES 2 1994						
Ice-free MIZ	0.05	0.08	0.01	0.0008	0.001	0.0015
Polar front	0.06	0.08	0.09	0.0007	0.001	0.0011

Accordingly one set of parameters was chosen to characterise the carbon metabolism (photosynthesis, growth, respiration, catabolism, exudation) of both phytoplankton groups (Table 4.III.). Furthermore this set of parameters holds for the whole Southern Ocean due to the lack of significant temperature dependence to be observed in the range -1.8 and +3.5°C(Figure 4.4.).

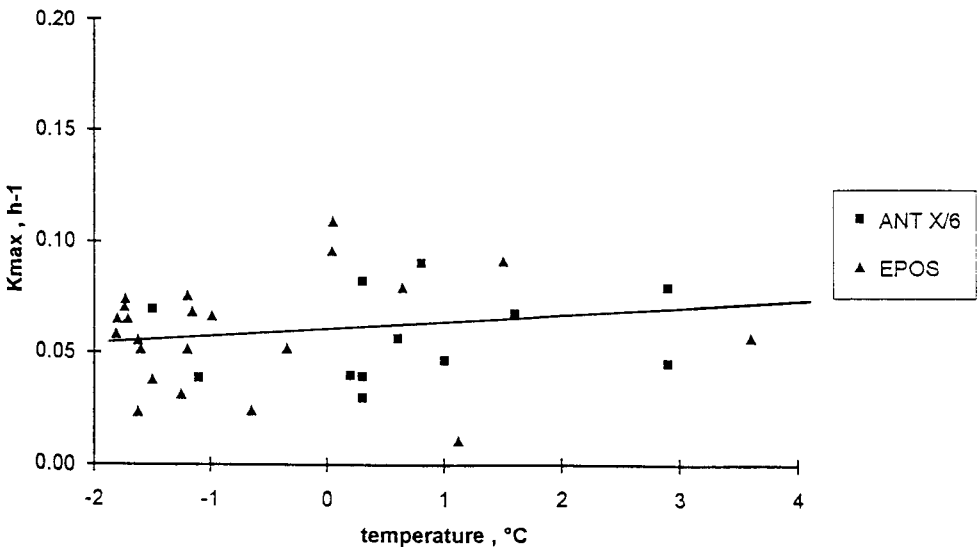

Figure 4.4.: Relationship between maximal photosynthetic capacity K_{max} and ambient temperature.

Diatoms and nanophytoflagellates physiological growth in the Southern Ocean then differentiates by the only physiology of Fe assimilation : the cellular Fe requirements and the kinetics parameters of Fe uptake. The observed better ability of nanoflagellates to outcompete micro-sized diatoms in the low-iron waters of the Southern Ocean (Sunda and Huntsman, 1995; Hutchkins, 1995) was designated by their higher affinity for dissolved iron uptake (low k_{Fe}) and their lower biochemical iron requirements. Half-saturation constant for Fe uptake by nanophytoflagellates and diatoms was chosen at respectively 0.02 nM (Price et al., 1994) and 1.8 nM. The latter concentration was calculated from Fe-enrichment experiments conducted in the Atlantic sector of the Southern Ocean (van Leeuw et al., 1996) when assuming that Fe supply in a low Fe environment stimulates the only diatom component of the phytoplankton community. Fe-phytoplankton requirement (Fe:C) was derived from literature (Morel, 1990; Brand, 1991; Sunda, 1991) and fixed at 0.12 and 0.0025 nM:µM for respectively diatoms and nanophytoflagellates.

Table 4.III.: SWAMCO parameters : AQUAPHY module

Parameters	Symbols	Values	Units
Photosynthesis			
Photosynthesic efficiency	α	0.00065	h^{-1} $(\mu Em^{-2}sec^{-1})^{-1}$
Optimal specific rate of photosynthesis	k_{max}	0.06	h^{-1}
Index of photoinhibition	β	0	h^{-1} $(\mu Em^{-2}sec^{-1})^{-1}$
Growth metabolism			
Maximal specific rate or R synthesis	ρmax	0.06	h^{-1}
Constant of R catabolism	k_R	0.06	h^{-1}
Maximal specific rate of F synthesis	μF_{max}	0.035	h^{-1}
Half-saturation constant of S assimilation	Ks	0.07	dimensionless
Maintenance Cst of basal metabolism	k_F	0.0005	h^{-1}
Energetic costs of F synthesis :	ξ		
ammonium source :		0.32	dimensionless
nitrate source :		0.70	dimensionless
Constant of exudation	ε	0.005	h^{-1}
Constant of cell autolysis	k_L	0.002	h^{-1}
Nutrient uptake			
Ammonium preference	γ	0.21	dimensionless
$f_{NH_4} = \gamma \frac{NH_4}{inorgN} + (1-\gamma)\frac{NH_4^{\delta}}{inorgN}$	δ	0.24	dimensionless
Half-saturation ct Fe uptake diatoms	K_{FeDIA}	1.8	nM
nanophytoplankton	K_{FeNANO}	0.03	nM
Diatom Fe content	FC_{DIA}	0.2	nM:µMC
Nanophyto.Fe content	FC_{NANO}	0.0025	nM:µMC
Diatom Si content	SiC_{DIA}	1.	µM:µMC
Phytoplankton N content	NC_F	0.2	µM:µMC

4.2.2. HBP : the protozooplankton model

Choice of state variables:

The protozoan community includes a large range of microorganisms able to graze on bacteria and/or on auto-and heterotrophic flagellates. To which extent the feeding behaviour of each protozoa is influenced by food concentration and quality, the latter determined by the relative importance of prey (bacteria versus flagellates) is not known and relies on the species. The feeding behaviour of antarctic protozoa was investigated during the ANTARES 2 expedition by running several food competitive experiments in temperature-controlled conditions. The experimental procedure is described in Menon et al. (1995) and in the material and methods section.

Shortly the methodology consists in measuring the kinetic parameters describing the ingestion rate of natural assemblages of protozoa in the presence of various concentrations of competitive prey: bacteria and flagellate. It has been demonstrated elsewhere (Menon et al., 1995) that the presence of one group of prey is not affecting the maximum protozoan ingestion rate on the other group of prey but rather would decrease the affinity of the predator for this latter prey when competition for the two groups of prey is significant. Physiologically, this decrease in affinity for the considered prey is expressed by a competitive-related change in the apparent half-saturation constant describing the protozoan ingestion rate in the presence of different concentration of the competitive prey.

Results of these experiments (Figure 4.5, 4.6) show that no significant competitive inhibition of the two kinds of tested prey could be evidenced, suggesting that the protozoan community of the Southern Ocean is highly food selective. Indeed maximum ingestion rates of protozoa on bacteria or flagellates and their apparent half-saturation constants were found to be independent of the concentration of flagellates (Figure 4.5) or bacteria (Figure 4.6). Consequently the protozoan community of the Southern Ocean can be considered as composed of two important groups characterised by their own diet : bactivorous flagellates and protistovorous microprotozoa.

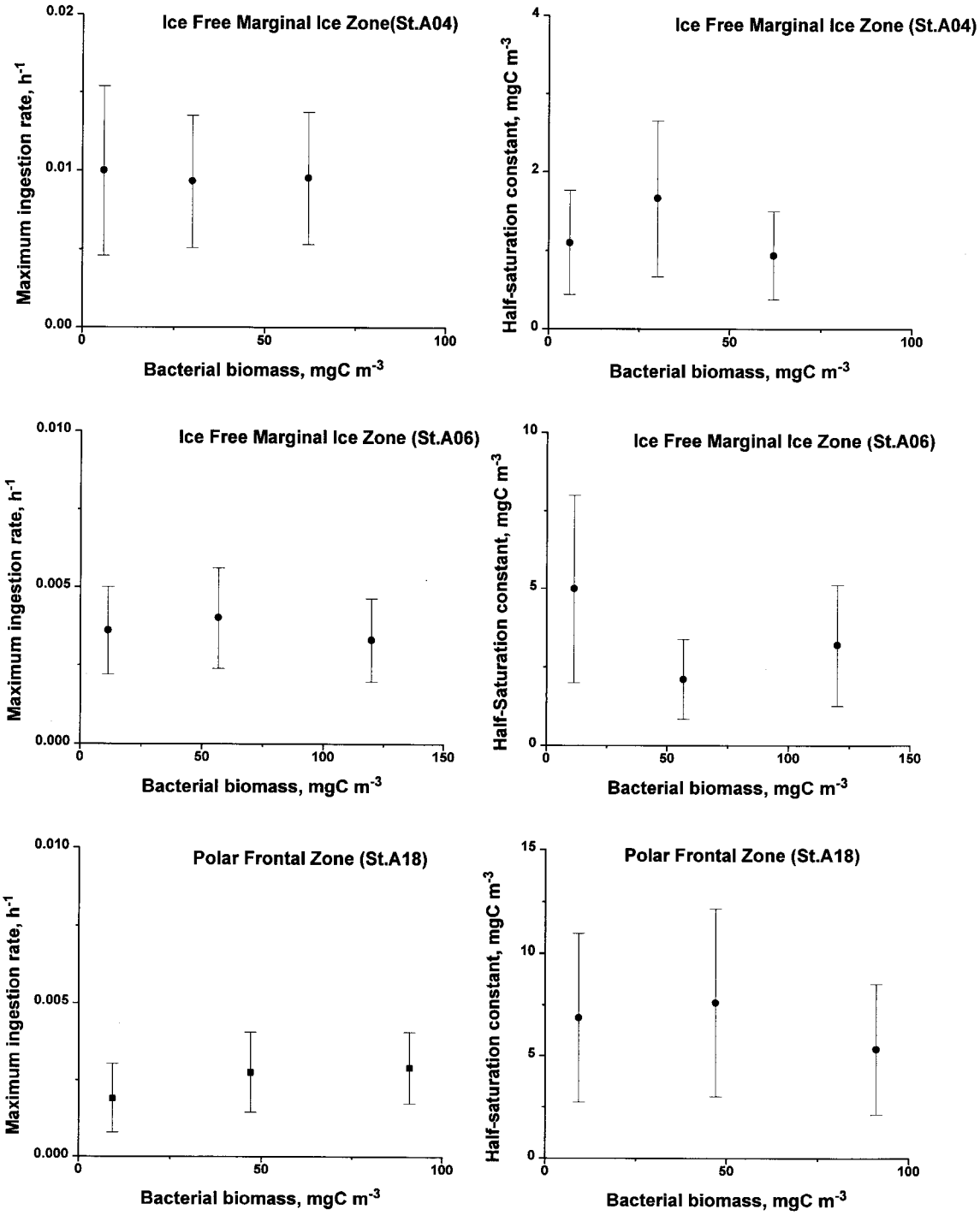

Figure 4.5: Effect of bacterial biomass on protozoan ingestion of flagellates.

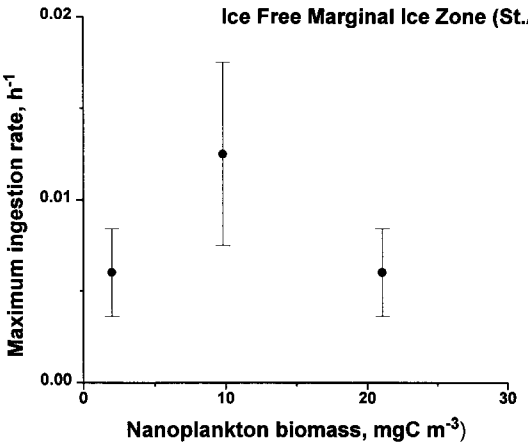

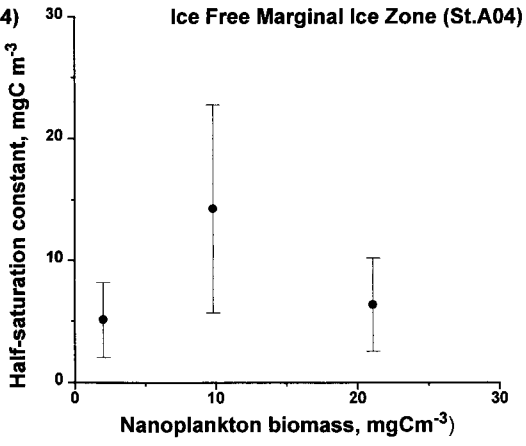

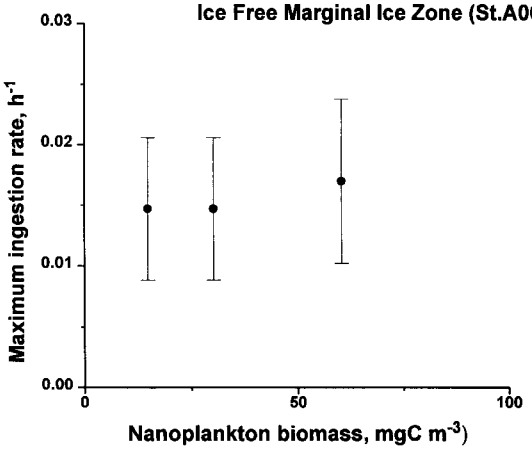

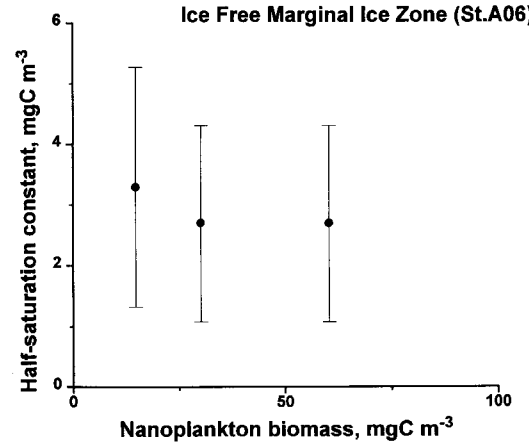

Figure 4.6: Effect of flagellate biomass on protozoan ingestion of bacteria.

Mathematical formulation:

The protozoan community is represented by two groups : the bactivorous flagellates HNF feeding on the only bacteria and the microzooplankton MCZ grazing on autotrophic and heterotrophic nanoflagellates. The whole community undergoes grazing pressure by metazoans and krill. Rate equations are the following :

$$\frac{dMCZ}{dt} = Y_{MCZ}\, ing_{MCZ} - l_{MCZ} - \beta g_j$$

$$\frac{dHNF}{dt} = Y_{HNF}\, ing_{HNF} - l_{HNF} - (1-\gamma)\, ing_{MCZ} - \gamma\, gj$$

In these equations :

- The protozoan ingestion rate is governed by food concentration and obeys Holling type II functional response analogous to a Michaelis-Menten kinetics above a threshold value THS below which no grazing is likely.

$$ing_{MCZ} = ing_{max_{MCZ}} \frac{PREY'}{PREY' + K_{PREY}} MCZ$$

$$ing_{HNF} = ing_{max_{HNF}} \frac{B'}{B' + K_B} HNF$$

with $PREY' = NANO + HNF - THS_{PREY}$

$B' = B - THS_B$

and ing_{maxMCZ}, ing_{maxHNF}, K_{PREY}, K_B, the maximum specific ingestion rates and half-saturation constants for respectively flagellates ingestion by microzooplankton and bacteria uptake by heterotrophic nanoflagellates.

- A constant fraction Y_{MCZ} and Y_{HNF}, of the ingested food by respectively microzooplankton and heterotrophic flagellates is converted in biomass, the remaining being respired.

- The rate of cell autolysis l_{MCZ} and l_{HNF} are described by first order kinetics :

$$l_{MCZ} = Kl_{MCZ}\, MCZ$$

$$l_{HNF} = Kl_{HNF}\, HNF$$

in which Kl_{MCZ} and Kl_{HNF} are first-order constants.

- γ is the fraction of microzooplankton grazing pressure on nanophytoplankton.

- βg_j and γg_j represent the part of metazoan and krill grazing pressure on respectively microzooplankton and heterotrophic nanoflagellates.

Parameters:

Protozoan feeding parameters were estimated from the experimental determination of the prey-dependence ingestion rate relationship conducted on protozoan communities sampled in the Atlantic and Indian sectors of the Southern Ocean (Becquevort, 1996; Figure 4.7, 4.8, Table 4.IV).

For both protozoan communities, there exists a food threshold value below which no grazing is occurring. Close to this food concentration, the protozoa is just able to maintain below it will starve (Heinbockel, 1978). Interestingly this food threshold is by far lower for protistovorous microprotozoa than for bactivorous flagellates emphasising the strong coupling between microprotozoa and their prey.

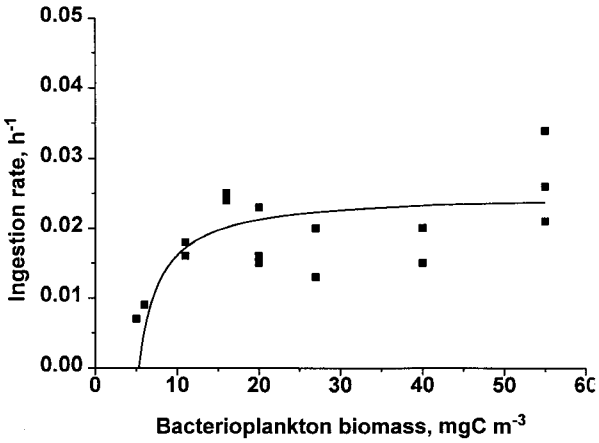

Figure 4.7: Functional feeding response of bactivorous protozoa.

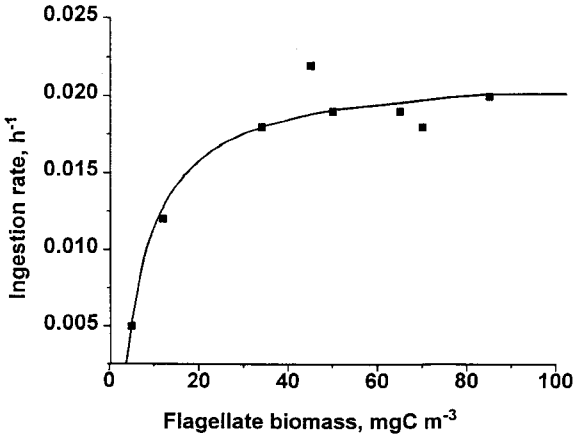

Figure 4.8: Functional feeding response of protistovorous microprotozoa.

Table 4.IV : SWAMCO parameters HBP module.

Parameters	symbols	values	units
Heterotrophic flagellates HNF			
Max. spec.ingestion rate	ing_{maxHNF}	0.025	h^{-1}
Bacteria threshold	THS_B	5.3	mgC m^{-3}
Half-saturation ct for bacteria ingestion	K_B	2.6	mgC m^{-3}
Growth efficiency	Y_{HNF}	0.3	dimensionless
Autolysis ct	KI_{HNF}	0.002	h^{-1}
HNF N:C ratio	NC_{HNF}	0.2	nM:µM
HNF Fe:C ratio	NC_{HNF}	0.0002	nM:µM
Microzooplankton MCZ			
Max. spec.ingestion rate	$ingmaxMCZ$	0.019	h^{-1}
Nanoplankton threshold	THS_{PREY}	1	mgC m^{-3}
Half-saturation ct for nanoplankton ingestion	K_{PREY}	3.4	mgC m^{-3}
Growth efficiency	Y_{MCZ}	0.3	dimensionless
Autolysis ct	KI_{MCZ}	0.002	h^{-1}
MCZ N:C ratio	NC_{MCZ}	0.2	nM:µM
MCZ Fe:C ratio	NC_{MCZ}	0.0002	nM:µM

4.2.2 HSB : the microbial loop model

Mathematical formulation:

The model of microbial loop dynamics (see for physiological basis Billen and Servais, 1989) considers one single bacterioplankton group B (including both free-living and attached bacteria on particles and aggregates) and 3 pools of dissolved organic substrates (monomers MS, rapidly biodegradable polymers H_1 and slowly biodegradable polymers H_2) for bacterioplankton development. Basically, bacterial growth is directly dependent on the concentration of monomeric substrates whilst most of the dissolved organic matter is in the form of macromolecules requiring extracellular hydrolyse.

Equation rates are the following :

$$\frac{dH_1}{dt} = -eH_1 + Q\,\text{supply}$$

$$\frac{dH_2}{dt} = -eH_2 + (1-Q)\,\text{supply}$$

$$\text{with supply} = l_i R_i + l_i F_i + l_{HNF} + l_{MCZ} + l_B + slp_{krill}$$

$$\frac{dMS}{dt} = eH_1 + eH_2 - \text{upt}\,MS + \varepsilon S$$

$$\frac{dB}{dt} = Y_B\,\text{upt}\,MS - l_B - ing_{HNF} - \xi g_j$$

In these equations :

- The extracellular hydrolysis eH_1 and eH_2 obey a Michaelis-Menten kinetics (Somville and Billen, 1983; Somville, 1984) characterized by two specific parameters - e_{imax}, K_{Hi} ($_i$ = $_{1,2}$) - owing to the different susceptibilities to extracellular hydrolysis of H_1 and H_2 :

$$eH_i = e_i\,max\frac{i}{K_{H_i} + {}_{H_i}}B$$

in which $_i$ = $_{1,\,2}$

- Q is the part to H_1 of macromolecules produced by phytoplankton, bacteria, protozoa, autolysis and by sloppy feeding krill.

- The sloppy feeding s1P is assumed to represent a constant fonction γ of krill grazing pressure.

- The uptake of direct substrates uptSM is assumed to obey a Michealis-Menten kinetics :

$$\text{uptMS} = b_{max} \frac{MS}{K_{MS} + MS} B$$

where b_{max} and K_{MS} are the maximum rate and half-saturation constant of substrate uptake by bacteria.

- A constant fraction Y_B of the amount of substrates taken up is used for biomass production, the remaining part being respired.

Parameters:

Most parameters were determined experimentally (Billen and Becquevort, 1991; Lancelot et al., 1992; Servais et al., 1987). Values are reported in Table 4.V). Contrasting with eucaryotic cells, bacterial activity in the Southern Ocean is strongly governed by ambient temperature (Billen and Becquevort, 1992). Accordingly, the model considers a temperature dependence of bacterial parameters described by the following sigmoid relationship :

$$\mu = \mu_{max} \left(0.1 + 0.9 \exp\left(-\frac{(Topt - T)^2}{dt^2}\right) \right)$$

with μ_{max} = max specific rate at optimal temperature
T = ambient temperature
Topt = optimal temperature
dt = sigmoid width

Tableau 4.V. SWAMCO parameters : HSB module

Parameters	Symbols	Values	Units
Heterotrophic flagellates HNF			
Max. rate of H_1 hydrolysis	e_{1max}*	0.75	h^{-1}
Max. rate of H_2 hydrolysis	e_{2max}*	0.25	h^{-1}
H_1 fraction in lysis products	Q	0.5	dimensionless
Half sat.ct for H_1 hydrolysis	K_{H1}	100	$mgCm^{-3}$
Half sat.ct for H_2 hydrolysis	K_{H2}	1000	$mgCm^{-3}$
Max. rate of monomers uptake	b_{max}*	0.18	h^{-1}
Half sat.ct for monomers uptake	K_{MS}	10	$mgCm^{-3}$
Growth efficiency	Y_B	0.25	dimensionless
Autolysis ct	Kl_B*	0.002	h^{-1}
Bacteria N:C ratio	NC_B	0.2	nM:µM
Bacteria Fe:C ratio	FC_B	0.0002	nM:µM
Temperature characteristics : parameters with *			
Optimal temperature	Topt	12	°C
Temperature interval	dt	5	°C

4.2.3 The inorganic loop

Mathematical formulation:

Nitrate, ammonium, iron and silicic acid are the inorganic nutrients considered by the model. Nitrate and ammonium - but ammonium preferably - and iron are taken up by the two phytoplankton groups and assimilated into the only functional constituents F. Silicic acid is used by the only diatoms. Only iron assimilation is explicitly described, while N and Si uptake are deduced from computed growth rate and cellular stoechiometry of biological state variables. Ammonium and dissolved iron can be occasionally taken up by bacteria and protozoa according to the N:C and Fe:C ratios of their food resources and their own biochemical requirements.

Ammonium and dissolved iron (Hutchins et al., 1995) are released by bacteria and protozoa as product of their metabolism. Regenerating processes are computed by comparing the nitrogen and iron content of food resources with the biochemical requirements of the micro-organisms.

Equation rates are the following :

$$\frac{dNO_3}{dt} = -(1 - f_{NH_4})\, sF_i\, NC_F$$

$$\frac{dNH_4}{dt} = -f_{NH_4}\, sF_i\, NC_F + regeN_B + regeN_{HNF} + regeN_{MCZ}$$

$$\frac{dFe}{dt} = -sF_{NANO}\, FC_{NANO} - sF_{DIA}\, FC_{DIA} - Y_B upt\, MS\, FC_B + rege\, Fe_{HNF} + rege\, Fe_{MCZ}$$

$$\frac{dSi}{dt} = -sF_{DIA}\, SiC_{DIA}$$

with :

$$regeN_B = uptMS\,(NC_{MS} - Y_B\, NC_B)$$

$$regeN_{HNF} = ing_{HNF}\,(NC_B - Y_{HNF}\, NC_{HNF});\quad regeFe_{HNF} = ing_{HNF}\,(FC_B - Y_{HNF}\, FC_{HNF})$$

$$regeN_{MCZ} = ing_{MCZ}\,(NC_{PREY} - Y_{MCZ}\, NC_{MCZ});\quad regeFe_{MCZ} = ing_{MCZ}\,(FC_{PREY} - Y_{MCZ}\, FC_{MCZ})$$

In these equations :

- NC_F, NC_{MS}, NC_B, NC_{HNF}, NC_{MCZ}, are the molar nitrogen:carbon ratios of respectively phytoplankton functional macromolecules, monomeric substrates, bacteria, heterotrophic nanoflagellates and microzooplankton; NC_{PREY} is the molar nitrogen:carbon ratio of the combined flagellates (autotrophic and heterotrophic) and is calculated at each time step.
- FC_{NANO}, FC_{DIA}, FC_B, FC_{HNF}, FC_{MCZ} are the molar Fe:C ratios specific to respectively nanophytoplankton, diatoms, bacteria, heterotrophic flagellates and microzooplankton. FC_{PREY} is the calculated Fe:C ratio of the combined flagellated population.
- $SI:C_{DIA}$ is the molar silicon content of functional macromolecules of diatoms.
- f_{NH4} is the ratio of phytoplankton ammonium uptake to the total inorganic nitrogen uptake. The empirical relationship (Table 4.I) relating f_{NH4} to ambient ammonium was derived from nitrogen uptake studies conducted in the Weddell Sea area (Goeyens et al., 1991).

  Stoechiometric ratios (Fe:N:C) were derived from literature. Values are reported in tables 4.III, 4.IV and 4.V for phytoplankton, protozooplankton and bacterioplankton respectively.

4.3 MODEL RESULTS

4.3.1 Validation : application of the swamco model to the ANTX/6 site

The ANTX/6 sampling site, at 6°W in the Atlantic sector of the Southern Ocean has been chosen for a first application of the SWAMCO coupled physical-biogeochemical model. This area is crossed by two contrasting water masses : the iron-depleted (~0.4nM) but sea-ice-associated southern branch of the ACC (~ 51-56°S) and the iron-enriched (1.8nM) Polar Frontal Jet (~ 47-50°S, Veth et al., 1996). Transects were repeatedly sampled over a one-month period, at the early beginning of the growth season, providing spatio-temporal distributions of dissolved iron (de Baar et al., 1996), chlorophyll a (Bathmann et al., 1996), nanophytoplankton and protozoa (Becquevort, 1996) for model calibration and validation.

Model implementation:

The SWAMCO model has been run at each half-degree of latitude between 47°S and 58°S, over a 40-day period (20th October-30th November 1992). As a first application, and for a better assessment of the performance of the 'biogeochemical component' of the coupled physical-biological model, advection by currents or wind drift has been neglected. This reduction of physical processes makes sense due to the larger scale of horizontal advection compared with the scale of vertical and biogeochemical terms of the mathematical model. Also, the stabilizing mechanisms occurring at the Polar Front i.e. the admixture of warmer subpolar waters from the North were not considered by the physical model. The temporal variation of the state variables were calculated according to the Eulerian procedure, using 0.5m as vertical resolution and 1h for time step integration. Exportation terms (mesozooplankton faecal pellets and diatom sedimentation) constitute a loss term for the surface waters.

Initial values of biological state variables were set at their minimum level, corresponding to biomasses recorded during the end-winter period (Table 4.VI.). Initial concentration of 0.4 and 2 nM was chosen for dissolved iron in the ACC and Frontal area respectively (de Baar et al., 1995; Table 4.VI.). Sea ice conditions and meteorological data reconstructed from continuous shipboard measurements and satellite information are the forcing function of the coupled physical-biological model.

Model results:

Due to the lack of high-resolution time-series of chemical and biological data at each simulated latitude - a general problem for ecological models calibration and validation -, the overall performance of the SWAMCO model was assessed by comparing model predictions and observations recorded in surface waters at the last sampled cross-section (Transect 11) of ANTX/6 cruise (Figure 4.9). Thus, simulations of Figure 4.9 encompass the early spring bloom event having occurred at the ANTX/6 over the preceding month.

Table 4.VI : SWAMCO model : initial values of state variables

State variables	Values	Units
F_{DIA}	1.6	mgC m^{-3}
R_{DIA}	0.2	mgC m^{-3}
S_{DIA}	0.2	mgC m^{-3}
R_{NANO}	0.2	mgC m^{-3}
S_{NANO}	0.2	mgC m^{-3}
F_{NANO}	1.6	mgC m^{-3}
HNF	1	mgC m^{-3}
MCZ	1	mgC m^{-3}
B	1	mgC m^{-3}
NO_3	31	µM
NH_4	0.2	µM
Fe	0.4 - 2	nM
H_1	5	mgC m^{-3}
H_2	200	mgC m^{-3}
MS	2.5	mgC m^{-3}
H_1N	0.04	µnM
H_2N	1.8	µnM
MSN	0.03	µnM

As a general trend, a good agreement is reached between predictions and available observations (Figure 4.9). Furthermore the model simulates quite well the spring bloom event in both water masses:

As observed (Bathmann et al., 1996; de Baar et al., 1995), the model predicts elevated chlorophyll a concentrations of 2-2.8 mg m^{-3} in the Polar Frontal Jet, while

phytoplankton of the ACC area is monotonously maintained at low chlorophyll a concentration below 0.5 mg m^{-3} (Figure 4.9a). Accordingly, predicted daily net primary production rates along the transect differ by about a factor 3 with elevated net daily primary production between 1000 and 1700 mgC m^{-2} d^{-1} in the Polar Frontal Jet and values typical of oligotrophic systems - around 100 mg m^{-2} d^{-1} - in the ACC area (Figure 4.9b).

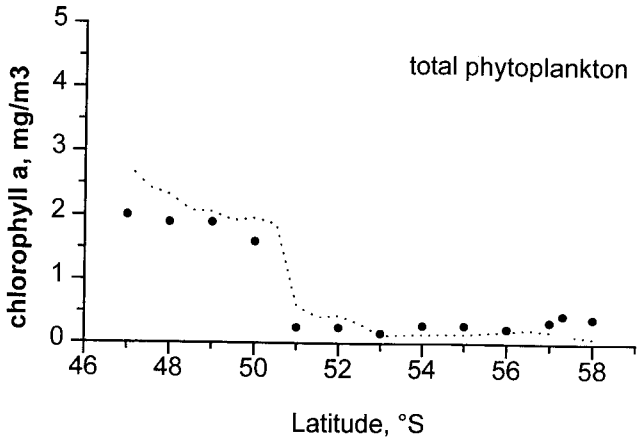

Figure 4.9a SWAMCO predictions at the ANTX/6 site : transect 11 predicted (solid line) and measured (solid circles) surface chlorophyll a

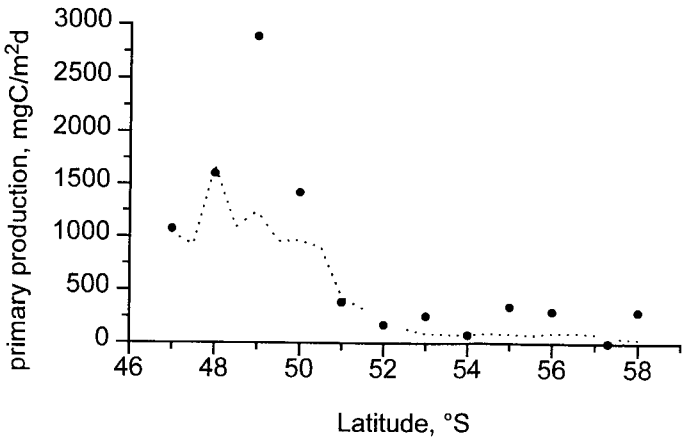

Figure 4.9b SWAMCO predictions at the ANTX/6 site : transect 11 predicted (solid line) and measured (solid circles) net primary production

In the iron-depleted ACC area, the predicted phytoplankton community is dominated by nanophytoplankton (Figure 4.9c), according to observation (Becquevort, 1996). Their biomass is keeping down by microzooplankton (Figure 4.9d) which grazing pressure is of the same order of magnitude as nanophytoplankton production (Figure 4.9ef). In perfect agreement with observation (de Baar et al., 1996), the model predicts a little decrease in dissolved iron from 0.4 to 0.38 nM over the one-month bloom period (Figure 4.9h). Such a low apparent utilization results from the strong coupling between iron nanophytoplankton uptake and iron regeneration associated with protozoa feeding activity (Figure 4.9e). Low availability of dissolved iron in HNLC marine systems would play a similar role as ammonium in oligotrophic open waters in structuring the ecological functioning of the marine ecosystem.

In the Polar Front, more than 90% of the predicted phytoplankton biomass is produced by diatoms (Figure 4.9g). The model predicts a diatom-chlorophyll a increase of 1.8 mg m^{-3} over the one-month simulated period and an iron and nitrate decrease of respectively 0.8 nM and 2 µM is simulated for the same period, in perfect agreement with measurements (de Baar et al., 1995). Interestingly enough nanophytoplankton is always present and maintained at low biomass (<0.5mg m^{-3}) due to the heavy grazing pressure of the ubiquitous microzooplankton (Figure 4.9ef).

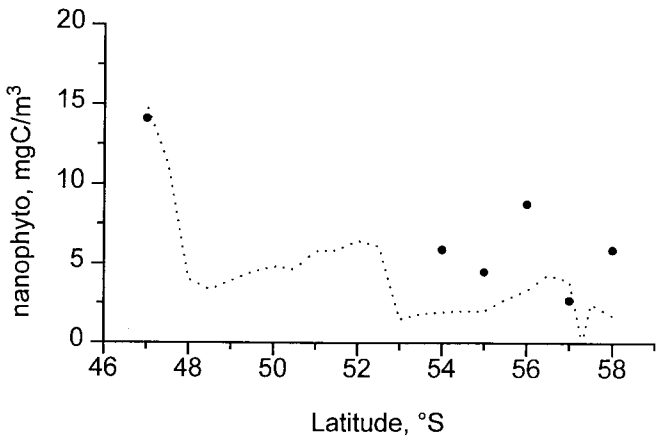

Figure 4.9c SWAMCO predictions at the ANTX/6 site : transect 11 predicted (line) and observed (solid circles) nanophytoplankton

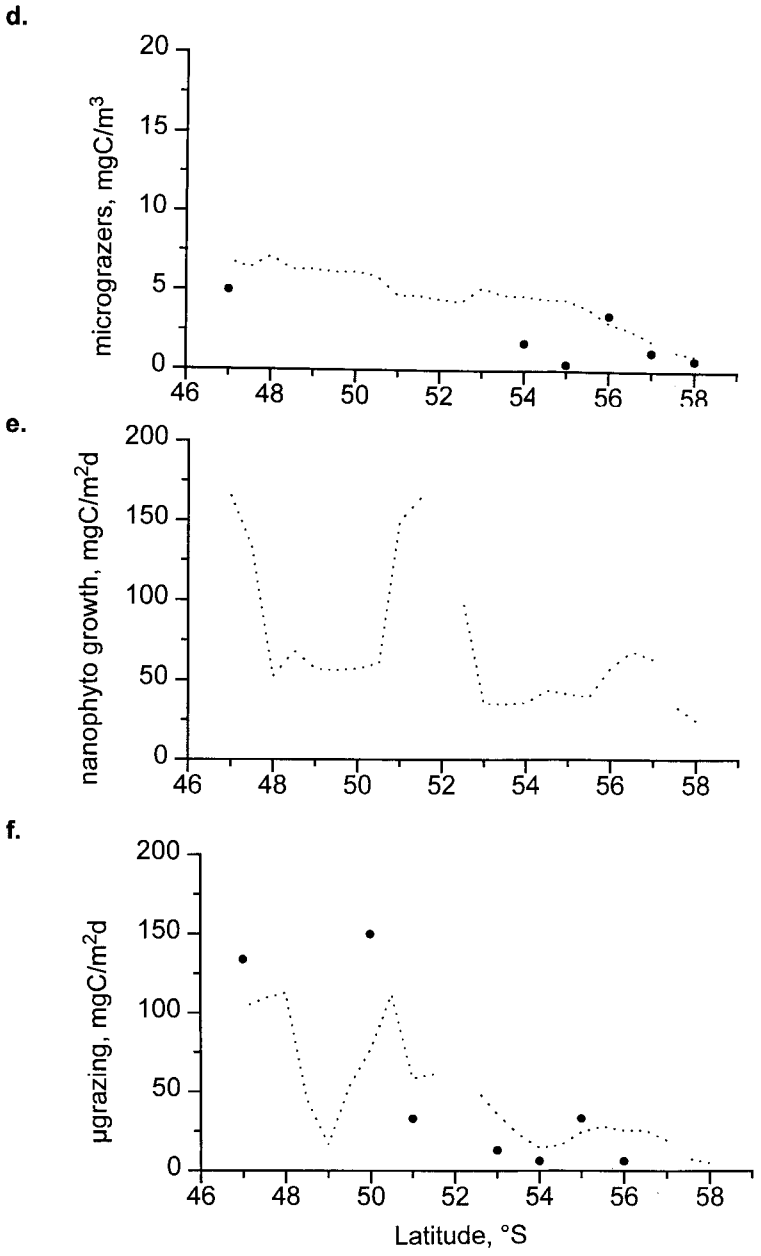

Figure 4.9 **SWAMCO predictions at the ANTX/6 site : transect 11**
d):predicted (line) and observed (solid circles) microzooplankton
e) predicted (line) and observed (solid circles) nanophytoplankton daily growth

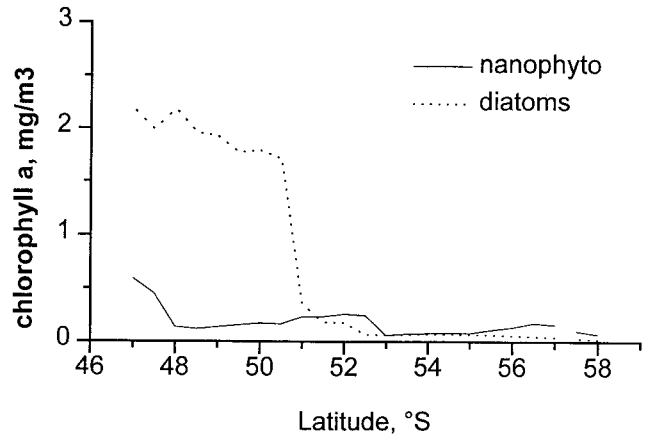

Figure 4.9g SWAMCO predictions at the ANTX/6 site : transect 11 predicted diatom- (solid line) and nanoplytoplankton- (dotted line) chlorophyll a distribution

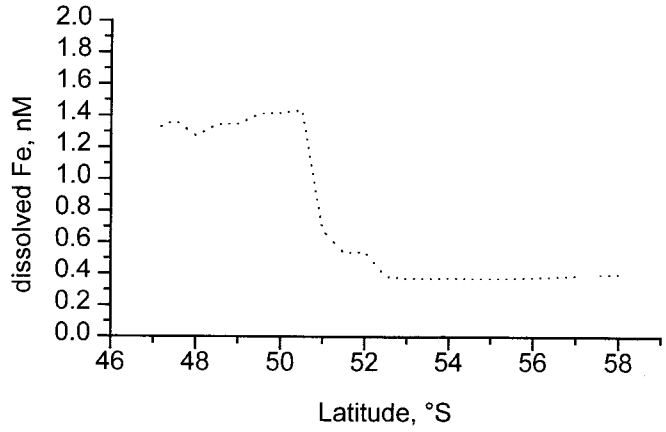

Figure 4.9h SWAMCO predictions at the ANTX/6 site : transect 11 predicted dissolved iron in surface waters.

4.3.2 SWAMCO scenarios : phytoplankton blooms and food web structure in the Southern Ocean : iron, krill, sea ice and wind

The capability of the SWAMCO model to address the paradoxical nature of the Southern Ocean and hence its role in global carbon cycle has been tested by running several scenarios under contrasting conditions. Particular attention was given to the physical, chemical and biological conditions that allowed diatom versus nanophytoplankton development i.e. the establishment of a dominated- linear food chain versus a microbial food web. Our previous analysis of the structure and functioning of the Antarctic food chain (chapter 3) indeed demonstrates that both the timing, the amplitude and the extent of Antarctic phytoplankton blooms are determined by the combined action of the light environment - under control of sea ice and wind stress -, grazing pressure by micro-, meso-zooplankton and krill and iron availability. The interplay between these factors is however not unique over the whole Southern Ocean, either temporaly or geographically. Furthermore, a spectrum of food chain structures is to be expected, between two extremes. Large diatoms developments controlled by krill swarm passages are forseen in iron-enriched neretic areas when meteorological conditions are favourable (high light, low wind). Low nanophytoplankton growth controlled by microzooplankton is expected in iron-low regions suffering severe meteorological conditions.

The generic property of the SWAMCO model is then determined by its ability to properly integrate the complex interaction between physical, chemical and biological factors as co-limiting agents of phytoplankton bloom developments and food-web structures in the Southern Ocean. This quality of the SWAMCO model has been appraised throughout its capability to properly simulate the diatom versus nanophytoflagellate dominances observed at ANTX/6 and EPOS sampled sites and by testing its response to several iron-enrichment scenarios.

Diatom, nanophytoplankton blooms at the ANTX/6 site : iron, sea ice and wind

Application of the SWAMCO model to the ANTX/6 site clearly evidences the key role of dissolved iron availability in driving phytoplankton bloom and structuring the phytoplankton community (Figure 4.10bc). Diatom-dominant phytoplankton biomass is simulated in the iron-rich Polar Frontal Jet (Figure 4.12b). Furthermore, the maximum biomass reached by the diatom development is determined by iron concentration (Figure 4.11ac) up to a maximum value which depends on the vertical stability of the surface waters (Figure 4.11b). Nanophytoplankton is maintained at low level by protozoan grazing pressure, independently of iron concentration (Figure 4.13).

Extremely low biomass of nanophytoplankton is predicted in the iron-deficient Antarctic Circumpolar Current as well as in the Polar Frontal Jet (Figure 4.10b). No ice-edge related phytoplankton bloom is simulated. To which extent the lack of phytoplankton development at the receeding ice-edge could be attributed to iron deficiency or light limitation owing to the severe meteorological conditions met at these latitudes was investigated by running SWAMCO iron-enrichment scenarios in the

ACC area (latitude 56°S). Model simulations show the positive response of diatoms to increasing ambient iron but when the upper mixed layer is stabilized at about 20m (Figure 4.13a). The frequent storm events prevailing during the first 25 days of the simulation (see predicted WML on Figure 4.10d) were preventing any bloom to develop. As simulated in the Polar Frontal Jet, nanophytoplankton biomass varies independently of iron availability and is maintained at low level by the ubiquitous herbivorous protozoan community (Figure 4.13b). From this it can be savely concluded that light was the major factor limiting phytoplankton development at the beginning of the investigated period. During the auspicious meteorological conditions met at the end of the cruise, iron limitation was the main factor preventing diatom to growth. Accordingly, the SWAMCO model reproduces quite well the observed stimulation of diatom growth after iron addition upon ice edge melting (de Baar et al., 1996; Figure 4.14)

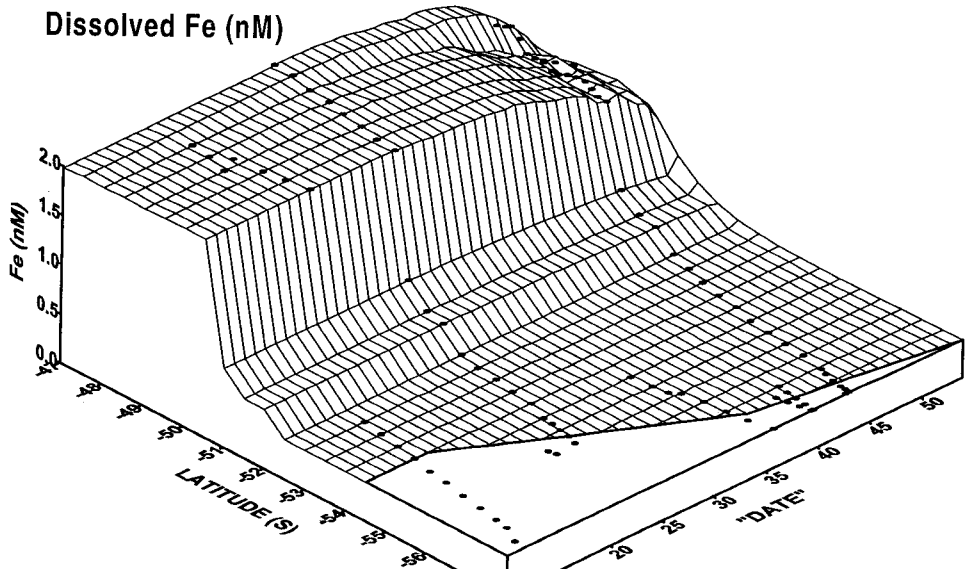

Figure 4.10a.: **swamco prediction of surface dissolved iron at the ANTX/6 site**

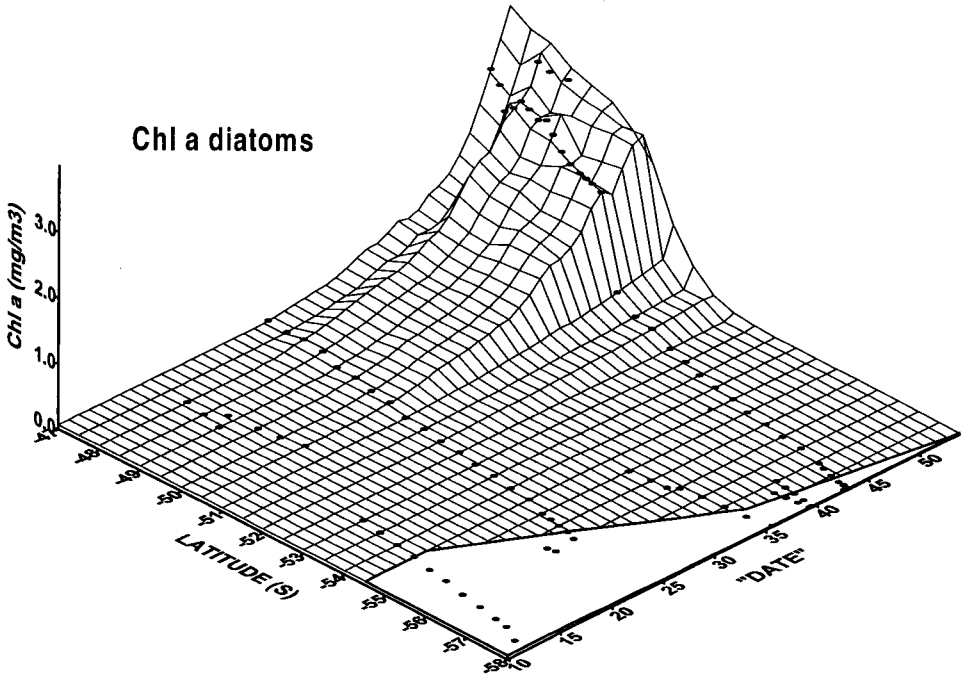

Figure 4.10b.: **swamco prediction of surface layer diatom-Chl.a at the ANTX/6 site**

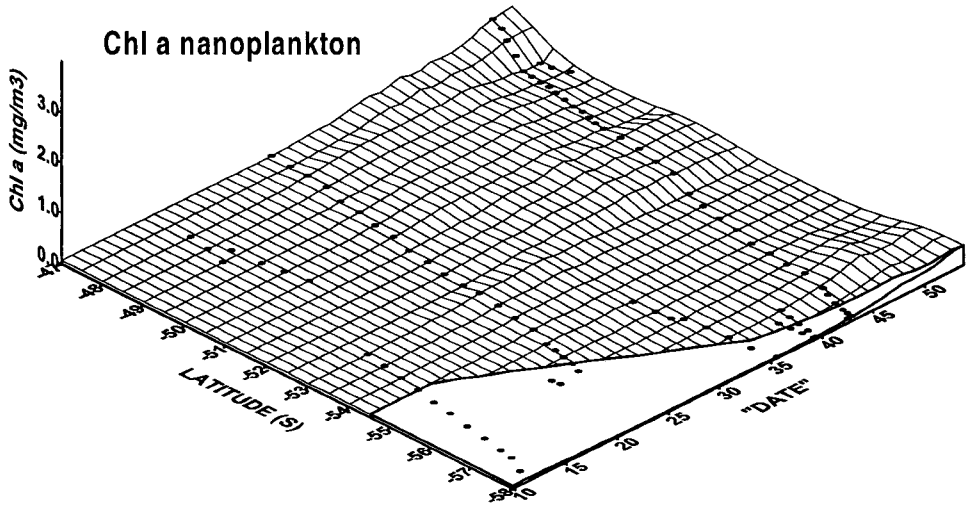

Figure 4.10c.: **swamco prediction of surface layer nanophytoplankton-Chl.a at the ANTX/6 site**

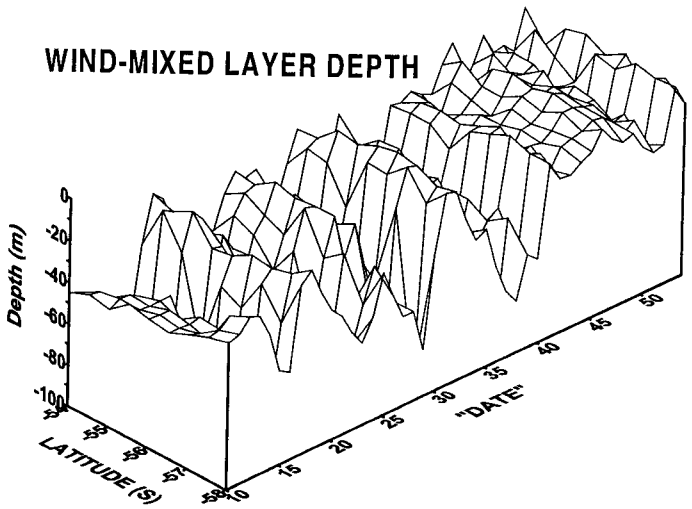

Figure 4.10d.: WML depth prediction at the ANTX/6 site

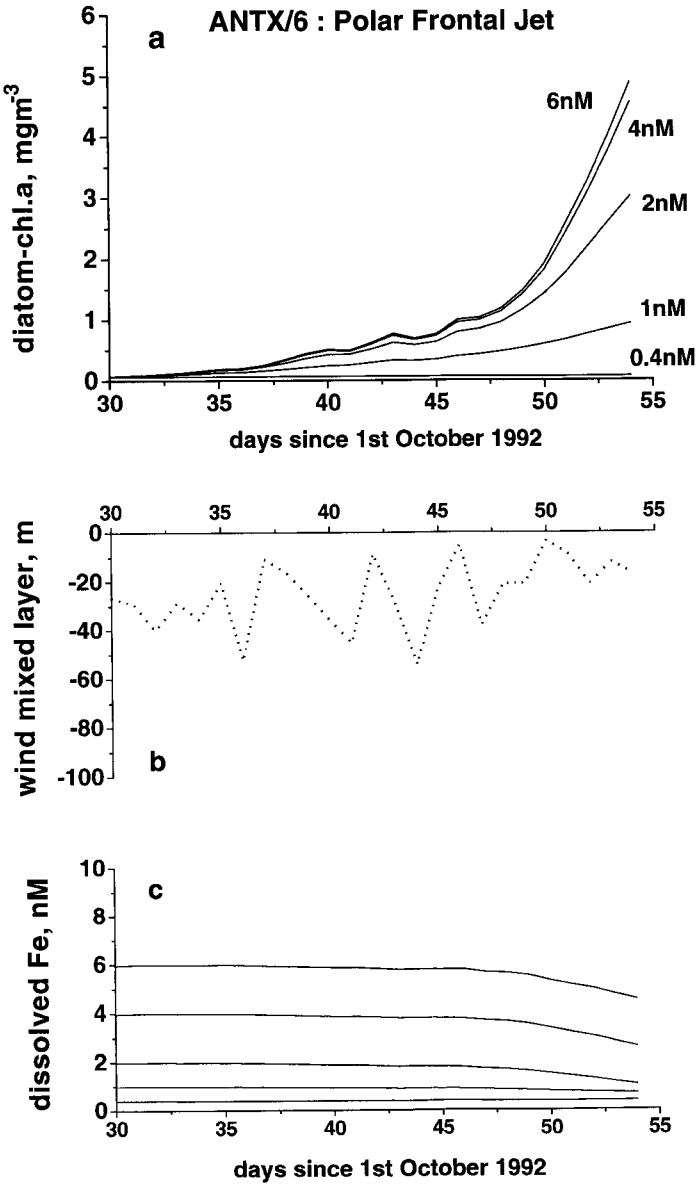

Figure 4.11 : **swamco predictions at latitude 47°S (ANTX/6 site, Polar Frontal Jet) : a) diatom development at different iron concentrations; b) wind mixed layer depth; c) dissolved iron**

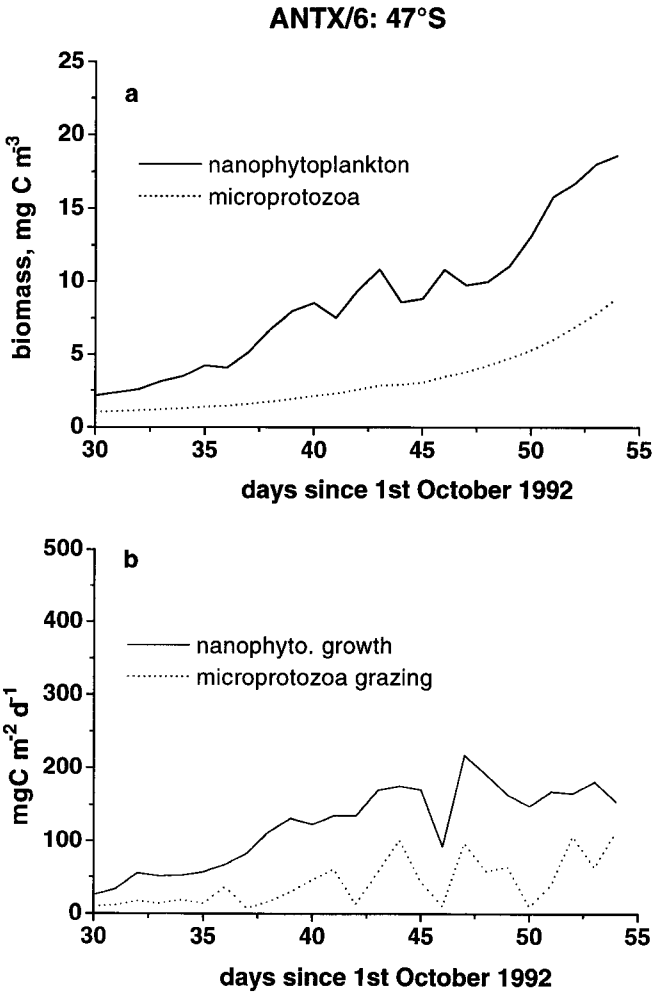

Figure 4.12.: **swamco predictions at latitude 47°S (ANTX/6 site, Polar Frontal Jet) : nanophytoplankton and micrograzers development.**

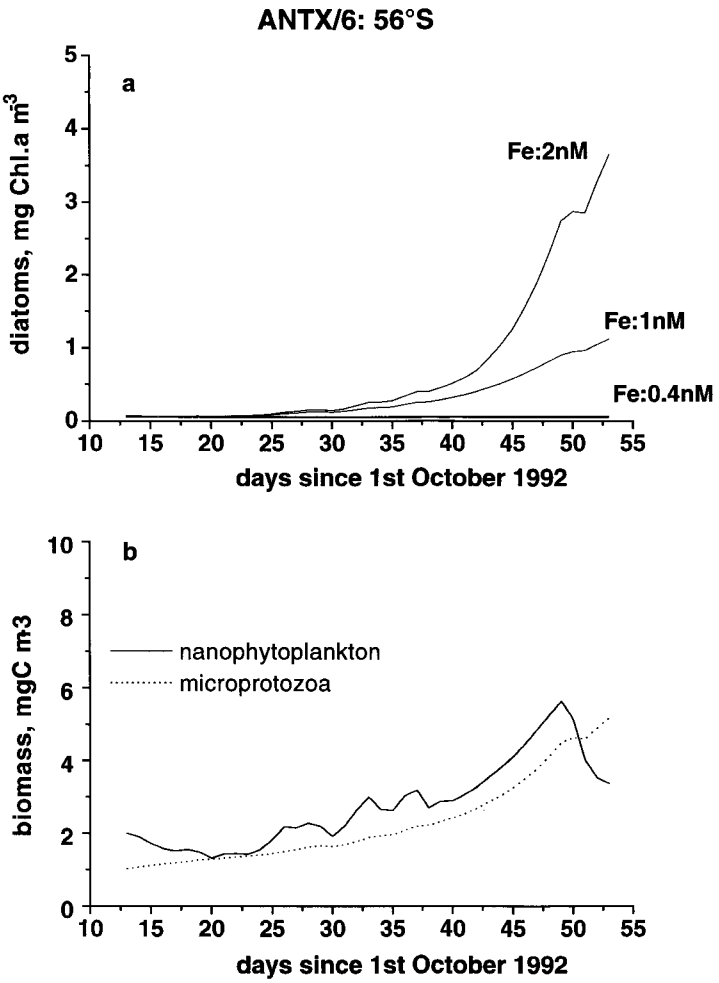

Figure 4.13. : **swamco predictions at latitude 56°S (ANTX/6 site, Antarctic Circumpolar Current) :a) diatom development at different iron concentrations; b) nanophytoplankton and micrograzers development.**

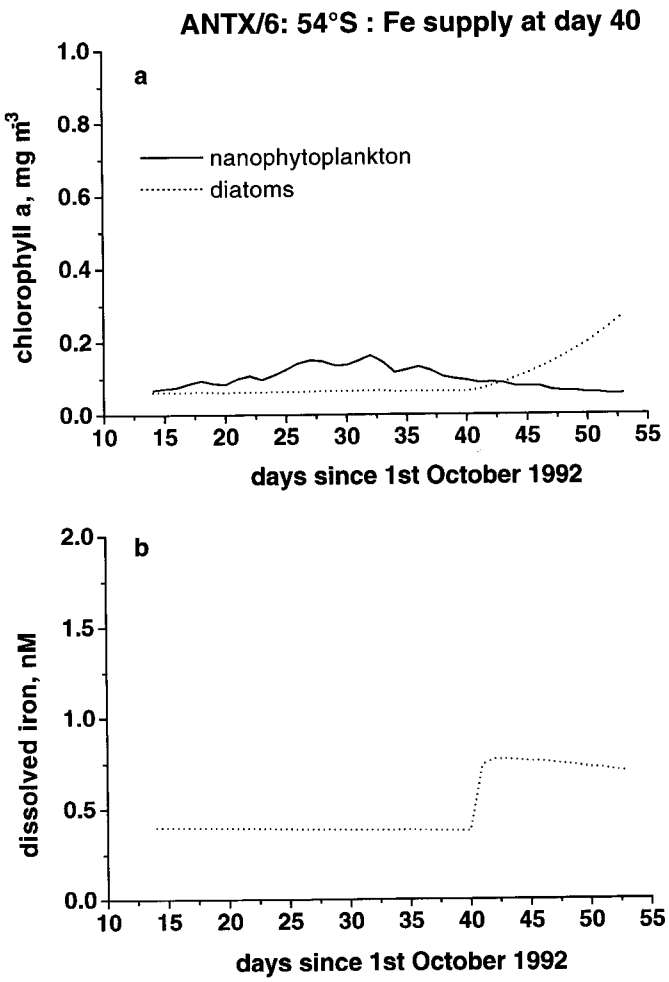

Figure 4.14.: **swamco predictions at latitude 54°S (ANTX/6 site, Antarctic Circumpolar Current) with supply of 0.5 nM Fe at day 40 (10 Nov.1992) : a) diatom and nanophytoplankton developme; b) dissolved iron concentration.**

Diatom, nanophytoplankton blooms at the EPOS site : iron, krill, sea ice and wind

The catastrophic impact of a krill swarm passage on the ecosystem structure and functioning of the Southern Ocean has been often suggested (Smetacek et al., 1990) but seldom reported. Such an event was by chance observed at the iron-rich EPOS site (latitude 59°S). In less than 6h, the blooming phytoplankton community shifted from a diatom- to a nanophytoplankton- dominated population (Figure 3.7). The ecological significance of krill as vecteur of change in ecosystem structure and functioning was determined, based on SWAMCO run scenarios simulating the observed krill swarm passage or lack of at latitude 59°S. Observed meteorological and sea ice conditions (Lancelot et al., 1993) were used as forcing function and initial dissolved iron concentration was set at 2nM (Nolting, 1991) but no extra iron supply was considered. The krill event was simulated by dropping, at day 40, the biological state variables to their initial value (Table 4.VI). The ingested biomass by krill was considered as lost for the simulated surface water column, being advected with krill or exported as fecal pellets to deeper waters. However, a sloppy feeding of 10% supplying dissolved organic matter in the surface layer was assumed.

Comparing predictions at latitude 59°S in the absence (Figure 4.15) or presence (Figure 4.16) of krill gives some insight on conditions that lead to the observed ecosystem structure change.

In the absence of Krill, a diatom-dominated phytoplankton bloom reaching 4 mg Chl.a m^{-3} is predicted at the receeding ice edge (Figure 15a). Clearly the diatom bloom enhancement is determined by the predicted increase of upper layer vertical stability driven by ice melting under auspicious meteorological conditions (Figure 4.15b); the height is controlled by iron availability (Figure 4.15c). No diatom bloom is predicted at the end of the simulation in spite of optimal light conditions (shallow upper mixed layer, Figure 4.15) due to iron depletion. The model predicts a concomitant early development of both nanophytoplankton and diatoms (Figure 4.15a). However, and in spite of favourable light conditions, predicted nanophytoplankton biomass never reaches concentrations higher than 1 mg Chl.a m^{-3} due to intense protozoan grazing pressure. Furthermore the model predicts a delay of less than 10 days between those primary and secondary producers the biomass of which is kept at very low level (Figure 4.15d).

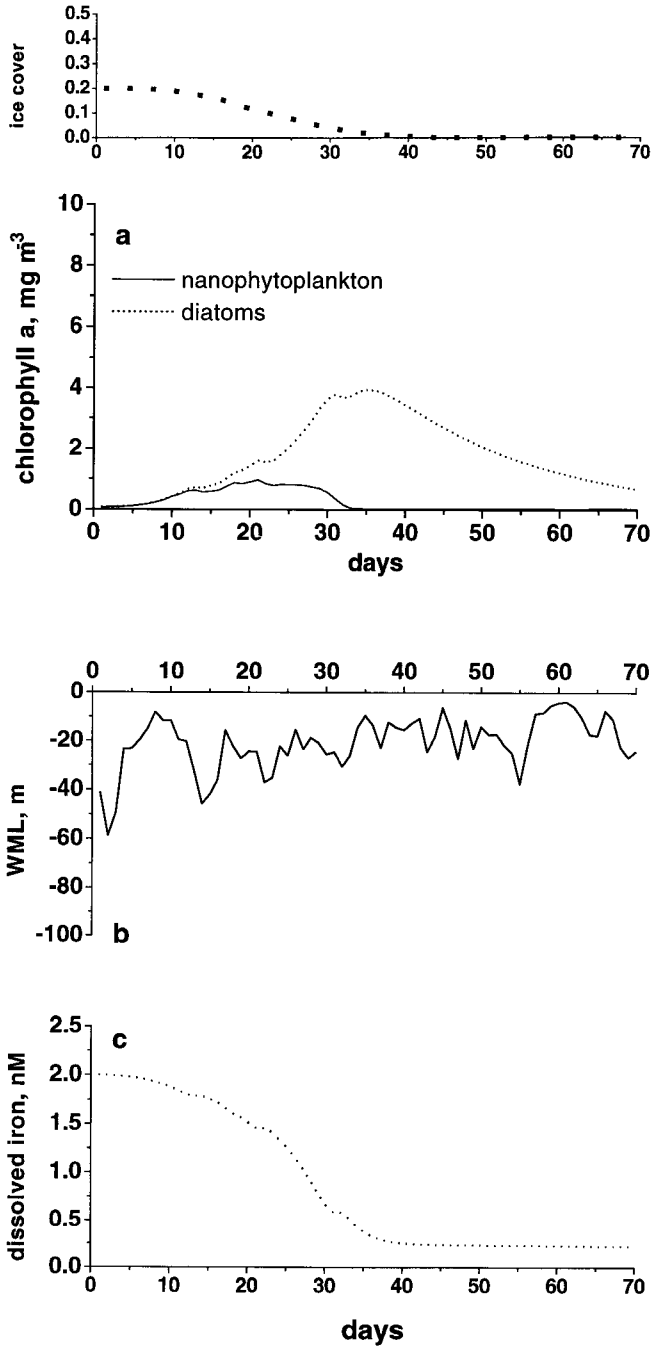

Figure 4.15: SWAMCO predictions at latitude 59°S (EPOS site) : no krill

Krill event happened at day 40 i.e. when maximum diatom biomass was reached and iron was depleted (Figure 4.15). After krill passage, a significant nanophytoplankton bloom of 5 Chl.a m^{-3} is predicted at the end of the simulation, when extremely favourable meteorological conditions were met (Figure 4.16). The succesfull development of the nanophytoplankton community was made possible because of increased water column stability and the elimination of micrograzers after krill ingestion (Figure 4.16). Reversely diatoms could not develop in spite of optimal light conditions due to growth limitation by iron shortage. Interestingly enough, the development of a second phytoplanton bloom entirely dominated by nanophytoplankters is predicted after diatom bloom vanishing by krill swarm passage. The intensity of this nanophytoplankton bloom is then strongly determined by the meteorological conditions prevailing over a 10 day-period, the necessary delay for micrograzer exponential development.

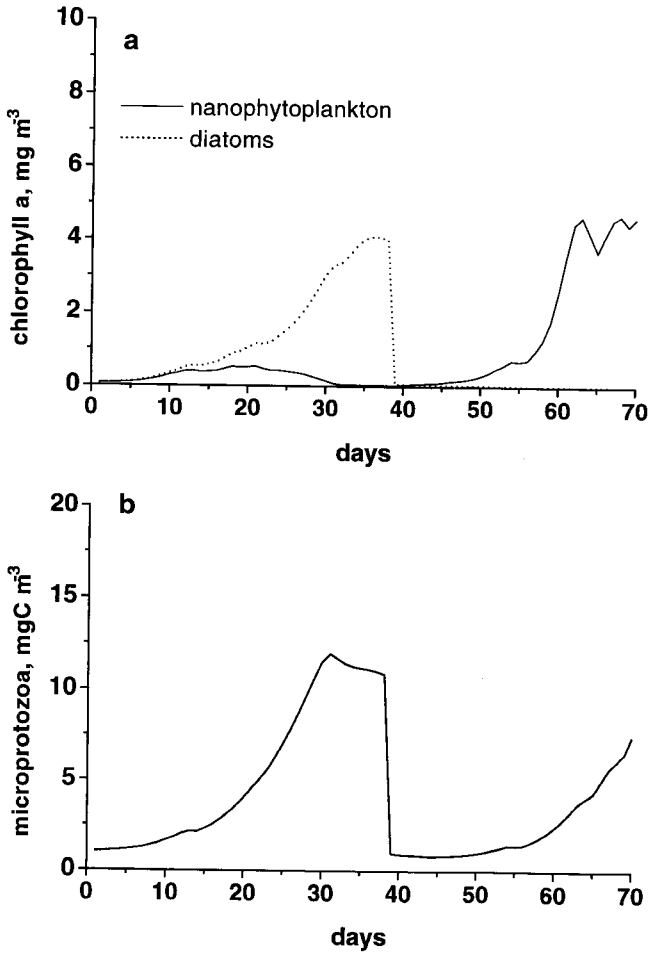

Figure 4.16: SWAMCO predictions at latitude 59°S (EPOS site) : krill swarm passage at day 40

5. CONCLUSION AND PERSPECTIVES

Observational analysis of the structure and functioning of the Antarctic pelagic food chain combined with SWAMCO model scenarios performed under contrasting meteorological, chemical and biological conditions conclude that the HNLC (High Nutrient Low Chlorophyll) conditions of the Southern Ocean are resulting from the successfull development of micrograzer-controlled nanophytoplanktonic communities in an iron-limited environment. Episodic diatoms blooms are well developping in iron-rich areas provided optimal light conditions are reached and maintained. These blooms are however very transient because of their great vulnerability to Krill swarm passage. Furthermore, and for both phytoplanktonic communities, light constitutes a major limiting factor in this extreme environment, driven by wind mixing and ice cover.

Furthermore, the Southern Ocean cannot be regarded as homogeneous with respect to sea-ice dynamics, meteorological conditions, dissolved iron and krill swarm distributions.

Large parts of the circumpolar Southern Ocean , especially the Antarctic Circumpolar Current, are traditionally renowned for experiencing violent and frequent storms. Those regions are consequently not the right place to assist intense phytoplankton development wathever iron availability could be. Areas with favourable weather circumstances for phytoplankton bloom development can be identified from the reconstruction of the 1992 monthly wind climate (Figure 5.1) based upon data from ECMWF (European Centre for Medium Range Weather Forecasts). Figure 5.1. clearly shows that the wind field is far from being uniform all over the Southern Ocean. Accordingly the ANTX/6 site was in the 'most wind-stressed' region while EPOS site occurred in areas with low wind speed. Highly favourable weather circumstances for phytoplankton development are also expected to occur in the Prydz Bay and the Ross Sea.

Subnanomolar concentration of dissolved iron, characteristic of upwelled deep waters (de Baar et al., 1995) can be considered as general for the Southern Ocean. Areas enriched with iron supply are then neretic waters - the continental shelf and the proximity of islands - , the Polar Frontal Jet, some ice-covered regions (Table 5.I).

Furthermore, krill does not distribute similarly around Antarctica (Figure 5.2).

Combining all this information, makes possible to identify key areas of the Southern Ocean where diatom bloom development and related carbon exportation are expected to occur. This would be of great help for identifying future field studies and improving carbon budget estimate at the scale of the global Southern Ocean.

However, and with respect to the large spectrum of physical, meteorological, chemical and biological conditions occurring in the Southern Ocean, its role in global

carbon cycling cannot be properly addressed without help of a coupled 3D physical-biogeochemical model of the Southern Ocean including the dynamics of sea-ice formation and ablation. As a first step in this direction the generic quality of the biogeochemical SWAMCO model describing C, N, Fe cycling through aggregated components of the pelagic ecosystem in fonction of light and iron conditions has been demonstrated throughout its successful application to visited sites. Future work would sake for coupling of the mechanistic SWAMCO model to a 3D physical model of the sea-ice-ocean system.

Table 5.I Iron distribution in the Southern Ocean

Site	dissolved iron, nM	Reference
Weddell/Scotia Sea	>1	Nolting et al., 1991
Drake passage		
inshore	5-7	Martin et al., 1990
offshore	0.1-0.9	
Ross Sea		
inshore	>1	Martin et al., 1990
offshore	<1	
Atlantic sector : 6°W		
ACC	<1	de Baar et al., 1996
Polar Front	>1	
Pacific sector : 89°W		de Jong et al., in prep.
subabtarctic	0.5	
Polar Front	0.6-1	
ACC	0.5	
cont. margin	0.6-1	

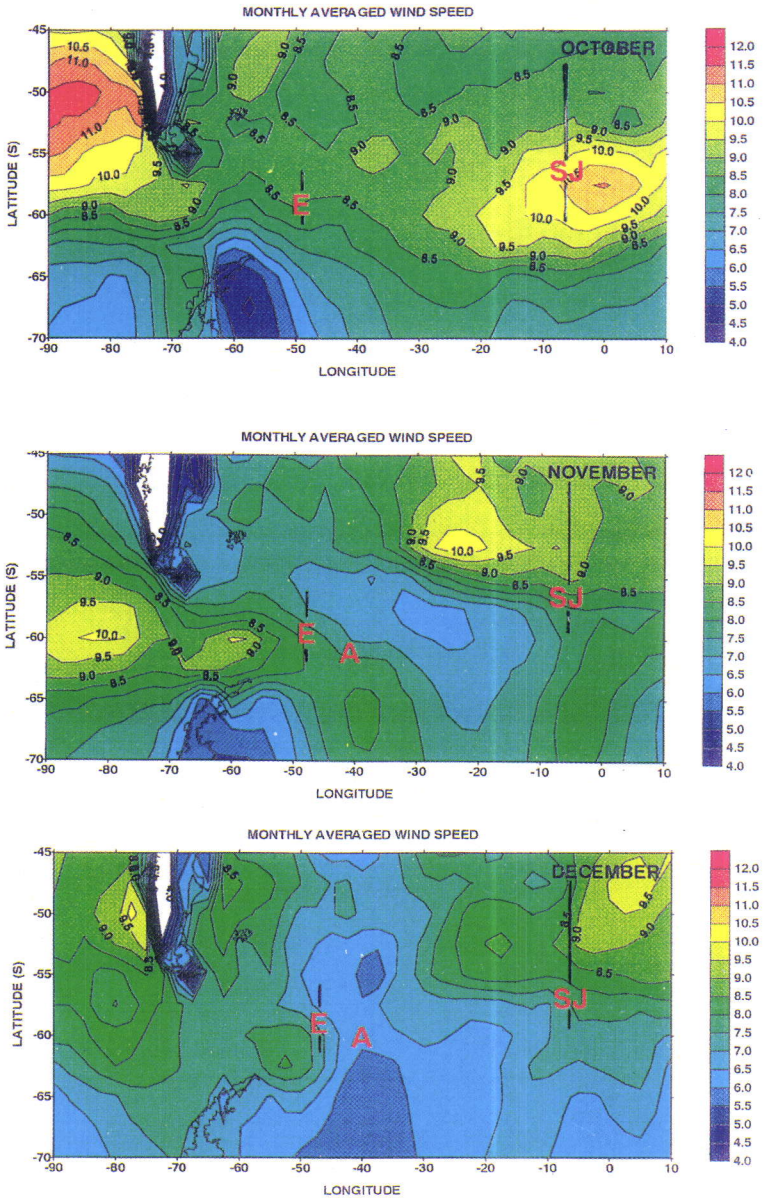

Figure 5.1 : Monthly averaged wind velocity (m s-1 estimated for Austral spring 1992 from ECMWF data. Regions investigated during the Ameriez (A), EPOS (E) and ANTX/6 (SJ) are indicated as well.

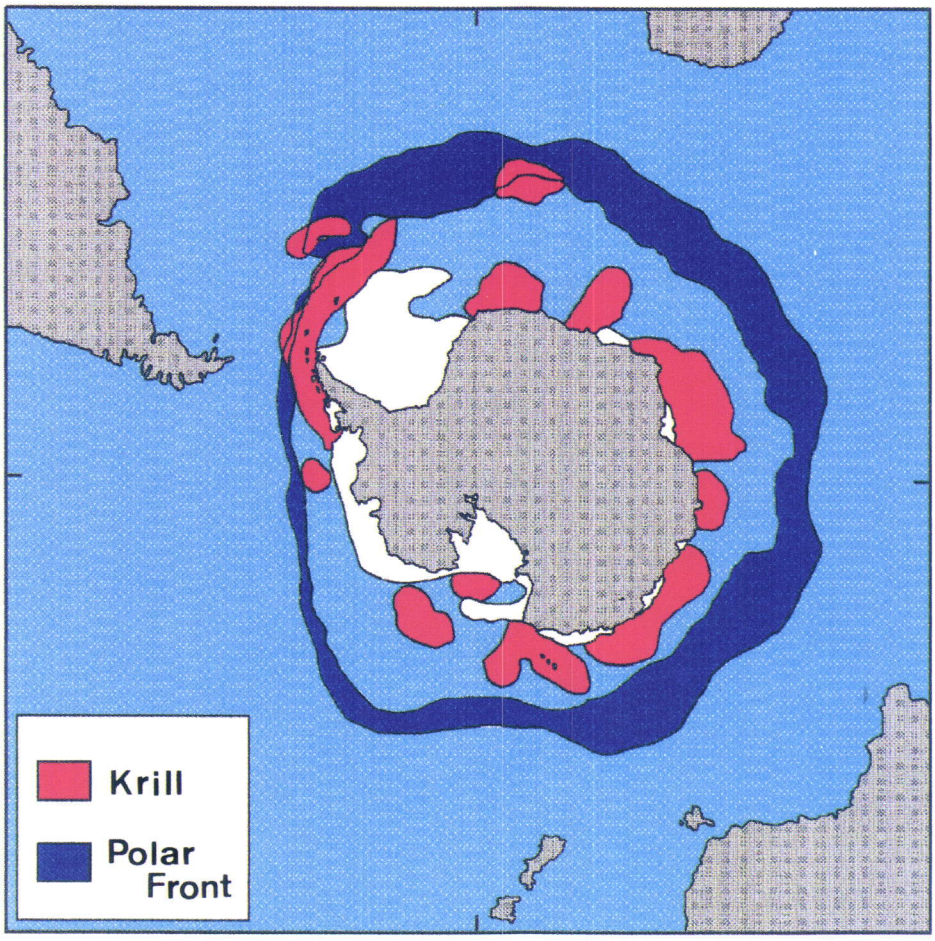

Figure 5.2 : Krill distribution in the Southern Ocean. Redrawn from

ACKNOWLEDGEMENTS

This work is a part of the Phase III of the Belgian Scientific Programme of Antarctic funded by SSTC (Brussels, Belgium). Most of data presented in this report were collected during two polar expeditions (ANTX/6 and ANTARES 2), in the scope of the international SO-JGOFS Program. We take the opportunity to express our gratitude to Victor Smetacek, Hein de Baar and Paul Treguer, the scientific responsible for the respectively German, Dutch and French SO-JGOFS Programme, who took an active part in the implantation and coordination of research activities.

We are especially grateful to the captain and the crew of RV Polarstern and RV Marion Dufresne for their helpful assistance during the cruise.

The scientific concepts and the generic biogeochemical model we developed is the fruit of ecological and geochemical-oriented discussions we had on board and later during meetings. We are especially grateful to Victor Smetacek and Hein de Baar. Our discussions were sometimes very hard but always delight and very fruitful. Also we than Kees Veth for the physical development of the model and for his great interest for biology.

Last but not least, all our thanks to our Belgian colleagues Leo Goeyens and Frank Dehairs who are our faithful cruise companions since 1988 and contribute to the success of the Belgian research activities in the scope of the SO-JGOFS Programme

6. REFERENCES

Archer, S.D., Leakey, R.J.G., Burkill, P.H. and Sleigh, M.A. Microbial dynamics in coastal waters of East Antarctica: herbivory by heterotrophic dinoflagellates. Marine Ecology Progress Series, submitted.

Bainbridge, A.E. 1980. Geosecs Atlantic expedition. V.2. Sections and profiles. U.S. GPO.

Bathmann, U.V., Scharek, R. and Dubischar, C. 1996. Chlorophyll and phytoplankton species distribution in the Atlantic sector of the Southern Ocean in spring. Deep Sea Res. In press.

Bathmann, U.V., Smetacek, V., de Baar, H., Fahrbach, E. and Krause, H. 1994. The expeditions ANTARKTIS X/6-8 of the Research Vessel "Polarstern" in 1992/93. Berichtze zur Polarforschung. 135-236 .

Becquevort, S. 1996. Nanoprotozooplankton of the Atlantic section of the Southern Ocean in early spring : biomass and feeding activities. Deep Sea Res. In press.

Becquevort, S., Mathot, S. and Lancelot, C. 1993. Interactions in the microbial community of the marginal ice zone of the northwestern Weddell Sea through size distribution analysis. Polar Biol. 12 : 211-218.

Bedo, A., Labat, J.P. and Mayzaud, P. 1995. In: ANTARES 2/MD 78. à bord du MARION-DUFRESNE 26 Janvier-23 Mars 1994. Institut Français pour la Recherche et la Technologie Polaires. 95-01, 164-168.

Bianchi, F., Boldrin, A., Cioce, F., Dieckmann, G., Kuosa, H., Larsson, A-M., Nöthig, E.-M, Sehlsted, P.-I., Socal, G. and Syversten, E.E. 1993. Phytoplankton distribution in relation to sea ice, hydrography and nutrients in the Northwestern Weddell Sea in early spring 1988 during EPOS. Polar Biol. 12 : 225-236.

Billen, G. and Servais, P. 1989. Modélisation des processus de dégradation bactérienne de la matière organique en milieu aquatique. In : Micro-organismes dans les écosystèmes océaniques. Bianchi et coll. Masson. 219-245.

Billen, G. and Becquevort, S. 1991. Phytoplankton-bacteria relationship in the Antarctic marine ecosystem, Polar Res. 10 : 245-263.

Borsheim, K.Y. and Bratbak G. 1987. Cell volume to cell carbon conversion factors for a bacterivorous Monas sp. enriched from seawater. Mar. Ecol. Prog. Ser. 36 : 171-175.

Burkill, P.H., Edwards, E.S. and Sleigh, M.A. 1995. Microzooplankton and their role in controlling phytoplankton growth in the marginal ice zone of the Bellingshausen Sea. Deep-Sea Res. 42 : 1277-1290.

Campbell, J.W. and Aarup, T. 1989. Photosynthetically available radiation at high latitudes. Limnol. Oceanogr. 34 : 1229-1243.

Cole, K.H. 1994. Effect of iron, manganese, copper and zinc enrichment on productivity and biomass in the subarctic Pacific. Limnol. Oceanogr. 36 : 1851-1864.

de Baar, H.J.W., Buma, A.G.J., Nolting, R.F., Cadée, G.C., Jacques, G. and Tréguer, P.J. 1990. On iron limitation of the Southern Ocean: experimental observations in the Weddell and Scotia Seas. Mar. Ecol. Progr. Ser. 65 : 105-122.

de Baar, H.J.W., de Jong, J.T.M., Bakker, D.C.E., Löscher, B.M., Veth, C., Bathmann, U. and Smetacek, V. 1995a. Importance of iron for plankton blooms and carbon dioxide drawdown in the Southern Ocean. Nature. 373 : 412-415.

de Baar, H.J.W., van Leeuwe, M.A., Scharek, R. and Goeyens, L. 1995b. Iron and Plankton Ecology of Polar and Subpolar Oceans. JGOFS Symposium Volume In IGBP Books Series. University Press, Cambridge. to be published.

de Baar, H.J.W., van Leeuwe, M.A., Scharek, R. and Goeyens, L., Koeve, W., Bakker, K.M.J. and Fritsche, P. 1996. Iron availability May Affect the Nitrate/Phosphate Ratio (A.C. Redfield) in the Antarctic Ocean. Deep-Sea Res. in press.

Denman, K.L. 1973. A time-dependant model of the upper ocean. Journal of Physical Oceanography. 3 : 173- 184.

Edler, L. 1979. Recommendations for marine biological studies in the Baltic Sea. Phytoplankton and Chlorophyll. Baltic Marine Biologists. 4 : 1-38.

El-Sayed, S.Z. 1984. Productivity of the Antarctic waters : a reappraisal. In : Marine phytoplankton and productivity, Holm-Hansen, Bolis, L. and Gilles, R., (Eds). Springer. 19-34.

Fiala, M. 1995. ANTARES 2/MD 78. à bord du MARION-DUFRESNE 26 Janvier-23 Mars 1994. Institut Français pour la Recherche et la Technologie Polaires. 95-01. 178pp .

Fiala, M. and Oriol, L. 1995. Biomasse des différentes classes de taille phytoplanctoniques dans l'Océan Indien Austral durant l'été. 1995. In: ANTARES 2/MD 78. à bord du MARION-DUFRESNE 26 Janvier-23 Mars 1994. Institut Français pour la Recherche et la Technologie Polaires. 95-01. 97-102.

Garrison D.L. 1991. An overview of the abundance and role of protozooplankton in Antarctic waters. Journal of Marine systems. 2 : 317-331.

Garrison, D.L., and Buck, K.R. 1989. Protozooplankton in the Weddell Sea, Antarctica: Abundance and distribution in the ice-edge plankton. Polar Biol. 9 : 341-351.

Garrison, D.L., Buck, K.R. and Fryxell, G.A. 1987. Algal assemblages in Antarctic pack ice and in ice-edge plankton. Journal of Phycology, 23 : 564-572.

Garrison D.L., Buck, K.R. and Gowing, M.M. 1991. Plankton assemblages in the ice edge zone of the Weddell Sea during the austral winter. Journal of Marine systems. 2 : 123-130.

Garrison D.L., Buck, K.R. and Gowing, M.M. 1993. Winter plankton assemblage in the ice edge zone of the Weddell and Scotia Seas: composition, biomass and spatial distributions. Deep-Sea Res. 40: 311-338.

Goeyens, L., Tréguer, P., Lancelot, C., Mathot, S., Becquevort, S., Morvan, J., Dehairs, J. and Baeyens, W. 1991. Ammonium regeneration in the Scotia-Weddell confluence area during spring 1988. Mar. Ecol. Progr. Ser.. vol. 78 : 241-252.

Hayes, P.K., Whitaker, T.M., Fogg, G.E. 1984. The distribution and nutient status of phytoplankton in the Southern Ocean between 20 and 70 °W. Polar Biol.3: 153-165.

Heinbokel, J.F. 1978. Studies on the functional role of tintinids in the Southern California Bight. I. Grazing and Growth Rates in Laboratory Cultures. Mar. Biol. 47 : 177-189.

Helbling, E.W., Villafane, V. and Holm-Hansen, O. 1991. Effect of iron on productivity and size distribution of Antarctic phytoplankton. Limnol. Oceanogr. 36 : 1879-1885.

Hempel, G. 1992. Weddell Sea Ecology, Results of EPOS, European "Polarstern" Study. Springer Verlag, Berlin Heidelberg ??p.

Hewes, C.D., Sakshaug, E., Reid, F.M. and Holm-Hansen, O. 1990. Microbial autotrophic and heterotrophic eucaryotes in Antarctic waters : Relationships between biomass and chlorophyll, aolenosine triphosphate and particulate organic carbon. Mar. Ecol. Progr. Ser. 63 : 27-35.

Holm-Hansen, O. and Mitchell, B.G. 1991. Spatial and temporal distribution of phytoplankton and primary production in the western Bransfield Strait region. Deep-Sea Res. 38 : 961-980

Hutchkins, D.A. 1995. Iron and the marine phytoplankton community. Prog. Phycol. Res. 11.

Jacques, G. and Panouse, M. 1991 Biomass and composition of size fractionated phytoplankton in the Weddell Sea Confluence area. Polar Biology, 11. 315-328

Jochem F.J., Mathot S. and B. Quéquiner (1995) Size-fractionated primary production in the open Southern Ocean in austral spring. Polar Biology. in press

Kiorboe, T. 1993. Turbulence, Phytoplankton Cell Size, and the Structure of Pelagic Food Webs. Advances in Marine Biology. 29: 1-72.

Klaas, C. 1996. Microprotozooplankton distributions and grazing impact in the Anatrctic Circumpolar Current. Deep-Sea Res. in press.

Lancelot, C., Veth, C. and Mathot, S. 1991a. Modelling ice-edge phytoplankton bloom in the Scotia-Weddell sea sector of the Southern Ocean during Spring 1988. J. Mar. Syst. 2 : 333-346.

Lancelot C., Billen, G., Becquevort, S., Mathot, S. and Veth, C. 1991b. Modelling carbon cycling through phytoplankton and microbes in the Scotia-Weddell Sea area during sea ice retreat. Mar. Chem. 35 : 305-324.

Lancelot, C., Mathot, S., Veth, C. and de Baar, H. 1992. On the factors controlling phytoplankton ice-edge blooms in the marginal ice zone of the north western Weddell Sea during ice retreat 1988 : Field observations and mathematical modelling. Polar Biol. 13(6) : 377-387

Lancelot, C., Mathot, S., Veth, C. and de Baar, H. 1993a. Factors controlling phytoplankton ice-edge blooms in the marginal ice-zone of the northwestern Weddell Sea during sea ice retreat 1988: field observations and mathematical modelling. Polar Biol. 13 : 377-387.

Lancelot, C., Mathot, S., Becquevort, S., Dandois, J.M. and Billen, G. 1993b. Carbon and nitrogen cycling through the microbial network of the marginal ice zone of the Southern Ocean with particular emphasis on the North Western Weddell Sea. In : Belgian Scientific Research Programme on Antarctica. Scientific results of Phase 2 (Feb.1989-Dec.1991), S. Caschetto, ed., Science Policy Office, Brussels. 1-103.

Lessard E.J. 1991. The trophic role of heterotrophic dinoflagellates in diverse marine environments. Mar. Microb. Food Webs. 5 : 49-58.

Löscher, B.M., de Jong, J.T.M., de Baar, H.J.W., Veth, C. and Dehairs, F. 1996. The distribution of Fe in the Antarctic Circumpolar Current. Deep-Sea Res. in press.

Martin, J.H. and Fitzwater, S.E. 1988. Iron deficiency limits phytoplankton growth in the North-East Pacific Subarctic. Nature. 331 : 341-343.

Martin, J.H., Coale, K.H., Johnson, K.S., Fitzwater, S.E., Gordon, R.M., Tanner, S.J., Hunter, C.N., Elrod, V.A., Nowicki, J.L., Coley, T.L., Barber, R.T., Lindley, S., Watson, A.J., Van Scoy, K., Law, C.S., Liddicoat, M.I., Ling, R., Stanton, T., Stockel, J., Collins, C., Anderson, A., Bidigare, R., Ondrusek, M., Latasa, M., Millero, F.J., Lee, K., Yao, W., Zhang, J.Z., Friederich, G., Sakamoto, C., Chavez, F., Buck, K., Kolber, Z., Greene, R., Falkowski, P., Chisholm, S.W., Hoge, F., Swift, R., Yungel, J., Turner, S., Nightingale, P., Hatton, A., Liss, P. and Tindale, N.W. 1994.Testing the iron hypothesis in ecosystems of the equatorial Pacific Ocean. Nature. 371 : 123-129.

Martin, J.H., Gordon, R.M., and Fizwater, S.E. 1990. Iron in Antarctic waters. Nature. 345 : 156-158.

Mathot, S. 1993. Phytoplankton in the marginal ice zone and its contribution to the annual primary production of the Southern Ocean. PhD thesis. Free University of Brussels, 200p.

Mathot, S., Becquevort, S. and Lancelot, C. 1991. Microbial communities from sea ice and adjacent water column at the time of ice melting in the northwestern part of the Weddell Sea. Polar Res. 10 : 267-275.

Mathot, S., Lancelot, C. and Dandois, J.M. 1992. Gross and net primary production in the Scotia Weddell sector of the Southern Ocean during spring 1988. Polar Biol. 12 : 321-332.

Mathot, S., Lancelot, C. and Garrison, D.L. Reevaluation on regional pelagic-and ice-based primary production in the Southern Ocean. submitted.

Menon, P., Becquevort, S., Billen, G. and Servais, P. 1996. Kinetics of Flagellate Grazing in the Presence of Two Types of Bacterial Prey. Microb. Ecol. 31: 89-101.

Menon, P., Lancelot, C. and Becquevort, S. 1995. In: ANTARES 2/MD 78. à bord du MARION-DUFRESNE 26 Janvier-23 Mars 1994. Institut Français pour la Recherche et la Technologie Polaires. 95-01. 154-163.

Mitchell, B.G. and Holm-Hansen, O. 1991. Observations and modelling of the Antarctic phytoplankton crop in relationship to mixing depth. Deep-Sea Res. 38 : 981-1008.

Morel, F.M.M., Rueter, J.G. and Price, N.M. 1991. Iron nutrition of phytoplankton and its possible importance in the ecology of ocean regions with high nutrient and low biomass. Oceanography. 4 : 56-61.

Nelson, D.M., Smith, W.O., Gordon, L.I. and Huber, B.A. 1987. Spring distribution of density, nutrients and phytoplankton biomass in the ice-edge zone of the Weddell-Scotia Sea. J. Geophys. Res. 92 : 7181-7190.

Nolting, R.F., De Baar, H.J.W., Van Bennekom, A.J. and Masson, A. 1991. Cadmium, copper and iron in the Scotia Sea, Weddell Sea and Weddell-Scotia Confluence (Antarctica). Mar. Chem. 35 : 219-243.

Nöthig, E.M. 1988. On the ecology of the phytoplankton in the southeasthern Weddell Sea (Antarctica) in january/february 1985. Berich Polarforsch. 53 : 1-118.

Platt, T., Gallegos, C.L. and Harrisson, W.G. 1980. Photoinhibition of photosynthesis in natural assemblages of marine phytoplankton. J. Mar. Res. 38 : 687-701.

Porter, K.G. and Y.S. Feig 1980. Use of DAPI for identifying and counting aquatic microflora, Limnol. Ocean. 25 : 943-948.

Price, N.M., Ahner, B.A. and Morel, F.M.M. 1994. The equatorial Pacific: Grazer controlled phytoplankton populations in an iron-limited ecosystem. Limnol. Oceanogr. 39 : 520-534.

Putt, M. and Stoecker, D.K. 1989. An experimentally determined carbon:volume ratio for marine 'oligotrichous' ciliates from estuarine and coastal waters. Limnol. Oceanogr. 34 : 1097-1103.

Putt, M. 1991. Development and evaluation of tracer particles for use in microzooplankton herbivory studies. Mar. Ecol. Prog. Ser. 77: 27-37.

Rublee, P.A. and Gallegos, C.L. 1989. Use of fluorescently labelled algae (FLA) to estimated microzooplankton grazing. Mar. Ecol.Progr. Ser. 51 : 221-227.

Sakshaug E. and Holm-Hansen, O. 1984. Factors governing pelagic production in polar oceans. In Marine phytoplankton and productivity, Lecture Notes in Coastal and Estuarine Studies. HOLM-HANSEN O., L. BOLIS and R. GILLES (Eds.), vol 8.

Sarthou, G., Jeandel, C., Brisset, L., Amouroux, D. and Donard, O. 1995. In: ANTARES 2/MD 78. à bord du MARION-DUFRESNE 26 Janvier-23 Mars 1994. Institut Français pour la Recherche et la Technologie Polaires. 95-01. 146-153.

Scharek, R.V., Smetacek, E., Fahrbach, E., Gordon, L.I., Rohardt, G. and Moore, S. 1994. The transition from winter to early spring in the eastern Weddell Sea, Antarctica: Plankton biomass and composition in relation to hydrography and nutrients. Deep-Sea Res. 41 : 1231 - 1250.

Servais, P., Billen, G., and Hascoët, M.C. 1987. Determination of the biodegradable fraction of dissolved organic matters in waters. Water Res. 21 : 445 -450.

Sherr F.B, Sherr E.B. and C. Pedros-Alio (1989) Silmutaneous measurement of bacterioplankton production and protozoan bacterivory in estuarine water. Marine Ecology Progress Series. 54 : 209-219.

Sherr, B.F., Sherr, E.B. and Fallon, R.D. 1987. Use of monodispersed fluorescently bacteria to estimate in situ protozoan bacterivory. Appl. Environ. Microbiol. 53 : 958-965.

Shuter, B., 1929. A model of physiological adaptation in unicellular algae. J. Ther.Biol., 78 : 519-552.

Simon M. and Azam F., 1989. Protein content and protein synthesis rates of planktonic marine bacteria. Mar. Ecol. Prog. Ser. 51 : 201-213.

Smetacek, V., Scharek, R. and Nothig, E.M. 1990. Seasonal and regional variation in the pelagial and its relationship to the life history cycle of krill. In : Antarctic Ecosystems : Ecological change and conservations, Kerny, R.and Hempel, G., (Eds). Springer Verlag, Berlin Heidelberg: 103-114.

Smith, W.O. and Nelson, D.M. 1985. Phytoplankton bloom produced by a receding ice edge in the Ross Sea: spatial coherence with the density field. Science. 227 : 163-166.

Smith, W.O.Jr and Nelson, D.M. 1986. The importance of ice-edge phytoplankton blooms in the Southern Ocean. Bioscience. 36 : 251-257.

Somville, M. 1984. Measurement and study of substrate specificity of exoglucosidase activity in eutrophic water. Appl. Environ. Microbiol. 48 : 1181-1185.

Somville, M. and Billen, G. 1983. A method for determination exoproteolytic activity in natural waters. Limnol. Oceanogr. 28 : 190-193.

Sullivan, C.W., Mc Clain, C.R., Comiso, J.C. and Smith, W.O. 1988. Phytoplankton standing crops within an Antarctic Ice Edge assessed by Satellite Remote Sensing. J. Geophys. Res. 93 : 12487-12498.

Sunda, W.G., Swift, D. and Huntsman. 1991. Low iron requirement for growth in oceanic phytoplankton. Nature. 351 : 55-57.

Talbot, V. 1995. Activité protéolitique and dynamique bactérienne en Océan Austral. Thesis. Université de la Mediterranée. 192 p.

Taylor G.T. and Haberstroh P.R. 1988. Microzooplankton grazing and planktonic production in the Bransfield Strait observed during the RACER program. Antarctic Journal of the United States. 23 : 126-128.

Utermöhl, H. 1958. Zur Vervollkommnung der quantitativen Phytoplankton - methodik. Mitt. int. Verein theor. angew. Limnol. 9: 1-38.

Van Franeker, J.A. 1989. Sea Ice Conditions. In: The expedition ANTARKTIS VII/3 (EPOS LEG 2) of RV "Polarstern" in 1988/1989. Hempel, I., Schalk, P.H. and Smetacek, V. (Eds). Berichtze zur Polarforschung. 65: 10 - 13.

Van Franeker, J.A. 1994. Sea-ice cover and Icebergs. In: The expeditions ANTARKTIS X/6-8 of the Research Vessel "Polarstern" in 1992/93. Bathmann, U.V., Smetacek, V., de Baar, H., Fahrbach, E. and Krause, H. (Eds). Berichtze zur Polarforschung, 135 : 17 - 22.

Van Leeuwe, M.A., Sharek, R., de Baar, H.J.W., de Jong, J.T.M. and Goeyens, L. 1996 Iron enrichment experiments in the Southern Ocean: Physiological responses of a plankton community. Deep-Sea Res. in press.

Veth, C. 1991a. The structure and evolution of the top layers of the water column across the marginal ice zone during spring 1988 in the Scotia-Weddell Sea sector of the Southern Ocean. Marine Chemistry. 35 : 63-76.

Veth, C. 1991b. The evolution of the upper water layer in the marginal ice zone, austral spring 1988, Scotia-Weddell Sea. J. Mar. Syst. 2 : 451-464.

Veth, C., Lancelot, C. and Ober, S. 1992. On processes determining the vertical stability of surface waters in the marginal ice zone of the north-western Weddell Sea and their relationship with phytoplankton bloom development. Polar Biol. 12 : 237-243.

Veth, C., Lancelot, C. and Ober, S. 1992. On processes determining the vertical stability of surface waters in the marginal ice zone of the north western Weddell Sea and their relationship with phytoplankton bloom development, Polar Biol. 12 :237-243.

Veth, C., Peeken I. and Scharek, R. 1996. Physical anatomy of fronts and surface waters in the ACC near the 6°W meridian during austral spring 1992. Deep Sea Res. (in press).

RESEARCH CONTRACT A3/02/001

ROLE OF THE MEIOBENTHOS IN ANTARCTIC ECOSYSTEMS

3

S. VANHOVE,
J. WITTOECK,
M. BEGHYN,
D. VAN GANSBEKE,
A. VAN KENHOVE,
A. COOMANS and
M. VINCX[1]

UNIVERSITEIT GENT
INSTITUUT VOOR DIERKUNDE
VAKGROEP MORFOLOGIE, SYSTEMATIEK EN ECOLOGIE
SECTIE MARIENE BIOLOGIE
K.L. Ledeganckstraat 35
B-9000 Gent
Belgium

[1] Corresponding author E-mail : magda.vincx@rug.ac.be

CONTENTS

ABSTRACT 1
1. INTRODUCTION 3

2. MATERIAL AND METHODS 4
2.1 Deep-sea study 4
2.2 Shallow-water study 5
2.3 Treatment of the meiofauna and nematodes 6
2.4 Environmental data of Signy Island 6
2.5 Statistical tests 7
2.6 *In situ* grazing experiments 7
2.7 Sediment-water nutrient concentration changes 8
2.8 Respiration 9

3. RESULTS 10
3.1 Meiobenthos in the deep-sea floor of the Weddell Sea 10
3.2 Meiobenthos in the low subtidal sediments of Signy Island 13
3.3 Relations between the meiobenthos and its environment in the deep-sea 14
3.4 Relations between the meiobenthos and its environment in the low subtidal 15
3.5 Flux of organic matter and nutrients through the benthic system and sediment-water interface at Signy Island 17

4. DISCUSSION 18
4.1 Comparison of Antarctic meiobenthic standing stock with similar systems all over the world 18
4.2 Meiobenthic relations with the trophic environment 19
4.3 Bentho-pelagic coupling: direction water column to sediments 22
4.4 Bentho-pelagic coupling: reverse direction and contribution of the meiobenthos to the mineralization processes: the case of Signy Island 23
4.5 Meiofaunal secondary production at Signy Island 28
4.6 Carbon balance at Signy Island 31

5. CONCLUSIONS 33
6. ACKNOWLEDGEMENTS 35
7. REFERENCES 36

ABSTRACT

To date meiobenthic research remained a big white spot in the systematic-ecological work on Antarctic zoobenthos. Therefore the relative importance of the meiofauna (organisms within the size range of 38-1000μm) in the Antarctic benthic community has been assessed by a combined field ecology and experimental approach. This was done in two contrasting conditions, *e.g.* the deep sea and low subtidal, where as to the depth of the water column the benthic characteristics were, respectively, indirectly or directly related to primary production. Deep-sea samples were collected at Kapp Norvegia and Halley Bay (Weddell Sea) during the EPOS- leg 3- campaign (summer 1989) with the RV Polarstern at depths between 200 and 2000 m. Samples for the ecological-experimental approach of the meiofauna in the low subtidal were taken at Signy Island (South Orkney Islands), at a water depth of 10 m, opposite the base of the British Antarctic Survey. This was done forthnightly during 18 months in 1991/92 and during the summer of 1994. A set of environmental variables (oxygen, pore-water nutrients, particulate and dissolved organic matter, sediment texture, chloroplastic pigments, bacteria and diatoms) were concurrently monitored.

Despite the apparent harshness of the Antarctic environment the meiofauna thrived with high productive stocks, sometimes much higher than their temperate and tropical relatives. Numbers and biomass were more or less seasonal and interannual varying (in the case of the subtidal meiofauna). Correlation with environmental factors revealed that depth, sediment texture, oxygen availability, variations in organic matter flux to the sediment surface, and hence food, governed the meiobenthic distribution patterns. Towards this, minimum nematode production constituted 2% of primary production in the pelagial and 11% of the downward flux of organic matter to the seabed.

The energetic position of the meiofauna, and their share in the remineralization processes and hence, reintroduction of regenerated nutrients and organic carbon through the sediment/water interface back into the water column, was inferred from flux measurements of nutrients, oxygen and organic matter. Grazing experiments with radiolabeled isotopes, used to quantify the carbon transfer between microbiota and their meiobenthic grazers (mainly epistratum and non-selective deposit-feeders), showed a clearance rate of 5.1 $.10^{-4}.h^{-1}$. Yet, about 10% of the annual benthic carbon production was grazed down by the nematodes. Nutrient and oxygen fluxes were measured from concentration changes in incubation chambers and vertical profiles in the sediment core. The results evidenced an efflux of ammonia and phosphate to the water column, and an uptake of nitrate and silicate by the sediments. Respiratory activity was

measured by a combined method of individual nematode and bulk sediment oxygen uptake. With an individual respiration of 0.89-2.77 nl $O_2.ind^{-1}.h^{-1}$ ($Q_{10} = 2$) the nematode community contributed to a substantial proportion of benthic remineralization processes (13-42% of the total benthic carbon demand was due to nematode respiration).

Secondary production by the nematode community at Factory Cove was among the highest in the world (P varying between 2.2 and 72.4 $gC.m^{-2}.y^{-1}$), and accounted for 9.4 % of total benthic production, 4.1 % of phytoplankton production and 11.9 % of microphytobenthic production.

From the flux measurements and production estimates it was suggested that, by using the substantial episodic food supply (both from water column and *in situ* production) very efficiently, the meiofauna might play a potentially important role in the energy-transfer through the differing benthic components and from the sediment back into the water column.

1. INTRODUCTION

Since the Belgian Antarctic Expedition by the Belgica (1897-1899) to the South Shetland Islands and the Antarctic Peninsula made the first collection of benthic animals, a lot of systematical-ecological work on Antarctic zoobenthos has been accomplished (reviewed by Arntz et al. 1994). Yet, meiobenthic studies remained a big white spot.

The meiofauna, defined as organisms within the size range of 38-1000μm, and generally dominated by nematodes and harpacticoid copepods, are in terms of abundance the most important metazoan group in marine sediments (Giere 1993). They harbour many different habitats in which they constitute a variety of feeding mechanisms, including herbivory, bacterivory, detritivory, predatory, scavenging, absorption and suspension-feeding (Wieser 1953; Tietjen 1980; Jensen 1982).

One major question to be addressed is how the meiofaunal component of the benthic system in the Southern Ocean responds to variations in organic matter flux to the sediment surface. Compared to other oceanic regions the pelagial of the Southern Ocean (*e.g.* south of 50°S) exhibits the unique feature of a very short, but extremely intense summer phytoplankton bloom, followed by a poor production period during the rest of the year. This is particularly so in coastal areas of the Antarctic continent and also in association with the melting of sea ice. As benthic communities depend heavily on the supply of resources from the water column above (Graf 1992), the seasonality, intensity and spatial heterogeneity of the vertical fluxes resulting from the pelagic production will certainly affect its size and structure.

The ultimate fate of deposited pelagic detritus is either long-term burial in the sediments, or remineralization via microbial and metazoan decomposition. Benthic regeneration of nutrients is likely to be a very important factor determining the productivity of the upper pelagial, especially in coastal waters where the water depth is small and where there is a close connection between the sediment and the water column. But also in the aphotic zone a quantity of nutrients is reintroduced into the water column as a result of benthic activity (Graf 1992). The meiobenthos play a regulatory role in these mineralization processes and flow of carbon, either directly via grazing and respiration, or indirectly by stimulting bacterial decomposition (Giere 1993).

The aim of the present study is to contribute to a better understanding of the role of the benthos in Antarctic ecosystems with a focus on the meiobenthos. We will attempt to find an answer on the following main questions:

1. What is the influence of the abiotic/biotic benthic environment, and hence the primary production in the water column, on meiofaunal distribution and activity in the bioturbation zone?

2. What is the nature of the carbon balance between sediment, sediment-water interface (nepheloid layer) and water column in the Antarctic ecosystem?

3. What is the role of the meiobenthos in the biogeochemistry of the sea floor, and remineralization of nutrients?

4. How can the pelagial be related to the benthos (*e.g.* bentho-pelagic coupling in the direction of the sediments towards the water column)?

Towards answering these questions we restrict our investigations to soft-bottom meiofauna. We will draw our attention to two contrasting conditions, *e.g.* the deep sea and low subtidal, where the benthic characteristics are respectively indirectly or directly related to primary production as to the depth of the water column. The major part of the composed problems will deal with field experience. Some questions will be evidenced with laboratory experiments.

2. MATERIALS AND METHODS

The methods used were more detailed described in Vanhove et al. (1995) and Vanhove et al. (*subm.)*.

2.1 Deep-sea study Fig.1 Table I.

Samples were collected at Kapp Norvegia and Halley Bay, Weddell Sea, (resp. 71-72°S, 12-13°W and 74-75°S, 25-29°W) during the EPOS ("European Polarstern Study") leg 3 cruise (ANT VII/4 : 13.1-10.3.1989) of RV Polarstern. The investigated bathymetric depth range was between 211 and 2080 m. The sediments mainly consisted of fine sands.
Samples were taken with a multicorer (MUC; each core = 25 cm^2; Barnett et al. 1984) for the deeper stations and a multibox corer (MG; each core = 240 cm^2 as described by Gerdes (1990) was used for the shallower sites. In both cases meiofauna were subsampled using 10 cm^2 plastic cores.

Table I: Station locality and sampling gear employed (MG: multiboxcorer; MUC: multicorer).

station	position S	W	depth (m)	sampling gear
Kapp Norvegia				
274	71°37,1′	012°10,9′	211	MG
277	71°39,8′	012°34,9′	405	MG
278	71°29,3′	012°32,1′	537	MG
292	71°03,8′	012°42,1′	561	MG
294	71°06,2′	012°03,8′	1199	MUC
295	71°07,9′	012°48,1′	2080	MUC
Halley Bay				
226	75°15,70′	025°48,60′	582	MUC
229	75°14,10′	026°14,00′	502	MUC
230	75°13,30′	027°00,10′	247	MUC
235	75°10,60′	027°35,40′	399	MUC
241	75°05,50′	028°00,40′	458	MUC
245	74°39,60′	029°42,10′	492	MUC
248	74°38,10′	029°39,50′	633	MUC
249	74°36,10′	029°41,50′	681	MUC
250	74°35,10′	029°40,20′	806	MUC
252	74°32,20′	029°17,70′	1183	MUC
253	74°08,20′	030°04,20′	1958	MUC

2.2 Low subtidal study Fig.1.

Samples were taken at Factory Cove at Signy Island, South Orkney Islands, Antarctica (60°43′S, 45°38′W), at a water depth of approximately 10 m at the Outer Mooring site, to the north-west of the cove, opposite the base of the British Antarctic Survey. Coring happened by SCUBA-diving forthnightly from April 27, 1991 to November 10, 1992, and twice during the austral summer of 1994 (January 26 and February 21). In summer open-water periods samples were taken by SCUBA diving from an inflatable boat at the bouy marked site; in winter samples were taken through a hole cut in the fast-ice. Although regular monthly samples have been taken, coverage has not been even, reflecting the difficulty of sampling in some months during late summer or early winter when unconsolidated pack-ice prevents both boating and snow-mobile travel.

2.3 Treatment of the meiofauna and nematodes

Further assessment of the sediment cores (*e.g.* extraction, examination and counting) followed the procedure recommended in Higgins and Thiel, (1988). The metazoan meiofauna was counted, and samples were subsequently manipulated for quantitative analysis of the nematodes. Assuming a specific gravity of 1.13 and a dry/wet weight ratio of 0.25, the meiofauna biomass was calculated from the dimensions of length and maximum width of ad random sets of nematodes (usual 100 to 200 nematodes per replicate), using the adjusted method of Andrassy (Soetaert 1989).
The nematodes were classified into the four feeding groups of Wieser (1953), distinguishing selective (1A) and non-selective (1B) deposit feeders, epistratum feeders (2A) and predators/omnivores (2B).

2.4 Environmental data of Signy Island

Oxygen availability was measured with a Platinum and saturated Calomel electrode at a constant temperature of 5 °C. Readings were done after 15 minutes on a Corning Ion Analyzer 150. For the quantification of pore-water nutrients sediment was extruded from the core tubes under N_2 atmosphere and passed through Whatman GF/C filters. The pore water samples were immediately frozen at -40 °C, and stored at -20 °C. Later the interstitial water was thawed and processed for the measurements of the concentrations of ammonia, nitrate, nitrite, phosphate and silicate with an A_{II} automatic chain (SAN^{plus} Segmented Fow Analyzer, SKALAR). The determination of ash free dry weight (AFDW) sediment was combusted at 550°C for 120 min and the loss in weight was quantified. Total particulate matter (TC and TN) was measured with a Carlo Erba NA-1500 analyzer. A Coulter^R LS Particle Size Analyzer was used to characterize the granulometry of the sand fraction (61.7-900 μm) and the pellite (clay + silt) content of the total sediment (0.4-900 μm). Dissolved organic carbon was measured, on a SKALAR (SK-12) DOC/TOC-analyzer on defrozen pore water. As a measure of microalgal biomass the concentrations of plant pigments in the sediments (*i.c.* chlorophyll a, c, β-carotenes, fucoxanthin) were determined. Fluorometrical measurements were done on aliquots filtered onto Whatman GF/F glass-fiber filters and extracted in 90% acetone on a Gilson HPLC-chain according to a slightly modified method of Mantoura and Llewellyn, (1983). Sediment samples (approx. 1 ml sediment) for the quantification of bacteria were preserved to a final concentration of 2 % sterile formaldehyde

solution, and stored in the fridge until enumeration was carried out by epifluorescence microscopy. Counting of diatoms was done with a Bürker-counter.

2.5 Statistical tests

The relation within environmental variables and between the meiofauna/nematode structure and environmental factors was tested using the non-parametric Spearman rank correlation analysis (Sokal and Rohlf, 1981).

2.6 *In situ* grazing experiments

In situ tracer experiments were done on the very fine sands of Factory Cove (shoveled from the upper layers of the sediment surface). The basic idea behind these experiments was: radiolabeled substrates are incorporated into microbes (by either photosynthesis or DNA- synthesis) which serve as food for meiofauna and thereby become labeled by their trophic activity. [Methyl-^{3}H]-thymidine (^{3}HTdR) and NaH^{14}C-bicarbonate (H$^{14}CO_3^-$) were used (3 replicates in three experiments of each label) to label respectively heterotrophic bacteria or autotrophic diatoms in the sediment. Therefore 100 μCi ^{3}HTdR or 60 μCi H$^{14}CO_3^-$ was added with a microliter syringe, underneath the sediment-water interface of 25 ml sediment samples (to respective final concentrations of 4 μCi.ml^{-1} ^{3}HTdR and 2.3 μCi.ml^{-1} H$^{14}CO_3^-$). The cores were incubated with label during maximal 5,5 hours, at a constant temperature of 5 °C. The incubation period was terminated by adding 4% formalin fixative. The uptake of label by microbes was measured on a sediment aliquot (from the surficial milimeters) filtered on 0.22 or 8 μm filters, respectively for bacteria and diatoms. Decantation and sieving (38 μm) of the remaining portion of the sample was done to remove the meiofauna from the sediment. Nematodes were sorted in a droplet of water into scintillation vials. The nematodes and the sediments were rinsed several times in sterile, deionized water to wash away unused (not incorporated) isotope. Measurements were performed on a LKB Wallac liquid-scintillation counter (model 1209). Corrections for diffusive uptake through the nematode cuticle were made with parallel, formaldehyde-poisoned (blank) controls (Carman et al. 1989); dark controls were performed to correct for the uptake of the isotope by the microbiota through non-photosynthetic processes and uptake of dissolved carbon ('drinking') by the nematodes.
The equation :

$$G = \frac{1}{t} \frac{\textit{activity nematodes at time } t}{(\textit{ activity microbiota at time } 0 + \textit{activity microbiota at time } t\ ) / 2}$$

with G = grazing rate , t (hours) = end of experiment

outlined by the three-compartment model of Daro (1978) and modified by Montagna (1984, 1993) for benthic systems, was used to calculate grazing rates. As isotope was introduced at the start of the experiment, and during incubation, labelling of microbiota occurred simultaneously to the grazing by nematodes. As a result, radioactive incorporation should increase linearly and that of the nematodes hyperbolically (nematode uptake lags microbial uptake). The latter assumes that grazers do not discriminate between microbes that take up label and those that do not.

2.7 Sediment-water nutrient concentration changes

Measurements were done on sediments from the same sampling site at Factory Cove (Outer Mooring, -10 m), in the usual perspex cores for meiofaunal sampling (10 cm^2, 10-15 cm length, closed with silicon rubber bungs), taken by SCUBA-diving and returned to the laboratory within 10 minutes. The upper water was immediately removed (but stored) in order to pick out the macrofauna. Amphipods were ubiquitous and it was impossible to take sediment samples without also including these organisms. Then a constant volume (50 ml) of the upper water was gently (to maintain an intact sediment-water interface) re-added to the surface of each core. Incubations were done at a constant temperature of 5°C after re-equilibration and aeration (in order to maintain *in situ* redox gradients) following the disturbance of coring and removal of macrofauna. The experiment here performed, was a closed system (e.g. closed cores from t_0), and lasted for 6 hours, with an interval of 60 minutes. A set of 12 cores were used, of which half were wrapped in tin foil paper (= dark control) to avoid light penetration and hence nutrient concentration changes due to photosynthesis. At t_0 the upper 2 cm and overlying water of the first set of two cores (light and dark) were frozen at -40 °C and stored for the later analysis of sediment texture, particulate organic carbon, nutrients and dissolved organic carbon. The incubation continued in the other cores and was terminated at t_1 for the next pair of cores, t_2... until the last pair of cores at t_6, at the end of the experiment. Water samples for the analysis of oxygen content were taken from the upper water of a parallel incubation chamber using a gassyringe (25 μl sample size) through self-sealing holes, and measured with a couloximeter (Peck

and Uglow, 1990). The upper water was never stirred. The methods used for the measurement of the concentration profiles were earlier described.

2.8 Respiration

Respiration measurements were performed in two different ways e.g. total sediment respiration and meiofaunal community respiration. For both type of experiments a Strathkelvin oxygen respirometer (1302, oxygen monitor 781) was used. Methods followed the descriptions of Moens et al. (*subm.*) and Nedwell (1989) and were done in a constant temperature room at 5°C. Each experiment was preceded by a measurement of the oxygen content with a couloximeter (see above) to calibrate the system.

sediment respiration Fig.2. Undisturbed sediment from the same sampling site at Factory Cove (Outer Mooring, -10 m) was taken by SCUBA-DIVING with a perspex core (63 mm internal diameter, 10-15 cm length, closed with rubber bungs). This sediment was returned to the laboratory within 10 minutes, and the macrofauna (mainly amphipods) was immediately removed. Incubations were done after re-equilibration (following the disturbance of coring and removal of macrofauna), aeration and adjustment of the hight of the water column to approximately 10 cm above the sediment. The core tube was closed with an airtight screw cap, through which protruded a dissolved oxygen electrode (Strathkelvin Instruments) into the water column. Constant stirring of the water, with a metal arrow protruding through the cap and connected with an induction motor, occurred without resuspending the surface sediment. The experiment was stopped when a linear oxygen decline could be discerned, usually after 90-100 minutes. The oxygen consumption was calculated from the decline in oxygen content. Preliminary measurement of oxygen uptake by sterile seawater (background respiration) in the absence of sediment did not decrease significantly. Dark and light measurements were performed in order to deduce the differential oxygen budget as a result of primary production and heterotrophic aerobic respiration.

individual respiration Fig.3. Individual meiofaunal respiration was measured using a 1000 μl chamber (RC 300) of the Strathkelvin electrode system. Because individual nematode consumption was less than the sensitivity of the apparatus, at least 100 nematodes of combined species were randomly hand-sorted, rinsed in aseptic (with antibiotics to block microbial respiration) water and finally pipetted in oxygen saturated *in situ* sterile water with an end volume of 1 ml.

Additional respiration measurements were done on other dominant meiobenthic groups, e.g. polychaetes and harpacticoid copepods, and on the prevalent macrobenthic amphipods. "Background respiration", defined as the change in oxygen concentration in a control chamber (separate experiment), was negligible.

$$R = \frac{x \cdot v \cdot z \cdot 60 \cdot 1000}{y \cdot t \cdot n}$$

with R = *respiration rate* $(ng\ O_2 \cdot ind^{-1} \cdot h^{-1})$

3. RESULTS

3.1 Meiobenthos in the deep-sea floor of the Weddell Sea Figs 4,5,6.

The meiofauna reached high densities up to almost 5000 individuals. 10 cm^{-2} (Fig.4A), and consisted mainly of nematodes (80-97%), harpacticoid copepods, polychaetes and kinorhynchs. The other taxa comprised together less than 4 % of the total meiofauna. All taxa were presented in table II. Part of this table was constructed with information from Herman and Dahms, (1992).
The mean length of the nematodes (averaged over about 7000 measurements) was generally situated between 700 and 1000 μm (Fig.4B). No consistent pattern along the transect was observed. Total biomass ranged between 0.1 and 0.8 $gC.m^{-2}$ and was higher close to the ice-shelf, and lower in offshore sediments (Fig.4C). The identifications of the nematodes gave a list of 140 genera covering 34 families. An average of 20-50 genera were found per station (Table III). Deposit and epistratum feeders with small buccal cavities (groups 1A, 1B and 2A), feeding on unicellular algae, bacteria and fungi, dominated the nematode assemblages. Predators were much less abundant (about 5 %) (Table III).

Table II : Meiofaunal composition in the deep Weddell Sea : occurrence of the permanent and temporal taxa throughout the transects. *Nematodes, Harpacticoids, Polychaetes, Kinorchynchs, Amphipods, Bivalves, Bryozoans, Coelenterates, Cumaceans, Gastrotrichs, Halacarids, Isopods, Loricifers, Oligochaetes, Ostracods, Priapulids, Tanaidaceans, Tardigrades and Turbellarians.*

	Kapp Norvegia						Halley Bay									
	274	277	278	292	294	295	226	229	235	241	245	248	249	250	252	253
Nema	●	●	●	●	●	●	●	●	●	●	●	●	●	●	●	●
Harp	●	●	●	●	●	●	●	●	●	●	●	●	●	●	●	●
Poly	●	●	●	●	●	●	●	●	●	●	●	●	●	●	●	●
Kino	●	●	●	●	●	●	●	●	●	●	●		●	●	●	●
Amph					●	●		●			●	●	●	●		
Biva	●	●	●	●	●	●	●	●	●	●	●	●	●	●	●	●
Bryo		●		●			●				●	●				
Coel	●	●	●	●			●	●	●	●	●				●	
Cuma						●				●	●	●				
Gast	●	●		●	●		●		●		●	●				
Hala	●	●		●	●	●	●	●		●	●	●	●	●	●	●
Isop		●		●			●	●	●	●	●	●	●	●	●	
Lori		●	●		●	●				●	●	●				
Olig	●	●	●	●	●	●	●		●		●	●	●	●		●
Ostr	●	●	●	●	●	●	●	●	●	●	●	●	●	●	●	●
Pria		●	●	●		●	●	●	●	●					●	
Tana	●	●	●	●	●		●	●	●	●	●	●	●	●		●
Tard	●	●		●	●	●	●	●	●	●	●		●	●	●	●
Turb		●	●	●	●		●	●	●	●					●	●

Table III: Comparison of meiofauna structure between the two deep-sea transects studied. Average values are added between brackets.

	KAPP NORVEGIA (211-2080 m; 19 repl)	HALLEY BAY (582-1958 m; 22 repl)
NEMATODES (N°.10 cm^{-2})	824 - 4915 (1994)	730 - 2291 (1586)
RELATIVE ABUNDANCE (%)	83 - 96	88 - 97
INDIVIDUAL LENGTH (mm)	0.7 - 1.0	0.7 - 1.0
INDIVIDUAL DWT (μg)	0.15 - 0.35	0.12 - 0.30
TOTAL BIOMASS (g $dwt.m^{-2}$)	0.13 - 0.97	0.09 - 0.65
GENERA : number	20 - 44 (34.2)	21 - 47 (33.5)
	Acantholaimus, Dichromadora, Microlaimus, Molgolaimus	Acantholaimus, Daptonema, Dichromadora, Leptolaimus, Microlaimus, Molgolaimus, Monhystera, Sabatieria
JUVENILES (%)	56	51
FEEDING COMPOSITION (%)		
1A	17 - 48 (31)	13 - 37 (23)
1B	25 - 38 (29)	20 - 44 (36)
2A	23 - 44 (34)	28 - 63 (40)
2B	3 - 7 (5)	2 - 12 (5)

From figure 5 it is obvious that the meiofauna at different bathymetric depths (e.g. 537 to 2080 m) had highest densities at the sediment surface, but deeper burrowing taxa were not unusual, and depths of 5-10 cm still comprised several numbers. The upper layers (0 to 2 cm) were dominated by epistratum feeders (2A: 40-60%). Non-selective deposit feeders populated deeper layers from 3-4 cm on (1B: 40-60%). Selective deposit feeders (1A) were quite evenly distributed throughout the sediment profile (average of about 20%) (Fig.6).

3.2 Meiobenthos in the low subtidal sediments of Signy Island Figs 7,8,9.

Meiobenthic density at Signy Island was around an average of 6.2 $.10^6$ ind.m^{-2}, and total biomass, based upon median individual nematode dwt around 1.4 g.m^{-2} (= 0.6 gC.m^{-2}). A number of 6 taxa indicated low diversity, dominated by nematodes (mean: 82%), harpacticoid copepods and ostrocods (Table IV). Other taxa were mainly turbellarians, bivalves, amphipods, polychaetes and gastrotrichs, halacarids, but they occurred in extreme low proportions (maximum 1% of total).

Table IV: Number of samplings on a total of 36 intervals related to meiobenthos densities in main taxa in the sediments of Factory Cove: total metazoan meiofauna, nematodes, harpacticoid copepods + nauplii, ostracods, others.

N°.10 cm^{-2}	Total	Nema	Harp	Ostr	Other
0	0	0	0	0	34
1 - 100	0	0	3	4	2
101 - 500	0	0	12	25	0
501 - 1000	2	3	15	6	0
1001 - 5000	11	18	6	1	0
5001 - 10000	16	12	0	0	0
> 10000	7	3	0	0	0

The community showed a more or less apparent seasonal fluctuation in which temporal high dimensions of density and biomass (Fig.7) alternated with periods of poor standing stocks. Similarly, interannual variation was weak and constructed by intermittent peaks and troughs during the first year. These observations were partly consistent with features within the environment. Organic matter and sediment texture appeared rather constant on a forthnightly and annual scale. Benthic chloropigments showed a strong seasonality, but annual differences could not be discerned from this study.
The temporal change of nematode genus composition (Fig.8A) was strongly constructed by *Neochromadora, Sabatieria, Daptonema* and *Aponema*. Together they comprised more than 80 %, revealing a trophic predominance of epistratum (2A) and non-selective deposit feeders (1B) throughout the year (Fig.8B).

In accordance to the prominent redox based biochemical gradients (of microbiota, chloropigments, pore-water nutrients, organic matter), the meiofauna was confined to the surface 2-3 centimeter layers (Fig.9). The observed patterns

were mainly constructed by the subsurface peaks of *Aponema* and continous decline of *Daptonema*. *Daptonema* always dominated the upper sediment layer.

3.3 Relations between the meiobenthos and its environment in the deep-sea.

Table V: Summary of significant Spearman Rank Order Correlations for meiofauna variables with environmental characteristics in the deep Weddell Sea sediments: total meiofauna density; total nematode biomass; individual nematode biomass; nematodes; kinorchynchs; harpacticoids; cnidarians; priapulids; nauplii; oligochaetes; tardigrades; ostracods; tanaidaceans; bivalves and polychaetes.

	tot dens	tot biom	ind biom	N° taxa	nem	kin	har	cni	pri	nau	oli	tar	ost	tan	biv	pol
depth	***	***	-	***	**	-	*	*	-	*	-	*	**	-	-	***
porosity	-	-	-	-	*	***	-	-	-	-	-	-	-	-	-	-
very coarse sand	-	-	-	-	-	*	-	-	-	-	*	-	-	-	-	-
sand	-	-	-	-	-	**	-	-	-	-	-	-	-	-	-	-
silt	-	-	-	-	*	***	-	-	-	-	-	-	-	-	-	-
clay	-	-	-	-	-	*	-	-	-	-	-	-	-	-	-	-
SiO_2	-	-	-	-	-	-	**	-	-	-	-	-	-	-	-	-
NO_3	-	-	-	-	-	-	-	-	-	*	-	-	-	*	-	-
Eh at -1 cm	*	-	-	-	*	*	-	-	*	-	-	-	-	-	-	-
ATP	*	*	-	-	*	**	-	-	**	-	-	-	-	-	-	*
organic carbon	-	-	-	-	-	**	-	-	-	-	-	-	-	**	-	-
organic nitrogen	-	-	-	-	-	-	-	-	-	-	-	-	-	**	-	-
biom bacteria	*	*	*	-	-	-	-	**	*	-	-	-	*	*	*	*
biom flagellates	*	*	-	*	-		-	**	*	-	-	-	**	-	***	***

*** : $p \leq .001$ ** : $.001 < p \leq .01$ * : $.01 < p \leq 0.05$

Statistical community analyses revealed a distinction between shelf, slope and deeper stations, with generally higher stocks in shallower nearshore bottoms (not presented). The main structuring forces were depth and food (ATP, organic matter, nanoflagellate and bacterial stocks) (Table V). Environmental data used for this analysis were obtained from other cruise scientists.

3.4 Relations between the meiobenthos and its environment in the low subtidal

A spearman rank analysis of the detrital food between the sediments and respectively the sediment traps and water column (Table VI) showed some correlations between the benthic chloropigments and the pigments and dry weight in the traps, and micro pigments in the water column. A strong association seemed to occur between the sedimentary pigments and nano pigments in the water column. The benthic POM-loading (TOC, TON) did not show any significant correlation.

Table VI: Probability levels of the Spearman rank correlation between detrital sources in the sediment (Chl-a, Chl-c, β-carotene, organic carbon and nitrogen) and respectively sediment trap (chlorophyll, phaeopigments, dry mass, ash free dry mass, carbon and nitrogen) and water column (micro Chl-a, micro phaeopigments, nano Chl-a and nano phaeopigments) in the sediments of Factory Cove, n=10.

	Sediment trap						Water column			
	Chl	Phaeo	dwt	AFDM	N	C	micro Chl-a	micro phaeo	nano Chl-a	nano phaeo
Chl-a		+	+							+ +
Fucoxanthins			+		+			+	+	+ + +
Chl-c	+	+ +	+						+	+ +
β-carotenes			+		+			+	+	+ + +
TOC										
TON										

+: $p \leq .05$ ++: $.05 < p \leq .01$ +++: $.01 < p \leq .001$

A subsequent correlation analysis between the meiofauna and environment (Table VII) revealed that the meiofauna was not related to the sedimentary detrital sources (except for nauplii and Chl-c) and only weakly to median grain size. Scattered relations were observed with food in sediment traps (*e.g.* bivalves, turbellarians, harpacticoid copepods and total density), and more consistent correlations were recognized with the temperature of the sea, and pigment concentrations in the water column (*e.g.* harpacticoid copepods, ostracods, turbellarians, total density and total biomass). No lag effect between

the succeeding densities and biomasses of meiofaunal populations and biomass of suspected food were identified from graphical outputs.

Table VII: Probability levels of the Spearman rank correlation between meiofauna and respectively sediment (Chl-a, Chl-c, fucoxanthin, β-carotene, organic carbon and nitrogen, median particle size, skewness, pellite), sediment trap (chlorophyll, phaeopigments, dry mass, ash free dry mass, carbon and nitrogen) and water column (NH_4, PO_4, temperature, micro Chl-a, micro phaeopigments, nano Chl-a and nano phaeopigments) at Factory Cove. Only the variables with a significant sign are added, n = 10 or 20.

	Sediment		Sediment trap				Water column					
	Chlc	med	Chl	Phaeo	dwt	ash	NH_4	PO_4	T°	micro Chl-a	micro phaeo	nano Chl-a
Amphipods												
Bivalves					+	+						
Harpacticoids : total					+	+			+			+
adults												
nauplii	+	- -										
Ostracods							+		+			+
Turbellarians		- -	+	+				- -	+ +	+ + +		+ + +
Taxa		-										
Nematodes					+	+ +		-	+ +		+	+ +
Total density					+	+ +		-	+ +		+	+ +
Total biomass									+			+ +

+ or -: $p \leq .05$ - - or + + : $.05 < p \leq .01$ + + +: $.01 < p \leq .001$

3.5 Flux of organic matter and nutrients through the benthic system and sediment-water interface at Signy Island

Food experiments Fig.10. The radioactivity that was abiotically fixed by the sediment (blank) and dark controls was low, and comparable to the t_0 measurements for the bicarbonate experiments, though much lower than the t_0 of the thymidine series, indicating that the thymidine was already incorporated in and/or attached to the bacteria and nematodes from the first minutes of the experiment (time between adding label to the different replicates). The assumptions (e.g. linear and hyperbolic uptake of respectively the microbes and nematode grazers) were satisfactory met for the $H^{14}CO_3^-$-experiments. In contrast, they were not at all met for the ^{3}HTdR-experiment. The replicability of the latter measures appeared erratic and less precise than those for $H^{14}CO_3^-$ uptake. Therefore only the clearance rate on autothrophs (diatoms) was calculated and amounted to $5.1 .10^{-4}.h^{-1}$.

Nutrient concentration changes Figs 11, 12. Taking the preliminary nature of the nutrient flux experiment (Fig. 11), it can be formulated that oxygen concentration changes were very fluctuating, but showed an overall decline in dark as well as light condition. The fluxes of the macro nutrients (nitrites, phosphates, ammonia and nitrates) were generally erratic and overwhelmingly dominated by NH_4^+, while the majority of the fluxes of organic matter (AFDW, particulate organic carbon and nitrogen, dissolved organic carbon) decreased during the course of 6 hours. The C:N weight ratio of organic matter in the surface 2 cm of sediment fluctuated between 5 and 8. Errors associated with the lack of stirring and the use of different cores for each time-interval could be the basis of these erratic patterns.
The macronutrient concentration profiles with depth during the summer in sediments of Factory Cove (Fig. 12), indicated always greater records in the pore waters compared to the overlying water. Ammonia and silicate increased with sediment depth, whereas oxygenated nitrogen decreased to an undetectable level from 3 centimeter depth. Phosphate remained stable.

Respiration

sediment oxygen demand (SOD) Table VIII. The oxic respiration by the entire sediment in light conditions was 30 to 50% of dark measurements. When removing the macrofauna (mainly amphipods) the SOD declined substantially (to almost one third of total uptake).

Table VIII: Parameters of the regression of oxygen decline (in $mg.l^{-1}$) against time in the sediment core respiration measurements.

	slope	R^2
light : without amphipods		
experiment 1	-0.005	0.87
experiment 2	-0.003	0.82
experiment 3	-0.004	0.94
experiment 4	-0.004	0.94
dark		
experiment 1 : without amphipods	-0.009	0.46
experiment 2 : with 20 amphipods	-0.025	0.92

Calculations of oxygen uptake rates by the experimental cores gave values of 0.068 (dark; without amphipods, 1.027 (dark; with amphipods) and 0.024 (light without amphipods) mg O_2 $.d^{-1}.31$ cm^{-2}, corresponding to 0.685, 10.353 and 0.24 mmol $O_2.m^{-2}.d^{-1}$.

individual respiration. The nematodes and amphipods consumed respectively 1.8 to 5.6 (average 3.97), and 8.12 $ng.ind^{-1}.h^{-1}$. Procedure effects made it impossible to get reliable results for harpacticoid copepods and polychaetes.

4. DISCUSSION

4.1 Comparison of Antarctic meiobenthic standing stock with similar systems all over the world

When comparing the variables in the deep Antarctic Weddell Sea with similar study results in literature, it is clear that high meiofauna densities were recorded comparable to Pacific, Atlantic and Arctic Ocean faunas (reviewed by Thiel 1983, Tietjen 1992). Only the oligotrophic warm sediments in the Mediterranean and Red Sea had significant poorer populations (Vanhove et al. 1995). This was clarified with a regression of meiofaunal densities with depth in the Southern (own data: triangles) and NE-Atlantic (data from Vincx et al. 1994: squares) Ocean (Fig. 13: own data superimposed on existing regression). The parameters were very comparable when our data were included in the regression ($Y = 6259 - 718$ ln depth, $R^2 = 0.748$).

The comparison of Signy results with temperate, tropical and polar inshore waters (reviewed by Rudnick et al. 1985 and given in table IX) showed that the numbers were generally much higher and comparable to the highest records all over the world. Only one study to date was richer (e.g. Narrangansett Bay) in terms of density and biomass.

Table IX: Comparison of total meiofauna density between Factory Cove, other comparable shallow waters and nearshore polar regions.

Location	Abundance range (* $10^6.m^{-2}$)
This study	4.9 - 13.2
Niantic River (Tietjen 1969)	1.2 - 5.0
Long Island Sound (Yingst 1978)	0.5 - 2.7
Narragansett Bay (Rudnick et al. 1985)	8.1 - 41.8*
Subantarctic (de Bovée and Soyer, 1975, Bouvy 1988)	0.0 - 15.5
Boreal (Elmgren 1975, Ankar and Elmgren, 1976, Elmgren et al. 1983, Wittoeck 1991)	0.5 - 7.9

* Foraminifers included

4.2 Meiobenthic relations with the trophic environment.

The pelagic regime of the high Antarctic is characterized by sudden and pronounced bloom events - phenomena which have an extra dimension in coastal and shelf ecosystems (Nöthig 1988; Wefer et al. 1990). With the variety and unpredictability of food sources in mind, it was expected that the meiofauna would develop strategies favourable to these particular environmental conditions. In our studies in the low subtidal and deep-sea sediments of Antarctica, correlations were sometimes rare and often not very explicative. Features such as a patchy primary production, with subsequent variable fluxes to the sea bed and their seasonal character, together with macrobenthic perturbation induce small and meso-scale variability between and within substrates, which can be different from meiobenthic distribution scales (Blanchard 1990; Santos et al. 1995). As a complement, high deviations between the replicates, presumably inherent to sampling and sorting, and specific responses to certain food quality and quantity (Romeyn and Bouwman, 1983; Carman and Thistle, 1985; Montagna et al. 1995) could have masked existing relationships.

Meiobenthic biota were, however, to some extent, spatially as well as temporally related to the available organic sources. Nematodes possess a wide range of buccal structures which are believed to reflect their diet (Wieser 1953). They were predominantly epistratum and deposit feeders in the Antarctic sediments. Correlations were therefore mainly attributed to close trophic interactions between the meiofauna and their suspected food, such as diatoms and bacteria.

The experimental evidence of these trophic couplings were variable. The choice of [^{3}H]-thymidine for grazing on bacteria was recently compared to the use of [^{14}C]-bicarbonate by microalgae (Montagna 1993). Thymidine is apparently not incorporated by either chemolithotrophic or sulfate-reducing bacteria and this type of experiment does not measure efficiently *in situ* grazing in muddy sediments. Moreover, label uptake by bacteria associated with the cuticle of meiofauna can be responsible for most of the meiofauna uptake, whereas meiofaunal [^{14}C]-bicarbonate uptake is not dominated by such absorption phenomena (Montagna 1993). Absorption can be estimated with inhibitor-control experiments, but this was not done during the current study.
The poor efficiency of the [^{3}H]-thymidine-experiments could be at the base of the failed experiments in our study. Although this lack of experimental evidence we still believe that some close trophic coupling could have existed between bacteria and meiofauna, as a certain degree of overlap in their dispersal patterns was visible in the vertical sediment profiles at Signy and in the transect sediments of the Weddell Sea. Evidence of such interrelationships was given by a high number of field studies (Meyer-Reil and Faubel, 1980; Giere 1993), and grazing rates on bacteria were very variable, ranging between 0.03 and 5.7 $.10^{-3}$ h^{-1}. Bacterial food was, generally, not limiting (Montagna 1984, Montagna and Bauer, 1988; Montagna and Yoon, 1991; Epstein and Shiaris, 1992).

The amount of carbon transferred from the phytobenthic compartment to the nematodes (i.e. the grazing rate) can be calculated from the bicarbonate clearance rate and standing stocks of diatoms, giving a flux of 3.1 and 1.5 $.10^{-3}$ $gC.m^{-2}.h^{-1}$ for January and February 1994, respectively (Table X). Yet, the biomass specific trophic turnover, defined as the time required for the total nematode population (with their respective standing stocks of 0.34 and 0.13 $gC.m^{-2}$) to consume the standing stock of microphytobenthos, would be respectively 4.6 and 3.6 days.

Table X: Nematode and microphytobenthic standing stock and trophic dynamic. Values are averaged over 2 cm of sediment at Factory Cove (-10 m); a conversion factor of C:Chl=40 (Darley 1977) for diatom carbon and a ratio of dwt/C=0.42 (Heip et al. 1985a) for nematode carbon was applied; the use of an approximate value of 0.18 μg dwt.nematode^{-1} was based upon dimensions from Jan/Feb 1992; a clearance of 5.1 .10^{-4}.h^{-1} was applied.

	January 1994	February 1994
nematode density (N°.10 cm^{-2})	4757	1834
standing stock (gC.m^{-2})		
nematodes	0.34	0.13
microphytobenthos	6.14	2.96
biomass specific grazing rate (10^{-3} gC.m^{-2}.h^{-1})	3.1	1.5
trophic turnover (h)	109.6	86.7

These biomass specific rates were well within the ranges found from nematodes in other localities 0.01 - 33.9 .10^{-3} gC.m^{-2}.h^{-1} (Admiraal et al. 1983; Montagna 1984; Blanchard 1991; Montagna et al. 1995). We have no idea of the turnover times of microphytobenthos in the Antarctics. Yet, as to get an idea of the grazing impact of nematodes on the microphytobenthos at Signy, the biomass specific grazing rate can be calculated as a percentage of microphytobenthic production. According to Gilbert (1991a), primary production amounted to 29.2, 13.1 and 16.3 .10^{-3} gC.m^{-2}.h^{-1} in respectively the early, middle and late summer of 1987/88, giving a mean value of 19.5 .10^{-3} gC.m^{-2}.h^{-1}. If we assume that primary production was the same in 1994, this would mean that grazing during January and February would be respectively about 16 and 8 % of the daily microphytobenthic production. These values indicate a modest role of nematode grazing in the turn-over of their autotrophic prey.

The results of the bicarbonate tracer technique for relating benthic autotrophs with their nematode grazers assumed that no recycling of label through respiration and/or excretion occurred, and label uptake was only from grazing activity. The use of a same clearance rate for calculating trophic dynamics in January and February could be partly clarified with regard to the study by Montagna et al. (1995), who found that the nematode clearance rate was very weakly related to microphytobenthos biomass (e.g. when offered more diatom cells, consumption reached a maximum rate). With the high microphytobenthic biomass during the austral summer in mind (Gilbert 1991b) one can reasonably assume that grazing was then at a same maximum rate in both months. In some

instances this is, however, very questionable as the field observations within the summer of 1994 showed a clear density/biomass response of the nematodes to changes in autotrophic food quantity.
Because of these shortcomings the calculated grazing rates should be treated as preliminary background information.

Summary. From the available information, one can cautiously accept that the meiobenthic relations with the suspected microbial food (bacteria and diatoms) could to some extent be explained by meiofauna grazing (this was also indicated by the high amount of diatom frustules observed in the gut of *Daptonema*). Yet, microbiota are not only of vital importance for the nutrition of meiofauna organisms, but in turn they are, though to a small degree, impacted by the meiobenthic community as well (per day, 6-8 % of the production is consumed). At present, only the trophic relations between nematode grazers and diatoms/bacteria were addressed. Not only the grazers, but also the deposit-feeders predominated the sediments. As to the poor relation between meiofauna and organic matter (i.c. particulate organic carbon), and also as documented by several authors, particulate detritus itself plays a minor role, whereas microbiota attached to detritus are the major food sources. Apart from the principle microbial foods, other dietary items such as yeast, fungi, amoebae, ciliates and foraminifera might also be important nutritious sources.

4.3 Bentho-pelagic coupling: direction water column to sediments.

Since benthic communities depend on the flux of organic sources from the pelagic for sustaining their standing stock and production important response mechanisms exist, following significant changes in the water column productivity (Rowe et al. 1991; Graf 1992; Sayles et al. 1994). These feed-backs are very complex, and difficult to measure if the quantity and especially quality of the organic material arriving at and burried in sediments is not known (Heip 1995). The amount of organic input depends on several factors, among which distance to the coast dominates. Its quality, and hence the quantity of biological utilizable food sources, depends on the degree of sedimentation and decomposition of primary products in the water column. This is inversely related to water depth.
Several authors have tried to couple meiobenthic population dynamics (abundance, biomass, diversity and reproductive output) to temporal and spatial patterns in the pelagial productivity. Evidence was given in diverse communities along the boreal, temperate, tropical and subantarctic longitudinal axis (reviews

by Thiel 1983; Heip et al. 1985a; Rudnick et al. 1985; Tietjen 1992) and this study adds to the available information.

deep sea. Total nematode biomass ranged from 0.087 to 0.966 g dwt.m^{-2}. Therefore, based on an annual P/B ratio of 4 and 69 (discussed below) the production of the meiofauna in this region was situated between a mean of 0.47 and 12.96 gC.m^{-2}.y^{-1}. The mean annual phytoplankton production off Kapp Norvegia reaches 24 gC.m^{-2}, and an annual carbon flux of 4.2 g.m^{-2} at 100 m depth (Wefer and Fisher, 1991). Hence, minimum nematode production calculated for this region was about 2 % of the primary production, and 11 % of the downward flux rates. Yet, a high percentage of the export flux was channeled into the meiobenthic communities of Kapp Norvegia.
It was found that foraminiferal standing stock and metabolism at abyssal depths can respond within a time-scale of a couple of days (Lutze et al. 1986; Gooday and Turley, 1990; Linke 1992). Except for one study on the nematode size spectra of the North-east Atlantic (Soltwedel et al. *subm*), no evidence was found for the response of deep-sea metazoan meiofauna to seasonal varying events in the pelagial. No temporal records were obtained from this deep-sea study, but meiofauna communities in the Weddell Sea, are also assumed to be affected by the seasonal character of the pelagial production. Because of the similar structure between Antarctic and other deep-sea meiobenthos, it is plausible that identical structuring forces will dominate, which in turn means that the meiofauna in the Antarctic deep sea will use the episodic food supply very efficiently.

low subtidal. Diverse bentho-pelagic relationships occur and will be outlined more in detail in the following sections.

4.4 Bentho-pelagic coupling: reverse direction and contribution of the meiobenthos to the mineralization processes: the case of Signy Island.

Southern Ocean sediments are the major repository for biogenic silica (De Master et al. 1983; Biggs et al. 1988) and reintroduction of silica, nitrogen and phosphorous may have a major effect on global nutrient cycling (Olson 1980; Gilbert et al. 1982; Rönner et al. 1983; Koike et al. 1986; Vidal et al. 1989; Kristensen et al. 1992; Nedwell and Walker, 1995). The finding that nutrients become depleted due to phytoplankton growth in the water column of Signy Island (Clarke et al. 1988), raises the idea that also at this site benthic nutrient

regeneration might determine the productivity of the upper pelagial (Nedwell et al. 1993).

The role of the macrobenthic amphipod fauna in Factory Cove (*Cheirmedon femoratus, Pontogonea rotundifrons, Tryphosa kerguelenii*), as stimulators of bacterial metabolism, are known to have a positive influence on early diagenic processes. Removing this fauna depressed sedimentary oxygen uptake by 33% and sedimentary release of ammonia by 50%. NH_4^+-excretion and stimulation of remineralization processes through bioturbation activity were the major cues for these observations (Nedwell and Walker, 1995).

The relative share of meiofauna in such processes is still vague, but some recent ideas were introduced. Through their bioturbation activity the meiobenthos mix the sediment and change its physico-chemical composition (Cullen 1973; Nehring et al. 1990; Aller and Aller, 1992). In organically enriched habitats with larger benthic deposit-feeders (such as Factory Cove), they are the primary organisms responsible for transferring phytodetritus through the sediment-water interface during the first few days after particle deposition. As sediments are important sites of degradation of organic matter, leading to the transfer of nutrients (oxygen, nitrogen, phosporous, silicate and carbon) through the sediment-water interface, this burial of sedimented phytoplankton enhances the initial decomposition processes (Webb and Montagna, 1993).

In the current appraisal a preliminary study was done on benthic remineralization including aerobic respiratory activity and nutrient fluxes in the nepheloid layer and meiofaunal bioturbation zone. The relative importance of the nematodes was inferred. The data are very preliminary and insufficient to establish an accurate balance (this was mainly due to the lack of replicates, working at 5°C instead of *in situ* temperatures and high sediment disturbance by eliminating macrofauna), but they should give a first idea of how the benthic realm functions in the global ecosystem of Factory Cove.

Nutrient concentration changes. The flux measurements were made under darkened and lightened conditions, in order to detect changes due to photosynthesis by benthic algae. However, the concentration changes of macro nutrients generally followed similar patterns. This result could have been a methodological effect. The dark controls were wrapped in tin foil, except for the top surface of the core, where a continous air supply was needed. It is known, as an adaptation to the occurrence of fast ice, that Antarctic diatoms are capable of surviving, but also effectively utilizing low photon emission (Gilbert 1991b). As a consequence, the low light intensities reaching the surface of the sediment cores in our experiment, could have been enough for micro-algal

activity, and hence differences between dark and light experiments would then be minute.

A point which merits attention, bearing in mind the tentative nature of the results, is the lowering of organic matter which could have been the results of benthic regeneration. The decrease of soluble phosporous, ammonia and nitrate could have been a signal of efflux of these nutrients to the water column. This would be supported by the finding that porewater nutrient concentrations of the 0-1 cm layer of sediment in our study were always greater than in the water column immediate above the sediment-water interface. Indeed, ammonia and phosphate were also much higher in the water immediate above the sediment than in the water column. However, nitrate and silicate were lower in the water immediate above the sediment compared to the water column, inferring that ammonia and phosphate were exported from, and nitrate and silicate were imported into, the sediments. The pore water nutrient concentration profiles in the sediment core showed a decrease in nitrate concentration below the top cm which was accompanied by an increase in ammonium concentration with a maximum reached at approximately the same depth horizon that nitrate became depleted. This suggest substantial denitrification at a depth from 3 cm on. The release of phosphorous and ammonia to the water column are both related to decomposition of organic matter (Libes 1992).

Table XI: Nutrient concentrations (μM) in the porewater of the sediments (maximum sediment slice value in the summer of 1994), in the overlying water immediate above the sediment (summer average of 1994) and in the pelagial of Borge Bay (average of summer minimum levels of 1988 to 1994, Clarke and Leakey, *subm.*). The arrows indicate the probable direction of nutrient flux, and the values underneath indicate the relative proportions (%) between the concentrations of the different water bodies.

	benthos		overlying water		pelagic
Ammonia	1600	----------> 4	60	---------->	< 0.005
Nitrate	36	----------> 17	6	<---------- 40	15
Phosphate	65	----------> 11	7	----------> 14	1
Silicate	360	----------> 8	29	<---------- 46	63

Nutrient exchange was more intensively and accurately studied by Nedwell and Walker, (1995). The sediment of Factory Cove was also found to be a sink of NO_3^-, but a source of NH_4^+ to the water column. These fluxes might impact the regenerated (ammonium based) production in the water column. Ofcourse the direction of these fluxes can vary quickly and depend on the oxygen conditions and microbial processes near the sediment-water interface, and on algal bloom deposition (Hansen and Blackburn, 1992). Nedwell and Walker, (1995) could not demonstrate seasonal differences.
The role of the meiofauna to this respect could not be deduced from the current experiments, but as meiofauna significantly enhance solute (O_2, NO_3^-, $Si(OH)_4$,..) transport at the sediment-water interface and in the bioturbation zone, they stimulate aerobic reaction rates and associated processes (Aller and Aller, 1992).

Sediment oxygen demand (SOD). Oxygen respiration is the principal mineralization process in the sediments, and SOD measurements yield a minimum estimate for C-flux in the sediment. Oxygen uptake by the benthos in Factory Cove in other years ranged between 53 and 90 mmol oxygen $m^{-2}.d^{-1}$ Nedwell 1989; Nedwell et al. 1993). This was in dark conditions with amphipod respiration included, with the seasonal variation taken into account. Our measurements with amphipods in the dark amounted to a maximum rate of 10.4 mmol oxygen $m^{-2}.d^{-1}$. This was a factor 5 to 9 lower than the above mentioned values.
Our respiration measurements were the resultant of chemical and biological processes and did not distinguish between the major organic matter mineralization mechanisms (e.g. aerobic respiration, denitrification and sulfate-reduction) in the coastal marine sediments of Signy Island. However, in organic-rich sediments, such as at Factory Cove, oxygen demand alone can substantially underestimate metabolims. To this respect, the above mentioned authors found that on an annual basis, 32 % of benthic organic matter mineralization was anoxic, with the proportion of anoxic compared with oxic mineralization higher during the winter (Nedwell et al. 1993). Bioturbation by the amphipods depressed sedimentary oxygen uptake by 33 % (Nedwell and Walker, 1995). When macrobenthos was eliminated in our measurements an anomalously low oxygen flux of 0.69 $mmol.m^{-2}.d^{-1}$ was measured. This would mean a decrease of oxygen uptake by almost 95 %.

Meiofaunal (individual) respiration. Short-term measurements make polarographic oxygen electrodes an interesting and reliable tool for routine measurements of meiofaunal respiration (Moens et al. *subm*). The metabolic rate of polar ectotherms, assessed by measuring oxygen consumption, is affected by numerous factors, among which temperature stress and physical disturbance are certainly important key factors. We tried to control this by carefully handling the nematodes under low temperatures. However, as to the use of a cold water bath, the transfer of the signal between the sample/electrode at low temperatures and the monitor at room temperatures, "background" oxygen consumption seem to be higher (Moens et al. *subm*). Therefore we did our measurements under at a constant ambient temperature of 5°C. The relevance of the observed respiration rates may therefore be questioned. We are aware of the many factors influencing oxygen demand in nematodes (Atkinson 1980), and of the complexity of adaptation of polar ectotherms to the polar temperatures (as extensively reviewed by Clarke 1983 and shown for an arctic terrestrial nematode, Procter 1987). By applying this method we assumed that the meiofauna had compensated their metabolic activity (e.g. exhibited similar respiration rates at laboratory and field conditions). Respiration rates of high Antarctic free-living marine nematodes have not been measured before. Thus we do not know their temperature-sensitivity and temperature optimum.

Nothwithstanding this we standardized the obtained rates to the ambient temperature at that period of the year (e.g. 0°C) using Q_{10} = 2. Price and Warwick, (1980) reported this value to be characteristic for meiobenthos which feed on seasonally unstable food sources - a situation which we regard as applicable to Antarctic sediments. Hence, the observed respiration rate of nematodes (1.26-3.92 nl $O_2.ind^{-1}.h^{-1}$ for nematode dwt of about 0.4 to 0.8 μg) amounts to 0.89-2.77 nl $O_2.ind^{-1}.h^{-1}$ (mean : 1.97) with a Q_{10} = 2, and serves as a first preliminary information, without emphasising weight and temperature specific rates. This was within the ranges of temperate marine nematodes at about 20°C (Warwick and Price, 1979; Nicholas 1984; Giere 1993; Ferris et al. 1995).

Partitioning of benthic community respiration. Remineralisation processes in the current sediments are highly active (12.3 mole $C.m^{-2}.y^{-1}$, Nedwell et al. 1993) and strong seasonal varying and major part of nutrient regeneration is due to microbial activity (e.g. sulfate reduction, denitrification and aerobic processes). Taking into account the percentage share of the respiration of amphipods (macrofauna) in the total SOD, 70% (= 8.61 $gC.m^{-2}.y^{-1}$) was taken up by the meio- and microbenthos. Considering the carbon utilization, at a respiration rate

of 1.97 $nl.h^{-1}.ind^{-1}$, the nematode population (based upon densities of January and February 1994) would consume in 1 year 1.6 to 4.2 mol $C.m^{-2}$. This would account for about 13-42% (mean approx. 25%) of the mean total benthic carbon demand (of own and Nedwell's measurements). Hence, respiration would be partioned among the three major benthic components with relative numbers for amphipods 30%, meiofauna 25% and microbiota 45%. Because of a multitude of factors affect meiofaunal respiration (e.g. size, age, composition, diurnal and seasonal variation of temperature, blooms, particle size) the estimate will be subject to considerable variation. In literature meiofaunal respiration accounted for 9-61 % of SOD (Lasserre 1976; Relaxans et al. 1992).

4.5 Meiofaunal secondary production at Signy Island Table XII.

The estimate of secondary production by the meiofauna was done in several indirect ways, all of which are only based upon the production of the major taxon (e.g. nematodes). The methods used originate from investigations in temperate regions and are based upon the observations that the reproduction of nematodes are continous, such that the generations in the field strongly overlap and individual cohorts cannot be distinguished.

1) The first approach was based upon reported annual P:B ratios for meiofauna (Heip et al. 1982, 1984, 1985a,b; Herman et al. 1984; Vranken and Heip, 1986). We used the extreme limits (P:B 4 to 64), and the common applied ratio of Gerlach (1971: P:B 9). The application of a wide range of possible annual P:B ratios will certainly govern real meiofauna production in the Antarctic.

2) The second method was based upon the experimental and field data of marine nematode species and the temperature regime Vranken et al. (1986) gives

regression (1) :

$$\log T_{min} = 2.202 - 0.0461\ t + 0.627 \log W$$

where :

$$\frac{1}{T_{min}} * D * 3$$

D = *days per month*; $\frac{1}{T_{min}}$ = *development rate*

Table XIII: Secondary production by the nematodes.

	mean	median
Individual dwt (μg) : total community	0.5 ± 0.23 (0.2 - 1.3)	0.2 ± 0.26 (0.1- 1.4)
Individual dwt (μg) : adults	0.7 ± 0.28 (0.3 - 1.3)	0.3 ± 0.14 (0.5- 1.4)
Total dwt (g C.m^{-2})	1.1 ± 1.16 (0.1 - 5.2)	0.6 ± 1.11 (0.1 - 5.6)
Production based on P:B ratios (gC.m^{-2}.y^{-1}) P:B = 4 P:B = 9 P:B = 69	 4.2 9.4 72.4	 2.2 5.0 38.4
Production based on equation (1) (gC.m^{-2}.y^{-1})	30.8	17.1
	January 1994	February 1994
Production based on equation (2) (gC.m^{-2}.y^{-1})	13.3	6.0

note : a factor of 0.42 was used to convert the nematode dwt to carbon values (Feller & Warwick, 1988).

This regression equation requires but a knowledge of the annual temperature regime of the habitat and the body mass of the adult females. The equation has, however, some speculative aspects. As we expect the antarctic meiofauna to be primarily influenced by food, rather than by temperature, the current estimates give only a small side of the full range of annual production variation (e.g. temperatures varied only about 2°C). Moreover, these calculations assume that the biomass turn-over (e.g. number of offspring per generation) was 3 and a temperature coefficient of Q_{10} = 2.95 was implied. In addition, we did not distinguish between the specific body weights of males and females, as we used the body mass values of adults of the total nematode community between April 1991 and January 1992. More detailed expertise is needed before any conclusive remark can be made.

The P:B ratio's calculated from the average total biomass over the months April 1991 to January 1992, and the total production based on these 10 months, is given in Table XIII.

Table XIII: Estimate of annual P:B ratio based upon equation (1).

	Mean	Median
Total production (mole $C.m^{-2}.y^{-1}$)	2.569	1.428
Average biomass (mole $C.m^{-2}$)	0.129	0.07
P:B	**19.9**	**20.4**

3) Warwick and Price, (1979) re-evaluated the general applied P/B ratio (Gerlach 1971) using an empirical relationship between respiration and production :

regression (2) :

$$\log P = 0.8262 \log R - 0.0948 \quad (kcal.m^{-2}.y^{-1})$$

In this calculation P and R are both expressed in Kcal; we assumed that 1gC = 12 Kcal (Crisp 1971).

By plotting the proportion of total production of each meiofaunal species, ranked in order of importance, Warwick (1982) found curves which fitted lognormal distributions. Yet, the partitioning of total secondary production by meiofauna species was quite equitable in a system dominated by epigrowth feeders (group 2A) and non-selective deposit-feeders (group 1B). This was, however, refuted by Kennedy (1994), who found that, although the numerical dominance of these feeding categories, the energetic importance of omnivore-predators, could not be ignored. Such stucture and functioning of the meiobenthic communities at Factory Cove are unknown. Because of the very low numbers of selective deposit feeders (group 1A) and predators/omnivores (group 2B), and because of the rather stable relative genus composition throughout the year, it is however likely that the relative importance (in terms of annual production) of the 2A and 1B groups, was equally shared. Therefore the mistake of applying the calculations on the total nematode community respiration, ignoring specific functional groups (like feeding type) and life stage might be less decisive in the sediments of Factory Cove with their low diversity and more or less stable community age structure.
As a conclusion the calculated estimates of secondary production by the meiofauna were between 2.2 and 72.4 $gC.m^{-2}.y^{-1}$ with a high probability of P laying between 10 and 20 $gC.m^{-2}.y^{-1}$.

4.6 Carbon balance at Signy Island.

The biomass balance at the water column-sediment interface and bentho-pelagic coupling for the nearshore region and from the meiofaunal point of view, is outlines by figure 14. All figures are expressed in mol $C.m^{-2}.y^{-1}$, and we focussed the fluxes on the meiobenthic point of view, with the bentho-pelagic link in mind. Additional information is gained from available literature.

Gilbert (1991b) measured primary production on the sediment surface (8.4 mol $C.m^{-2}.y^{-1}$) and Whitaker (1982) in the water column above (7.2-24.1 mol $C.m^{-2}.y^{-1}$). The sedimentation (9.1-35.8 mol $C.m^{-2}.y^{-1}$) and production of organic carbon (10.6 mol $C.m^{-2}.y^{-1}$) was given by Nedwell et al. (1993) and Tanner and Herbert, (1981). No estimates were available for the annual production of the macrofauna.

Silicate and nitrate was found to be transported to the sediments, whereas ammonium and phosphate are exported towards the water column. The flux rates were not quantified, but indications that the sediments might sustain regenerated production in the water column infer that these fluxes might be high (Nedwell and Walker, 1995).

The importance of meiofauna in the carbon budget is given by their secondary production rates (0.18-6.0 mol $C.m^{-2}.y^{-1}$). These are minimum and maximum estimates based on mean and median dimensions (see above) of nematode length and width in the forthnightly samples of 1991-1992. When considering a mean production of 1 mol $C.m^{-2}.y^{-1}$ (from the new P:B ratio, see above), the meiofauna represented a minimum of 9.4% of total benthic carbon production, 4.1% of phytoplankton production and 11.9% of microphytobenthic production. The annual production was comparable with the highest production reported from various regions (Bouvy 1988). This is in accordance with the finding that food input both from *in situ* benthic production and pelagial activity was higher than major nearshore areas.

The relative share of meiobenthos in carbon flow is given by their metabolic rates. Grazing on autotrophs (1.1-2.3 mol $C.m^{-2}.y^{-1}$) constituted 10.4% and respiration by the nematode community (1.6-4.2 mol $C.m^{-2}.y^{-1}$) 21.7% of annual benthic organic carbon production. The latter was based upon metabolic rates at $Q_{10} = 2$ (see above). Both fluxes were extrapolated from rates obtained in the

summer months (January and February 1994), and might give overestimates of the true rates.
Grazing on bacteria and benthic organic carbon (POC and DOC) could not be quantified, and other food items, such as flagellates, ciliates, fungi, .. were not taken into account, and other fluxes such as temporary burial, resuspension and geological deposition of organic matter below the bioturbated zone are similarly unknown. We disregarded mortality and predation by macrofauna.

Sources of bias.
-The data are not from the same year. This could be a source of bias as seasonality and interannual variability in the sediments of Factory Cove is very high (Clarke et al. 1988). To minimize this aspect we tried to bring together the reported extremes (minima and maxima), so that the budget may be applicable over several years.

-Influence of temperature in the flux rates. As to overcome the problem of oxygen electrode uptake rates using a cold water bath, we did our measurements in a constant temperature room at 5°C. All the other experiments (including grazing, nutrient fluxes, respiration) were done under similar conditions, and hence at a same constant temperature of 5°C. To minimize this shortcoming we scaled respiration rates down to the ambient temperatures, with a Q_{10} = 2. The choice is, however, arbitrary and using another Q_{10} can drastically alter our conclusions. The conversion was not done for the calculation of other fluxes (e.g. SOD and grazing). To our opinion applying such fixed ratios without having any knowledge on the differential influence of temperature and food in Antarctic benthic communities would lead to other biases.
- Because of the lack of statistical proof and pooling of core measurements, the fluxes (based on metabolic processes of the meiofauna) in the carbon budget should be treated with caution.

In summary. With their high production, grazing and respiratory activity, it seems like that meiofauna respond efficiently to the extreme Antarctic environment, and that they form a potentially important step in the energy web. However, it should be stressed that the energy transfer is not a simple matter of a step-by-step progression through conventional trophic levels. The dynamics of benthic assemblages as a whole is difficult to understand, and the substraction of one functional group with its characteristic species, sizes and ages is even

more complex. Therefore we recognize the simplicity of our budget, but it should offer instructive information for further research.

5. CONCLUSIONS

-The meiofauna community in the deep Weddell Sea was rich in terms of abundance and biomass, and exhibited a high level of heterogeneity. The meiofaunal communities in the deep sea were not very different from those in other continental shelf and slope assemblages (e.g. concerning patchiness, standing stock, diversity, relation with environment). It was suggested that the structure and functioning of the different assemblages mirrored events that occurred in the water column. When applying a minimum nematode production for this region about 2 % of the primary production, and 11 % of the downward flux rates was channeled into the meiobenthic communities.

-The sediment~ of Factory Cove were populated by a flourishing meiobenthic community. A strongly reduced benthic environments with distinct zonation patterns of food and oxygen triggered their vertical distribution. The overall temporal shift in meiofauna/nematode variables was consistent with temporal changes of available food (microbiota and chloropigments), and stressed therefore the tight coupling between the benthos and the rich, but high seasonal depositional pelagic.

-We could cautiously accept that the meiobenthic relations with the suspected microbial food (bacteria and diatoms) were to some extent explained by meiofauna grazing (e.g. about 10% of annual benthic carbon production). Moreover, microbiota were not only of vital importance for the nutrition of meiofauna organisms, but in turn they were impacted by the meiobenthic community as well.

-The estimate of secondary production by the meiofauna in this region, obtained from several indirect ways, and based upon the production of the major taxon (e.g. nematodes) gave very high values.

-When standardizing the individual respiration to ambient temperature the observed respiration rate of nematodes were within the ranges of temperate marine nematodes at about 20°C. Thus, considering the carbon utilization by

the nematode community, the meiofauna at Factory Cove accounted for about 13-42% of the mean total benthic carbon demand, and 22% of annual benthic organic production.

-Comparison of nutrient concentrations in the porewater, in the nepheloid layer and in the water column, and experimental evidence for concentration changes in the sediment inferred that ammonia and phosphate were exported from, and nitrate and silicate were imported into, the sediments. It was suggested that substantial denitrification occurred at a depth from 3 cm on, and that the observed fluxes might impact the regenerated (ammonium based) production in the water column.

Our conception of carbon exchanges in the coastal system of Signy Island give some valuable information, but it is far from fully understood.

General conclusion

From the field data of density and biomass, the relative importance of the meiobenthos in the Southern Ocean was derived. Despite the apparent harshness of the environment the Antarctic meiofaunal taxa thrives with high standing stocks and production, sometimes much higher than their temperate and tropical relatives. This implies that the meiofauna uses the episodic food supply, both from water column and *in situ* production very efficiently. Flux measurements of organic matter (e.g. grazing), nutrients (concentration changes) and oxygen (oxidative respiration), suggest that the meiofauna may provide an important pathway by which deposited and *in situ* organic matter is channeled through the differing benthic components and from the sediment back into the water column.

ACKNOWLEDGEMENTS

The research presented in this paper was performed under the auspices of the the Scientific Research Programme on Antarctica-Phase III from the Belgian State-Prime Minister's Federal Office for Scientific, Technical and Cultural Affairs (DWTC), and Institute for the Encouragement of Scientific Research in Industry and Agriculture (IWT). Samples were collected during the European "Polarstern" Study (EPOS) sponsored by the European Science Foundation and the Alfred Wegener Institute for Polar and Marine Research, Germany, and by the summmer and winter parties at Signy Island, British Antarctic Survey, United Kingdom, for which we are very grateful. Many gratitudes also to the technical staff of the Marine Biology Section of our Institute, with special reference to G. De Smet, D. Schram, I. Seys, M. Bruyneel, A. Vierstraete and R. Coolen. Finally we acknowledge Dr R.L. Herman for stimulating discussions.

REFERENCES

Admiraal, W., Bouwman, L.A., Hoekstra, L. and Romeyn, K. 1983. Qualitative and quantitative interactions between microphytobenthos and herbivorous meiofauna on a brackish intertidal mudflat. Int. Revue ges. Hydrobiol. 68 (2) : 175 - 191.

Aller, R.C. and Aller, J.Y. 1992. Meiofauna and solute transport in marine muds. Limnol. Oceanogr. 37 (5) : 1018 - 1033.

Ankar, S. and Elmgren, R. 1976. The benthic macro- and meiofauna of the Anskö-Landsort area (northern Baltic proper). Contr. Askö Lab Univ Stockholm 11 : 1 - 115.

Arntz, W.E., Brey, T. and Gallardo, V.A. 1994. Antarctic zoobenthos. Oceanogr. Mar. Biol. Ann. Rev. 32 : 241 - 304.

Atkinson, H.J 1980. Respiration in nematodes. In : Nematodes as biological models, vol 2. Zucker-Man, B.M. (Ed.), Academic press, New York : 101 - 142.

Barnett, P.R.O., Watson, J. and Connelly, D. 1984. A multiple corer for taking virtually undisturbed samples from shelf, bathyal and abyssal sediments. Oceanol. Acta 7 : 399 - 408.

Biggs, D.C., Berkowitz, S.P., Altabet, M.A., Bidigare, R.R., DeMaster, D.J., Dunbar, R.B., Leventer, A., Macko, S.A., Nottrouer, C.A. and Ondrusek, M.E. 1988. A coopereative study of upper-ocean particulate fluxes in the Weddell Sea. In : Proceedings of the Ocean Drilling Program, 113. Initial reports, Weddell Sea, Antarctica. Stewart, N.J. (Ed.), College station, Texas, A & M University : 77 - 86.

Blanchard, G.F. 1990. Overlapping microscale dispersion patterns of meiofauna and microphytobenthos. Mar. Ecol. Prog. Ser. 74 : 99 - 107.

Blanchard, G.F. 1991. Measurement of meiofauna grazing rates on microphytobenthos: is primary production a limiting factor? J. Exp. Mar. Biol. Ecol. 147 : 37 - 46.

Bouvy, M. 1988. Contribution of the bacterial and microphytobenthic microflora in the energetic demand of the meiobenthos in an intertidal muddy sediment (Kerguelen Archipelago). PSZNI: Mar. Ecol. 9(2) : 109 - 122.

Carman, K.R. and Thistle, D. 1985. Microbial food partitioning by three species of benthic copepods. Mar. Biol. 88 : 143 - 148.

Carman, K.R., Dobbs, F.C. and Guckert, J.B. 1989. Comparison of three techniques for administering radiolabeled substrates to sediments for trophic studies: uptake of label by harpacticoid copepods. Mar. Biol. 102 : 119 - 125.

Clarke, A. 1983. Live in cold waters: the physiological ecology of polar marine ectotherms. Oceanogr. Mar. Biol. Ann. Rev. 21 : 341-453.

Clarke, A. and Leakey, R.J.G. *subm.*. The seasonal cycle of phytoplankton and the microbial community in a nearshore Antarctic marine ecosystem. Limnol. Oceanogr.

Clarke, A., Holmes, L.J. and White, M.G. 1988. The annual cycle of temperature, chlorophyll and major nutrients at Signy Island, South Orkney Islands, 1969-82. Br. Antarct. Surv. Bull. 80 : 65 - 86.

Crisp, D.J. 1971. Energy flow measurements. In: Methods for the study of marine benthos. Holme, N.A. and McIntyre, A.D. (Eds). IBP Handbook N°16. Blackwell Scientific Publications, Oxford : 197 - 279.

Cullen, D.J. 1973. Bioturbation of superficial marine sediments by interstitial meiobenthos. Nature 242 : 323 - 324.

Darley, W.M. 1977. Biochemical composition. In: The biology of diatoms. Werner, D. (Ed.) Blackwell Scientific Publications, Oxford : 208.

Daro, M.H. 1978. A simplified 14C method for grazing measurements on natural planktonic populations. Helgoländer wiss. Meeresunters. 31 : 241 - 248.

de Bovée, F. and Soyer, J. 1975. Le méiobenthos de l' Archipel de Kerguelen. Premières données quantitatives. CR Acad Sc Paris 280 (D) : 2369 - 2372.

De Master, D.J., Nittrouer, C.A. and Hoffmann, P.A. 1983. Biogenic silica accumulation on the Antarctic continetal shelf. US Antarct. J. 18 : 132 - 134.

Elmgren, R. 1975. Benthic meiofauna as indicator of oxygen conditions in the Northern Baltic proper. Merentutkimuslait Julk 239 : 265 - 271.

Elmgren, R., Rosenberg, R. and Andersen, A.B. 1983. Benthic macro- and meiofauna in the Gulf of Bothnia (Northern Baltic). Finnish Marine Research 250 : 3 - 18.

Epstein, S.S. and Shiaris, M.P. 1992. Rates of microbenthic and meiobenthic bacterivory in a temperate muddy tidal flat community. App. Env. Microbiol. 58 (8) : 2426 - 2431.

Feller, R.J. and R.M. Warwick 1988. Energetics. In: Introduction to the study of meiofauna. Higgins, R.P. and Thiel, H. (Eds). Smithsonian, Washington DC : 181 - 196.

Ferris, H., Lau, S. and Venette, R. 1995. Population energetics of bacterial-feeding nematodes, respiration and metabolic rates based on CO_2 production. Soil Biol. Biochem. 27(3) : 319 - 330.

Gerdes, D. 1990. Antarctic trials of the multi-box corer, a new device for benthos smapling. Polar Rec. 26(156) : 35 - 38.

Gerlach, S.A. 1971. On the importance of marine meiofauna for benthos communities. Oecolgia 6 : 179 - 190.

Giere, O. 1993. Meiobenthology. The microscopic fauna in aquatic sediments. Springer-Verlag Berlin Heidelberg : 328p.

Gilbert, N.S. 1991a. Primary production by benthic microalgae in near-shore marine sediments of Signy Island, Antarctica. Polar Biol. 11 : 339 - 346.

Gilbert, N.S. 1991b. Microphytobenthic seasonality in near-shore marine sediments at Signy Island, South Orkney Islands, Antarctica. Est. Coast. Shelf. Sci. 33 : 89 - 104.

Gilbert, P.M., Biggs, D.C. and McCarthy J.J. 1982. Utilization of ammonium and nitrate during austral summer in the Scotia Sea. Deep Sea Res. 29 : 837 - 850.

Gooday, A.J. and Turley, C.M. 1990. Responses by benthic organisms to inputs of organic material to the ocean floor: a review. Philosophical Transactions of the Royal Society of London, A 331 : 119 - 138.

Graf, G. 1992. Benthic-pelagic coupling : a benthic view. Oceanogr. Mar. Biol. Ann. Rev. 30 : 149 - 190.

Hansen, L.S. and Blackburn, T.H. 1992. Effect of algal deposition on sediment respiration and fluxes. Mar. Biol. 112 : 147-152.

Heip, C. 1995. Eutrophication and zoobenthos dynamics. Ophelia 41 : 113 - 136.

Heip, C., Herman, P.M.J. and Coomans, A. 1982. The productivity of marine meiobenthos. Academiae Analecta 44(2) : 1 - 20.

Heip, C., Herman, R. and Vincx, M. 1984. Variability and productivity of meiobenthos in the Southern Bight of the North Sea. Rapp. P.-v. Réun. Cons. int. Explor. Mer 183 : 51 - 56.

Heip, C., Vincx, M. and Vranken, G. 1985a. The ecology of marine nematodes. Oceanogr. Mar. Biol. Ann. Rev. 23 : 399 - 489.

Heip, C., Herman, P.M.J., Smol, N., Van Brussel, D. and Vranken, G. 1985b. Energy flow through the meiobenthos. In: Benthic studies of the Southern Bight of the North Sea and its adjacent continental estuaries. Heip, C. and Polk, Ph. (Eds.). Concerted Actions Oceanography. Final Report. vol 3: Biological Processes and Translocations. Ministry of Scientific Policy, Brussels, Belgium. 226 p.

Herman, R.L. and Dahms H.U. 1992. Meiofauna communities along a depth transect off Halley Bay (Weddell Sea-Antarctica). Polar Biol. 12 : 313 - 320.

Herman, P.M.J., Vranken, G. and Heip, C. 1984. Problems in meiofauna energy-flow studies. Hydrobiologia 118 : 21 - 28.

Higgins, R.P. and Thiel, H. 1988. Introduction to the study of meiofauna. Smithsonian Institution Press, Washington, D.C. London, 488 p.

Jensen, P. 1982. Diatom-feeding behaviour of the free-living marine nematode *Chromadorita tenuis*. Nematologica 28 : 71 - 76.

Kennedy, A.D. 1994. carbon partitioning within meiobenthic nematode communities in the Exe estuary, UK. Mar. ecol. Prog. Ser. 105 : 71 - 78.

Koike, I., Holm-Hansen, O. and Biggs, D.C. 1986. Inorganic nitrogen metabolism by Antarctic phytoplankton with special reference to ammonium cycling. Mar. Ecol. Prog. Ser. 30 : 105 - 116.

Kristensen, E.S., Syvertsen, E.E. and Farbrot, T. 1992. Nitrogen uptake in the Weddell Sea during late winter and spring. Polar. Biol. 12 : 245 - 251.

Lasserre, P. 1976. Metabolic activities of benthic icrofauna and meiofauna : recent advances and review of suitable methods of analysis. In: The benthic boundary layer. McCave I.N. (Ed.). Plenum publ. Co, New York : 95 - 142.

Libes, S.M. 1992. An introduction to marine biogeochemistry. Wiley & Sons, Inc., 734 p.

Linke, P. 1992. Metabolic adaptations of deep-sea benthic formaninfera to seasonally varying food input. Mar. Ecol. Prog. Ser. 81 : 51 - 63.

Lutze, G.F., Pflaumann, U. and Weinholz, P. 1986. Jungquartäre Fluktuationen der benthischen Foraminiferenfaunen in Tiefsee-Sedimenten vor NW-Afrika. Eine Reaktion auf Produktivitätsänderungen im Oberflächenwasser. 'Meteor' Forsch.-Ergebn. C40 : 163 - 180.

Mantoura, R.F.C. and Llewellyn, C.A. 1983. The rapid determination of algal chlorophyll and carotenoid pigments and their breakdown products in natural waters by reverse-phase high-performance liquid chromatography. Anales Chimie Analytique 151 : 297 - 314.

Meyer-Reil, L.-A. and Faubel, A. 1980. Uptake of organic matter by meiofauna organisms and interrelationships with bacteria. Mar. Ecol. Prog. Ser. 3 : 251 - 256.

Moens, T., Vierstraete, A., Vanhove, S., Verbeke, M. and Vincx, M. *subm.* A handy method for measuring meiobenthic respiration.

Montagna, P.A. 1984. *In situ* measurement of meiobenthic grazing rates on sediment bacteria and edaphic diatoms. Mar. Ecol. Prog. Ser. 18 : 119 - 130.

Montagna, P.A. 1993. Radioisotope technique to quantify *in situ* microbivory by meiofauna in sediments. In: Handbook of methods in aquatic microbial ecology, (Kemp, P.F., Sherr, B.F., Sherr, E.B. and Cole, J.J. (Eds). Lewis publishers, Boca Raton, FL : 745 - 753.

Montagna, P.M. and Bauer, J.E. 1988. Partitioning radiolabeled thymidine uptake by bacteria and meiofauna using blocks and poisons in benthic feeding studies. Mar. Biol 98 : 101 - 110.

Montagna, P.A. and Yoon, W.B. 1991. The effect of freshwater inflow on meiofaunal consumption of sediment bacteria and microphytobenthos in San Antonio Bay, Texas, U.S.A. Est. Coast. Shelf. Sci. 33 : 529 - 547.

Montagna, P.A., Blanchard, G.F. and Dinet, A. 1995. Effect of production and biomass of intertidal microphytobenthos on meiofaunal grazing rates. J. Exp. Mar. Biol. Ecol. 185 : 149 - 165.

Nedwell, D.B. 1989. Benthic microbial activity in an Antarctic coastal sediment at Signy Island, South Orkney Islands. Est. Coastal Shelf Sci. 28 : 507 - 516.

Nedwell, D.B. and Walker, T.R. 1995. Sediment-water fluxes of nutrients in an Antarctic coastal environment : influence of bioturbation. Polar Biol 15 : 57 - 64.

Nedwell, D.B., Parkes, R.J., Upton, A.C. and Assinder, D.J. 1993. Seasonal fluxes across the sediment-water interface, and processes within sediments. Phil. Trans. R. Soc. Lond. A 343 : 519 - 529.

Nehring, S., Jensen, P. and Lorenzen, S. 1990. Tube-dwelling nematodes: tube construction and possible ecological effects on sediment-water interfaces. Mar. Ecol. Prog. Ser. 64 : 123 - 128.

Nicholas, W.L. 1984. The biology of free-living nematodes. 2nd edition. Clarendon press, Oxford.

Nöthig, E.-M. 1988. Untersuchungen zur Ökologie des Phytoplanktons im südöstlichen Weddellmeer (Antarktis) im Januar/Februar 1985. Ber. polarforsch. 53.

Olson, R.J. 1980. Nitrate and ammonium uptake in Antarctic waters. Limnol. Oceanogr. 25 : 1064 - 1074.

Peck, L.S. and Uglow, R.F. 1990. Two methods for the assessment of the oxygen content of small volumes of seawater. J. Exp. Mar. Biol. Ecol. 141 : 53 - 62.

Price , R. and Warwick, R.M. 1980. The effect of temperature on the respiration rate of meiofauna. Oecologia 44 : 145 - 148.

Procter, D.L.C. 1987. Respiration rates of *Chiloplacus* sp. and other arctic nematodes at low and high temperatures. Polar Biol. 7 : 303 - 306.

Relaxans, J.-C., Etcheber, H., Castel, J., Escaravage, V. and Auby, I. 1992. Benthic respiratory potential to sedimentary carbn quality in seagrass beds and oyster parks in the tidal flats of Arcachon Bay, France. Est. Coast. Shelf Sci., 34 : 157 - 170.

Romeyn, K. and Bouwman, L.A. 1983. Food selection and consumption by estuarine nematodes. Hydrobiol. Bull. 17 : 103 - 109.

Rönner, U., Sørensen, F. and Holm-Hansen, O. 1983. Nitrogen assimilation by phytoplankton in the Scotia Sea. Polar Biol. 2 : 137 - 147.

Rowe, G.T., Sibuet, M., Deming, J.W., Tietjen, J. and Khripounoff, A. 1991. Total sediment biomass and preliminary estimates of organic carbon residence time in deep-sea benthos. Mar. Ecol. Prog. Ser. 79 : 99 - 114.

Rudnick, D.T., Elmgren, R. and Frithsen, J.B. 1985. Meiofaunal prominence and benthic seasonality in a coastal marine ecosystem. Oecologia (Berlin) 67 : 157 - 168.

Santos, P.J.P., Castel J. and Souzy-Santos, L.P. 1995. Microphytobenthic patches and their influence on meiofaunal distribution. Cah. Biol. Mar. 36 : 133 - 139.

Sayles, F.L., Martin, W.R. and Deuser, W.G. 1994. Response of benthic oxygen demand to particulate organic carbon supply in the deep sea near Bermuda. Nature 371 : 686 - 689.

Soetaert, K. 1989. An ecological-systematical study of the deep-sea meiofauna and nematode communites in the western Mediterranean Sea. Ph.D. thesis, university of Gent, Belgium, 306 p.

Sokal, R.R. and Rohlf, F.J. 1981. Biometry (second edition). Freeman W.H. and company, New York, 859 p.

Soltwedel, T., Pfannkuche, O. and Thiel, H. *subm.* The size structure of deep-sea metazoan in the NE Atlantic: nematode size spectra in relation to environmental variables.

Tanner, A.C. and Herbert, R.A. 1981. Nutrient regeneration in maritime Antarctic sediments. Kieler Meeresforsch. 5 : 390 - 395.

Thiel, H. 1983. Meiobenthos and nanobenthos of the deep sea. In: The sea, volume 8. Rowe, G.T. (Ed). Wiley & Sons, New York : 167 - 230.

Tietjen, J.H. 1969. The ecology of shallow water meiofauna in two New England estuaries. Oecologia (Berlin) 2 : 251 - 291

Tietjen, J.H. 1980. Microbial-meofaunal interrelationship: a review. Microbiology : 335 - 338.

Tietjen J.H. 1992. Abundance and biomass of metazoan meiobenthos in the deep sea. In: Deep-sea food chains and the global carbon cycle. Rowe, G.T. and Pariente, V. (Eds). Kluwer Academic Publishers, the Netherlands : 45 - 62.

Vanhove, S., Lee, H.J., Beghyn, M., Van Gansbeke, D., Brockington, S. and Vincx, M. *subm.* The metazoan meiofauna in an Antarcitc coastal sediment : link with biochemical gradients and temporal shifts in the ecosystem.

Vanhove, S., Wittoeck, J., Desmet, G., Van den Berghe, B., Herman, R.L., Bak, R.P.M., Nieuwland, G., Vosjan, J.H., Boldrin, A., Rabitti, S. and Vincx, M. 1995. Deep-sea meiofauna communities in Antarctica : structural analysis and relation with the environment. Mar. Ecol. Prog. Ser. 127 : 65 - 76.

Vidal, M., Romero, J. and Camp, J. 1989. Sediment-water nutrient fluxes : preliminary results of *in situ* measurements in Alfaques Bay, Ebro River Delta. In: Topics in marine biology. Ros, J.D. (Ed.). Scient. Mar. 53(2-3) : 505 - 511.

Vincx, M., Bett, B.J., Dinet, A., Ferrero, T., Gooday, A.J., Lambshead, P.J.D., Pfannkuche, O., Soltwedel, T. and Vanreusel, A. 1994. Meiobenthos of the deep Northeast Atlantic. Adv. Mar. Biol. 30 : 1 - 88.

Vranken, G. and Heip, C. 1986. The productivity of marine nematodes. Ophelia 26 : 429 - 442.

Vranken, G., Herman, P.M.J., Vincx, M. and Heip, C. 1986. A re-evaluation of marine nematode productivity. Hydrobiologia 135 : 193 - 196.

Warwick, R.M. 1982. The partitioning of secondary production among species in benthic communities. N.J.S.R. 16 : 1 - 16.

Warwick, R.M and Price, R. 1979. Ecological and metabolic studies on free-living nematodes from an estuarine mud-flat. Est. Coast. Shelf. Sci. 9 : 257 - 271.

Webb, D.G. and Montagna, P.A. 1993. Initial burial and subsequent degradation of sedimented phytoplankton: relative impact of macro- and meiobenthos. J. Exp. Mar. Biol. Ecol. 166 : 151 - 163.

Wefer, G. and Fischer, G. 1991. Annual primary production and export flux in the Southern Ocean from sediment trap data. Mar. Chem. 35 : 597 - 613.

Wefer, G., Fischer, G., Fütterer D.K., Gersonde, R., Honjo, S. and Ostermann, D. 1990. Particle sedimentation and productivity in Antarctic waters of the Atlantic sector. In: Geological history of the polar oceans : Arctic versus Antarctic. Bleil, U. and Thiede, J. (Eds). Kluwer Academic Publishers : 363 - 379.

Whitaker, T.M. 1982. Primary production of phytoplankton off Signy Island, South Orkneys, The Antarctic. Proc. R. Soc. Lond., B214 : 169 - 189.

Wieser, W. 1953. Die Beziehung zwischen Mundhöhlengestalt, Ernährungsweise und Vorkommen bei freilebenden Marinen Nematoden. Eine ökologisch-morphologische Studie. Arkiv Für Zoologie 2(4) : 439 - 484.

Wittoeck, J. 1991. Ecologische studie van het meiobenthos van West-Groenland (Disko Island). Ms thesis, university of Gent, Belgium : 1 - 84.

Yingst, J.Y. 1978 Patterns of micro- and meiofaunal abundance in marine sediments, measured with the adenosine triphosphate assay. Mar. Biol. 47 : 41 - 54

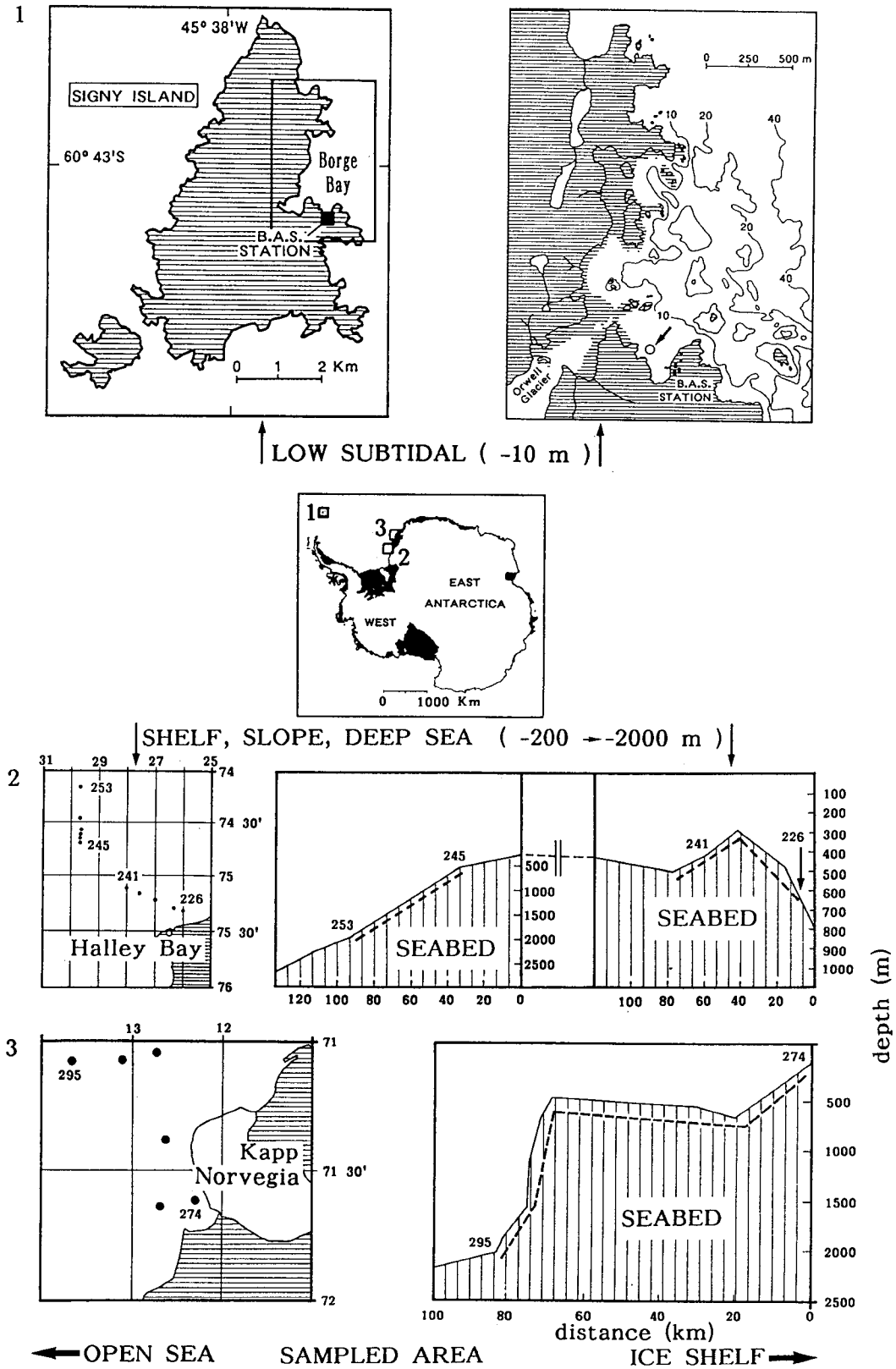

Fig.1: Station location in the low subtidal(1)and deep sea(2&3)of Antarctica; the outer stations of each transect are indicated(see table I).

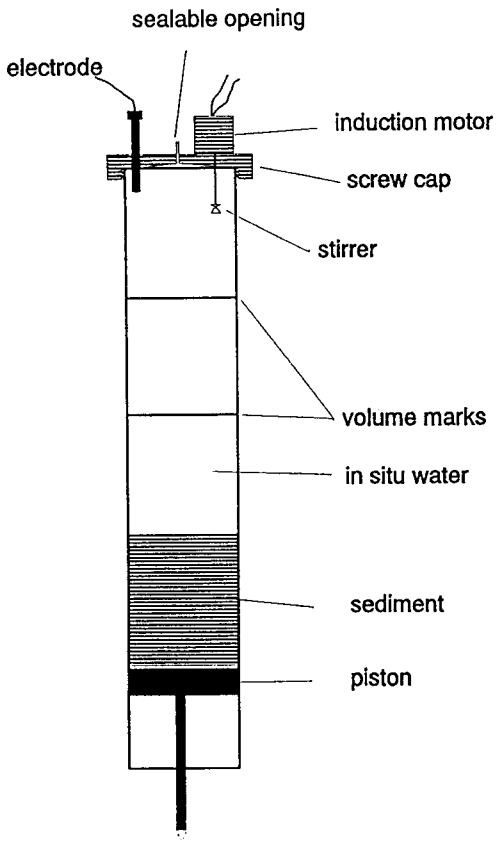

Figure 2 : Respiration chamber (core) to measure total sediment oxygen uptake.

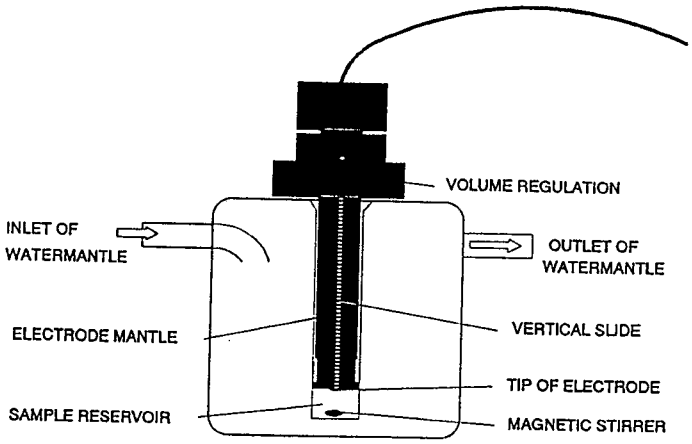

Figure 3 : Respiration chamber (RC 300) of the Strathkelvin electrode system to measure individual faunal oxygen uptake

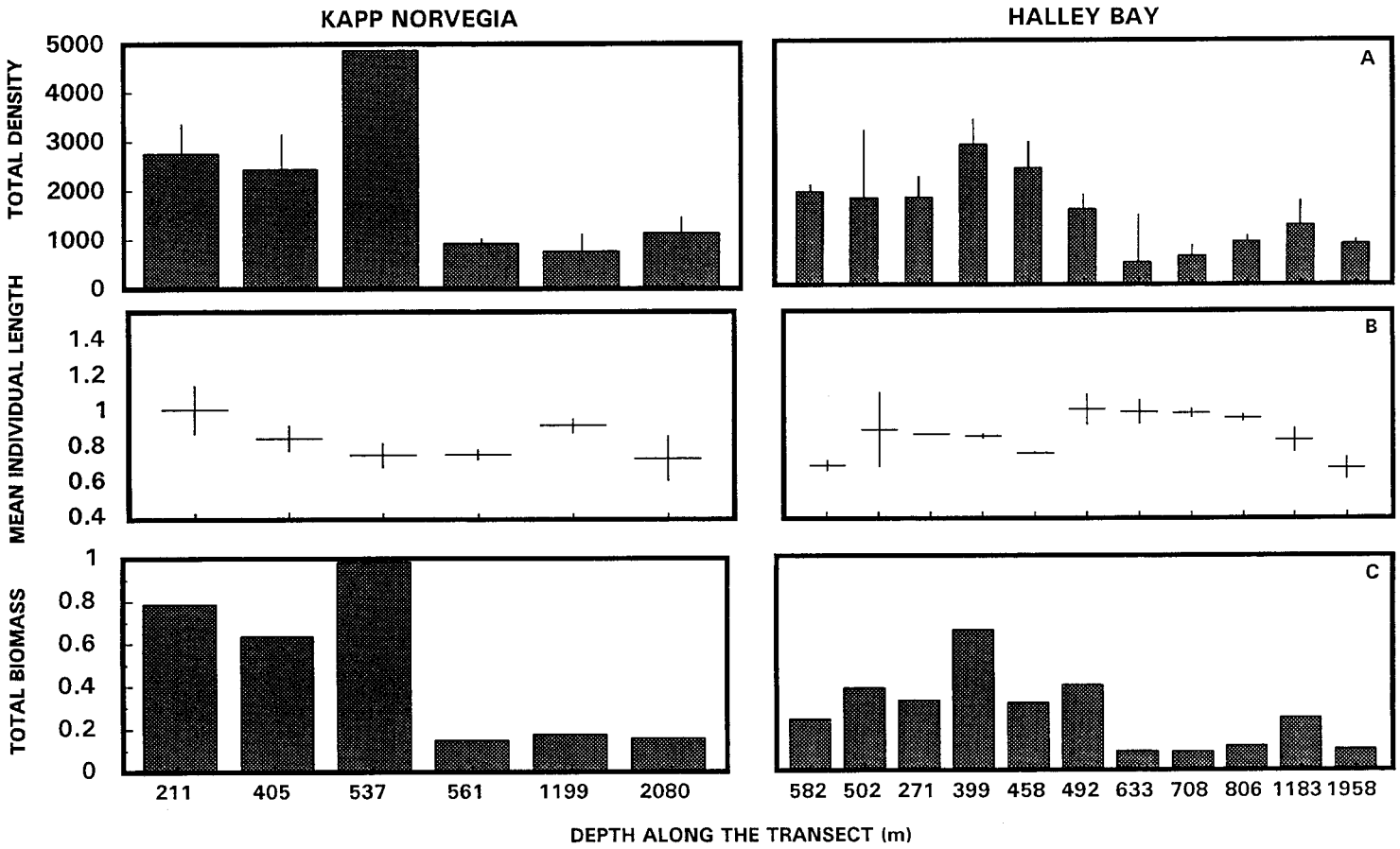

Figure 4 : Meiobenthos in the deep-sea floor of the Weddell Sea,
A) total density (N°.10 cm-2, SD), B) total biomass (g.m-2), C) mean individual nematode length (mm, SD)

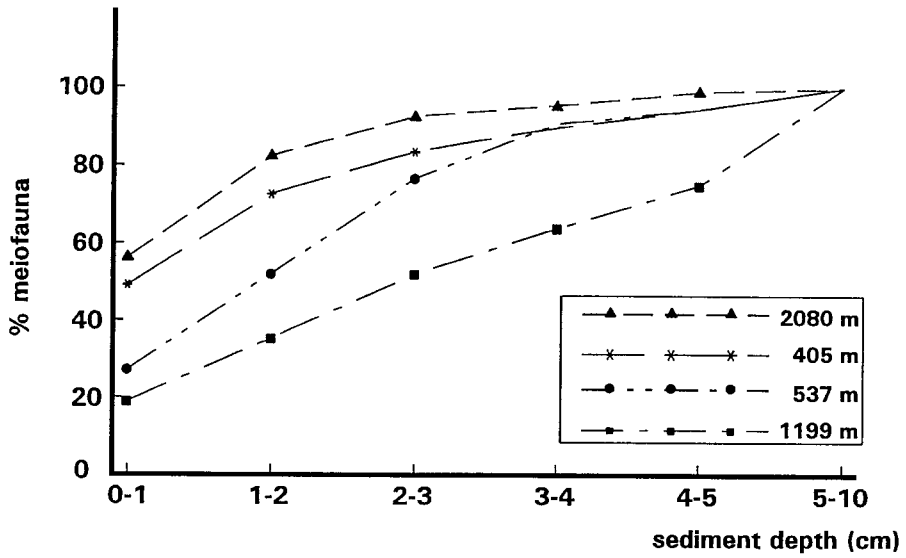

Figure 5 : Cumulative percentage curves of the depth penetration of meiofauna in the sediment profile at four stations in the deep Weddell Sea.

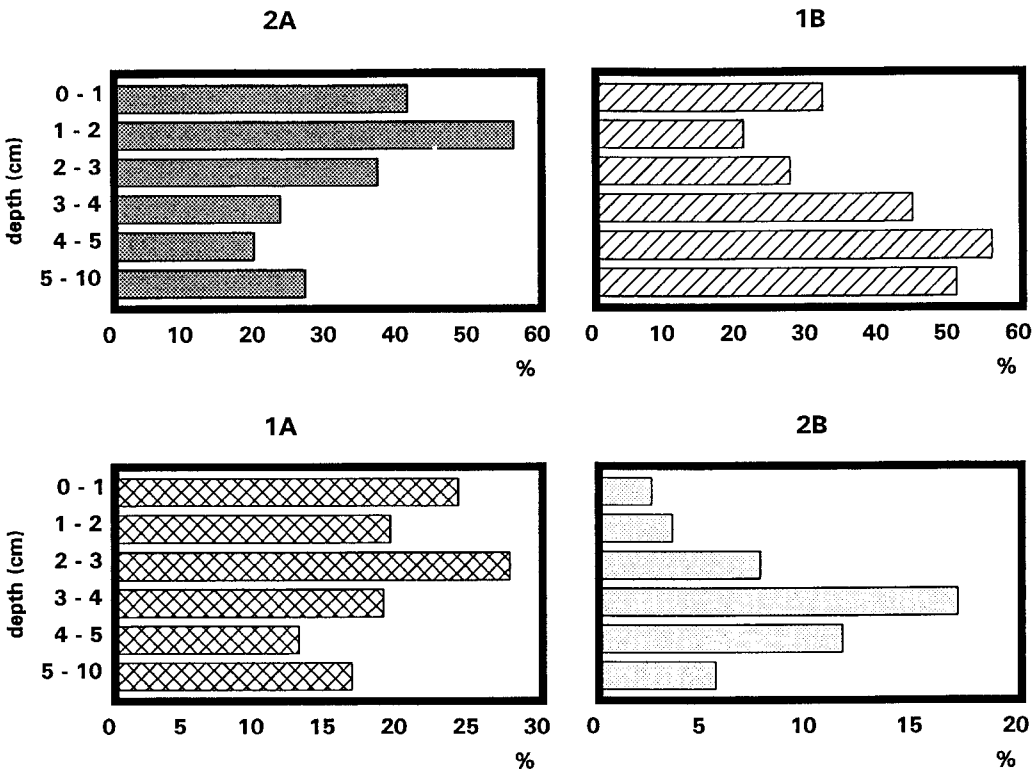

Figure 6 : Trophic composition of the nematodes in the sediment layers of a deep Weddell Sea station (2080 m). The values are percentages of the total at each layer.

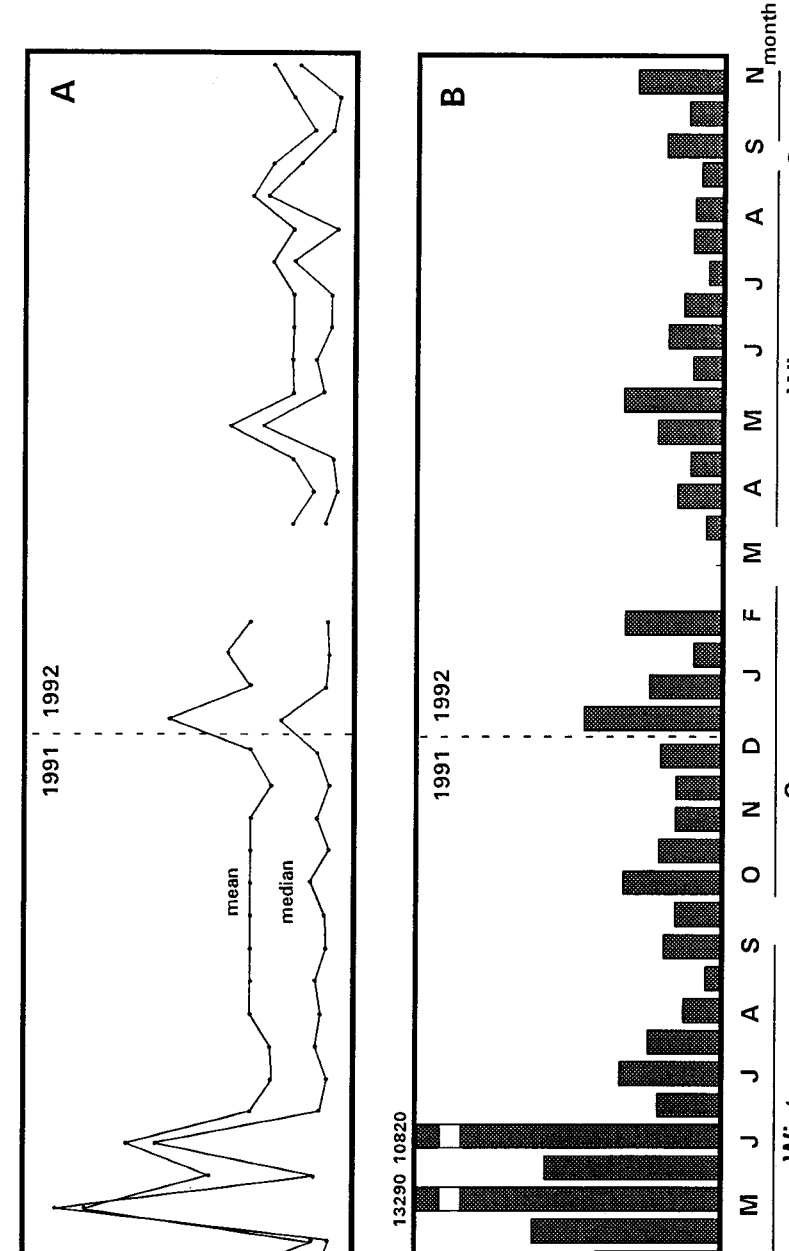

Figure 7 : A) Mean and median individual dwt (μg), and B) total biomass (μg dwt 10 cm-2) of the nematodes in the sediments of Factory Cove.

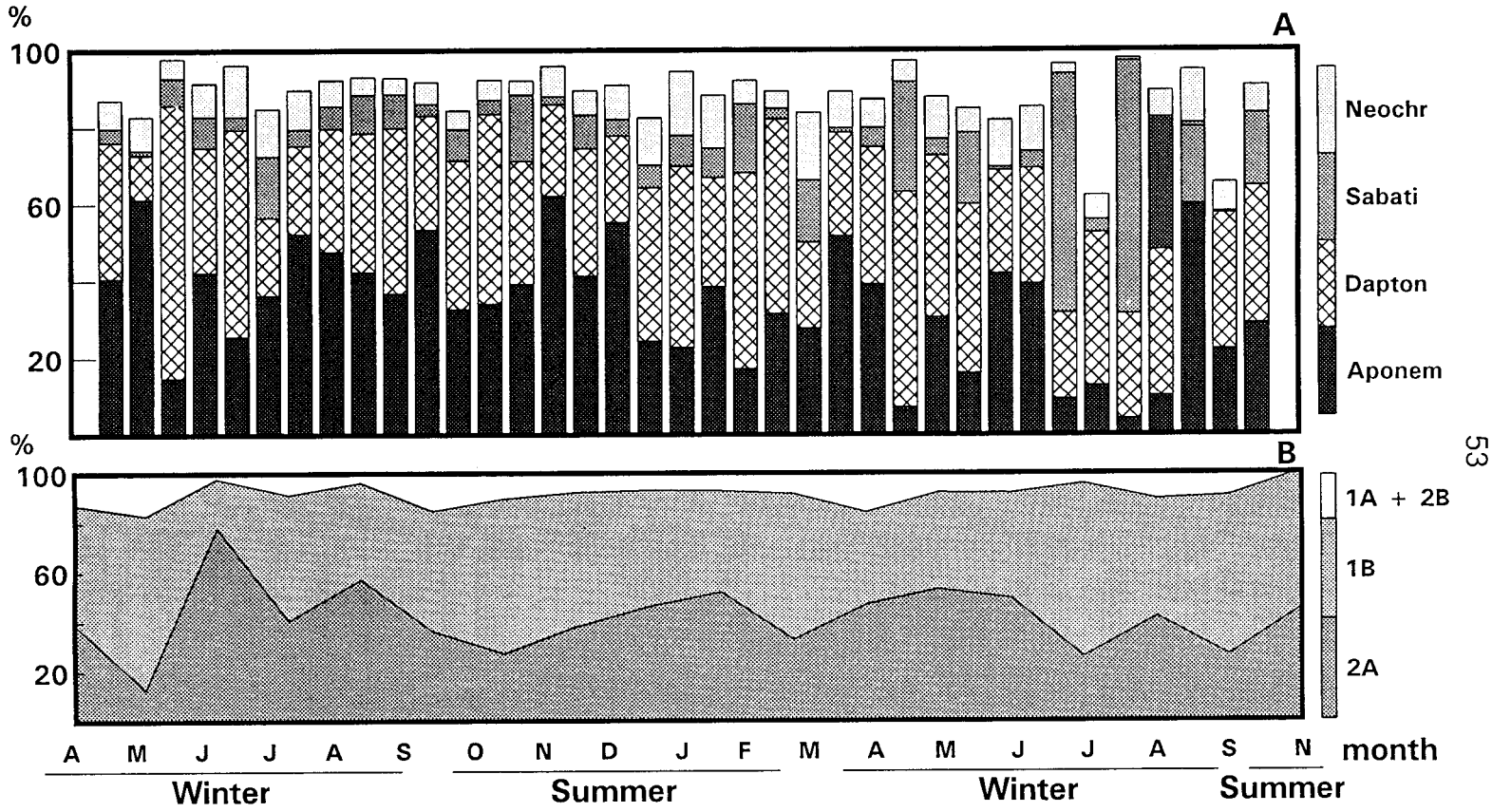

Figure 8 : A) Nematode genus and B) trophic composition in the sediments ofFactory Cove (% of total)
Neochr: Neochromadora, Sabati: Sabatieria, Dapton: Daptonema, Aponem: Aponema.

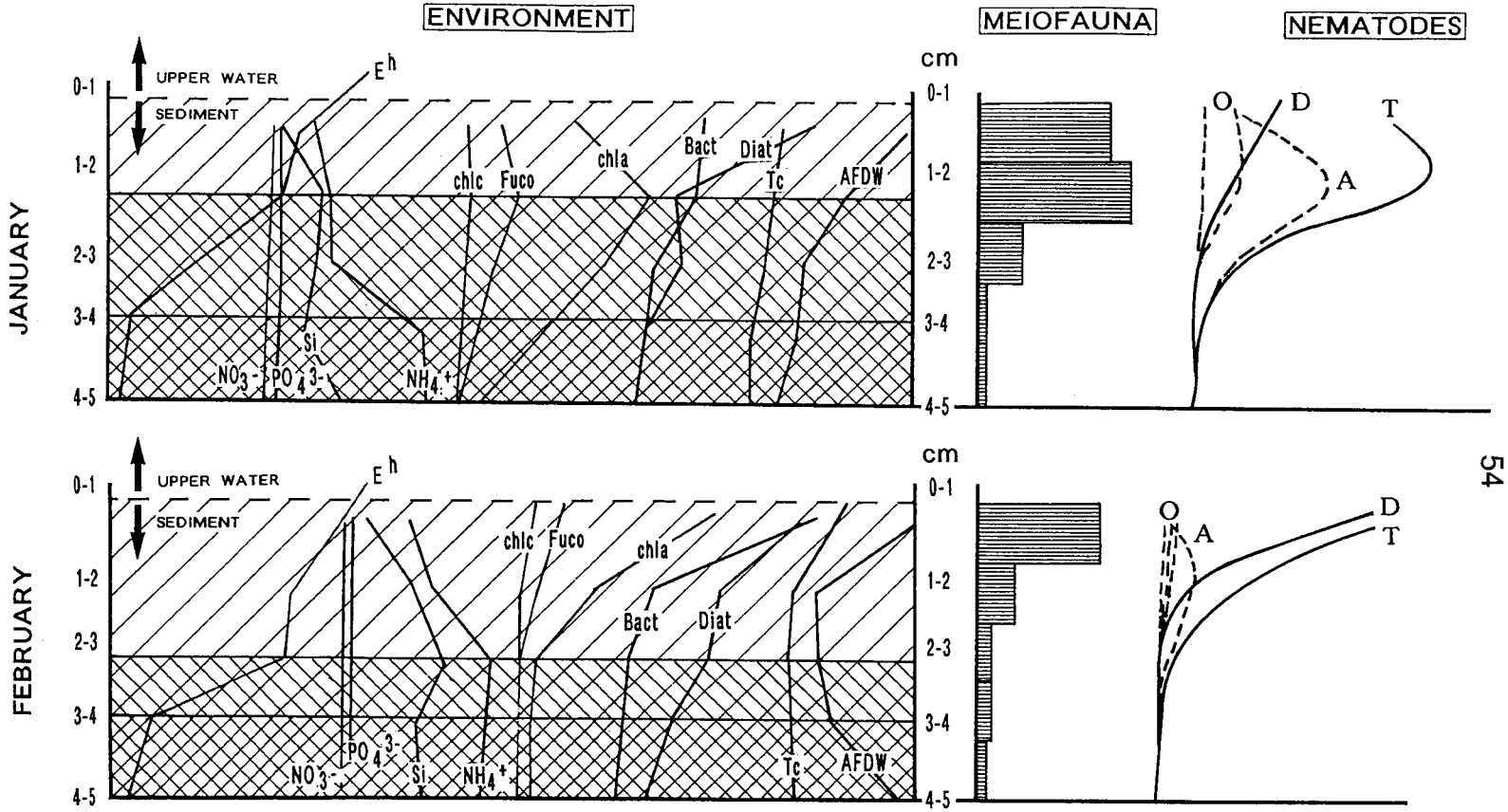

Figure 9 : Schematic presentation of biogeochemical concentration profiles and meiofauna distribution patterns within the sediments of Factory Cove: summer 1994 (for data the reader is referred to Vanhove et al. subm.). T: Total nematodes; A: *Aponema*; D: *Daptonema*; O: Others = *Chromadorita, Diplolaimella, Microlaimus, Neochromadora*.

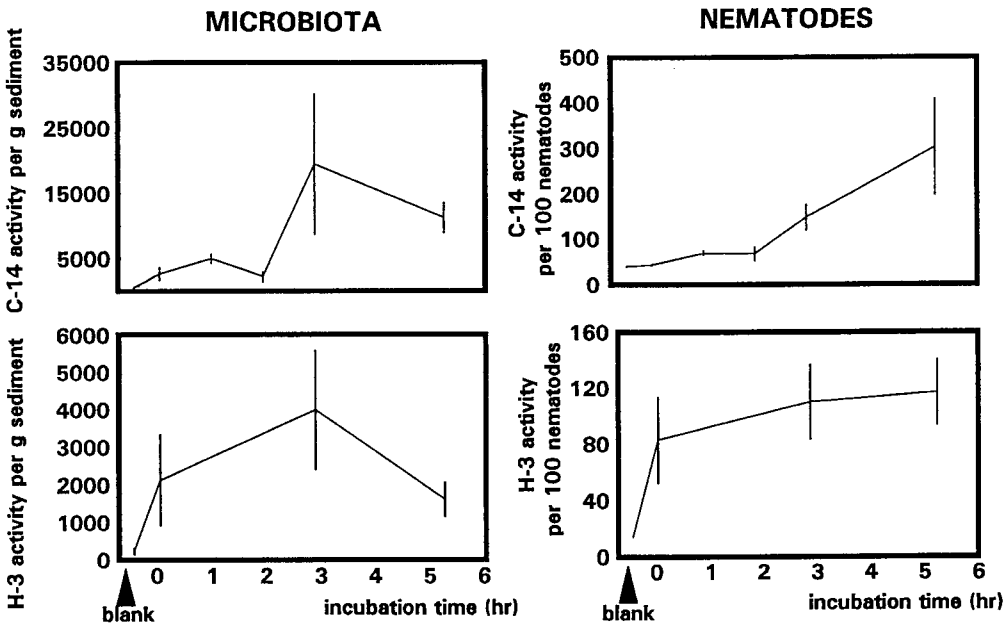

Figure 10 : Radio-isotope incorporation into the microbiota and nematodes. The data are mean and SD of three experiments.

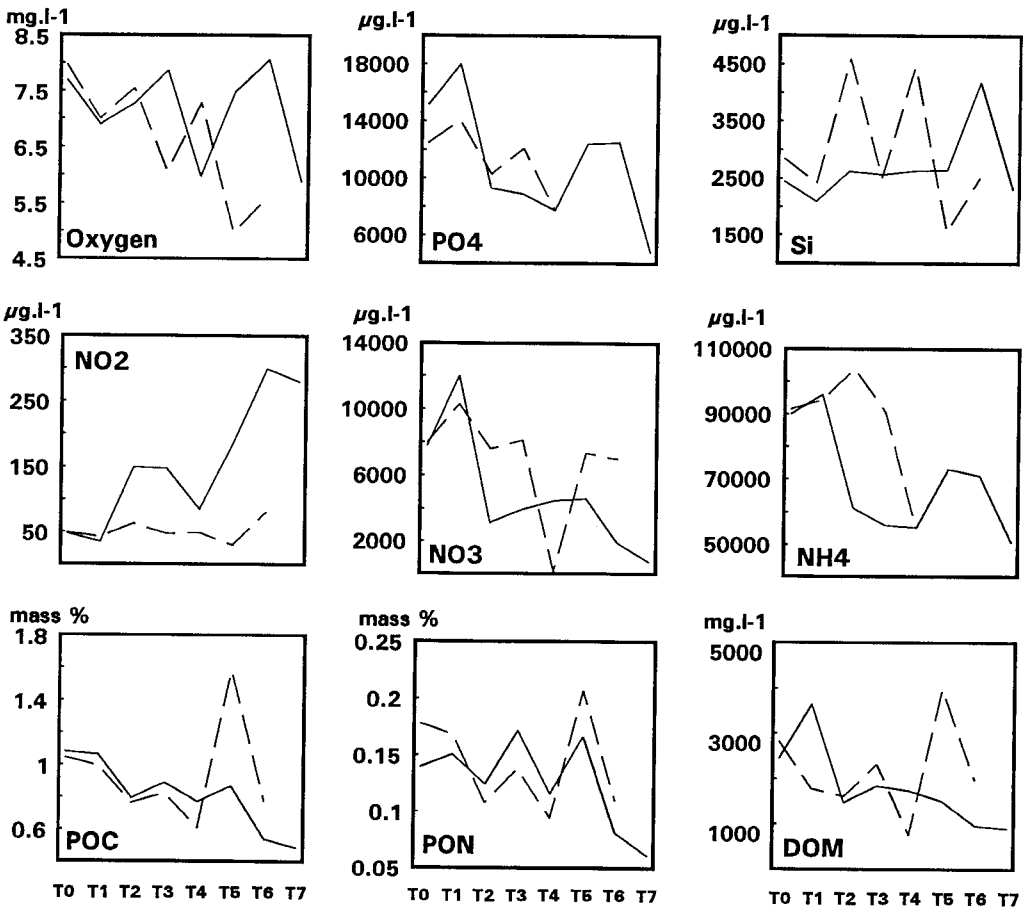

Figure 11 : Concentration changes of oxygen, nitrogen, carbon and phosporous organics and inorganics in the sediments of Factory Cove in March 1994. Solid lines represent light conditions; dashed lines are measurements in the dark.

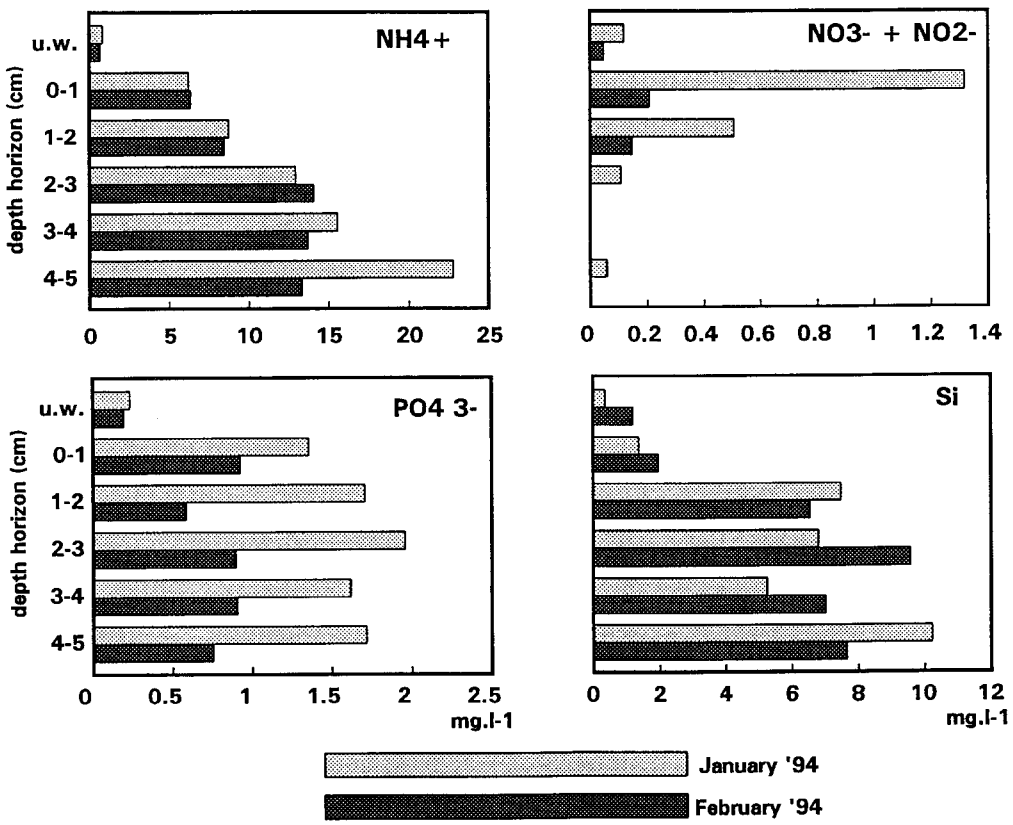

Figure 12 : Concentration profiles of dissolved pore water nutrients in the sediments of Factory Cove during the austral summer 1994.

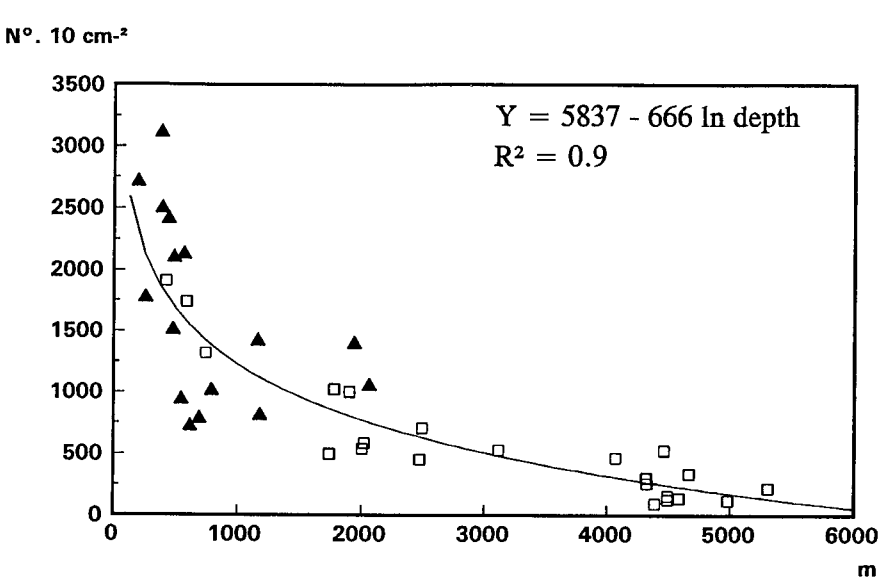

Figure 13 : Meiofaunal densities in the Weddell Sea (triangles), superimposed on the regression of meiofauna numbers with depth in the NE Atlantic Ocean (squares) by Vincx et al. 1994.

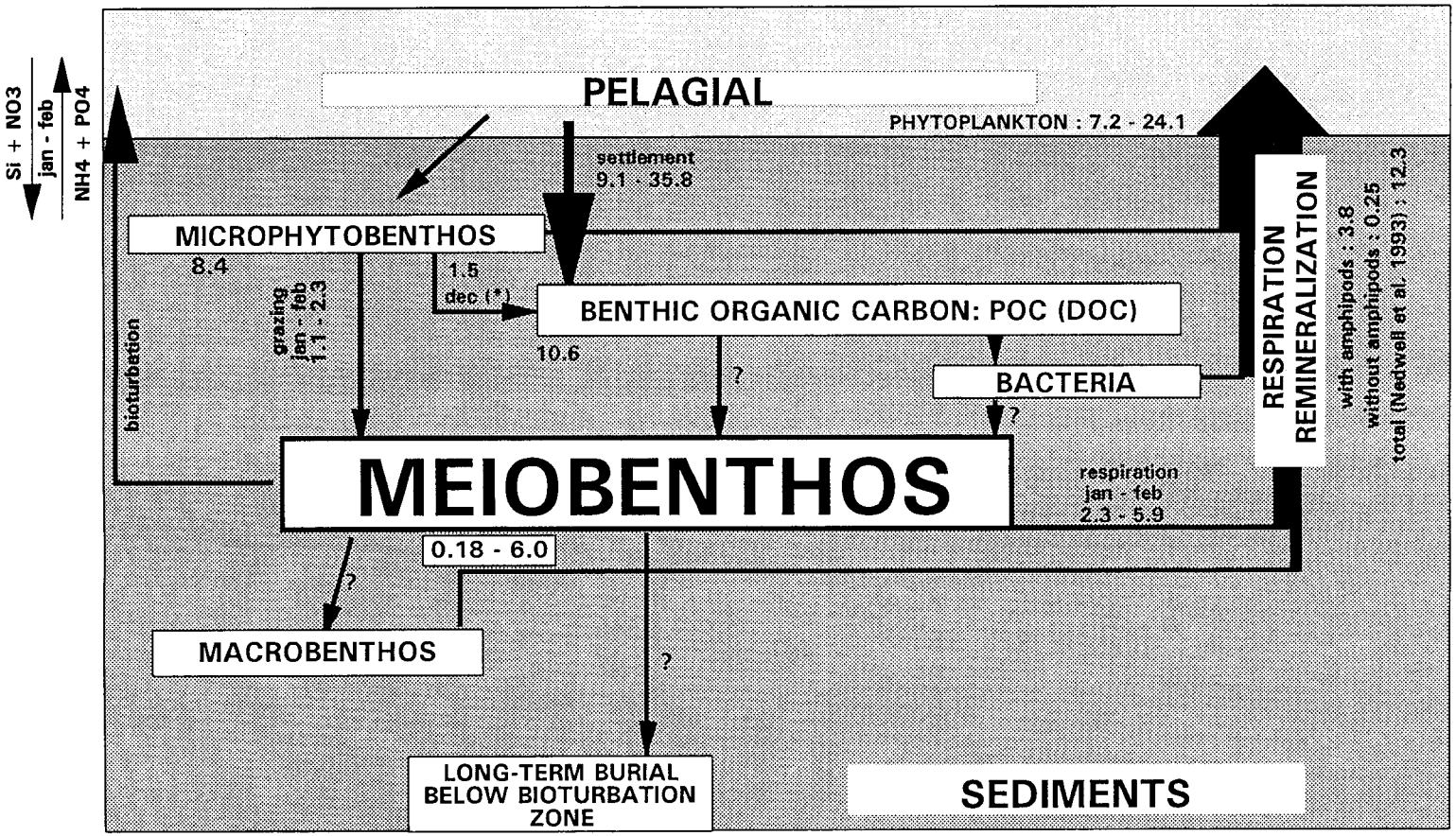

Figure 14: role and position of the meiobenthos in the ecosystem of Factory Cove : numbers reflect rates of carbon production and fluxes (mol C.m-2.y-1).